UNIVERSIDAD NACIONAL AUTÓNOMA DE MÉXICO

POSGRADO EN CIENCIAS BIOLÓGICAS

FACULTAD DE MEDICINA

BIOLOGÍA EXPERIMENTAL

ESTUDIO DE LA MODULACIÓN EJERCIDA POR FRUCTANOS DURANTE EL ESTRÉS INFLAMATORIO INTESTINAL INDUCIDO POR DISRUPTORES QUÍMICOS DE LA BARRERA INTESTINAL Y DE LA ARGININA DEIMINASA DE GIARDIA

TESIS

QUE PARA OPTAR POR EL GRADO DE:

DOCTORA EN CIENCIAS

PRESENTA:

M. EN C. FERNÁNDEZ LAINEZ CYNTHIA

TUTOR PRINCIPAL DE TESIS:

DR. GABRIEL LÓPEZ VELÁZQUEZ

INSTITUTO NACIONAL DE PEDIATRÍA, S.S.

CO-TUTOR DE TESIS:

PROF. PAUL DE VOS

FACULTAD DE CIENCIAS MÉDICAS, UNIVERSIDAD DE GRONINGEN

COMITÉ TUTOR:

DRA. MARIETTA TUENA SANGRI †

INSTITUTO DE FISIOLOGÍA CELULAR, UNAM

DRA. LILIÁN YÉPEZ MULIA

INSTITUTO MEXICANO DEL SEGURO SOCIAL

CIUDAD UNIVERSITARIA, CDMX, SEPTIEMBRE, 2023

UNIVERSIDAD NACIONAL AUTÓNOMA DE MÉXICO

POSGRADO EN CIENCIAS BIOLÓGICAS

FACULTAD DE MEDICINA

BIOLOGÍA EXPERIMENTAL

ESTUDIO DE LA MODULACIÓN EJERCIDA POR FRUCTANOS DURANTE EL ESTRÉS INFLAMATORIO INTESTINAL INDUCIDO POR DISRUPTORES QUÍMICOS DE LA BARRERA INTESTINAL Y DE LA ARGININA DEIMINASA DE GIARDIA

TESIS

QUE PARA OPTAR POR EL GRADO DE:

DOCTORA EN CIENCIAS

PRESENTA:

M. EN C. FERNÁNDEZ LAINEZ CYNTHIA

TUTOR PRINCIPAL DE TESIS:

DR. GABRIEL LÓPEZ VELÁZQUEZ

INSTITUTO NACIONAL DE PEDIATRÍA, S.S.

CO-TUTOR DE TESIS:

PROF. PAUL DE VOS

FACULTAD DE CIENCIAS MÉDICAS, UNIVERSIDAD DE GRONINGEN

COMITÉ TUTOR:

DRA. MARIETTA TUENA SANGRI †

INSTITUTO DE FISIOLOGÍA CELULAR, UNAM

DRA. LILIÁN YÉPEZ MULIA

INSTITUTO MEXICANO DEL SEGURO SOCIAL

CIUDAD UNIVERSITARIA, CDMX, SEPTIEMBRE, 2023

COORDINACIÓN GENERAL DE ESTUDIOS DE POSGRADO
COORDINACIÓN DEL POSGRADO EN CIENCIAS BIOLÓGICAS
ENTIDAD (FACULTAD DE MEDICINA)
OFICIO: CGEP/CPCB/FMED/0525/2023
ASUNTO: Oficio de Jurado

M. en C. Ivonne Ramírez Wence
Directora General de Administración Escolar, UNAM
P r e s e n t e

Me permito informar a usted que en la reunión ordinaria del Comité Académico del Posgrado en Ciencias Biológicas, celebrada el día **08 de mayo de 2023** se aprobó el siguiente jurado para el examen de grado de **DOCTORA EN CIENCIAS** de la estudiante **FERNÁNDEZ LAINEZ CYNTHIA** con número de cuenta **098012509** con la tesis titulada **"ESTUDIO DE LA MODULACIÓN EJERCIDA POR FRUCTANOS DURANTE EL ESTRÉS INFLAMATORIO INTESTINAL INDUCIDO POR DISRUPTORES QUÍMICOS DE LA BARRERA INTESTINAL Y DE LA ARGININA DEIMINASA DE GIARDIA",** realizada bajo la dirección del **DR. GABRIEL LÓPEZ VELÁZQUEZ,** quedando integrado de la siguiente manera:

Presidente:	DR. LUIS FELIPE JIMÉNEZ GARCÍA
Vocal:	DR. SERGIO ENRÍQUEZ FLORES
Vocal:	DR. ARTURO CARLOS II BECERRA BRACHO
Vocal:	DR. LUBBERT DIJKHUIZEN
Secretario:	DRA. LILIÁN YÉPEZ MULIA

Sin otro particular, me es grato enviarle un cordial saludo.

A T E N T A M E N T E
"POR MI RAZA HABLARÁ EL ESPÍRITU"
Ciudad Universitaria, Cd. Mx., a 27 de junio de 2023

COORDINADOR DEL PROGRAMA

POSGRADO EN CIENCIAS BIOLOGICAS
COORDINACIÓN

DR. ADOLFO GERARDO NAVARRO SIGÜENZA

c. c. p. Expediente del alumno

AGNS/RCHT/EARR/rcht

AGRADECIMIENTOS INSTITUCIONALES

Al Posgrado en Ciencias Biológicas, UNAM

A la Facultad de Ciencias Médicas, RUG

El presente trabajo de tesis tuvo los siguientes apoyos financieros:

Recursos Fiscales para Investigación Instituto Nacional de Pediatría 2019/062

Programa de Talento Abel Tasman, Universidad de Groningen

CONACyT 260625

Al comité tutor:

Dra. Marietta Tuena Sangri †

Dra. Lilián Yépez Mulia

Dr. Gabriel López Velázquez (Tutor principal)

Prof. Paul de Vos (Cotutor)

En el marco del programa de doble doctorado entre la Universidad Nacional Autónoma de México y la Universidad de Groningen, la investigación descrita en esta tesis se llevó a cabo en el Laboratorio de Biomoléculas y Salud Infantil del Instituto Nacional de Pediatría y en el Grupo de Inmunoendocrinología del Centro Médico Universitario de Groningen (UMCG) y la Universidad de Groningen (RUG).

Agradecimientos a título personal

Clama a mí, y yo te responderé, y te enseñaré cosas grandes y ocultas que tú no conoces. Jeremías 33:3

Dios mío, cinco años han pasado desde que comencé esta aventura, ¡estoy muy feliz de haber terminado! Gracias por concederme lograrlo.

Esta hazaña no hubiera sido posible sin el apoyo de mi familia, amigos, colegas y profesores, a quienes les dedico las siguientes palabras:

Mis más profundo agradecimiento a mis alma mater la Universidad Nacional Autónoma de México (UNAM), la Universidad de Groningen y el Centro Médico Universitario (UMCG). Me siento profundamente satisfecha y agradecida con estas instituciones por darme la oportunidad de adquirir una formación académica de excelencia, la cual está rindiendo buenos frutos y me permitió establecer redes de colaboración para mi futura vida académica como investigadora.

A los miembros del jurado, Dr. Luis Felipe Jiménez García, Dr. Sergio Enríquez Flores, Dr. Arturo Carlos II Becerra Bracho, Prof. Lubbert Dijkhuizen, y Dra. Lilián Yépez Mulia, gracias por sus valiosas observaciones y sugerencias, las cuales mejoraron esta tesis.

A los miembros de mi comité tutoral de la UNAM. Doctora Lilián Yépez Mulia, le agradezco enromemente todas sus sugerencias y observaciones durante las evaluaciones semestrales. Todas ellas enriquecieron el proyecto y mi formación académica. Mi muy especial agradecimiento y reconocimiento a la Profesora Marietta Tuena Sangri quien recientemente nos dejó, sus enseñanzas, sus preguntas tan certeras, mismas que siempre me llevaban a la reflexión, y su trato humano cálido, siempre los llevaré en mi corazón.

A mis tutores, el Prof. Gabriel López-Velázquez y Prof. Paul de Vos.

Querido Gabriel, ¡tengo tanto que agradecerte! Desde aquellos ayeres cuando aceptaste dirigir mis estudios de posgrado. Para empezar, gracias por haber confiado en mi potencial, más aún, ¡gracias por hacerme ver el potencial que ni yo misma creía que tenía! Todo lo que he logrado lo debo en gran parte a tu apoyo incondicional. Compartiste tu visión tan progresista de lo que debe ser un doctor en ciencias y expandiste mis horizontes más allá de las fronteras de nuestro país y de nuestro continente. Por todo ello te estaré eternamente

agradecida. Ahora que seremos colegas, estoy segura de que seguiremos colaborando y enfrentando los retos venideros en nuestra vida académica.

Querido Paul, nunca olvidaré nuestras reuniones semanales, donde junto con una taza de café, siempre me compartiste tu amplia experiencia académica. Gracias por la confianza y el apoyo que siempre me diste, especialmente en los momentos más difíciles durante mi estancia en Groningen por problemas de salud. También quisiera agradecerte por invertir tu tiempo en enseñarme cómo escribir artículos académicos. Siempre me sentí tratada por tí con gran calidez humana, lo cual siempre atesoraré.

A la Doctora Marcela Vela Amieva, para usted tengo un agradecimiento muy especial por haberme apoyado desde siempre. ¡Este logro es en gran parte a su apoyo! Todo lo que aprendí está al servicio de nuestro laboratorio y al servicio de nuestros pacientes con errores innatos del metabolismo, para seguir creciendo y haciendo nuestro trabajo, ¡el cual disfrutamos!

A mis compañeros del Laboratorio de Errores Innatos del Metabolismo y Tamiz, Sara Guillén, Lizbeth López, Aída Hernández, Jaime Torres, Ricardo Morales, y Sandra Vázquez, gracias por su apoyo, especialmente durante mi ausencia.

A “Los Intocables”, Itzhel, Sergio, Nacho y Luis, ustedes fueron grandes maestros durante mi etapa de estudios de maestría, para posteriormente convertirse en mis amigos. ¡Gracias por todo!

Por último, pero no menos importante, a mis queridos padres Leonel y María Eugenia, mis hermanas Diana, Ada y Moni, mis cuñados Armando y Ricardo, y mis sobrinos Paulo y Celina, muchas gracias por aguantar y comprender mis ausencias, porque para obtener este logro los sacrifiqué muchas veces. Gracias por siempre alimentarme con su cariño y brindarme apoyo siempre que lo necesité. ¡Nunca olvidaré los maletones con los que regresaba de México a Groningen, siempre llenos de mis frituras mexicanas preferidas, dotación de chiles y hasta el lavadero! Ustedes fueron un alisciente muy importante para trabajar duro todos los días.

Para mís amados padres

ÍNDICE

RESUMEN

Existe evidencia científica sustancial acerca de los beneficios a la salud del consumo de fibras dietéticas (FDs), tales como los fructanos, sin embargo, los mecanismos que subyacen dichos beneficios no son del todo conocidos. Por ello, en la presente tesis, en los **capítulos 2 al 6**, estudiamos cómo los fructanos de tipo graminano (GTFs por sus siglas en inglés) extraídos de la planta *Agave tequilana* y los fructanos de tipo inulina (ITFs, por sus siglas en inglés) extraídos de la planta de achicoria (*Cichorium intybus)* impactan a la imunidad y a la función de la barrera intestinal. Además, también comparamos los efectos entre ambos tipos de fructanos. Para ello, nuestros modelos de estudio fueron las diferentes células especializadas que constituyen el epitelio intestinal. Como células tipo enterocito incluímos a las células Caco-2 y T84, como células productoras de mucosa incluimos a la línea celular tipo caliciforme o goblet LS174T, y como representantes de las células inmunes intestinales, incluímos a las células dendríticas (DCs). A nivel de las células intestinales tanto epiteliales como caliciformes, mediante estudios de resistencia transepitelial y de expresión génica, demostramos el efecto protector de los fructanos en la barrera epitelial intestinal, tanto en condiciones fisiológicas, como en condiciones de estrés inducido por moléculas que dañan la barrera intestinal. En las DCs demostramos que éstas exhibieron una respuesta antiinflamatoria cuando fueron expuestas a los fructanos. Más aún, demostramos que dichas respuestas reguladoras de las DCs son más fuertes cuando son expuestas al medio de cultivo que fue previamente utilizado por las células intestinales, mismas que a su vez, fueron incubadas en presencia de los fructanos. Yendo más allá del contexto celular, también estudiamos los efectos que tienen los fructanos sobre receptores del sistema inmune de tipo Toll (TLRs), los cuales se especializan en la detección de moléculas provenientes de agentes infecciosos en el intestino, para dar lugar a la activación de cascadas de señalización que culminan en la producción de citocinas proinflamatorias para combatir la infección. Encontramos que los fructanos del agave poseen un fuerte efecto inhibidor de la activación inducida de los TLRs 2 y 4. Basados en estudios de docking molecular, propusimos una explicación mecanística para este fenómeno biológico observado. Propusimos que dicho efecto inhibitorio de la activación de TLR2 y TLR4 podría ser debido a la competencia de los GTFs con el sitio de unión al agonista natural de dichos TLRs.

El conocimiento generado contribuye alentendimiento de cómo los fructanos estudiados contribuyen al mejoramiento de la salud, lo cual podría ser de utilidad en el diseño de alimentos que prevengan efectivamente y protejan de la disfunción de la barrera intestinal o de los procesos inflamatorios en el intestino.

En la segunda parte de esta tesis, estudiamos la importancia de los TLRs como parte de la comunicación entre el hospedero y parásitos intestinales, todo esto en el contexto de la infección intestinal por *Giardia lamblia*, la cual es una de las principales causas de diarrea provocada por parásitos protistas a nivel mundial. En el **capítulo 7** estudiamos la interacción de los TLRs con uno de los factores de virulencia de *G. lamblia*, la enzima arginina deiminasa (GlADI). A partir de estudios en líneas celulares que expresan de manera independiente cada uno de los TLRs, encontramos que GlADI puede activar a los TLRs 2 y 4 en una manera dependiente de la dosis. También encontramos que la estructura tridimensional de GlADI es fundamental en la inmunomodulación ejercida. Mediante docking molecular predijimos que GlADI se une al TLR2 mediante la interacción con residuos de aminoácidos localizados cerca de del sitio de unión del ligando, así como a aminoácidos importantes para la dimerización de TLR2. También encontramos que GLADI interactúa tanto con el TLR4, como con su proteína accesoria MD2. Finalmente, la incubación de DCs parecidas a las de infantes, en presencia de GlADI provocó una liberación aumentada de las citocinas proinflamatorias TNFα y IL-1β, pero

disminuyó la liberación de la citocina MCP-1. Este estudio demuestra que GlADI participa en la inmunomodulación de Giardia con el hospedero en una manera dependiente de la estructura, y que dicha inmunomodulación es ejercida mediante los TLRs.

El tratamiento de primera línea de la giardiasis incluye la administración de metronidazol y nitazoxanida. Sin embargo, algunas cepasd de *Giardia* son resistentes a estas terapias. Entonces, la búsqueda de terapias alternativas para combatir la giardiasis aún es necesaria. En el **capítulo 1** estudiamos a GlADI como un blanco potencial para el diseño de nuevos fármacos contra la giardiasis. Para ello, realizamos estudios de docking molecular y espectroscópicos pata investigar la interacción potencial de GlADI con los fármacos omeprazol, rabeprazol, aurotiomalato y sulbutiamina. Utilizamos estos fármacos midificadores de cisteínas debido a que la estructura primaria de GlADI es rica en residuos de cisteínas. También realizamos ensayos de inactivación enzimática con los cuatro fármacos y encontramos que todos ellos inactivaron a GlADI en un modo dependiente de la dosis; sin embargo, sólo el omeprazol y el rabeprazol disminuyeron la sobrevivencia de *Giardia* con la inhibición simultánea de la actividad de GlADI. Los estudios de docking molecular revelaron que estos fármacos se unen a diferentes residuos de cisteínas. El rabeprazol fue el único fármaco que dañó la capacidad de enquistamiento de Giardia. Estos hallazgos demuestran el promisorio papel de GlADI como blanco contra la giardiasis. También demostramos la potencial actividad antigiardiásica del rabeprazol, y que ésta se lleva a cabo a través de un mecanismo de modificación de cisteínas.

Finalmente, en el **capítulo 8** se discuten de manera global los resultados presentados.

ABSTRACT

Substantial scientific evidence exists about the health benefits of dietary fibers (DFs) such as fructans, however, the underlying mechanisms of those benefits are not well understood. Therefore, in the present thesis, from **chapter 2 to 6**, we studied how graminan-type fructans (GTFs) from *Agave tequilana* plant and inulin-type fructans (ITFs) extracted from chicory plant (*Cichorium intybus)* impact on immunity and integrity of the intestinal barrier. Moreover, we compared the effects of both fructans. To that end, our study models were the different specialized cells that constitute the intestinal epithelium. As enterocyte-like cells we included Caco-2 and T84 cells, as goblet-like cells we included LS174T cells, and as representatives of the gut immune system we included dendritic cells (DCs). At the intestinal cells level, as epithelial as goblets, through transepithelial resistance and genetic expression, we demonstrated the protective effect of fructans in the intestinal epithelial barrier. On DCs, we demonstrated that they showed an anti-inflammatory effect when they were exposed to fructans. Moreover, we demonstrated that such regulatory responses were stronger when they were exposed to the spent medium used by Caco-2 cells, which were previously incubated in presence of fructans. Going further, we also studied the effects of fructans on Toll-like receptors (TLRs), which are specialized in the detection of molecules from gut pathogenic agents, this activates signaling cascades that end in the production of proinflammatory cytokines for defending the organism from infection. We found that agave fructans possess a strong inhibitory effect of the induced activation of TLR2 and TLR4, which could be due to the competition of GTFs for the natural agonist binding site of TLRs.

In the second part of this thesis, we studied the importance of TLRs as part of the crosstalk between host and parasites in the context of intestinal infection by *Giardia lamblia,* one of the leading causes of diarrhea provoked by protist parasites worldwide. In **Chapter 7** we studied TLR interaction of one of *G. lamblia* virulence factors, the enzyme arginine deiminase (GlADI). From studies in cell lines that independently express each TLR, we found that GlADI activates TLR2 and TLR4 in a dose-dependent fashion. We also found that 3D structure of GlADI is fundamental in the immunomodulation exerted. By molecular docking we predicted that GlADI binds to TLR2 through amino acid residues located next to the ligand binding site, as well as with amino acids important for TLR2 dimerization. We also found that GlADI interacts with both TLR4 and MD2 protein. Finally, incubation of human infant-like DCs in the presence of GlADI provoked an enhanced release of the pro-inflammatory cytokines TNFα and IL-1β but decreased the release of MCP-1. This study demonstrates that GlADI participates in Giardia-host immunomodulation in a structure-dependent fashion and that this immunomodulation is exerted via TLRs.

The first line of treatment for giardiasis includes administration of metronidazole and nitazoxanide. However, strains of *Giardia* might be resistant to these therapies. Thus, the research on alternative therapies against giardiasis is needed. In **Chapter 2** we studied GlADI as a potential target for the design of new drugs against giardiasis. To that end, molecular docking as well as spectroscopic studies were applied to investigate the potential interaction of GlADI with omeprazole, rabeprazole, aurothiomalate and sulbutiamine. We used these cysteine-modifying drugs since the primary structure of GlADI is rich in cysteine residues. We also performed GlADI enzymatic inactivation assays with the four drugs and found that all of them inactivated GlADI in a dose-dependent manner, however, only omeprazole and rabeprazole decreased *Giardia* survival with the simultaneous inhibition of GlADI activity. Molecular docking studies revealed that these drugs bind to different cysteine residues. Rabeprazole was the only drug that impaired Giardia encystment capacity. These findings demonstrate the promising role of GlADI as target against giardiasis. We also demonstrated the potential anti-giardial activity of rabeprazole, and that it is through a cysteine-modification mechanism.
Finally, in **Chapter 8** the results presented in this thesis were discussed.

INTRODUCCIÓN

Parte 1

El incremento global en la incidencia de enfermedades no transmisibles está directamente influenciado por el estilo de vida moderno. El sedentarismo y la dieta occidental enriquecida con grasas y carbohidratos de alto índice glicémico, junto con una inclusión insuficiente de fibra dietética (FD), son las principales causas de este escenario. Por el contrario, el alto consumo de FD ayuda al envejecimiento saludable y disminuye el riesgo de desarrollar enfermedades crónicas. El tracto gastrointestinal (GI) y el sistema inmune intestinal juegan un papel importante en dicho círculo virtuoso; sin embargo, los mecanismos que subyacen dichos efectos benéficos no han sido completamente comprendidos. Debido a su naturaleza química, las FDs pasan por el sistema digestivo y alcanzan el intestino prácticamente sin ser digeridas. Después de la interacción de las FDs con la cubierta del intestino delgado, se ha observado un sistema inmune fortalecido y un reforzamiento de la función de la barrera epitelio intestinal. Estos efectos llamados "directos" resultan de la interacción de las FDs con los receptores de reconocimiento de patrones (PRRs, por sus siglas en inglés), tales como los receptores tipo Toll (TLRs), con la concomitante inmunomodulación del hospedero. Un grupo importante de fibras dietéticas que ha demostrado poseer efectos directos benéficos son los fructanos. Los fructanos son carbohidratos a base de fructosa, cuya longitud de cadena o grado de polimerización (GP) es variable. Aquellos extraídos de plantas son carbohidratos no estructurales, solubles en agua, que sirven como reservorios de energía. En Europa, los fructanos extraídos de la planta de achicoria (*Cichorium intybus*) son los suplementos alimenticios de fibra más ampliamente consumidos. Mientras que en regiones como Latinoamérica las plantas de la familia del agave, i.e. *Agave tequilana*, que son endémicas de la región, representan una fuente rica en fructanos. Estos fructanos también podrían ser utilizados como fuente de FD para la suplementación de alimentos. Los fructanos de la achicoria y los del agave son estructuralmente diferentes. Los fructanos de la achicoria pertenecen al grupo de los fructanos de tipo inulina (ITFs, por sus siglas en inglés), esto es debido a que son polímeros unidos únicamente por enlaces $\beta(2\rightarrow1)$. Dichos ITFs tienen una estructura lineal. Mientras que los fructanos del agave pertenecen a los fructanos de tipo graminano (GTFs, por sus siglas en inglés), debido a que constan de una mezcla de enlaces $\beta(2\rightarrow1)$ y $\beta(2\rightarrow6)$, lo cual les confiere una estructura ramificada. La evidencia científica acerca de los beneficios a la salud de los fructanos de la achicoria es sustancial; sin embargo, estos beneficios no han sido del todo estudiados para los fructanos del agave. Es por ello que en la presente tesis estudiamos el efecto de los fructanos del agave en la inmunomodulación y en la función de la barrera intestinal. Además, comparamos estos efectos, con los efectos de los fructanos de la achicoria.

Además de la extensa evidencia del efecto prebiótico de los fructanos, también denominado "*indirecto*", su consumo ha demostrado jugar un papel importante en el desarrollo del sistema inmune, principalmente mediante su unión a los receptores de reconocimiento de patógenos (PRRs, por sus siglas en inglés), causando efectos anti-inflamatorios y potenciando la eficacia de vacunas. Mediante estudios *in vitro* se ha observado que el co-cultivo de fructanos con células epiteliales intestinales, fortalece la función de la barrera y previene la adhesión de microorganismos patógenos. El efecto directo de los fructanos en la inmunomodulación y en la función de la barrera intestinal ha sido más estudiado para los ITFs que para los GTFs.

Introducción

Los fructanos de tipo graminano (GTFs, por sus siglas en inglés) son fibras dietéticas /FDs) ampliamente reconocidas por sus potenciales beneficios a la salud en la prevención o tratamiento de enfermedades no transmisibles, tales como la enfermedad inflamatoria intestinal, la diabetes tipo 2, la obesidad y el cáncer. Estos fructanos también han sido aplicados exitosamente como prebióticos en fórmulas infantiles. Sin embargo, no se sabe si los GTFs poseen capacidad inmunomoduladora y en qué medida, y si este efecto es dependiente del tamaño del fructano y de su estructura. Tampoco se sabe si los GTFs son capaces de proteger la barrera epitelial intestinal de agentes disruptores y de sus efectos de inflamación, ni si este efecto podría ir más allá de la barrera intestinal, alcanzando las células del sistema inmune que residen por debajo e intercaladas entre el epitelio intestinal, tales como las células dendríticas. Los mecanismos que subyacen los beneficios a la salud de los GTFs tampoco son del todo conocidos. Es por ello que en la presente tesis estudiamos cómo los GTFs de direrente tamaño impactan a la imunidad y a la función de la barrera intestinal. Además, también comparamos los efectos de los GTFs con los sabidos efectos de los fructanos de tipo inulina (ITFs, por sus siglas en inglés). El entendimiento de cómo los GTFs contribuyen al mejoramiento de la salud, podría ser de utilidad en el diseño de alimentos que prevengan efectivamente y protejan de la disfunción de la barrera intestinal o de los procesos inflamatorios en el intestino. Más aún, disectar si los efectos de los GTFs son dependientes de su estructura o de la longitud de su cadena, podría ayudar en el diseño de opiones terapéuticas individualizadas.

Durante los años recientes se han tenido avances sustanciales en el entendimiento y la determinación de los efectos de los fructanos de la achicoria y el agave tanto en la salud como en la enfermedad, así como en sus mecanismos de acción. El efecto indirecto prebiótico de estas fibras dietéticas ya ha sido ampliamente demostrado tanto en estudios *in vitro* como *in vivo* en ensayos clínicos.

Los efectos directos a nivel del sistema inmune de las fibras dietéticas han sido gran sujeto de investigación durante la déada pasada. En el intestino delgado hay una amplia oportunidad de que las fibras interactúen con el epitelio y las células del sistema inmune tales como las células dendríticas y los linfocitos intraepiteliales, los cuales expresan los PRRs, tales como los TLRs. A este respecto, los fructanos también han demostrado actuar vía esta misma ruta y contribuir así a la homeostasis disparando la transducción de señales subsecuentes en las células del sistema inmune intestinal, con lo que al final se traduce en un efecto regulador o de tolerancia. Sin embargo, al mismo tiempo se ha demostrado que no todos los fructanos tienen la misma eficacia, y que dichos efectos dependen principalmente de la estructura, largo de cadena y dosis del fructano aplicado. El uso de tecnologías modernas tales como la metabolómca para una caracterización más profunda del alcance de los fructanos en la salud humana y en los estados de enfermedad, podrían ser útiles para tener mayor evidencia de cómo los fructanos impactan en la salud (O'Conell, et. al. 2020, Spacova, et. al. 2020).

En diferentes partes del mundo los fructanos se extraen de diferentes plantas. Debido a que estos fructanos pueden diferir en grande manera, es esencial no generalizar acerca de sus beneficios a la salud, sino estudiarlos de manera individual. Cada fructano podría actuar de manera diferente y por ende, podría tener diferentes beneficios a la salud. Es por ello que el conocimiento generado hasta la fecha acerca de los fructanos del agava y de la achicoria, contribuye al diseño de opciones terapéuticas más personalizadas en un escenario profiláctico (Reimer, et. al. 2020). Los campos potenciales de aplicación de los fructanos pueden ser a nivel de soporte de un envejecimiento saludable (Kiewiet, et. al. 2021), en el mejoramiento de la efectividad de las vacunas (Vogt, et. al. 2017), o en la prevención del desarrollo y severidad de enfermedades. Los fructanos

incluso podrían coadyuvar en el tratamiento de enfermedades de tipo inflamatorio, tales como algunos desórdenes intestinales, la diabetes y el cáncer (Li, et. al. 2020, Padilla Camberos, et. al. 2018, Hiel, et. al. 2020, De Preter, et. al. 2013).

Durante los años recientes nuevos hallazgos sobre los mecanismos por los cuales los fructanos ejercen sus efectos benéficos a la salud se han descubierto, y al mismo tiempo se ha demostrado que dichos efectos dependen grandemente de la estructura del fructano aplicado, así como de la edad y el estado de salud del hospedero (Roberfroid, et. al. 2005). Para maximizar los efectos y llegar a la dosis óptima, es necesario generar más evidencia acerca de cuáles fructanos deberían ser aplicados para grupos específicos de pacientes, permitiendo un abordaje más especializado para la prevención de enfermedades.

Parte 2

Acerca de la enzima arginina deiminasa de *Giardia lamblia* como interlocutor durante la comunicación hospedero-parásito

Durante nuestros estudios de inmunomodulación por los fructanos y la importancia de los TLRs en este fenómeno, nos preguntamos si un mecanismo similar podría participar también en la inmunomodulación inducida por organismos patógenos tales como *Giardia lamblia*, el cual tiene la capacidad de sortear el ataque del sistema inmune (Axelrad, et al. 2020).

El parásito *Giardia lamblia* es un organismo eucarionte que se encuentra dentro de las primeras causas de diarrea provocada por protistas en el mundo (Lalle, et al. 2018). Los niños, los adultos mayores y las personas inmunocomprometidas son los más afectados por este parátiso. *G. lamblia* infecta el intestino delgado causando giardiasis, la cual en la mayoría de los casos es autolimitante. Sin embargo, las formas crónicas de la enfermedad pueden llevar a una variedad de anormalidades intestinales, que pueden ir desde los cambios microscópicos, a atrofia severa de vellosidades que asemeja al síndrome de malabsorción intestinal o a la enfermedad de intestino irritable, los cuales llevan a la pérdida de peso y a la intolerancia nutrientes tales como la lactosa (Troeger, et. al. 2007, Hemphill, et al. 2019).

Hasta la fecha ya se han descrito varios mecanismos causantes de giardiasis. Por ejemplo, se sabe que *G. lamblia* reside en estrecha proximidad a las células intestinales (Benchimol, et. al. 2011). Sin embargo, los mecanismos finos que expliquen la variabilidad de síntomas clínicos observada y los distintos grados de severidad de la giardiasis, no son del todo comprendidos. Este parásito ha desarrollado múltiples mecanismos para evadir al sistema inmune. Uno de ellos es la variación antigénica, la cual le dificulta al sistema inmune el reconocimiento del parásito (Nash, et al. 2003). Se hipotetiza que *G. lamblia* puede liberar factores de virulencia específicos, tales como la enzima arginina deiminasa (ADI) para perturbar el metabolismo de las células epiteliales del intestino, inhibiendo las reacciones inmunológicas efectoras, tales como la producción de óxido nítrico, el cual a su vez inhibe el crecimiento del parásito en el intestino, y posiblemente también afecta la función de la barrera inestinal (Touz, et al. 2008).

La arginina deiminasa de *G. lamblia* (GlADI) es una enzima que puede jugar un papel importante en la virulencia del parásito. Cataliza la primera reacción de la vía de la arginina dihidrolasa, la cual es utilizada por G. lamblia para la generación de ATP (Rópolo, et al. 2010). Más aún, *G. lamblia* es considerada una proteína con actividad "*moonlighting*" (Jeffery, et. al. 1999), esto debido a que además de su función canónica metabólica, también lleva a cabo otras actividades, tales como su actividad de peptidil-arginina deiminasa, al catalizar la conversión de residuos de arginina a citrulina en algunas proteínas. También se ha observado que GlADI puede ser traslocada desde el citoplasma al núcleo para participar en procesos de regulación génica (Touz, et. al. 2008). Más aún, también se ha descrito el papel inmunogénico de GlADI, pues se observó que puede activar a mastocitos de rata, que incrementa la producción de citocinas proinflamatorias como la IL-6 y el TNF-α (Muñoz Cruz, et al. 2018). También se ha demostrado que GlADI provoca secreción de TNF-α e IL-10 en células dendríticas derivadas de monocitos (Banik, et. al. 2013).

El tratamiento de la giardiasis incluye la administración de fármacos anti-parasitarios tales como el metronidazol y la nitazoxanida. Sin embargo, la aparición de cepas multiresistentes a estos tratamientos de primera línea ya se ha documentado (Leitsch, et. al. 2015). Por lo tanto, la necesidad del desarrollo de nuevos antigiardiásicos aún sigue vigente. Para dicho desarrollo, el reposicionamiento de fármacos se ha aplicado en la búsqueda de terapias antigiardiásicas alternativas (Farha, et. al. 2019), siendo los inhibidores de la bomba de protones como el rabeprazol, uno de los fármacos propuestos (García Torres, et. al. 2016). El rabeprazol ha demostrado tener capacidad de inhibir enzimas de *G. lamblia* que son claves en su metabolismo energético, tales como la enzima glucolítica triosafosfato isomerasa, al mismo tiempo que disminuyen la sobrevida del parásito (García Torres, et. al. 2016, Reyes-Vivas, et. al. 2014, López Velázquez, et. al. 2019).

Considerando las versátiles e importantes funciones de GlADI en la sobrevida de *G. lamblia*, y debido al papel que juega esta enzima en la evasión del sistema inmune del hospedero, en la presente tesis ahondamos el estudio de GlADI como un potencial blanco de los PPIs, así como en su papel inmunomodulador via TLRs. Esto último debido a que a pesar de que ya se sabe del papel imnunomodulador que posee GlADI, el mecanismo por el cual se lleva a cabo dicho efecto es aún desconocido. Esta enzima incluso tiene la capacidad de apoyar la interacción hospedero-parásito (Ringqvist, et. al. 2008) y cambiar esta función para adaptar al parásito al ambiente del hospedero. Este podría ser otro mecanismo de *G. lamblia* por el cual se explique la variabilidad de cuadros clínicos y severidad en pacientes con giardiasis. Algunos de los estudios llevados a cabo en la presente tesis contribuyen al entendimiento de cómo GlADI participa en el balance entre los factores patogénicos, versus los factores protectores del hospedero durante la giardiasis.

Conceptualización y descripción de la tesis

Parte 1

Los fructanos de tipo graminano (GTFs, por sus siglas en inglés) son fibras dietéticas /FDs) ampliamente reconocidas por sus potenciales beneficios a la salud en la prevención o tratamiento de enfermedades no transmisibles, tales como la enfermedad inflamatoria intestinal, la diabetes tipo 2, la obesidad y el cáncer. Estos fructanos también han sido aplicados exitosamente como prebióticos en fórmulas infantiles. Sin embargo, no se sabe si los GTFs poseen capacidad inmunomoduladora y en qué medida, y si este efecto es dependiente del tamaño del fructano y de su estructura. Tampoco se sabe si los GTFs son capaces de proteger la barrera epitelial intestinal de agentes disruptores y de sus efectos de inflamación, ni si este efecto podría ir más allá de la barrera intestinal, alcanzando las células del sistema inmune que residen por debajo e intercaladas entre el epitelio intestinal, tales como las células dendríticas. Los mecanismos que subyacen los beneficios a la salud de los GTFs tampoco son del todo conocidos. Es por ello que en la presente tesis estudiamos cómo los GTFs de direrente tamaño impactan a la imunidad y a la función de la barrera intestinal. Además, también comparamos los efectos de los GTFs con los sabidos efectos de los fructanos de tipo inulina (ITFs, por sus siglas en inglés). El entendimiento de cómo los GTFs contribuyen al mejoramiento de la salud, podría ser de utilidad en el diseño de alimentos que prevengan efectivamente y protejan de la disfunción de la barrera intestinal o de los procesos inflamatorios en el intestino. Más aún, disectar si los efectos de los GTFs son dependientes de su estructura o de la longitud de su cadena, podría ayudar en el diseño de opiones terapéuticas individualizadas.

En el **Capítulo 3**, estudiamos la interacción de dos GTFs con diferente peso molecular con los receptores tipo Toll (TLRs por sus siglas en inglés). Se determinó si la interacción inducía activación o inhibición de los TLRs. Para ello, células de tipo monocitos que expresan todos los TLRs fueron expuestas a concentraciones crecientes de los dos GTFs. Depués, aplicamos inhibidores de las vías MyD88 y TRIF que llevan a la activación de NF-κB/AP-1 para determinar mediante cuál vía los GTFs interactúan con los TLRs. Posteriormente, estudiamos la interacción de los GTFs con cada uno de los TLRs adicionándolos a lineas de células HEK que expresan cada uno de los TLRs de manera independiente. Luego aplicamos docking molecular para identificar si el tamaño y la estructura ramificada de los GTFs tiene influencia en su interacción específica con los TLRs y si estos fructanos establecen interacciones con residuos aminoaciles de los TLRs que son clave para la unión con sus ligandos naturales o para la formación de sus unidades funcionales, por ejemplo la dimerización. Finalmente, estudiamos el impacto que tienen los GTfs en las respuestas de las DCs. Determinamos el perfil de citocinas de las células dendríticas (DCs) las cuales fueron estimuladas con los GTFs. Para comparar entre las estructuras lineales y ramificadas de los fructanos, todos estos efectos de los GTFs se compararon con los de ITFs de cadena similar.

En el **Capítulo 4**, estudiamos el efecto protector de los GTFs de cadenas corta y larga en la función de la barrera intestinal, misma que fue irrumpida por tres moléculas que la impactan mediante diferentes vías de señalización celular. Para ello, monocapas de la línea intestinal celular T84 fueron preincubadas en presencia de los GTFs. Posteriormente, el ionóforo de calcio A23187, el acetato de forbol-13 miristato (PMA, por sus siglas en inglés), y la toxina fúngica deoxinivalenol (DON), moléculas que dañan la barrera epitelial intestinal, fueron adicionadas a las células. Estos estresores incrementan el calcio intracelular o activan las vías de la proteína

cinasa tipo C (PKC, por sus siglas en inglés) o la cinasa activada por mitógeno (MAPK, por su siglas en inglés). La resistencia transepitelial (TEER, por su siglas en inglés) de las células T84 preincubadas con los GTFs se midió mediente el sistema de sensado de la impedancia célula-sustrato y se comparó con la TEER de células que fueron expuestas únicamente a los disruptores. También estudiamos si los GTFs son capaces de prevenir la producción de la citocina proinflamatoria 8 (IL-8) por las cálulas epiteliales intestinales. La concentración de IL-8 se determinó mediante un ensayo de ELISA a partir de los sobrenadantes de los cultivos de las células T84. Nuevamente, para comparar entre los efectos de fructanos ramificados versus fructanos lineales, todos estos efectos de los GTFs fueron comparados con los de ITFs de longitud de cadena similar.

No se sabe si los GTFs pueden proteger contra la desregulación de las proteínas de las uniones estrechas inducida por los bien conocidos disruptores A23187 y DON, ni si estos efectos son similares a los de los ITFs. Por ello, en el **Capítulo 5** estudiamos los efectos de los GTFs de diferentes tamaños en la expresión de los genes que codifican para proteínas uniones estrechas en células intestinales Caco-2, bajo condiciones fisiológicas e inflamatorias, y los comparamos con los efectos de los ITFs. Luego, determinamos si los GTFs pueden prevenir la inflamación provocada por los agentes disruptores. Para ello, medimos la citocina proinflamatoria IL-8 producida por las células Caco-2. También determinamos si estos efectos se extienden a a las células del sistema inmune que residen por debajo e intercaladas en la barrera epitelial intestinal. Para ello, se expuso a DCs a los GTFs y a los ITFs y se determinó el perfil de citocinas mediante la tecnología Luminex. Después, para investigar si las células epiteliales, cuando son puestas en contacto con los GTFs producen alguna señal que mejore o potencíe las respuestas de las DCs, expusimos a las DCs al medio de cultivo utilizado por las células Caco-2, seguido de la determinación del perfil de citocinas.

Intercaladas entre los enterocitos y otros componnentes del epitelio intestinal, se encuentran las células caliciformes o goblets (GCs, por su terminología en inglés). Estas GCs son células especializadas en la síntesis de mucosa. Aún no se sabe si los GTFs pueden influir la expresión de genes que codifican para proteínas relacionadas a la mucosa o al estrés del retículo endoplásmico, y en qué medida. En el **Capítulo 6** en GCs, determinamos la expresión de los genes *MUC2*, *TFF3*, *GAL3ST2*, y *CHST5,* los cuales codifican para proteínas de la mucosa intestinal. También estudiamos los genes *HSPA5* y *XBP1*, los cuales están relacionados al estrés del retículo endoplásmico. Para determinar si los GTFs poseen un efecto protector de una inflamación inducida, o de la disrupción de la barrera de mucosa y del estrés del retículo endoplásmico (RE), las GCs fueron expuestas a la citocina proinflamatoria TNFα o al inhibidor de la glicosilación tunicamicina (Tm). Como marcador de inflamación cuantificamos la concentración de IL-8 a partir de los sobrenadantes celulares. En otros experimentos, todos estos estudios fueron replicados en presencia de dos ITFs de diferente longitud de cadena para comparar si había un efecto dependiente del tipo de fructano en nuestros hallazgos.

Parte 2

Inspirados por el papel esencial de los TLRs en la inmunomodulación inducida por fructanos, en la segunda parte de esta tesis, estudiamos la importancia de los TLRs y el parásito intestinal *Giardia lamblia*. La infección por *G. lamblia* es la tercer causa más común de diarrea a nivel mundial, con cerca de 300 millones de casos anuales reportados. En el **Capítulo 2 (artículo requisito)** nos propusimos estudiar las potenciales interacciones de la enzima arginina deiminasa de *G. lamblia* (GlADI), un factor de virulencia de *Giardia* con los

TLRs, así como las respuestas de células dendríticas similares a las de infantes después de ser expuestas a esta enzima. Para ello, estandarizamos la sobreexpresión y purificación de GlADI en un sistema bacteriano, y expusimos células monocíticas que expresan todos los TLRs a concentraciones crecientes de GlADI. Después, para determinar cuáles TLRs están involucrados en la activación, aplicamos concentraciones crecientes de GlADI a líneas celulares HEK que expresan cada uno de los TLRs de manera independiente. Debido a el fármaco de reposicionamiento rabeprazol ha demostrado capacidad antigiardiásica, también nos preguntamos y estudiamos si este fármaco puede influir en la capacidad inmunomoduladora de GlADI y en qué medida, así como en la respuesta de las células dendríticas inducida por GlADI.

En el **Capítulo 7** estudiamos a GlADI como blanco contra la giardiasis. Para ello, primero realizamos estudios de docking molecular con los compuestos reactivos a grupos tiol, el s-metil metanotiosulfonato (MMTS), el ácido di-tio-bis-nitrobenzóico (DTNB), así como los fármacos reactivos a tioles aprobados para su uso comercial en humanos, el rabeprazol, la sulbutiamina y el aurotiomalato. Este docking molecular se realizó para predecir el modo de unión de estas moléculas a la estructura tridimensional de GlADI. Posteriormente, utilizamos la GlADI recombinante en ensayos de inhibición de la actividad enzimática con las moléculas anteriormente mencionadas, también realizamos estudios espectroscópicos para seguir la alteración estructural inducida por estas moléculas y para identificar fármacos potencialmente efectivos. También estudiamos si los cuatro fármacos antes mencionados son capaces de inhibir la actividad celular de GlADI y de ejercer un efecto citotóxico en ambos estadios de vida de *Giardia*, el trofozoito y el quiste. Para ello, la actividad de GlADI se determinó a partir de lisados de trofozoitos que fueron preincubados con los cuatro fármacos. Se determinó la capacidad de enquistamiento en estos trofozoitos que fueron incubados con los fármacos. Finalmente, los resultados obtenidos en esta tesis serán discutidos en el **Capítulo 8**.

Capítulo 1

ARTÍCULO REQUISITO

Multilevel approach for the treatment of giardiasis by targeting arginine deiminase

Cynthia Fernández-Lainez [a,b,c], Ignacio de la Mora-de la Mora [d], Itzhel García-Torres [d], Sergio Enríquez-Flores [d], Luis A. Flores-López [d,e], Pedro Gutiérrez-Castrellón [f], Lilian Yépez-Mulia [g], Felix Matadamas-Martínez [g], Paul de Vos [b], Gabriel López-Velázquez [d,*]

[a] Laboratorio de Errores Innatos del Metabolismo y Tamiz, Instituto Nacional de Pediatria, Ciudad de México 04530, Mexico.

[b] Immunoendocrinology, Division of Medical Biology, Department of Pathology and Medical Biology, University of Groningen and University Medical Center Groningen, 9700 Groningen, The Netherlands.

[c] Posgrado en Ciencias Biológicas, Universidad Nacional Autónoma de México, Ciudad de México 04510, Mexico.

[d] Laboratorio de Biomoleculas y Salud Infantil, Instituto Nacional de Pediatria, Ciudad de México 04530, Mexico.

[e] CONACYT-Instituto Nacional de Pediatria, Secretaria de Salud, Ciudad de México 04530, Mexico.

[f] Hospital General Dr. Manuel Gea González, Ciudad de México 14080, Mexico.

[g] Unidad de Investigación Médica en Enfermedades Infecciosas y Parasitarias, UMAE Hospital de Pediatría, Centro Médico Siglo XXI, Instituto Mexicano del Seguro Social, Ciudad de Mexico 06720, Mexico.

Artículo requisito. Publicado en International Journal of Molecular Sciences 2021, 22, 9491. https://doi.org/10.3390/ijms22179491

International Journal of
Molecular Sciences

MDPI

Article

Multilevel Approach for the Treatment of Giardiasis by Targeting Arginine Deiminase

Cynthia Fernández-Lainez [1,2,3], Ignacio de la Mora-de la Mora [4], Itzhel García-Torres [4], Sergio Enríquez-Flores [4], Luis A. Flores-López [4,5], Pedro Gutiérrez-Castrellón [6], Lilian Yépez-Mulia [7], Felix Matadamas-Martínez [7], Paul de Vos [2] and Gabriel López-Velázquez [4,*]

1 Laboratorio de Errores Innatos del Metabolismo y Tamiz, Instituto Nacional de Pediatría, Ciudad de Mexico 04530, Mexico; lainezcynthia@hotmail.com
2 Immunoendocrinology, Division of Medical Biology, Department of Pathology and Medical Biology, University of Groningen and University Medical Centre Groningen, Hanzeplein 1, 9700 RB Groningen, The Netherlands; p.de.vos@umcg.nl
3 Posgrado en Ciencias Biológicas, Universidad Nacional Autónoma de México, Ciudad de Mexico 04510, Mexico
4 Laboratorio de Biomoléculas y Salud Infantil, Instituto Nacional de Pediatría, Ciudad de Mexico 04530, Mexico; ignaciodelamora@yahoo.com.mx (I.d.l.M.-d.l.M.); itzheltorres@hotmail.com (I.G.-T.); sergioenriquez@ciencias.unam.mx (S.E.-F.); luisbiolexp@gmail.com (L.A.F.-L.)
5 CONACYT-Instituto Nacional de Pediatría, Secretaría de Salud, Ciudad de Mexico 04530, Mexico
6 Hospital General Dr. Manuel Gea González, Ciudad de Mexico 14080, Mexico; inpcochrane@gmail.com
7 Unidad de Investigación Médica en Enfermedades Infecciosas y Parasitarias, UMAE Hospital de Pediatría, Centro Médico Siglo XXI, Instituto Mexicano del Seguro Social, Ciudad de Mexico 06720, Mexico; lilianyepez@yahoo.com (L.Y.-M.); felixmatadamas@yahoo.com.mx (F.M.-M.)
* Correspondence: glv_1999@ciencias.unam.mx; Tel.: +52-5510840900 (ext. 1726)

Abstract: Giardiasis represents a latent problem in public health due to the exceptionally pathogenic strategies of the parasite *Giardia lamblia* for evading the human immune system. Strains resistant to first-line drugs are also a challenge. Therefore, new antigiardial therapies are urgently needed. Here, we tested giardial arginine deiminase (GlADI) as a target against giardiasis. GlADI belongs to an essential pathway in *Giardia* for the synthesis of ATP, which is absent in humans. In silico docking with six thiol-reactive compounds was performed; four of which are approved drugs for humans. Recombinant GlADI was used in enzyme inhibition assays, and computational in silico predictions and spectroscopic studies were applied to follow the enzyme's structural disturbance and identify possible effective drugs. Inhibition by modification of cysteines was corroborated using Ellman's method. The efficacy of these drugs on parasite viability was assayed on *Giardia* trophozoites, along with the inhibition of the endogenous GlADI. The most potent drug against GlADI was assayed on *Giardia* encystment. The tested drugs inhibited the recombinant GlADI by modifying its cysteines and, potentially, by altering its 3D structure. Only rabeprazole and omeprazole decreased trophozoite survival by inhibiting endogenous GlADI, while rabeprazole also decreased the *Giardia* encystment rate. These findings demonstrate the potential of GlADI as a target against giardiasis.

Keywords: *Giardia*; drug repurposing; proton pump inhibitor; sulbutiamine; aurothiomalate; omeprazole; rabeprazole

Citation: Fernández-Lainez, C.; de la Mora-de la Mora, I.; García-Torres, I.; Enríquez-Flores, S.; Flores-López, L.A.; Gutiérrez-Castrellón, P.; Yépez-Mulia, L.; Matadamas-Martínez, F.; de Vos, P.; López-Velázquez, G. Multilevel Approach for the Treatment of Giardiasis by Targeting Arginine Deiminase. *Int. J. Mol. Sci.* **2021**, *22*, 9491. https://doi.org/10.3390/ijms22179491

Academic Editor: Mohammad Hassan Baig

Received: 8 July 2021
Accepted: 20 August 2021
Published: 31 August 2021

1. Introduction

Current drug discovery techniques against parasites aim at the identification of essential pathogenic targets, which, after inhibiting their functionality, could be lethal for the pathogenic organisms. In addition, anti-virulence therapy is based on disarming the pathogens and preventing them from causing disease. The latter is increasing because virulence factors enhance the ability of pathogens to colonize and resist the immunity

of their hosts. Hence, therapeutic strategies directed at the molecules that participate at different levels in the life cycle of pathogens might be helpful in the treatment of the illness, but also in repressing the dissemination of the disease. Such a strategy might also be helpful in the fight against giardiasis.

Human giardiasis is an inflammation-driven diarrhea caused by the protist, *Giardia lamblia* [1], which has developed a broad range of mechanisms to escape the host immune system [2]. *Giardia* should not fall on deaf ears; it is a eukaryote more ancient than humans and is still epidemic, despite the tremendous advances in healthcare. *Giardia* is a microaerophilic organism that lacks the tricarboxylic acid cycle and oxidative phosphorylation, but has acquired enzymes of likely lateral gene transfer origin that support fermentative glycolysis [3], the arginine dihydrolase pathway [4,5], and substrate-level ATP generation [6–8].

Drug repurposing for the treatment of giardiasis based on cysteine-modification mechanisms directed at glycolysis has previously been proposed [9–11]. Since cysteines are highly reactive amino acids and are widely distributed in the proteome of *Giardia* [12], strategies based on the use of thiol-reactive drugs could target several important proteins of this disease that are still neglected. In this line, the short-term use of proton pump inhibitors (PPIs) is well tolerated, with few side effects [13]. Moreover, commercially available PPIs are active in vitro against *Giardia* trophozoites in the range of albendazole [14] and also retain their activity for metronidazole and nitazoxanide-resistant strains [11]. Such a landscape appears propitious for designing effective therapies based on thiol-reactive drugs against *Giardia* and for widening the spectrum of repurposable drugs for giardiasis.

In recent years, new drug targets have been studied in the search for efficient compounds against protozoa [9,15–17]. Based on this, we studied the giardial arginine deiminase (GlADI) as a crucial biomolecule essential for *Giardia* survival and involved in disease progression. To better support GlADI as a druggable target in *Giardia*, we studied its reactivity to s-methyl methanethiosulfonate (MMTS) and dithio-bis-nitrobenzoic acid (DTNB), to demonstrate the capacity of thiol-reactive compounds to inactivate this enzyme. Afterward, we assayed the commercially approved drugs omeprazole, rabeprazole, sulbutiamine, and aurothiomalate as repurposed drugs for giardiasis (Figure S1). Furthermore, we established the potential of these drugs for use as antigiardiasics by assaying them from a molecular perspective, using in silico studies, as well as biochemical and cellular studies. We found that rabeprazole is the most promising drug for repurposing against giardiasis, since it inactivates the enzyme activity of GlADI, disturbs its structure, provokes *Giardia* trophozoites death, and diminishes encystation.

2. Results

2.1. Cysteine Modification Underlies GlADI Inactivation

Since the complete 3D structure of GlADI is still unknown, homology modeling was used to identify potential inhibitors by docking [18]. We used the crystallographic structure of the arginine deiminase from *Mycoplasma arginini* as a template to model the GlADI 3D structure. This led to a number of observations. First, it revealed the abundance and distribution of the Cys residues in the three-dimensional arrangement of the homodimer, and second, it allowed us to identify the preferential binding sites of the highly Cys-reactive compounds MMTS and DTNB on the protein surface. After in silico approximations, the effect on the enzyme activity of MMTS and DTNB was determined in vitro, and finally, the free cysteine content was determined using Ellman's method to establish the underlying mechanism of inactivation by modification of cysteines.

GlADI has the longest known C-terminal domain among the described arginine deiminases. Through the dimer, 26 of the 32 Cys residues can be observed (Figure 1A and Figure S2). Of all modeled Cys residues, 13 show more than a 10% accessible surface area (ASA) (Table 1). The model was helpful in showing the distribution of the catalytic triad [19], which includes Cys 424, Glu 226, and His 280 amino acid residues (Figure 1B). The blind docking performed on the entire surface of the homodimer identified potential

binding sites for MMTS and DTNB. Representative binding sites for each compound are shown in Figure 1C,D. After the in silico approximations, the effect of MMTS and DTNB on the GlADI enzyme activity was assayed in vitro. The interaction between these compounds and GlADI caused inactivation of the enzyme in a dose-dependent manner (Figure 1E,F).

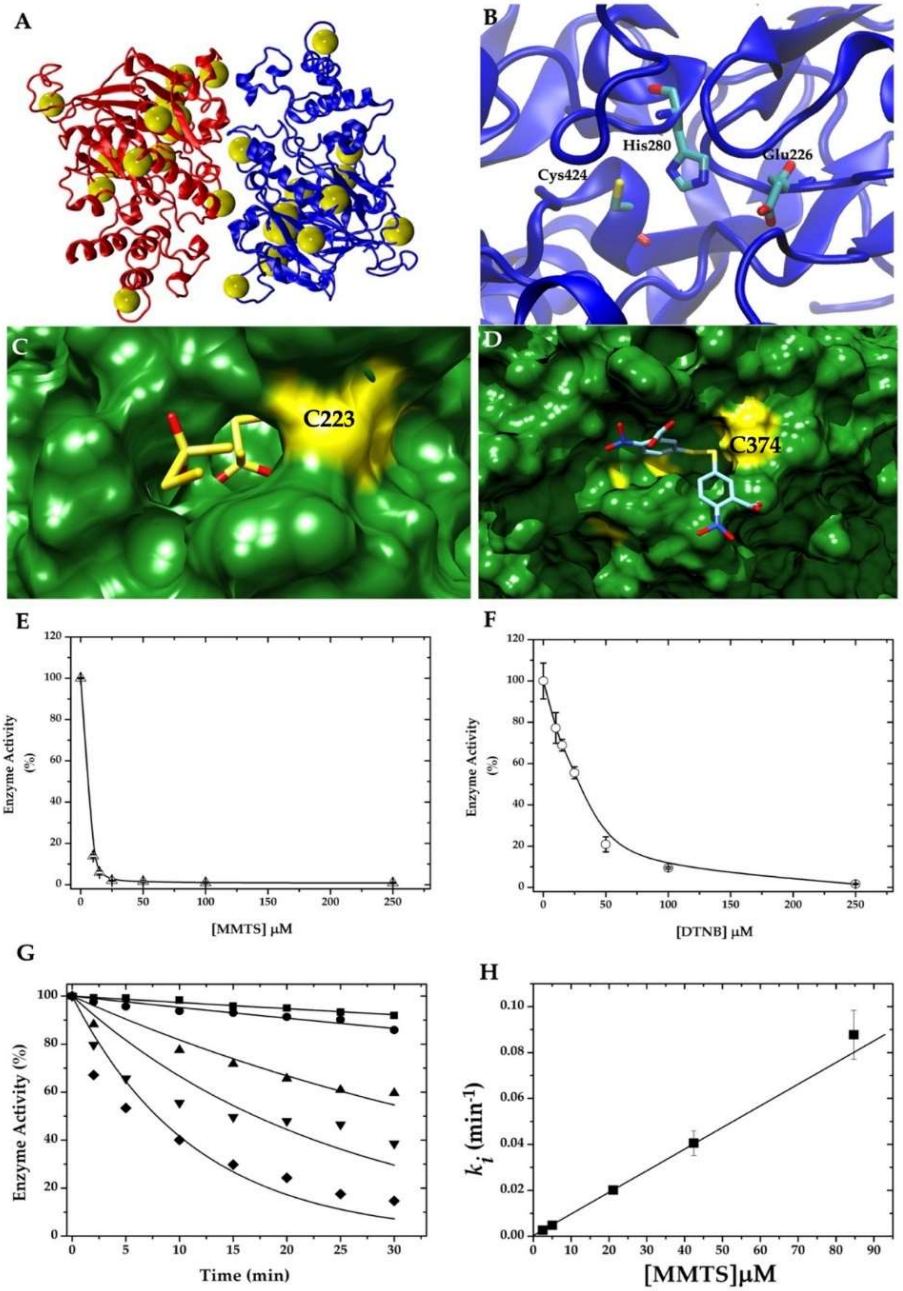

Figure 1. Arginine deiminase from *Giardia* as a potential target for cysteine reactive compounds. (**A**) Homology model showing the high content and distribution of cysteine residues (yellow spheres). (**B**) active site showing the catalytic triad. (**C**) representative docking with MMTS, and (**D**) with DTNB. Cysteine residues interacting with both molecules are indicated in bold type. Residual enzyme activity of recombinant GlADI after incubation with increasing concentrations of (**E**) MMTS or (**F**) DTNB. (**G**) Kinetics of GlADI inhibition by using 2. 5 (■), 5 (●), 20 (▲), 45 (▼), and 85 μM (◆) of MMTS. Inactivation rate constants at different MMTS concentrations were fitted to a linear equation model, where the slope represents the second−order inactivation rate constant (**H**).

Table 1. Cys residues with more than 10% ASA.

Cys Position	ASA (%)	Chain
329	71.3/46.5	A/B
396	66.2/31.4	A/B
300	63.3/58.1	A/B
374	24.1/28.0	A/B
271	25.1	A
223	21.1	B
118	16.4/15.8	A/B
216	15.4	B
52	13.7	A

Since MMTS resulted in the most efficient inhibition of GlADI (Figure 1E), we calculated its pseudo-first-order inactivation rate constant. The results show that the kinetics of inhibition using different concentrations of MMTS decays following a mono-exponential function (Figure 1G). Notwithstanding, the parameters used to adjust each data series were the same; those from 42 μM MMTS (▼) showed the lowest R^2 value (0.74, whereas the rest of the concentrations showed R^2 values above 0.9). This yielded an increased error for this *ki* value, but it did not prevent the linear fitting to calculate the second-order rate constant (k_2). The data of the slopes fitted onto a straight-line (Figure 1H) with a k_2 value of 15.68 ± 0.9 M^{-1} s^{-1}.

Concerning the underlying mechanism, the observed change of free cysteines before and after the treatments supports the inactivation being caused by a Cys-modification process (Table 2).

Table 2. Number of modified Cys residues per monomer.

Giardial Arginine Deiminase (GlADI)	Number of Modified Cys/Monomer
+DTNB (250 μM)	6 ± 0.1
+MMTS (250 μM)	6 ± 0.3
+Omeprazole (750 μM)	2 ± 0.9
+Rabeprazole (750 μM)	5 ± 0.3
+Sulbutiamine (750 μM)	2 ± 0.9
+Aurothiomalate (750 μM)	5 ± 0.5

Untreated GlADI shows 9 ± 0.9 free Cys/monomers. GlADI treated with 1mM TCEP shows 16 ± 0.5 free Cys/monomers.

2.2. GlADI Is Inactivated by Thiol-Reactive Drugs Not Previously Applied for Giardiasis

Based on the in vitro susceptibility of GlADI to being inactivated through a cysteine modification process, we studied four different thiol-reactive drugs: omeprazole, rabeprazole, sulbutiamine, and aurothiomalate, which are known to be safely used in humans but not for giardicidal purposes. As expected, the docking performed on the surface of the enzyme showed several possible binding sites near cysteine residues for all the studied drugs (representative binding sites for each drug are shown in Figure 2A–D). Moreover, an overall view of the GlADI monomer A shows the putative binding sites of the studied molecules on the general topography of the protein (Figure 3).

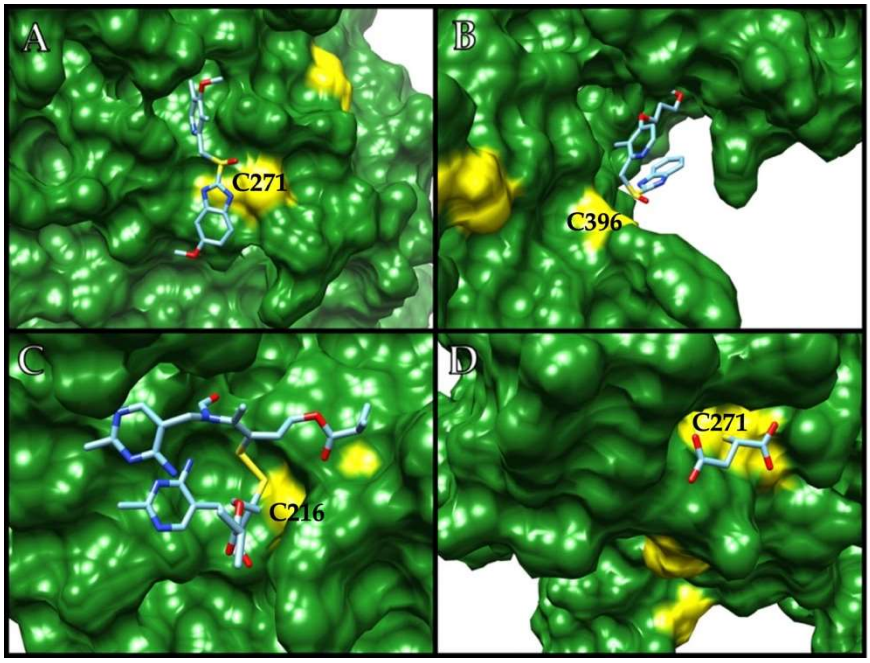

Figure 2. Representative docking of GlADI with (**A**) omeprazole, (**B**) rabeprazole, (**C**) sulbutiamine, and (**D**) aurothiomalate. Cysteine residues near the binding sites are yellow-colored. Cysteine residues interacting with each of the molecules are indicated in bold type.

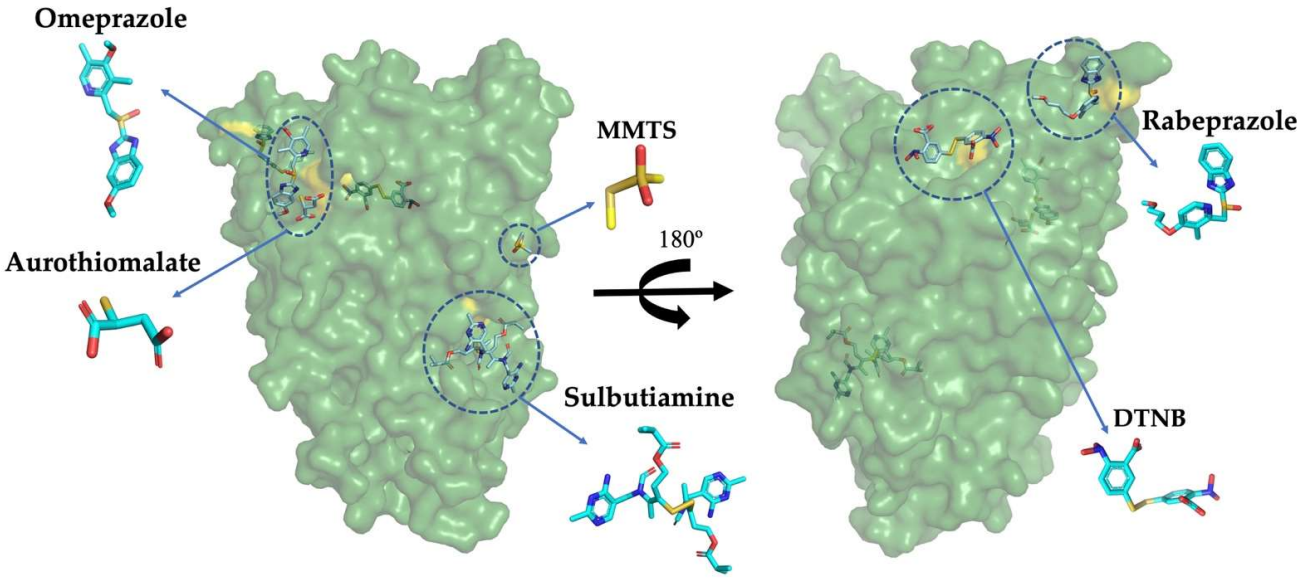

Figure 3. Two views of the GlADI monomer A rotated 180°, showing the global distribution of all the studied molecules in their putatively best ranked binding sites. To make the visualization easier, the structure is displayed with 50% transparency.

In agreement with the in silico prediction, all of these drugs were able to inhibit recombinant GlADI in vitro in a dose-dependent manner (Figure 4A–D). However, the number of modified cysteines on GlADI was different for each compound (Table 2). To further support Cys-modification as the underlying mechanism for GlADI inactivation, albendazole was assayed as a giardicidal but non-thiol-reactive drug. As expected, albendazole did not produce any inactivation of GlADI (Figure 4E).

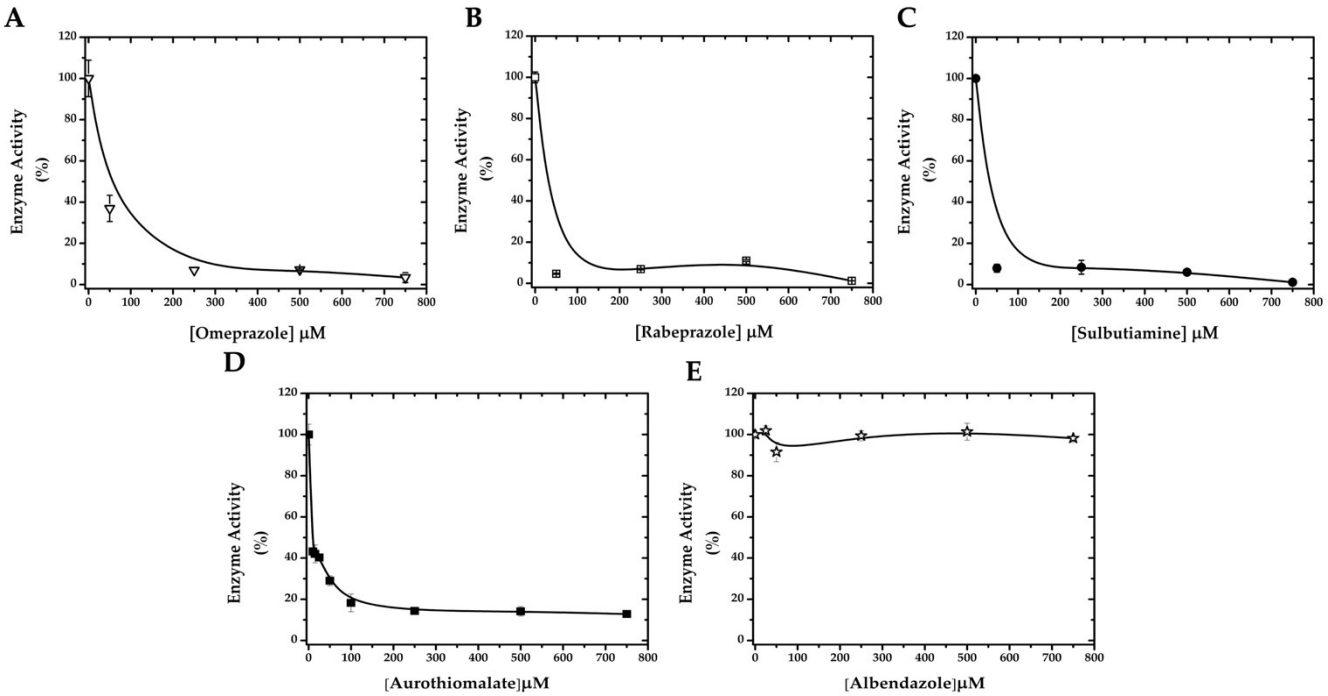

Figure 4. Effect of repurposing drugs approved for use in humans on the enzyme activity of GlADI. The enzyme was incubated with increasing concentrations of omeprazole (**A**), rabeprazole (**B**), sulbutiamine (**C**), aurothiomalate (**D**), and albendazole (**E**).

Since rabeprazole showed an efficient inhibition of the enzyme activity on recombinant GlADI (Figure 4B), we calculated the pseudo-first-order inactivation rate constant for this drug (Figure 5A,B). The results show that the kinetics of inhibition using different concentrations of rabeprazole decay following a mono-exponential function (Figure 5A). This data fitted onto a straight-line with a second-order rate constant (k_2) value of 6.72 $\pm$ 0.2 M^{-1} s^{-1} (Figure 5B).

To quantify the potential conformational changes of GlADI 3D structure by rabeprazole, fluorescence spectroscopy at 295 nm excitation wavelength was performed to monitor tryptophan residues. The intensity of intrinsic fluorescence decreased as a result of rabeprazole concentration (Figure 5C).

2.3. Targetable Cysteines in GlADI Are Possibly Limited by the Presence of Disulfide Bridges in the Native Structure

The amino acid sequence of GlADI revealed the presence of 16 Cys residues per monomer. This number of Cys residues was corroborated and deduced by sequencing the gene coding the recombinant enzyme we had previously studied (data not shown). Nonetheless, the maximum number of Cys residues accessible for the Ellman's reagent was six per monomer in the native enzyme and nine after denaturation. Conversely, when breaking all the disulfide bonds under reducing conditions, Ellman's reagent was able to detect the 16 Cys-residues per monomer after denaturing (Table 2).

2.4. Drug Susceptibility of Giardia Trophozoites Discloses the Efficacy of the Proposed Drugs

Relying on druggability prediction can generate ambiguous expectations, and final effects need to be determined on a cellular level. Therefore, we also determined *Giardia* trophozoites inhibition by the four drugs we found promising in our in silico and in vitro predictions. This revealed that only the PPIs showed a dose-dependent giardicidal effect on trophozoites by inactivation of the endogenous cellular GlADI (Figure 6).

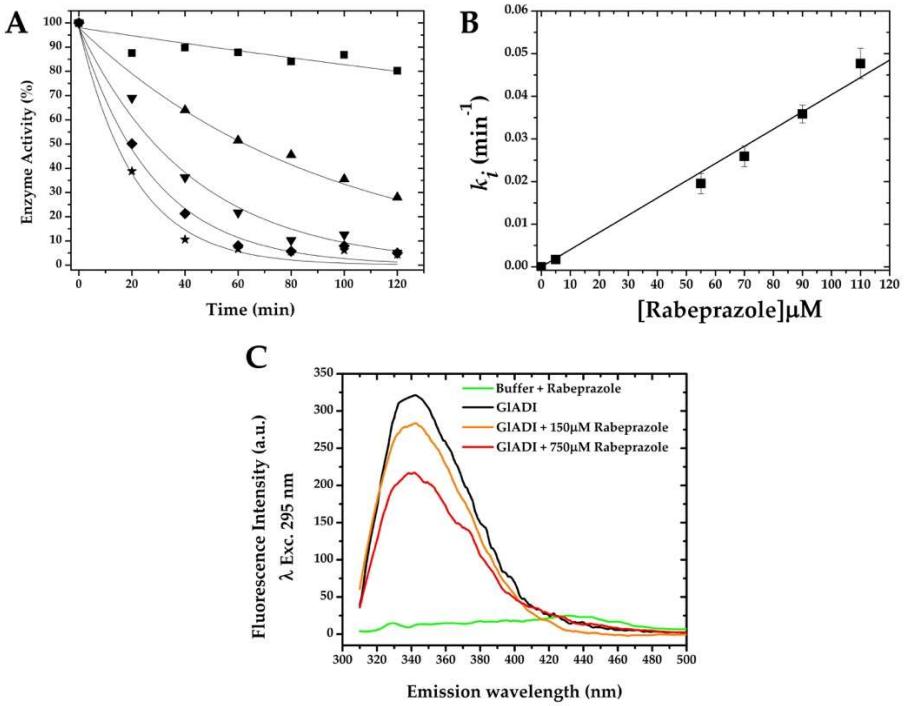

Figure 5. Effect of rabeprazole on the inactivation and intrinsic fluorescence of GlADI. (**A**) GlADI was incubated with 5 (■), 55 (▲), 70 (▼), 90 (◆), and 110 μM (★) of rabeprazole at 25 °C. (**B**) Inactivation rate constants at each concentration were plotted and fitted to a linear equation model, where the slope represents the second-order inactivation rate constant. (**C**) Measure of the fluorescence intensity of GlADI in the presence and absence of rabeprazole.

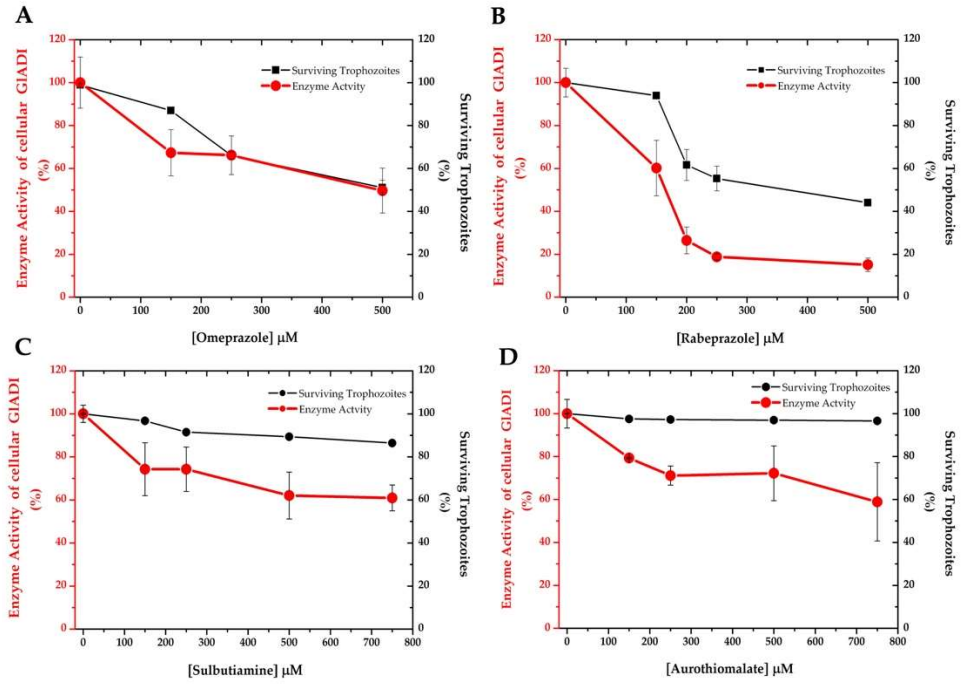

Figure 6. Effect of repurposing drugs on *Giardia* trophozoite survival and on the enzyme activity of endogenous GlADI. Omeprazole and rabeprazole exerted a concomitant effect on these parameters (**A**,**B**), whereas sulbutiamine and aurothiomalate did not (**C**,**D**).

2.5. Rabeprazole Impairs Giardia Encystment

Cyst formation is a requirement for surviving environmental stresses during the transmission of *Giardia*. This infective form of the parasite represents a target for blocking

its dissemination [20]. The findings shown herein prompted us to investigate the effect of rabeprazole on the encystment process of *Giardia*. As shown above, rabeprazole decreases trophozoite viability (Figure 6B). We found that it also significantly affects encystation (p = 0.001) (Figure 7). Contrary to what was previously proposed as the role of GlADI in the control of the encystation process [21], we found a significant decrease of cyst production between rabeprazole treated and untreated trophozoites (Figure 7). Moreover, the trophozoites that survived the treatment with rabeprazole were 97% less efficient at encysting than those not treated.

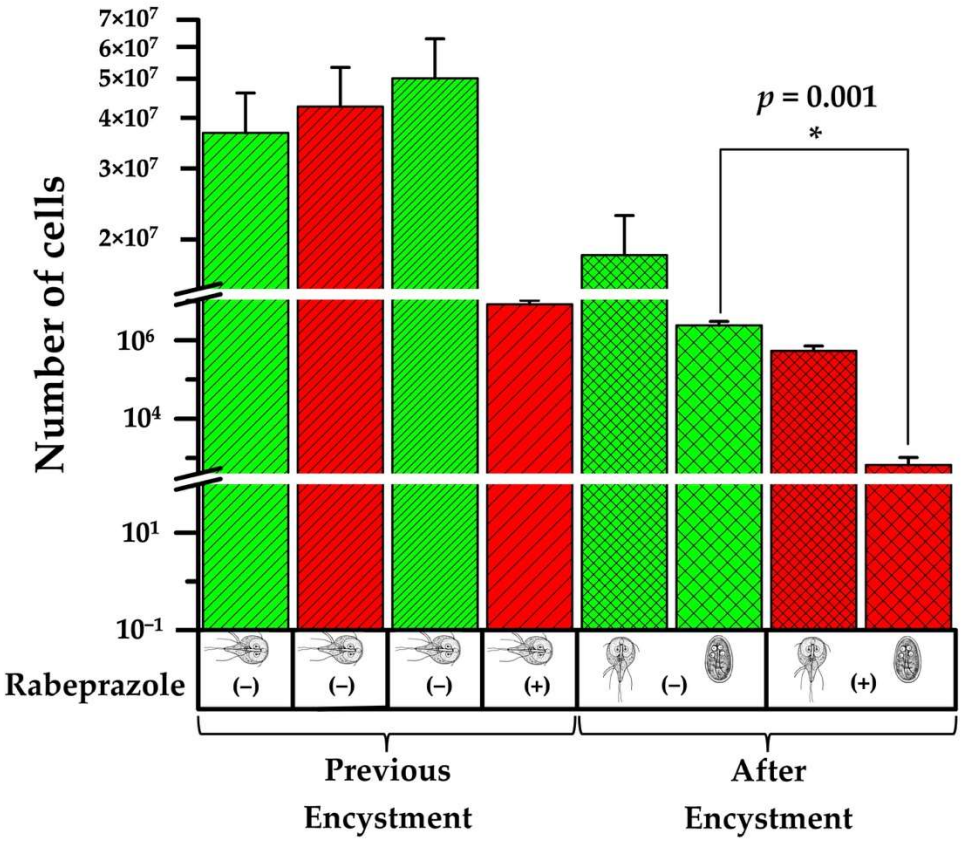

Figure 7. Impairment of *Giardia* encystment by rabeprazole. Green columns represent the control group (without rabeprazole), and the red columns represent the experimental group (exposed to rabeprazole). From left to right, the first two columns represent the number of cells grown to confluence at the beginning of the experiment in TYI−S−33 culture medium. The next two columns represent the number of cells grown in pre-encystment culture medium. The last four columns represent the number of cells grown in encystment culture medium. These results are the medium ± SD of three assays, with three technical replicates.

3. Discussion

The screening for new giardicidal drugs is undoubtedly a priority, since drug resistance and treatment failures are increasing [22]. As GlADI is absent in the human host, this enzyme is an attractive target for drug design against giardiasis [23]. Computational studies have enhanced the ability to pose reasonable and testable hypotheses for drug repositioning purposes. Therefore, druggability predictions have become part of the validation of a therapeutic target, to avoid intractable targets [24]. Nonetheless, the critical nature of these approaches is evident in cases where data gathered from in silico predictions do not ensure their efficiency in subsequent in vitro studies.

Based on computational docking, benzimidazole derivatives apart from PPIs have been proposed as potential inhibitors of GlADI [18]. Since the primary structure of GlADI is enriched with cysteine residues, we performed computational approaches to find poten-

tial inhibitors with an underlying cysteine-modification mechanism of action. With this approach, we found several thiol-reactive compounds (including some repurposing drugs) with promising binding regions on GlADI. Furthermore, all the thiol-reactive compounds studied in silico demonstrated high efficacy for inhibiting recombinant GlADI when they were assayed in vitro.

The number of modified cysteines in GlADI was variable according to the thiol-reactive compound assayed. This is possibly related to the accessibility of each cysteine residue, but it also might be because more than one Cys can contribute to the inactivation of the enzyme. It is noteworthy that the number of accessible cysteines in denatured conditions indicated the presence of at least three disulfides. Such a condition had already been reported for other giardial proteins (i.e., variable surface proteins, triosephosphate isomerase) [25,26], with structural and functional implications in some cases [27]. This should be further studied to better understand the biological meaning of these disulfides.

The calculated second-order inactivation constants (k_2) were in the range of others previously determined for different giardial enzymes [9]. Indeed, the value of the k_2 obtained for rabeprazole (Figure 5A,B) was 2.5-fold higher than that of rabeprazole, inhibiting the giardial triosephosphate isomerase [9], which means this drug possesses a higher efficiency for inhibiting GlADI than inhibiting triosephosphate isomerase. This would indicate that GlADI is a target more easily reached by rabeprazole than other targets previously proposed for this drug, such as triosephosphate isomerase. Therefore, since GlADI belongs to the arginine dihydrolase pathway, this route would be impaired in a more immediate manner than glycolysis.

It is known that thiol-reactive drugs do not reach all Cys present in a protein and, even if a Cys is modified, it does not always exert a deleterious effect on the protein [11]. Nonetheless, we were able to register functional and structural disturbances on GlADI after exposing it to the assayed thiol-reactive drugs and compounds. The fluorescence emission spectra of GlADI showed both a decrease of 67% in quantum yield at an excitation wavelength of 295 nm and a blue shift of 6 nm when exposed to rabeprazole. This fluorescence decrease could implicate potential conformational changes in the protein structure, which would expose tryptophan residues to the milieu [28,29], probably weakening the stability of the GlADI structure. On the other hand, the blue shift is suggestive of a compaction effect on its 3D structure that could be impair the interactions of GlADI with other molecular elements; either with those of the microorganism itself or those of the host.

Drug repurposing, defined as finding new indications for existing drugs [30], is of particular interest for coping with giardiasis. Compared with developing drugs de novo, which is of very high cost (10 to 17 years and 800 million USD), drug repurposing significantly reduces both the time and money needed. However, repurposable drugs also have to succeed at a cellular level. In line with this, we found that of the four computationally identified drugs, only omeprazole and rabeprazole were able to efficiently inhibit cellular GlADI and exert a cytotoxic effect on trophozoites. Despite having succeeded in inhibiting GlADI in vitro, sulbutiamine and aurothiomalate were less effective against the cellular enzyme. They did not cause more than 40% inhibition of cellular GlADI activity, and they only slightly impacted the viability of trophozoites.

Sulbutiamine is a molecule consisting of two thiamin (B1vitamin) molecules bound together by a disulfide and is a lipophilic drug that is useful in alleviating fatigue [31]. Sulbutiamine specifically inactivates a glycolytic enzyme of *Encephalitozoon intestinalis* through interaction with cysteine residues [32], but it has not been tested in vitro against the parasites. Aurothiomalate exhibits anti-inflammatory properties, mediated through its reactivity with protein sulfhydryl groups [33]. Despite inhibiting recombinant GlADI, sulbutiamine and aurothiomalate were unable to inhibit cellular GlADI and effectively induce trophozoite death. These drugs are possibly inefficient for crossing the cell membrane of the trophozoites, or they could decrease the giardicidal activity by interacting with other molecules before reaching GlADI. This highlights the importance of corroborating the tests done with molecular targets in their cellular context.

In light of these findings, we focused on the capacity of GlADI as a druggable target for giardiasis using rabeprazole as an efficient repurposable drug. Our results show that encystment is impaired when a GlADI inhibitor such as rabeprazole is used. This could be due to the fact that *Giardia* uses ammonia from arginine metabolism to drive the synthesis of glucosamine-6-phosphate for cyst wall polysaccharide biosynthesis [34]. Moreover, the trophozoites treated with rabeprazole lack an essential source of ammonia, which might impair their capacity to produce the cyst wall. The use of rabeprazole might therefore help to ameliorate the dissemination of giardiasis by altering the cyst production. To the best of our knowledge, this is the first study where rabeprazole demonstrated its ability to target the encystment process of *Giardia*.

4. Materials and Methods

4.1. Reagents and Drugs

All reagents were purchased from Sigma–Aldrich (St. Louis, MO, USA) unless otherwise specified. Isopropyl-β-D-thiogalactopyranoside (IPTG) was from AMRESCO LLC (Cochran Road Solon, OH, USA); reduced nicotinamide adenine dinucleotide (NADH) was purchased from Roche (Penzberg, Upper Bavaria, Germany); Immobilized Metal Affinity Chromatography (IMAC) resin was purchased from Bio-Rad (Hercules, CA, USA); and Amicon Ultra 30 kDa filters were from Millipore Corporation (Billerica, MA, USA). Sulbutiamine was purchased from Santa Cruz, Biotechnology (Dallas, TX, USA).

4.2. Homology Modeling

In a previous work [18], two homology models based on the crystallographic structures of arginine deiminase from *Pseudomonas aeruginosa* and *M. arginini* were found to be the most appropriate templates for the modeling of 3D GlADI structure. Based on its described homodimer quaternary structure, ADI from *M. arginini* was selected as a template. The amino acid sequence of GlADI (NCBI reference: XP_001705755) [34] was obtained from the NCBI database. To build the three-dimensional model, the complete sequence of 580 amino acids was submitted to SWISS-MODEL of the Expasy Server (https://swissmodel.expasy.org/ (accessed on 11 November 2018)), the crystallographic coordinates from *M. arginini* ADI (Protein Data Bank code 1S9R [35]) were uploaded as a template. We used the VMD molecular graphics program to show the distribution of cysteine residues for the total GlADI dimer and show the catalytic residues' distribution [36].

4.3. Docking

For docking studies, SwissDock server (http://www.swissdock.ch/docking (accessed on 5 March 2020)) was used, and the structure of the homology model of GlADI was analyzed as target, with s-methyl methanethiosulfonate (MMTS), dithio-bis-nitrobenzoic acid (DTNB), omeprazole, rabeprazole, sulbutiamine, and aurothiomalate as ligands. Ligands were obtained from ChemSpider (http://www.chemspider.com (accessed on 3 March 2020)) and PubChem Compound (https://www.ncbi.nlm.nih.gov/pccompound/ (accessed on 3 March 2020)) databases and adjusted to mol2 format with VMD. All structures were energy minimized with Chimera software [37], and with the resulting new coordinates, docking calculations were carried out with the mentioned server. The results were loaded and visualized with Chimera software [37].

4.4. Expression and Purification of Recombinant GlADI

The arginine deiminase gene from *Giardia lamblia* was cloned into the pET28a (+) vector (Novagen), as previously described [38]. pET28a (+) vector adds an N−terminal His6x tag to the protein. To over-express GlADI, this vector was used to transform the Rosetta 2 (DE3) pLysS *Escherichia coli* strain. This *E. coli* strain was grown in 250 mL of Terrific Broth culture medium supplemented with kanamycin and chloramphenicol at a final concentration of 50 μg/mL (each one). Cells were incubated at 37 °C until 0.8–1.0 of absorbance at 600 nm was reached. The overexpression was induced by the addition of isopropyl thio-β-

Dgalactoside (IPTG) at a final concentration of 1 mM for 16 h at 16 °C. Cells were harvested by centrifugation at 2370× *g* at 12 °C for 5 min (pellets were stored at −80 °C until further use). Pellets were weighed and resuspended in 25 mL of lysis buffer containing 50 mM sodium phosphate monobasic (H_2NaO_4P), 300 mM sodium chloride (NaCl), 20% glycerol, 4 µM β-mercaptoethanol, lysozyme (1 µg/mL), and protease inhibitor cocktail (1 mL of stock solution per 20 g of wet weight of *E. coli* cells). The buffer was adjusted at pH 8.0. The bacterial suspension was disrupted by sonication and centrifuged at 7690× *g* for 1 h at 4 °C. Protein purification was performed by IMAC using a Profinity Ni^{2+} charged resin previously equilibrated with lysis buffer. The soluble protein fraction was passed through an IMAC column three times, and the recombinant GlADI was purified with a gradient of 20–250 mM imidazole. The purified protein was dialyzed against lysis buffer and concentrated to a volume of 250 µL using Amicon ultrafiltration units. Due to the low stability of GlADI in solution, the N-terminal His6x tag was not cleaved. The concentration of purified GlADI was spectrophotometrically determined (Spectrophotometer Cary 50, Agilent Technologies, Santa Clara, CA, USA) at 280 nm using the extinction coefficient of ε_{280} = 60,250 M^{-1} cm^{-1} [39]. The purity of the enzyme was analyzed by sodium dodecyl sulfate-polyacrylamide gel electrophoresis technique (16% SDS–PAGE) and stained with colloidal Coomassie Brilliant Blue.

4.5. Enzyme Activity Assays

The enzyme activity of GlADI was determined by monitoring the conversion of L-arginine to citrulline. The reaction was based on that reported by Weickmann [40] and modified by Li [19], with slight modifications by us. Briefly, the reaction mixture at pH 8.0 in buffer containing 50 mM sodium phosphate monobasic (H_2NaO_4P), 300 mM sodium chloride (NaCl), and 20% glycerol was added with 8 mM L-arginine, 10 mM α-ketoglutaric acid, 0.2 mg/mL glutamate dehydrogenase (GIDH) as coupling enzyme, and 0.2 mM NADH. The reaction was initialized by adding the recombinant enzyme or soluble extracts from trophozoites to the reaction mixture. Enzyme activity was spectrophotometrically measured by monitoring NADH oxidation at 340 nm, at 25 °C.

4.6. Enzyme Inactivation Assays of Recombinant GlADI and Second-Order Inactivation Constants

The sulfhydryl reagents, thiol-reactive drugs, and albendazole solutions were freshly prepared in lysis buffer before use, as previously described [11,32,41]. The GlADI inactivation assays were performed at a protein concentration of 0.5 mg/mL in lysis buffer for 2 h at 25 °C. Aliquots from these incubations were withdrawn and assayed for enzyme activity, as described above. The reaction was initiated by adding 17 µg/mL of GlADI to the reaction mixture. The data are reported as the percentage of residual activity. Results are from at least four technical repetitions.

Pseudo-first-order inactivation rate constants (k_1) were obtained at MMTS concentrations ranging from 2.5 to 85 µM, whereas the concentration for rabeprazole varied from 5 to 110 µM, at the times indicated in Figure 4. Aliquots were removed from the samples and assayed for residual activity in the reaction mixture described above. Data were adjusted to a mono-exponential decay model, $A_R = A_0\, e^{-kt}$, where A_R is the residual activity at time t, A_0 is the activity at time 0, and k is the pseudo-first-order inactivation rate constant [41]. The slopes of the linear plots (k_1) versus the concentration of MMTS and rabeprazole correspond to the second-order inactivation constant k_2 (M^{-1} s^{-1}).

4.7. Fluorescence Emission Spectra

Fluorescence experiments were performed using a Perkin–Elmer LS55 spectrofluorometer at 25 °C and a protein concentration of 65 µg/ mL. The intrinsic fluorescence of the enzymes was determined at an excitation wavelength of 295 nm, and the emission spectra were recorded from 310 to 500 nm, with an integration time of 1 s, using excitation and emission slits of 3 nm. Each spectrum was the average of three scans with two experimental repetitions. The spectra of blanks were subtracted from those containing protein.

4.8. Quantification of Free Cysteines after Drug Treatments

The Cys residues were determined using Ellman's reagent under non-denaturing and denaturing conditions [42]. To carry out the experiments, 0.5 mg/mL of GlADI was incubated, either without compounds or with 250 μM DTNB and MMTS, separately, or with 750 μM omeprazole, rabeprazole, sulbutiamine, or aurothiomalate, separately. Each mix was incubated for 2 h at 25 °C. After the incubation period, the samples were extensively washed by ultrafiltration with Centricon filters to eliminate the excess drug, and the protein concentration was estimated by determining the absorbance at 280 nm. Next, the free Cys content of the samples was spectrophotometrically quantified as follows: the basal absorbance of 1 mM DTNB and 5% SDS dissolved in lysis buffer was measured at 412 nm (ε 412 nm = 13.6 mM/cm), and the increase in absorbance following the addition of 200 μg of protein was monitored. The number of modified Cys residues was indirectly calculated by subtracting the number of free Cys residues in the derivatized enzyme (treated with the drugs) from the number of free Cys residues in the enzyme in the absence of the drugs. The results represent the mean ± SD of at least four independent experiments.

4.9. Drug Susceptibility of Trophozoites and Cellular GlADI Activity Assays

G. lamblia WB strain was acquired from the American Type Culture Collection (ATCC) and cultured, harvested, and maintained as previously described [27]. Trophozoites were cultured in the presence of increasing concentrations of omeprazole, rabeprazole, sulbutiamine, or aurothiomalate for 24 h at 37 °C, at the concentrations shown in Figure 5. At the end of the treatment period, the tubes were decanted to preserve only the adhered trophozoites (trying to keep only living cells, and without mixing with dead cells). Nonetheless, the living and dead trophozoites were counted from these supernatants to register the total viability after the treatments. The culture tubes were washed three times with phosphate-buffered saline (PBS), pH 7.4, and chilled on ice for 20 min, and then the trophozoites were counted to standardize the assays by the number of cells. The cells were disrupted with five cycles of freeze–thaw cycles in liquid N_2 and 42 °C, in lysis buffer. Disrupted cells were centrifuged at 15,700× *g* for 20 min at 4 °C, and the supernatants were withdrawn for analysis of residual GlADI activity using the coupled method mentioned above, at 25 °C. We considered 100% to be the enzyme activity registered for the cultures without drugs.

4.10. Induction to Encystment in the Presence of Rabeprazole

G. lamblia WB strain trophozoites were cultured as mentioned above and harvested in the exponential phase of growth (~2 × 10^6 cells/mL). Encystation was accomplished following the method described by Boucher and Gillin with modifications [43]. Briefly, trophozoites were counted in a hemocytometer chamber and added to pre-encystation medium containing TYI-S-33 growth medium (pH 7.1) with the antibiotics ceftazidime (500 μg/mL; PiSA Laboratories) and ampicillin (500 μg/mL; Sigma-Aldrich, St. Louis, MO, USA), but no bovine bile. The culture tubes (borosilicate glass screw-capped tubes of 8 mL) were divided into 2 groups of three tubes each per assay. The experimental group was supplemented with 150 μM rabeprazole. Pre-encystation cultures were grown for 24 h at 37 °C. The tubes were inverted eight times, and the unattached trophozoites and medium were discarded. The attached trophozoite monolayers were refed with fresh encystation medium consisted of pre-encystation medium adjusted to pH 8.0 with 1 M NaOH and supplemented with bovine bile (7.5 mg/mL, final concentration) and lactic acid (hemi-calcium salt, 5 mM, final concentration), and grown for 48 h at 37 °C. The experimental group was kept in a 150 μM rabeprazole condition. Parasites were harvested and counted to report the number of trophozoites and cysts per group.

4.11. Statistical Analyses

Data were analyzed with GraphPad Prism™ software (version 8.2.1 for Windows™, San Diego, CA, USA). The normal distribution of data was assessed with the Shapiro–Wilk test. Normally distributed data were analyzed with one-way ANOVA, followed

by Dunnett's multiple comparisons adjustment. Non-parametric distributed data were analyzed with the Mann–Whitney U test or Friedman test, followed by Dunn's multiple comparisons adjustment test. Results are expressed as mean ± SD or as the median and interquartile range (IQR) for data with parametric and non-parametric distribution, respectively. A p-value < 0.05 was considered to be statistically significant.

Supplementary Materials: The following are available online at https://www.mdpi.com/article/10.3390/ijms22179491/s1, Figure S1: Studied molecules 2D chemical structure, Figure S2: Multiple sequence amino acid alignment of ADI enzyme from *G. lamblia* and different organisms.

Author Contributions: Conceptualization, G.L.-V., C.F.-L.; Supervision, G.L.-V.; Methodology, G.L.-V.; Investigation, C.F.-L., I.d.l.M.-d.l.M., I.G.-T., S.E.-F., L.A.F.-L., L.Y.-M., F.M.-M.; Formal analysis, P.G.-C.; Funding acquisition, G.L.-V., P.G.-C.; Writing original draft, C.F.-L., G.L.-V.; Writing—review and editing, G.L.-V., P.d.V. All authors have read and agreed to the published version of the manuscript.

Funding: This research was funded by Programa de Recursos Fiscales para Investigación from Instituto Nacional de Pediatría, grant number 2019/062.

Institutional Review Board Statement: Not applicable.

Informed Consent Statement: Not applicable.

Data Availability Statement: Data is contained within the article.

Acknowledgments: C.F.-L. is grateful for the support of Abel Tasman Talent Program Sandwich from the University of Groningen-University Medical Center, UG/UMCG in collaboration with Universidad Nacional Autónoma de México, UNAM, and CONACyT 260625.

Conflicts of Interest: The authors declare no conflict of interest.

Abbreviations

DTNB	Dithio-bis-nitrobenzoic acid
MMTS	S-methyl methanethiosulfonate
GlADI	Arginine deiminase from *G. lamblia*
PPI	Proton pump inhibitor
ATP	Adenosine triphosphate
ASA	Accessible surface area
Cys	Cysteine
a.u.	Arbitrary units
k_i	Pseudo-first-order inactivation rate constant
k_2	Second-order rate constant
TCEP	Tris(2-carboxyethyl)phosphine
SD	Standard deviation
SDS	Sodium dodecyl sulfate
ATCC	American Type Culture Collection
PBS	Phosphate-buffered saline

References

1. Gavinho, B.; Rossi, I.V.; Evans-Osses, I.; Lange, S.; Ramirez, M.I. Peptidylarginine deiminase inhibition abolishes the production of large extracellular vesicles from Giardia intestinalis, affecting host-pathogen interactions by hindering adhesion to host cells. *Biorxiv* **2019**, *10*, 586438. [CrossRef]
2. Lagunas-Rangel, F.A.; Bermúdez-Cruz, R.M. Epigenetics in the early divergent eukaryotic Giardia duodenalis: An update. *Biochimie* **2019**, *156*, 123–128. [CrossRef] [PubMed]
3. Lindmark, D.G. Energy metabolism of the anaerobic protozoon Giardia lamblia. *Mol. Biochem. Parasitol.* **1980**, *1*, 1–12. [CrossRef]
4. Schofield, P.; Costello, M.; Edwards, M.; O'sullivan, W. The arginine dihydrolase pathway is present in Giardia intestinalis. *Int. J. Parasitol.* **1990**, *20*, 697–699. [CrossRef]
5. Schofield, P.J.; Edwards, M.R.; Matthews, J.; Wilson, J.R. The pathway of arginine catabolism in Giardia intestinalis. *Mol. Biochem. Parasitol.* **1992**, *51*, 29–36. [CrossRef]
6. Adam, R.D. Biology of Giardia lamblia. *Clin. Microbiol. Rev.* **2001**, *14*, 447–475. [CrossRef]

7. Han, J.; Collins, L.J. Reconstruction of sugar metabolic pathways of Giardia lamblia. *Int. J. Proteom.* **2012**, *2012*, 1–9. [CrossRef]
8. Mendis, A.; Thompson, R.; Reynoldson, J.; Armson, A.; Meloni, B.; Gunsberg, S. The uptake and conversion of l-[U14C-] aspartate and l-[U14C-] alanine to 14CO2 by intact trophozoites of Giardia duodenalis. *Comp. Biochem. Physiol. B Comp. Biochem.* **1992**, *102*, 235–239. [CrossRef]
9. García-Torres, I.; Marcial-Quino, J.; Gómez-Manzo, S.; Vanoye-Carlo, A.; Navarrete-Vázquez, G.; Colín-Lozano, B.; Gutiérrez-Castrellón, P.; Sierra-Palacios, E.; López-Velázquez, G.; Enríquez-Flores, S. Proton pump inhibitors drastically modify triosephosphate isomerase from Giardia lamblia at functional and structural levels, providing molecular leads in the design of new antigiardiasic drugs. *Biochim. Et Biophys. Acta (BBA)-Gen. Subj.* **2016**, *1860*, 97–107. [CrossRef]
10. López-Velázquez, G.; Fernández-Lainez, C.; de la Mora-de, J.I.; de la Portilla, D.C.; Reynoso-Robles, R.; González-Maciel, A.; Ridaura, C.; García-Torres, I.; Gutiérrez-Castrellón, P.; Olivos-García, A. On the molecular and cellular effects of omeprazole to further support its effectiveness as an antigiardial drug. *Sci. Rep.* **2019**, *9*, 1–14.
11. Reyes-Vivas, H.; Castillo-Villanueva, A.; Yépez-Mulia, L.; Hernández-Alcántara, G.; Figueroa-Salazar, R.; García-Torres, I.; Gómez-Manzo, S.; Méndez, S.T.; Vanoye-Carlo, A.; Marcial-Quino, J. Giardial Triosephosphate Isomerase as possible target of the cytotoxic effect of omeprazole in Giardia. *Antimicrob. Agents Chemother.* **2014**, *58*, 7072–7082. [CrossRef] [PubMed]
12. Emery-Corbin, S.J.; Grüttner, J.; Svärd, S. Transcriptomic and proteomic analyses of Giardia intestinalis: Intestinal epithelial cell interactions. *Adv. Parasitol.* **2020**, *107*, 139–171. [CrossRef] [PubMed]
13. Lalle, M.; Hanevik, K. Treatment-refractory giardiasis: Challenges and solutions. *Infect. Drug Resist.* **2018**, *11*, 1921. [CrossRef]
14. Pérez-Villanueva, J.; Romo-Mancillas, A.; Hernández-Campos, A.; Yépez-Mulia, L.; Hernández-Luis, F.; Castillo, R. Antiprotozoal activity of proton-pump inhibitors. *Bioorg. Med. Chem. Lett.* **2011**, *21*, 7351–7354. [CrossRef]
15. Delgado-Maldonado, T.; Nogueda-Torres, B.; Espinoza-Hicks, J.C.; Vázquez-Jiménez, L.K.; Paz-González, A.D.; Juárez-Saldívar, A.; Rivera, G. Synthesis and biological evaluation in vitro and in silico of N-propionyl-N′-benzeneacylhydrazone derivatives as cruzain inhibitors of Trypanosoma cruzi. *Mol. Divers.* **2020**, *24*, 1–12.
16. Leitsch, D.; Müller, J.; Müller, N. Evaluation of Giardia lamblia thioredoxin reductase as drug activating enzyme and as drug target. *Int. J. Parasitol. Drugs Drug Resist.* **2016**, *6*, 148–153. [CrossRef]
17. Moreno-Herrera, A.; Cortez-Maya, S.; Bocanegra-Garcia, V.; Banik, B.K.; Rivera, G. Recent advances in the development of broad-spectrum antiprotozoal agents. *Curr. Med. Chem.* **2021**, *28*, 583–606. [CrossRef]
18. Trejo-Soto, P.J.; Aguayo-Ortiz, R.; Yépez-Mulia, L.; Hernández-Campos, A.; Medina-Franco, J.L.; Castillo, R. Insights into the structure and inhibition of Giardia intestinalis arginine deiminase: Homology modeling, docking, and molecular dynamics studies. *J. Biomol. Struct. Dyn.* **2016**, *34*, 732–748. [CrossRef]
19. Li, Z.; Kulakova, L.; Li, L.; Galkin, A.; Zhao, Z.; Nash, T.E.; Mariano, P.S.; Herzberg, O.; Dunaway-Mariano, D. Mechanisms of catalysis and inhibition operative in the arginine deiminase from the human pathogen Giardia lamblia. *Bioorg. Chem.* **2009**, *37*, 149–161. [CrossRef] [PubMed]
20. Aguilar-Díaz, H.; Carrero, J.C.; Argüello-García, R.; Laclette, J.P.; Morales-Montor, J. Cyst and encystment in protozoan parasites: Optimal targets for new life-cycle interrupting strategies? *Trends Parasitol.* **2011**, *27*, 450–458. [CrossRef] [PubMed]
21. Touz, M.C.; Rópolo, A.S.; Rivero, M.R.; Vranych, C.V.; Conrad, J.T.; Svard, S.G.; Nash, T.E. Arginine deiminase has multiple regulatory roles in the biology of Giardia lamblia. *J. Cell Sci.* **2008**, *121*, 2930–2938. [CrossRef]
22. Riches, A.; Hart, C.J.S.; Trenholme, K.R.; Skinner-Adams, T.S. Anti-Giardia Drug Discovery: Current Status and Gut Feelings. *J. Med. Chem.* **2020**, *63*, 13330–13354. [CrossRef] [PubMed]
23. Rópolo, A.S.; Feliziani, C.; Touz, M.C. Unusual proteins in Giardia duodenalis and their role in survival. *Adv. Parasitol.* **2019**, *106*, 1–50. [CrossRef]
24. Hajduk, P.J.; Huth, J.R.; Tse, C. Predicting protein druggability. *Drug Discov. Today* **2005**, *10*, 1675–1682. [CrossRef]
25. Papanastasiou, P.; Bruderer, T.; Li, Y.; Bommeli, C.; Köhler, P. Primary structure and biochemical properties of a variant-specific surface protein of Giardia. *Mol. Biochem. Parasitol.* **1997**, *86*, 13–27. [CrossRef]
26. López-Velázquez, G.; Molina-Ortiz, D.; Cabrera, N.; Hernández-Alcántara, G.; Peon-Peralta, J.; Yépez-Mulia, L.; Pérez-Montfort, R.; Reyes-Vivas, H. An unusual triosephosphate isomerase from the early divergent eukaryote Giardia lamblia. *Proteins* **2004**, *55*, 824–834. [CrossRef]
27. Reyes-Vivas, H.; Diaz, A.; Peon, J.; Mendoza-Hernandez, G.; Hernandez-Alcantara, G.; De la Mora-De la Mora, I.; Enriquez-Flores, S.; Dominguez-Ramirez, L.; Lopez-Velazquez, G. Disulfide bridges in the mesophilic triosephosphate isomerase from Giardia lamblia are related to oligomerization and activity. *J. Mol. Biol.* **2007**, *365*, 752–763. [CrossRef] [PubMed]
28. Ladokhin, A.S. Fluorescence spectroscopy in peptide and protein analysis. *Encycl. Anal. Chem. Appl. Theory Instrum.* **2006**.
29. Hernández-Alcántara, G.; Rodríguez-Romero, A.; Reyes-Vivas, H.; Peon, J.; Cabrera, N.; Ortiz, C.; Enríquez-Flores, S.; López-Velázquez, G. Unraveling the mechanisms of tryptophan fluorescence quenching in the triosephosphate isomerase from Giardia lamblia. *Biochim. Et Biophys. Acta (BBA)-Proteins Proteom.* **2008**, *1784*, 1493–1500. [CrossRef]
30. Tobinick, E.L. The value of drug repositioning in the current pharmaceutical market. *Drug News Perspect.* **2009**, *22*, 119–125. [CrossRef] [PubMed]
31. Starling-Soares, B.; Carrera-Bastos, P.; Bettendorff, L. Role of the Synthetic B1 Vitamin Sulbutiamine on Health. *J. Nutr. Metab.* **2020**, *2020*, 9349063. [CrossRef] [PubMed]

32. García-Torres, I.; De la Mora-De la Mora, I.; Hernández-Alcántara, G.; Molina-Ortiz, D.; Caballero-Salazar, S.; Olivos-García, A.; Nava, G.; López-Velázquez, G.; Enríquez-Flores, S. First characterization of a microsporidial triosephosphate isomerase and the biochemical mechanisms of its inactivation to propose a new druggable target. *Sci. Rep.* **2018**, *8*, 8591. [CrossRef] [PubMed]
33. Wood, P.L.; Khan, M.A.; Moskal, J.R. Mechanism of action of the disease-modifying anti-arthritic thiol agents D-penicillamine and sodium aurothiomalate: Restoration of cellular free thiols and sequestration of reactive aldehydes. *Eur. J. Pharmacol.* **2008**, *580*, 48–54. [CrossRef] [PubMed]
34. Morrison, H.G.; McArthur, A.G.; Gillin, F.D.; Aley, S.B.; Adam, R.D.; Olsen, G.J.; Best, A.A.; Cande, W.Z.; Chen, F.; Cipriano, M.J. Genomic minimalism in the early diverging intestinal parasite Giardia lamblia. *Science* **2007**, *317*, 1921–1926. [CrossRef]
35. Berman, H.M.; Westbrook, J.; Feng, Z.; Gilliland, G.; Bhat, T.N.; Weissig, H.; Shindyalov, I.N.; Bourne, P.E. The Protein Data Bank. *Nucleic Acids Res.* **2000**, *28*, 235–242. [CrossRef] [PubMed]
36. Humphrey, W.; Dalke, A.; Schulten, K. VMD: Visual molecular dynamics. *J. Mol. Graph.* **1996**, *14*, 33–38. [CrossRef]
37. Chimera, U. A visualization system for exploratory research and analysis. Pettersen EF, Goddard TD, Huang CC, Couch GS, Greenblatt DM, Meng EC, Ferrin TE. *J. Comput. Chem.* **2004**, *25*, 1605–1612.
38. Muñoz-Cruz, S.; Gomez-García, A.; Matadamas-Martínez, F.; Alvarado-Torres, J.A.; Meza-Cervantez, P.; Arriaga-Pizano, L.; Yépez-Mulia, L. Giardia lamblia: Identification of molecules that contribute to direct mast cell activation. *Parasitol. Res.* **2018**, *117*, 2555–2567. [CrossRef]
39. Pace, C.N.; Vajdos, F.; Fee, L.; Grimsley, G.; Gray, T. How to measure and predict the molar absorption coefficient of a protein. *Protein Sci.* **1995**, *4*, 2411–2423. [CrossRef] [PubMed]
40. Weickmann, J.L.; Fahrney, D.E. Arginine deiminase from Mycoplasma arthritidis. Evidence for multiple forms. *J. Biol. Chem.* **1977**, *252*, 2615–2620. [CrossRef]
41. Enríquez-Flores, S.; Rodríguez-Romero, A.; Hernández-Alcántara, G.; Oria-Hernández, J.; Gutiérrez-Castrellón, P.; Pérez-Hernández, G.; Mora, I.d.l.M.d.l.; Castillo-Villanueva, A.; García-Torres, I.; Mendez, S.T. Determining the molecular mechanism of inactivation by chemical modification of triosephosphate isomerase from the human parasite Giardia lamblia: A study for antiparasitic drug design. *Proteins Struct. Funct. Bioinform.* **2011**, *79*, 2711–2724. [CrossRef] [PubMed]
42. Ellman, G.L. A colorimetric method for determining low concentrations of mercaptans. *Arch. Biochem. Biophys.* **1958**, *74*, 443–450. [CrossRef]
43. Boucher, S.E.; Gillin, F.D. Excystation of in vitro-derived Giardia lamblia cysts. *Infect. Immun.* **1990**, *58*, 3516–3522. [CrossRef] [PubMed]

CAPÍTULO 2

Cynthia Fernández-Lainez[1,2,3], Gabriel López-Velázquez[4], Paul de Vos[1]

[1]Immunoendocrinology, Division of Medical Biology, Department of Pathology and Medical Biology, University of Groningen and University Medical Center Groningen, Hanzeplein 1, 9700 RB Groningen, The Netherlands.

[2]Laboratorio de Errores Innatos del Metabolismo y Tamiz, Instituto Nacional de Pediatría, S.S., Ciudad de México, México

[3]Posgrado en Ciencias Biológicas, Universidad Nacional Autónoma de México UNAM, Ciudad de México, México.

[4]Laboratorio de Biomoléculas y Salud Infantil, Instituto Nacional de Pediatría, S.S., Ciudad de México, México

Publicado en: *Fernández-Lainez C., López-Velázquez G., de Vos P. Health benefits of inulin- and agavin-type fructans in food: impact on microbiota, immune and gut barrier function under physiological and inflammatory conditions. En:* ***The Book of Fructans, Edited by: Van den Ende, W., Toksoy Oner, E. 2023, Elsevier, ISBN: 9780323854108. DOI: https://doi.org/10.1016/B978-0-323-85410-8.00015-6***

The Book of Fructans

Edited by

Wim Van den Ende
Professor, Biology Department, KU Leuven University, Leuven, Belgium

Ebru Toksoy Öner
Professor, Bioengineering Department, Marmara University, Istanbul, Turkey

ACADEMIC PRESS
An imprint of Elsevier

Academic Press is an imprint of Elsevier
125 London Wall, London EC2Y 5AS, United Kingdom
525 B Street, Suite 1650, San Diego, CA 92101, United States
50 Hampshire Street, 5th Floor, Cambridge, MA 02139, United States
The Boulevard, Langford Lane, Kidlington, Oxford OX5 1GB, United Kingdom

Notices
Knowledge and best practice in this field are constantly changing. As new research and experience broaden our understanding, changes in research methods, professional practices, or medical treatment may become necessary.

Practitioners and researchers must always rely on their own experience and knowledge in evaluating and using any information, methods, compounds, or experiments described herein. In using such information or methods they should be mindful of their own safety and the safety of others, including parties for whom they have a professional responsibility.

To the fullest extent of the law, neither the Publisher nor the authors, contributors, or editors, assume any liability for any injury and/or damage to persons or property as a matter of products liability, negligence or otherwise, or from any use or operation of any methods, products, instructions, or ideas contained in the material herein.

ISBN: 978-0-323-85410-8

Publisher: Nikki P. Levy
Acquisitions Editor: Megan R Ball
Editorial Project Manager: Kyle Gravel
Production Project Manager: Rashmi Manoharan
Cover Designer: Matthew Limbert

Typeset by TNQ Technologies

Chapter 13

Health benefits of Inulin and Agavin-type Fructans in Food: Impact on Microbiota, Immune and Gut Barrier Function

Cynthia Fernández-Lainez[1,2,3], Gabriel López-Velázquez[4] and Paul de Vos[1]

[1]*Immunoendocrinology, Division of Medical Biology, Department of Pathology and Medical Biology, University of Groningen and University Medical Center Groningen, Groningen, the Netherlands;* [2]*Laboratorio de Errores Innatos del Metabolismo y Tamiz, Instituto Nacional de Pediatría, Ciudad de México, México;* [3]*Posgrado en Ciencias Biológicas, Universidad Nacional Autónoma de México UNAM, Ciudad de México, México;* [4]*Laboratorio de Biomoléculas y Salud Infantil, Instituto Nacional de Pediatría, Ciudad de México, México*

1. Introduction

Economic, technological, and social changes have influenced lifestyle and feeding habits, especially in Western society. This has impacted the health of the population. One of these changes in food habits is the lowering of intake of dietary fibers. This lowering of intake of dietary fibers is associated with an increased risk of developing a growing list of Western diseases such as irritable bowel syndrome (IBS), cancer, type 2 diabetes, and metabolic syndrome (Dreher, 2018). Enhanced intake of dietary fibers has been shown to prevent many diseases and is associated with better general health (Roberfroid, 2002). An important family of dietary fibers is fructans. This fructose-based oligo- and polysaccharides are produced by some bacteria, fungi, and higher plants (Pérez-López & Simpson, 2020). Fructans are water-soluble reserve polysaccharides representing the main nonstructural pool of carbohydrates in many plants including chicory, wheat, and agave, the latter performing crassulacean acid metabolism (CAM) (Raveh et al., 1998; Van den Ende, 2013).

Fructans have been the subject of study in the last decades because of their potential health benefits. They pass the stomach without major hydrolysis to fructose and are resistant to human digestive enzymes. They reach the colon where intestinal microbiota with microbial enzymes ferment the fructans which leads to the production of microbial metabolic products such as short-chain fatty acids (SCFA), which can beneficially influence health at several levels (Lambertz et al., 2017). Here, microbiota-dependent effects of fructans will be considered as "*indirect effects*". These *indirect* health effects, depending on microbiota, include reduced risk for the development of some cancers, enhancement of calcium absorption, and avoiding the adhesion of pathogens to the intestinal epithelium. One of the most important *indirect* effects of fructans is their property to selectively stimulate beneficial gut bacteria, the so-called prebiotic effect (Gupta et al., 2019), contributing to healthy aging and prevention of the development of chronic diseases (Lambertz et al., 2017).

Other more recently discovered health benefits of fructans include their *direct* binding to immune receptors on cells of the gut immune barrier of the small intestine, beneficially influencing immune development and gut barrier function (Bermudez-Brito et al., 2015; Jeurink et al., 2013; Vogt et al., 2014). Therefore, we will refer to these as *direct* beneficial effects, achieved by the direct interaction of fructans with gut epithelial cells and cells of the gut immune system.

As many health benefits have been described for fructans, but also because health benefits according to current insight are highly fructan dependent on fructan-type and degree of polymerization (DP), we reviewed in the present chapter the current scientific evidence for health benefits of specific fructans extracted from chicory and agave plants, which are two of the most commonly used fructans in the food industry. We especially focused on the reported effects of different types of fructans on gut microbiota and regulatory effects on immunity and gut barrier as these seem to be the main targets of fructans and the current explanation for the majority of beneficial effects of fructans. This impact can start as early as in the first weeks after birth till an advanced age. We therefore will also review current insight on the current knowledge of the

The Book of Fructans. https://doi.org/10.1016/B978-0-323-85410-8.00015-6

impact of fructans on infant microbiota and gut immune barrier development as well as the impact on the prevention of disease.

2. Characteristics of plant fructans

Fructans serve as reserve compounds for some plant species, such as chicory, Jerusalem artichokes, asparagus, garlic, leak, and onion (Flamm et al., 2001; López & Urías-Silvas, 2007). Fructans can also function as osmoprotectants during drought periods (López et al., 2003). Fructans are water soluble and have a chemical flexible structure (Pérez-López & Simpson, 2020). In dicot plants, fructan synthesis starts with the transfer of fructose between two sucrose molecules, creating β-(2,1) fructosyl-fructose bonds. Therefore, they can be denoted as GF_n, where G and F represent glucosyl and fructosyl units respectively, and n depicts the number of fructose units in the polymer. In the fructan chain, the starting monomer can also be a D-fructopyranosyl residue, then F_n is used to denote these molecules (Roberfroid, 2005). Fructans, de novo synthesized from plants, are obtained by hot water extraction. They consist of a mixture of polymers with variable DP (chain length). DP refers to the number of repeating fructose units. DP is used to classify fructans in such a way, that polymers with a chain length < 10 are known as short-chain fructans (often referred to as fructooligosaccharides or FOS (or FOSs) in the literature), and those with a DP > 10 are referred to as long chain fructan polysaccharides (e.g., inulin). See Chapter 1 for more details on plant fructan structures.

All these fructans are considered to be nondigestible carbohydrates (NDCs) as they cannot be hydrolyzed by the human saliva and small intestinal digestive enzymes, which is due to the β-configuration of the anomeric C2 in the fructose monomers (Kelly, 2008; Roberfroid, 2005). Fructans are traditionally used as fat replacers and as prebiotics in the food industry (Apolinário et al., 2014; Shoaib et al., 2016; Vandeputte et al., 2017). Fructans have also been used in pharmaceutical applications as vehicles for drug delivery or as a cryoprotectant (Barclay et al., 2016). Two of the most commonly used fructans are those extracted from chicory (*Cichorium intybus)* and agave plants (Apolinário et al., 2014). Chicory is the most important source of inulin for the food industry, due to its high inulin content (> 80%) (Fan et al., 2016; Stephen & Phillips, 2006). Fructans from the *Agavaceae* family represent around 60% of their total soluble carbohydrates. Agave plants are an alternative source for fructan extraction (Moreno-Vilet et al., 2016), especially in Latin America.

2.1 Chicory and agave fructans

Fructans from chicory roots are of the inulin type (only β(2,1) linkages). These inulin-type fructans (ITFs) have variable DPs. Here, we use the terms short chain inulin (scITF) for fructans with DP 3−10, and the term long-chain inulin (lcITF) for fructans with DP > 10.

Fructans extracted from Agave are a mixture of β(2-1) and β(2,6) glycoside linkages, making them readily soluble in water. Agavin is commonly extracted from the leaves and stem of the plant and applied. Leaf agavin has a DP of 3−8. They contain single α-D-Glc*p* residues in the terminal and internal positions and (2,1)-linked β-D-Fru*f* residues only. This is different in stems where fructans are composed of a mixture of several structures with a α-D-Glc*p* residue in terminal and 6-linked positions. They contain also (2,1) and (2−6)-linked β-D-Fru*f* residues with branched oligomeric repeating units (Praznik et al., 2013). For DP 3−10 agavin we will use the term short-chain agavin fructans (scAFs), and the term long-chain agavin fructans (lcAFs) will be used for agavin with DP > 10.

Physicochemical characteristics of agavin such as DP and water solubility have been shown to be plant-age dependent. These physicochemical characteristics can vary according to the climate or environmental conditions where plants were cultivated (Mancilla-Margalli & Lopez, 2006; Mellado-Mojica & López, 2012).

3. Health benefits of chicory inulin and agavin from Agave

3.1 The gastrointestinal immune barrier

Before discussing the health benefits of chicory and agavin, it is essential to explain the characteristics of the gastrointestinal immune barrier on which fructans act.

The intestinal epithelial cells (IECs) represent the physical barrier between the intestinal lumen and the internal host-milieu (Camilleri et al., 2012). The gastrointestinal barrier is formed by a continuous mono-layer composed of several cell types. These cells can be classified in absorptive cells (enterocytes and colonocytes) and secretory cells (goblet cells and Paneth cells) (Pinto & Clevers, 2005). Secretory cells contribute to intestinal health and barrier function through the

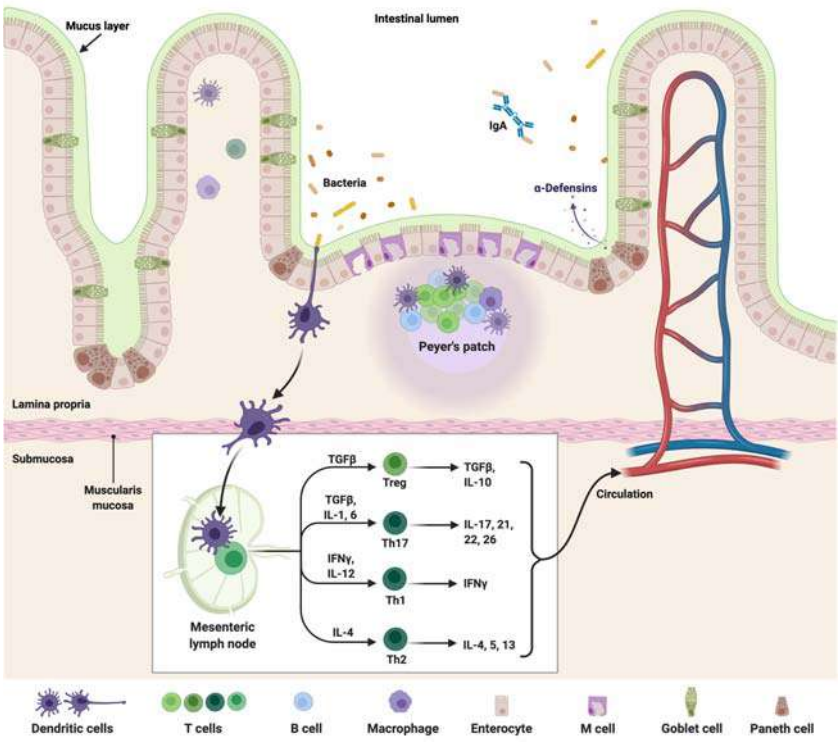

FIGURE 13.1 Schematic representation of gastrointestinal immune barrier. Crosstalk between IECs and GALT is necessary to maintain intestinal homeostasis. *Figure produced with BioRender.*

production of mucus proteins and antimicrobial peptides (Kim & Ho, 2010). Underneath the IECs, gut-associated lymphoid tissue (GALT) is located. GALT is constituted by the lamina propria, Peyer's patches, and the lymph nodes Fig. 13.1 (Dubois et al., 2005; Johansson & Kelsall, 2005; MacPherson et al., 2004; Sato & Iwasaki, 2005).

The IECs and the GALT have many pathways for crosstalk allowing induction of tolerance for beneficial microbiota, but also allowing detection and formation of appropriate responses to pathogenic microorganisms and parasites. To initiate these responses, the transport of luminal antigens through dendritic cells (DC) and macrophages is necessary. This generates meticulously regulated immune responses required for maintaining intestinal homeostasis (Mowat, 2003).

3.2 Indirect mechanisms of immunomodulation: prebiotic activity of chicory and agave fructans

3.2.1 Human gut microbial colonization

The gut is containing 100 trillion bacteria that contribute to the utilization of food components and produces health-promoting fermentation products that human cells cannot manufacture (Derrien & van Hylckama Vlieg, 2015). During the past decade it has become accepted that a healthy microbiome is essential for the prevention of disease and that dysbiosis, i.e., disturbed microbiota composition is associated with many diseases in humans as well as in animals (Carding et al., 2015).

Human intestinal colonization starts upon birth when the neonate gets in contact with vaginal maternal microbiota. As of that moment, microorganisms become a pertinent member of the gastrointestinal tract of the infant and is also the start of the development of many processes including immune, metabolic and neurologic programming. The way this programming occurs depends on the type of intestinal microbiota colonizing the neonatal intestine during the first days of life (Gabriel et al., 2018; Sestito et al., 2020). This initial colonization in the newborn is very sensitive and determined by many factors including the mode of birth, gestational age, and whether breast feeding or infant formula is applied (Walker, 2014). Consequently, the reference for a "healthy microbiome" is currently the intestinal microbiota of term-born infants, vaginally born, and exclusively breastfed (Chambers & Townsend, 2020; Collado et al., 2012).

In breastfed infants, the colonization of the microbiota is under the tight control of different human milk components. One of the most important human milk-component driving this colonization by microbiota is the so-called human milk oligosaccharides (hMOs). These hMOs comprise a family of 200 nondigestible sugars that prepare the human gut for colonization and may also serve as a growth substrate for the microbiota in neonates (Holscher et al., 2017). The hMOs are

unique for humans and not found in such an abundancy and variation in other species (Bode, 2012; Thurl et al., 2010). Besides their impact on shaping the intestinal microbiome (Cheng, Akkerman, et al., 2020; Cheng, Kiewiet, et al., 2020), hMOs and/or their fermentation products have been shown to have other beneficial functions such as inducing reduction of intestinal infections by inhibition of pathogenic adhesion (Ackerman et al., 2018; Jantscher-Krenn et al., 2012; Kong, Cheng, et al., 2020), stimulation and maturation of the immune system by interacting directly with components of the immune system (Cheng et al., 2019, 2021) and enhancing the intestinal barrier function (Figueroa-Lozano & de Vos, 2019; Kong, Cheng, et al., 2020; Kong et al., 2019).

In infants in which exclusive breast feeding is not an option, which is in about 75% of all infants (Theurich et al., 2019; Victora et al., 2016), cow-milk-derived infant formulas are used. These cow-milk-derived infant formulas do not have any hMO or bovine hMO-like molecule that can substitute the function of hMOs. As a consequence, the intestinal microbiota of breastfed infants is having a higher abundance of *Bifidobacteriaceae* and decreased or absence of pathogens such as *Clostridium* and *Enterobacteriaceae,* compared to infants receiving infant formula (Cheng, Kiewiet, et al., 2020). To overcome these differences in microbiota composition, significant efforts have been undertaken to find supplements for infant formula that mimic some of the functions of hMOs. Currently, a few molecules have been approved for human application and are cost-effective enough to allow application. These include galactooligosaccharides (GOS), pectins, and ITFs (Kong, Faas, et al., 2020; Rodriguez-Herrera et al., 2019; Wiciński et al., 2020).

3.2.2 Fructans in infant formula

Depending on the geographical location fructans of chicory or agave have been applied in infant formula to mimic the prebiotic functions of hMOs. In Europe, it is mostly chicory inulin that is applied in infant formula while in Latin America it is mostly agave fructans. The beneficial effects of ITFs and AFs alone or in combination with hMOs have been widely accepted in infant formula (Costalos et al., 2008; Holscher et al., 2012; Kapiki et al., 2007; Knol et al., 2005; López-Velázquez et al., 2015; Wernimont et al., 2015). The beneficial effects go beyond prebiotic effects. Also, digestive tolerance and adequacy of support of neonatal growth have been demonstrated (Closa-Monasterolo et al., 2013; López-Velázquez et al., 2013; Vandenplas et al., 2020). During recent years it has also been shown that the intestinal microbiota composition of neonates fed with fructan-supplemented infant formulas is improved and resembles that of breastfed infants (Borewicz et al., 2019; Holscher et al., 2012; Wernimont et al., 2015). Table 13.1. This type of microbiota is considered to be a healthy microbiota and associated with the prevention of stomach cholic, infection, and allergy (Arslanoglu et al., 2008; Fukuda et al., 2011; Ivakhnenko & Nyankovskyy, 2013; Moro et al., 2006), strengthening of intestinal epithelial barrier (Ulluwishewa et al., 2011), enhancement of mucosal immunity (Chambers & Townsend, 2020) and prevention of intestinal pathogen growth and adhesion (López-Velázquez et al., 2013; Martínez-Ortega et al., 2020; Ortega-Gonzalez, 2014). The way fructans support this will be discussed later in this chapter.

3.2.3 Fermentation products of chicory and agave fructans alone, or in symbiotic combination with bacteria

An important function of fructans in infant formulas is the stimulation of the production of microbial fermentation products such as SCFAs. These include SCFAs such as acetate, propionate, and butyrate (Rawi et al., 2020). In recent years it has become accepted that the action of these SCFAs rather than the changes in microbiota are responsible for health benefits (Kim et al., 2013; Macia et al., 2015). Among the benefits of SCFAs are the prevention of intestinal colonization with pathogens or parasites by decreased pH and increasing frequency and lowering softness of stool (Davis et al., 2017), as well as stimulation of immune responses (Table 13.2). However, the beneficial effects of fermentation products of fructans are dependent on the age of the infant and the type of prebiotic supplemented. That not all prebiotics have the same effects but that specific chemistries play a role was also demonstrated with ITFs because the DP greatly matters. In a recent study, we studied and compared the in vitro fermentation of scITFs and lcITFs. We compared fermentation by inocula of 2-week and 8-week-old, breastfed neonates. The results were remarkable. We showed that both microbiotas of 2-week and 8-week-old neonates preferred trisaccharides from scITFs, which were consumed in the first hours of fermentation, while the lcITFs remained practically intact. The digests taken from both fecal inocula were also tested for immunomodulatory capacity on immature DCs obtained from the umbilical cord of infants. This experiment again illustrated the chain length- dependent effects of ITFs as the fermentation products of lcITFs attenuated DCs proinflammatory responses stronger than scITFs (Logtenberg et al., 2020) (Table 13.2).

In addition to the prevention of intestinal colonization with pathogens, SCFAs and other fermentation products of fructans have, however, other beneficial effects, which are not restricted to infants. It has been shown that fermentation products of fibers such as fructans also support epithelial barrier function and immune responses. Van den Abbeele et al.

TABLE 13.1 Prebiotic effect of inulin-type fructans and agave fructans in clinical trials.

Fructan	Concentration (g/100 mL)	Subjects	Study design	Outcome	References
GOS/FOS mixture (9:1)	0.8	Infants, aged 7−8 weeks ($N = 68$)	Randomized, double-blind, placebo-controlled intervention study. Infants were randomly allocated into 2 groups: Formula (SF) and Formula + prebiotics (OSF). A group of breastfed (BF) infants was included as a reference. At study onset and after 4 and 6 weeks, fecal samples were examined for a number of *Bifidobacteria*, pH, SCFAs, and lactate.	OSF versus SF: ↑ *Bifidobacteria*, ↓ stool pH, ↑ acetate, ↓ propionate. OSF fermentation profile is more similar to that of the BF group.	Knol et al. (2005)
FOS	0.4	Preterm infants aged 1−14 days ($N = 56$)	A prospective double-blind study. Healthy formula-fed infants received either formula with prebiotic FOS ($N = 36$) or placebo ($N = 20$) for 14 days. Fecal samples were collected on inclusion day and on day 7. The number of *Bifidobacteria*, stool characteristics, and somatic growth were recorded.	FOS versus Placebo: ↑ *Bifidobacteria*, ↑ bacteroides, ↑ stool frequency, ↓ *Escherichia coli*, ↓ enterococci.	Kapiki et al. (2007)
GOS/lcFOS mixture (9:1)	0.4	Term infants whose breastfeeding stopped at 14 days old ($N = 160$)	Prospective, double-blind, study. Comparison of growth, acceptability, and proportion of *Bifidobacteria* and clostridia in the stool flora of formula-fed infants. Infants were randomly assigned to a group fed with standard formula with GOS/lcFOS (PBF group) or the same formula without added prebiotics (STF group). Stool samples were taken at the beginning and end of the 6-week study, and the number of *Bifidobacteria* and clostridia was determined.	PBF versus STF: ↑ *Bifidobacteria*, ↑ stool frequency, ↑ stool softness, ↓ *E. coli*, ↓ clostridia.	Costalos et al. (2008)
GOS/lcFOS mixture (9:1)	0.4	Full-term formula-fed (FF) infants ($N = 139$).	Randomized, controlled, double-blind, prospective clinical trial. FF infants were randomized to consume a partially hydrolyzed whey formula with (PRE) or without (CON) prebiotic mixture. Fecal bacteria, pH, and SCFA were assessed at baseline, 3 and 6 weeks. A breastfed group (BF) was included as a reference.	PRE versus CON: ↑ *Bifidobacteria*, ↓ fecal pH. FF versus BF: ↑ *Clostridium*, ↑ SCFAs.	Holscher et al. (2012)
scITF/lcITF mixture (1:1)	0.8	Term healthy neonates ($N = 300$)	Double-blind, randomized, placebo-controlled, and parallel trial. Neonates were randomized to infant formula either with (SYN1) or without (C) prebiotic. A reference group of breastfed (BF) infants was included. Stool samples were collected at inclusion and at 3 months. Microbiota analyses, stool frequency, and characteristics were determined.	SYN1 versus C: ↑ *Bifidobacteria*, ↓ *Bacteroides*, ↓ *Enterobacteriaceae*.	Closa-Monasterolo et al. (2013)

Continued

TABLE 13.1 Prebiotic effect of inulin-type fructans and agave fructans in clinical trials.—cont'd

Fructan	Concentration (g/100 mL)	Subjects	Study design	Outcome	References
Oligofructose	0.3	Infants aged 1 −13 days ($N = 95$)	Multicenter, prospective, double-blind, controlled study. Infants were randomized to the α-lactalbumin-enriched control formula (CF) or identical formula with oligofructose (EF). Stool samples were collected at baseline and after 1, 2, 4, and 8 weeks, to evaluate the impact of prebiotic-supplemented infant formula on fecal microbiota, stool characteristics, and hydration. Infants fed with human milk (HM) were included as a reference group.	EF versus CF: ↑ *Bifidobacteria*, softer stools.	Wernimont et al. (2015)
scAF, lcAF, and scAF/lcAF mixture (1:1.5)	0.5	Term infants aged 20 + 7 days ($N = 600$)	Randomized, double-blind, controlled trial. Infants were split in 5 groups: 1) Formula + Probiotics + scAF + lcAF. 2) Formula + Probiotics + lcAF. 3) Formula + Probiotics + scAF. 4) Formula + Probiotics. 5) Only formula. A breastfed (BF) group was included as a control. Fecal samples were collected at the onset and at the end of the study (3 months). Changes in gut microbiota were determined.	Group 1 Vs Group 5: ↑ *Bifidobacteria*, ↓ *Enterobacteriaceae*, ↓ *Clostridium*.	López-Velázquez et al. (2015)
GOS/lcFOS mixture (9:1)	0.6	Term infants aged 2 −12 weeks ($N = 443$)	Comparison of the composition of fecal microbiota from infants recruited in previous BINGO and KOALA birth cohort studies. Three groups of infants were included according to their type of feeding: Formula-fed fortified with prebiotics (BINGO cohort, BFF), mixed feeding (breast-milk + formula, MF), and formula-fed without prebiotics (KOALA cohort, KFF). A breastfed group (BF) was included.	BFF versus BF: ↑ *Bifidobacteria*, ↑ *Blautia*, ↑ *Dorea*, ↑ *Granulicatella*, ↑ *Eubacterium*, ↑ *Catenibacterium*, ↓ *Parabacteroides*. KFF versus BF: ↓ *Bifidobacteria*, ↓ *Lactobacillus*, ↓ *Halomonas*, ↓Aeribacillus, ↑ *Barnesiella*, ↑ *Alistipes*, ↑ *Escherichia-Shigella*, ↑*Veillonella*, ↑ *Flavonifractor*, ↑ *Clostridium*, ↑ *Lachnospiraceae*.	Borewicz et al. (2019)

FOS, Fructooligosaccharides; *GOS*, galactooligosaccharides; *lcAF*, long chain agave fructans; *lcITF*, long-chain inulin-type fructans; *scAF*, short chain agave fructans; *scITF*, short chain inulin-type fructans.

(2018) tested the impact of the fermentation products from ITFs and that of arabinoxylo-oligosaccharides (AXOS) after fermentation by adult microbiota on transepithelial electrical resistance (TEER) of Caco-2 cell monolayers. Caco-2 cells were cocultured in a transwell system with THP1-derived macrophages in order to assess the immune effect of the fermentation products that were in contact with Caco-2 cells. Fermentation products coming from both inulins and AXOS stimulated the gut barrier by increasing TEER. Immune function was also enhanced, as an increase of NF-κB, IL-10 and IL-6 was observed in the THP-1 cells (Van den Abbeele et al., 2018).

The prebiotic effect of fructans has also been demonstrated in adults. scAFs and lcAFs, as well as some nonfructan dietary fibers such as predigested calices from *Hibiscus sabdariffa* (*Hb*) plant, were fermented by fecal microbiota of

TABLE 13.2 In vitro studies of the prebiotic effect of fermentation products of inulin-type fructans and agave fructans alone, or in symbiotic combination with bacteria.

Fructan (DP)	Concentration	Experiment design	Results	References
FOS Native inulin	1:10 (v/v) in 54 mL of standard ileal efflux medium.	In vitro study of FOS fermentation by a pool of fecal microbiota from 4 exclusively breastfed infants. Fecal samples were collected at 2 and 8 weeks old. Microbial composition, SCFAs production, and cytokine profiles of immature DCs were determined.	2 weeks-old fecal samples: Utilized trisaccharides in FOS and native inulin with DP3-8. 8 weeks-old fecal samples: ↑ *Bifidobacterium*, degraded native inulin with DP < 16. Fermentation products of both prebiotics attenuated proinflammatory cytokines produced by DCs, but they were stronger with native inulin.	Logtenberg et al. (2020)
lcAFs (DP 30−60) scAFs (OF, DP 10−30)	7.5 g/d	Study of the changes in adult gut microbiota upon addition of AFs, OF and other food ingredients in a dynamic in vitro model of the human colon (TIM-2). A pool of fecal samples donated by three donors aged 28−47 years old was prepared and 70 mL were inoculated to TIM-2, which already had the prebiotics. Samples were taken at the onset, 24, 48 and 72h of the fermentation. Simulated ileal effluent medium was used as control. Microbiota composition and SCFAs production were determined.	AFs: ↑ formic acid, acetic:propionic:butyric acid molar ratio 42:16:40. OF: ↑ *Bifidobacterium*, ↑ *Catenibacterium*, ↑ butyric acid, acetic:propionic:butyric acid molar ratio 33:20:45. ↑ SCFAs production (175 mmol) after 72 h fermentation.	Sayago-Ayerdi et al. (2020)
Inulin (FIB) (DP 3−60) AXOS (average DP6)	5 g/L	In vitro fermentation study of fecal inocula from three human donors, coupled to cocultures of Caco-2 cells and THP1 macrophages. Fermentation was carried out in anaerobiosis for 48 h at 37°C. Microbial activity and composition, gut barrier function, and macrophage cytokine expression in response to inulin/AXOS fermentation were evaluated for each subject. A control of inocula without prebiotics was included.	FIB: ↑ *Firmicutes*, ↑ *Actinobacteria*, ↓ *Lentisphaerae*, ↓ *Verrucomicrobia*, ↑ Propionate, ↑ Butyrate, ↓ branched-SCFAs, ↑ TEER, ↑ NF-κB, ↑ IL-10, ↑ IL-6. AXOS: ↑ *Bacteroidetes*, ↑ Actinobacteria, ↓ *Lentisphaerae*, ↓ *Verrucomicrobia*, SCFAs production was donor-dependent, ↓ branched-SCFAs, ↑ NF-κB, ↑ IL-10, ↑ IL-6.	Van den Abbeele et al. (2018)
scGOS lcGOS scFOS lcFOS	0%.2% (wt/vol) in MRS medium without glucose	In vitro study to evaluate the ability of utilization of GOS and FOS prebiotics by a collection of Bifidobacterial species in pure culture and coculture. Medium supplemented with each prebiotic was inoculated with bifidobacterial strains at 1% (vol/vol). Growth and oligosaccharide utilization of the different *Bifidobacterium* strains was tested.	*B. bifidum* and *B. longum* subsp. *longum* utilized short-chain GOS and FOS. *B. breve* and *B. longum* subsp. *infantis* could metabolize both short-chain and long-chain GOS and FOS. In coculture, *B. breve* was numerically dominant over *B. longum* subsp. *infantis.*	(Sims & Tannock, 2020)

Continued

TABLE 13.2 In vitro studies of the prebiotic effect of fermentation products of inulin-type fructans and agave fructans alone, or in symbiotic combination with bacteria.—cont'd

Fructan (DP)	Concentration	Experiment design	Results	References
FOS (DP 2−8) Inulin (DP 2 −60)	5, 15, and 20 mg/mL in M9 minimal medium and DMEM medium	In vitro study of the effect of addition of FOS or inulin to *P. aeruginosa* to evaluate its pathogenicity. Bacteria were cultured at 37°C, for 24h in a medium with or without the addition of FOS and inulin. Growth capacity of biofilm formation, and motility behavior were determined. Cytokine profiles and NF-κB pathway proteins of infected rat macrophages were also determined, as well as endotoxin-A concentration in infected rat IEC cells.	FOS: ↓ growth, ↓biofilm formation, ↓ swarming and twitching, ↓ endotoxin-A, ↓cytokine response of rat primary monocytes to *P. aeruginosa* coculture, activation of NF-κB pathway in IEC cells.	Ortega-González et al. (2014)
lcITF DP (10 −60)	0.5 mg/mL	In vitro study of the effect of lcITF alone or combined with *Lactobacillus acidophillus* W37 (LaW37), *L. brevis* (LbW63), and *L. casei* W56 (LcW56), on epithelial barrier function of caco-2 cells. LW37 was challenged with *Salmonella thyphimurium* (STM). Transepithelial electrical resistance (TEER), gene expression, and IL-8 production were studied.	lcITF: Regulation of 128 genes related to energy metabolism. LaW37: ↑ regulation of 26 genes related to tight junctions, ↓ regulation of the canonical NF-κB pathway, ↑ TEER, prevention of STM-induced barrier disruption, ↓ IL-8 secretion.	Lepine et al. (2018)
lcITF DP (10 −60)	0.5, 1 and 5 mg/mL	In vitro study of the effect of lcITF alone or in symbiosis with *Lactobacillus acidophillus* W37 (LaW37), on Toll-like receptor (TLRs) signaling and cytokine secretion by DCs. The effect of media of intestinal epithelial cells (IEC) exposed to both ingredients and their combination (caco-spent medium, CSM) was determined. The effects of DC responses against *Salmonella thyphimurium* (STM) were also investigated.	lcITFs: Direct stimulation of TLR2, 3, and 5. LaW37: Activated TLR2, stimulation of a proinflammatory phenotype in DCs. LaW37-CSM: ↑ IL-8, TNFα and IL-1ra. lcITFs + -LaW37: Activated TLR2, 3 and 5, attenuation of DCs response. lcITFs + LaW37-CSM: Regulatory cytokine, synergistic enhancing effects on IL-6 and IL-8 production.	Lepine et al. (2018)
lcITF	0.114 g/d/kgBW 0.114 g/d/kgBW $+5 \times 10^9$ CFU/d/piglet	In vivo study to investigate whether lcITFs alone or in combination with *L. acidophillus* strain W37 (LaW37) can support vaccination efficacy against *S. typhimurium* (STM) of neonatal piglets. The influence of the intervention on the gut microbiota of piglets was also studied. The animals received supplementary feed until sacrifice. The piglets were vaccinated when they were 25 days old. On days 52−54 the animals were challenged with STM.	lcITFs: ↑ postweaning feed efficiency, ↑ fecal consistency. lcITFs + LaW37: ↑ *Prevotellaceae*, ↓ *Lactobacillaceae* in feces, enhanced vaccination efficacy 2-fold during STM challenge.	Lepine et al. (2019)

TABLE 13.2 In vitro studies of the prebiotic effect of fermentation products of inulin-type fructans and agave fructans alone, or in symbiotic combination with bacteria.—cont'd

Fructan (DP)	Concentration	Experiment design	Results	References
Inulin	1.0%, 1.5%, and 2.0% (w/v) of MRS broth	In vitro analysis of different probiotics and prebiotics for proposing an optimal probiotic prebiotic symbiotic preparation. Incubation for 48h at 37°C of 5 Lactobacillus strains, in MRS medium supplemented with inulin, maltodextrin, corn starch, β-glucan, or apple pectin. Probiotic growth, SCFAs production, differences in lactate isomers produced, and enzymatic profiles were tested. The influence of the prebiotic used on the antagonistic activity of probiotics against pathogenic bacteria was also studied.	Growth, metabolic profile, and antagonistic activity of the probiotics toward selected pathogens were the most favorable when 2% (w/v) of inulin was used. The symbiosis of inulin with the *Lactobacillus* strains studied was proposed as a promising mixture for positively impacting host's GIT health and functionality.	(Slizewska and Chlebicz-Wójcik, 2020)

AXOS, arabinoxylo-oligosaccharides; *DCs,* Dendritic cells; *FOS,* fructooligosaccharides; *GIT,* gastro-intestinal tract; *GOS,* galactooligosaccharides; *IEC,* intestinal epithelial cells; *lcAFs,* long chain agave fructans; *lcITF,* long-chain inulin-type fructans; *OF,* oligofructose; *scAFs,* short chain agave fructans; *SCFAs,* short-chain fatty acids; *scITF,* short chain inulin-type fructans; *wt,* weight.

donors with an age between 25 and 57 years. The fecal inoculum was applied to a dynamic in vitro model of the human colon (TIM-2) while supplemented with fructans. Fermentation of scAFs led to the highest production of butyric acid compared with the lcAFs and the predigested calices from Hb. These scAFs also strongly supported the expansion of *Bifidobacteria* (Sáyago-Ayerdi et al., 2020) (Table 13.2).

ITFs have also been studied in symbiotic combinations, *i.e.*, probiotic—prebiotic combinations. Many health benefits have been attributed to symbiotic combinations of fructans with probiotics, including improvement of the intestinal absorption of minerals (Abrams et al., 2005), or better regulation of appetite (Delzenne et al., 2005), and decreased symptoms during inflammatory intestinal injury (Shiou et al., 2013). However, only a few have been experimentally confirmed such as prevention of infection. Our research group has studied the impact of the symbiotic combination of different strains of *Lactobacillus* in the presence and absence of lcITFs for the prevention of *Salmonella typhimurium* (STM) infection. Firstly, in an in vitro model of STM infection, the STM-associated epithelial barrier disruption of Caco-2 cells monolayers was prevented by the presence of *Lactobacillus acidophillus* strain W37 (LaW37) (Lépine & de Vos, 2018; Lépine et al., 2018). Moreover, to gain insight into the immune effect of the lcITFs/LaW37 combination, DCs were used. As DCs are localized in-between IECs, they sense and detect gut-luminal antigens coming from beneficial microbiota or pathogenic microbes. DCs produce specific cytokines to initiate a tolerogenic or inflammatory response. To study how DCs would respond to lcITFs/LaW37 symbiotic combination, DCs exposed to STM-challenge in the presence or absence of medium from Caco-2 cells which were previously exposed to lcITFs/LaW37 symbiotic combination. When DCs were exposed to STM without medium, it was shown that a strong proinflammatory cytokine response was induced. This response, however, was more regulatory and attenuated when the DCs were exposed to medium from Caco-2 cells that were pre-exposed to lcITFs/LaW37 symbiotic combinations. Especially, the TNF-α response in DCs was significantly reduced (Lépine & de Vos, 2018) (Table 13.2). Secondly, using neonatal piglets as a model for infants, we studied whether dietary intervention with the symbiotic lcITFs/LaW37 combination was associated with a better development of gut microbiota and a better clearance of STM. We found that piglets receiving the symbiotic combination had reduced STM infection. This effect of reduced infection was probably due to the gut barrier-enhancing effect of the symbiotic combination (Lépine et al., 2019) (Table 13.2).

The symbiotic combination of five different *Lactobacillus* strains with five prebiotics extracted from diverse natural sources (inulin, maltodextrin, corn starch, β-glucan, and apple pectin) was also tested. The production of SCFAs, probiotic growth, and antagonistic activity of the probiotic strains toward pathogenic bacteria, such as *Salmonella* spp. or *Listeria monocytogenes* were measured. The growth, metabolic profile, as well as the antagonistic activity toward selected pathogens was the most favorable when inulin was used as carbon-source (Slizewska & Chlebicz-Wójcik, 2020).

3.3 Direct effects of fructans on immune cells

Considerable advances have been made in understanding and acknowledging the *direct* immunomodulatory effects of chicory and agave fructans. Our group and others have studied and proposed some of the mechanisms underlying these *direct* effects of fructans on host cells such as the binding of fructans to pathogen recognition receptors (PRRs), the enhancement of gut barrier function, and the impact of fructans on immune cell responses. Moreover, we have shown that this immune beneficial effect is strongly dependent on the identity of the fructans such as the chain-length, or linear versus branched structure (Vogt et al., 2013).

3.3.1 Binding of fructans to pathogen recognition receptors

One of the proposed mechanisms underlying the immunomodulating effect of ITFs relies on their ability to bind to PRRs on gut immune cells, such as PRRs present on DCs and intraepithelial lymphocytes (Kong, Faas, et al., 2020). These PRRs are Toll-like receptors (TLRs), nucleotide-binding oligomerization domain-containing proteins (NODs), Dectins, and RIG-I-like receptors (Kanneganti, 2020). The natural function of PRRs is to recognize conserved molecular structures that are broadly shared among pathogens, such as bacterial lipo-polysaccharides (LPS) (Takeda & Akira, 2004) and also beneficial microorganisms of the microbiota (Lebeer et al., 2010). These structures are known as pathogen-associated molecular patterns (PAMPs) (Sundaram & Kanneganti, 2021). Once PRRs recognize a substantial dose of specific carbohydrate moieties of PAMPs, signaling is activated for the production of an immunogenic response, through the secretion of proinflammatory or regulatory cytokines (Abreu, 2010) (Fig. 13.2).

Vogt et al. (2013) tested the effect of ITFs of different chain-lengths extracted from chicory on the cytokine release by human peripheral blood mononuclear cells (PMBCs). These PMBCs were stimulated with four different ITFs, followed by the determination of some pro- and antiinflammatory cytokines. Chain-length-dependent differences in ITFs stimuli were found, scITFs induced an antiinflammatory balance in IL-10/IL-12 cytokine ratios, compared to the lcITFs. To understand these effects, studies on reporter-cell lines expressing PRRs were performed and demonstrated that ITFs can bind and activate specifically TLRs and NODs. It was shown that ITFs are able to signal directly on immune cells via TLRs, primarily TLR2, while TLR4, 5, 7, 8, and NOD2 were mildly activated. Moreover, the stimulation resulted in the activation of the Nuclear Factor kB/Activating protein-1 promoter (NF-B/AP-1), and as such signaling was highly dependent on the myeloid differentiation primary response protein 88 (MyD88) pathway (Vogt et al., 2013) which indicates that effects are mainly TLR dependent.

Vogt et al. (2014) also studied the impact of ITFs on intestinal epithelial cell barrier function. This was done on stressed T84 cells in which gut barrier function was disrupted by the proinflammatory reagent phorbol 12-myristate 13-acetate (PMA). They showed that the barrier disruption by PMA could be prevented when cells were preincubated with scITFs. Also, it was shown that the protective effects of the specific stressor PMA could be explained by the impact of the

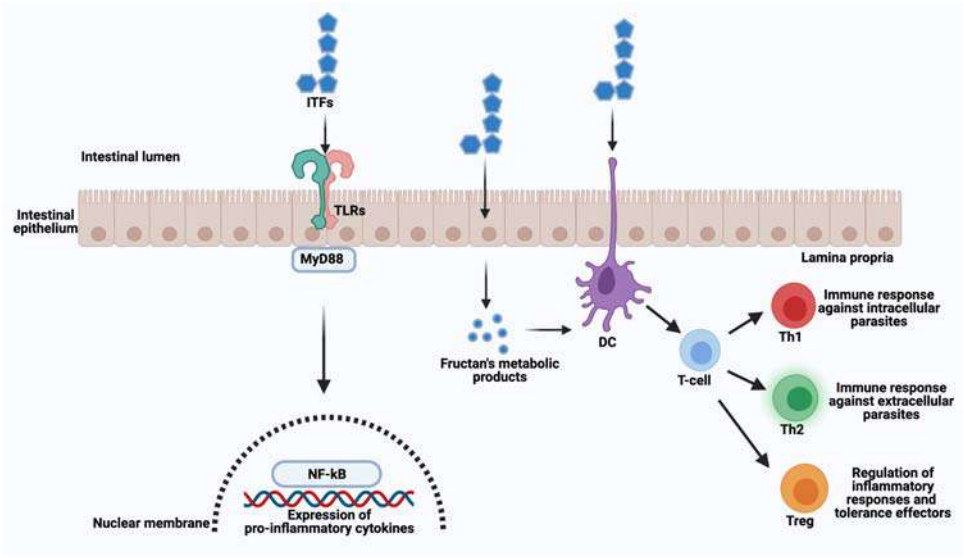

FIGURE 13.2 Representation of the *direct* beneficial effects of ITFs on gut immune barrier cells. *DC*, dendritic cells; *ITFs*, Inulin-type fructans. *Figure produced with BioRender.*

ITFs on TLRs receptors, specifically, TLR2. This was shown by applying an anti-TLR2 blocking antibody that prevented the protective effect of ITFs (Vogt et al., 2014).

3.3.2 Enhancement of gut barrier function

There are other components of the intestinal epithelium that are important for its adequate barrier function, such as the glycocalyx. The glycocalyx serves as a scaffold for the binding of intestinal microbiota and by doing so it contributes to barrier function. The glycocalyx is composed of glycans and proteins. The predominant glycosaminoglycans in glycocalyx are heparan sulfate (HS) and hyaluronic acid (HA). Recently the effect of dietary fibers on the maturation of the glycocalyx of intestinal epithelial cells was studied by Kong and collaborators (Kong et al., 2019). This maturation is important for the adequate development of gut barrier function and colonization by microorganisms in infants. ITFs of different DPs were applied to a Caco-2 intestinal epithelial cell line for 5 days. The thickness and area coverage of adsorbed albumin, HS, and HA in the glycocalyx were determined by immunofluorescence staining. ITFs increased glycocalyx development in a structure-dependent fashion. There was a DP-dependent effect. While scITFs selectively increased HS thickness, lcITFs significantly increased the area coverage of HA. These differential effects may account for the previously observed beneficial effects of these fructans on gut microbiota, as glycocalyx provides anchoring sites for bacterial adhesion. This effect could also provide a mechanistic explanation of the enhancement of the epithelial barrier function observed after treating cells with ITFs (Kong et al., 2019).

3.3.3 Impact of fructans on immune cell responses

Another mechanism by which ITFs can exert their beneficial effects on health is the decrease in concentration of inflammatory markers produced by immune cells such as DCs. In the intestinal epithelium, dendrites of DCs can protrude from the underlying lamina propria, between enterocytes to sense the contents of intestinal lumen and recognize PAMPs, as well as other antigens, and contribute to priming of immune responses but also induce tolerance (Fig. 13.2). Bermudez-Brito and colleagues investigated the effect of five commonly consumed fibers, including chicory inulin, on the cytokine production of DCs. First, they analyzed whether the direct contact of chicory inulin with DCs activated them, by measuring their production of cytokines. It was also determined if DCs were affected by bioactive factors produced by IECs after being stimulated with the studied fibers. To this end, an in vitro coculture system was used, which simulates the natural crosstalk between epithelial and immune gut cells. This coculture system is based on a 24-well plate, which has two compartments, the conventional well (basolateral side), and a smaller transwell that is suspended within the well. The bottom of the transwell is a permeable membrane that allows the flow of medium from the transwell to the lower chamber. DCs were seeded in the basolateral side of the plate and IECs were cultured in the transwell inserts. IECs were stimulated with the fibers. After stimulation with the fibers, cytokine production of DCs was measured. The authors found that chicory inulin only profoundly activated DCs when the DCs were stimulated simultaneously with supernatants from IECs that were also prestimulated with inulin (Caco-spent medium). However, in the coculture system, the proinflammatory cytokines IL-12, IL-6, and IL-8 were decreased by chicory inulin. Furthermore, in order to assess whether TLRs were involved in DCs activation, DCs were exposed to Caco-spent medium, in the presence and absence of MyD88 inhibitor. MyD88 is an adapter protein that links TLRs with down-stream signaling for the cytokine production. Caco-spent medium without inulin enhanced the production of proinflammatory cytokines in DCs, and this effect was strongly attenuated by inulin. When the assay was performed in the presence of MyD88 inhibitors, the attenuating effect was reduced. This demonstrates the dependency on the interaction of chicory inulin with TLRs. Finally, the effects of DCs stimulated with Caco-spent medium (DC-SM) on T-cell polarization were determined. To this end, naive T-cells were exposed to cocultures of DC-SM followed by the measuring of Th1, Th2, Th17, and Treg cytokines. Chicory inulin led to changes in Th1 cytokines but also reduced the Th2 cytokine IL-6, whereas the Treg cytokine IL-10 production was decreased. Based on all these findings, the authors proposed that an interplay between IECs, chicory inulin, and immune cells is necessary for inducing the regulatory immune effect of this dietary fiber (Bermudez-Brito et al., 2015).

Next, Bermudez-Brito and colleagues also studied the beneficial effect of galactooligosaccharides (GOS), chicory inulin as well as other dietary fibers such as sugar beet pectin, wheat arabinoxylan, barley β-glucan, and two digestion-resistant starches, in the context of bacterial infections that are commonly found in immunocompromised patients. To that end, the above-mentioned transwell system was used for mimicking the in vivo situation in the gut. The cocultures were treated with the Gram-negative bacilli *Sphingomonas paucimobilis* (*S. paucimobilis*). These bacteria were used as a model for the impact of an opportunistic pathogen that induces too strong immune responses and is difficult to eradicate with antibiotics therapy. Chicory inulin was one of the fibers that showed the strongest attenuation of the inflammatory effects provoked by *S. paucimobilis* infection, as IL-12 and TNFα were drastically decreased by inulin treatment. It was

also found that the IL-10/IL-12 ratio was significantly skewed toward more regulatory responses in the presence of chicory inulin and therefore effective in responses against pathogenic organisms that provoke too strong responses and are difficult to eradicate (Bermudez-Brito et al., 2016).

In order to gain more insight into the impact of the DP of ITFs on immunity, an in vivo study was performed. Fransen et al. (2017) fed conventional mice, as well as germ-free mice with two well-defined ITFs: scITFs and lcITFs. The authors found no differences in gut microbiota composition and fecal SCFAs production between mice fed with ITFs and untreated controls. Regarding immune cell populations, it was found that ITFs can modulate the immune system, as in Peyer patches (PPs), both ITFs induced a higher number of Th1 cells. Moreover, this immune modulation was ITF chain-length dependent, as in MLNs, only scITFs induced higher percentages of Treg cells and CD4+ T-cells expressing the activation marker CD69. Also, in MLNs, it was found that scITFs increased $CD11b^{-}CD103^{-}$ DCs and decreased $CD11b^{+}CD103^{+}$ DCs. As a result of the gene expression analysis in the ileum, an enhancement of the expression of the glycosylation gene 2-alpha-L-fucosyltransferase 2 (Fut2) and other IL-22-dependent genes was found. This finding was irrespective of the molecular weight or length of the applied ITF. The enhanced expression of Fut2 is associated which expedited microbial colonization and reduced chances of pathogenic infections. We therefore believe that Fut2-induced upregulation by ITFs is a novel but the crucial mechanism by which ITFs contribute to improved colonization of microbiota and support beneficial health effects in children fed with inulin-containing infant formula (Fig. 13.3).

The analysis of gene expression in PPs revealed that scITFs induced lower CD80 expression by $CD11b^{-}CD103^{-}$ DCs. While lcITFs modulated B-cell responses in the germ-free mice, as some of the genes involved in antibody production, such as IgD and CD20 were upregulated. Based on all the above-mentioned evidence, the authors demonstrated direct immune effects of ITFs in vivo, furthermore, such immunomodulation is ITF structure-dependent (Fransen et al., 2017).

scITFs and lcITFs were also tested in an animal model for autoimmune diabetes, i.e., NOD-mice (Chen et al., 2017). Consistent with previous studies, it was found that lcITFs, but not scITFs, enhanced regulatory CD25+ Foxp3+ CD4+ regulatory T cells, decreased cytotoxic IL17A+ CD4+ Th17 cells, and modulated cytokine production toward a more regulatory profile in the pancreas, spleen, and colon. This, but also the enhanced expression of gut barrier-enhancing tight junction proteins and SCFA explains the antidiabetogenic effect of lcITFs. Next-generation sequencing analysis revealed that lcITFs also enhanced *Firmicutes/Bacteroidetes* ratio and enriched modulatory *Ruminococcaceae* and *Lactobacilli*. The regulatory effects of lcITFs in the pancreas were subsequently tested in a pancreatitis model in mice. Also, here lcITFs but not scITFs were effective in attenuating inflammation in the pancreas via similar gut barrier-enhancing effects (He et al., 2017).

The immunomodulatory effect of agavin is not that well studied as for chicory inulin, but there are a few studies demonstrating that also agavin has direct immune-stimulating effects. For example, Moreno-Vilet et al. (2014) studied

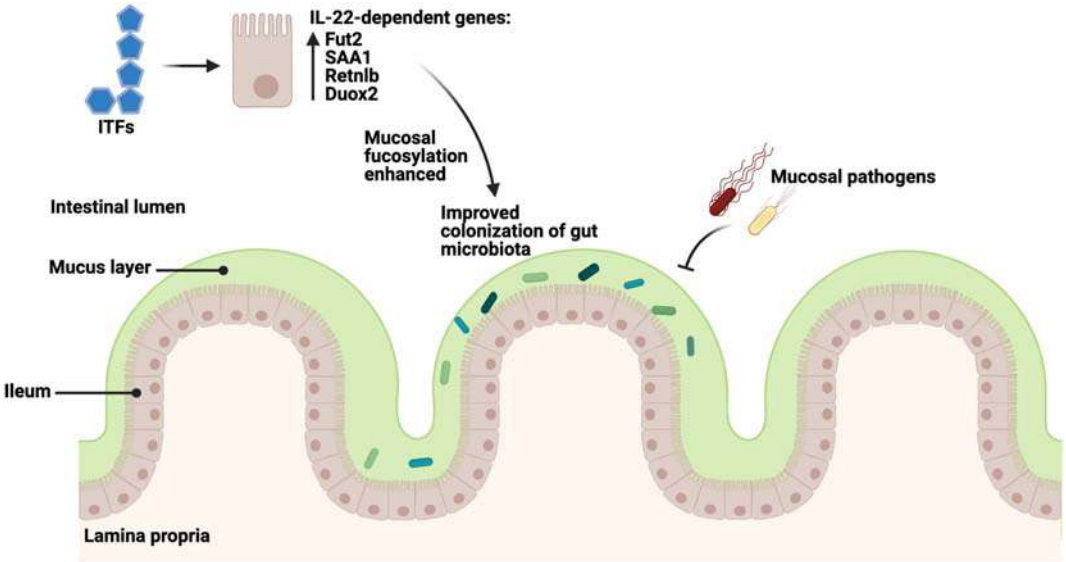

FIGURE 13.3 Inulin-type fructans up-regulate in vivo the microbial adhesion molecule Fuc2 independently of whether short or long-chain ITFs were given (Fransen et al., 2017). *DUOX2*, dual oxidase 2; *Fut2*, 2-alpha-L-fucosyltransferase; *SAA1*, serum amyloid A1; *RETNLB*, resistin like beta. *Figure produced with BioRender.*

in vitro the role of chicory and agave fructans, alone or in combination with probiotics as activators of the immune system. Activation, proliferation, and differentiation of T cells was measured. This was done on T-cells isolated from peripheral blood mononuclear cells that were incubated with agave and chicory fructans, alone or in combination with *Lactobacillus* strains. The early activation of lymphocytes was measured through the expression of CD69-positive cells. Also, the expression of T-bet and FOXP3 transcription factors for lymphocyte differentiation was measured. Agave fructans were the strongest stimulators of T-bet and FOXP3 transcription factor. The authors suggest on the basis of the results that fructans might stimulate intestinal T-cell mediated host defenses and prevent the possible manifestation of clinical disease (Moreno-Vilet et al., 2014).

The efficacy of agave fructans to prevent or attenuate immune-mediated disease has been studied in the autoimmune disorder systemic lupus erythematosus (SLE). In a study by Gutiérrez-Nava et al. (2017), a mice model of SLE was generated by intraperitoneal administration of tetramethylpentadecane to female mice. Compared with the SLE positive control group, the group of SLE animals that received treatment with agave fructans showed a significant decrease in all the SLE biomarkers such as knee articular diameter, proteinuria levels, antinuclear autoantibodies, and proinflammatory cytokines. The authors suggest that the antiinflammatory effect of agave fructans observed might be due to their immunomodulatory ability, at different levels. Agave fructans may also participate in the activation of TLRs 2 and 4 but this remains to be experimentally verified (Peshev & Van den Ende, 2014). Also, a possible effect of agave fructans in the modulation of the characteristic SLE Th2-type immune response was suggested. Finally, the authors concluded that antiinflammatory effect could be another mechanism by which agave fructans would be acting as modulators of SLE development in their animal model (Gutiérrez-Nava et al., 2017).

The immune-stimulating effects of inulin-type fructans (ITFs) have also been shown in humans in a vaccination study. It was demonstrated in a double-blind placebo-controlled trial by Vogt et al. (2017) that ITFs dietary supplementation improved immune responses to hepatitis B virus. To that end, 40 healthy volunteers were supplemented with a single dose of scITFs or lcITFs for 14 days. All the subjects were vaccinated against hepatitis B on day 7. At the end of the trial, blood anti-Hbs antigen titer (HBsAg) was measured. It was found that both ITFs induced TLR2 activation in a dose-dependent fashion, but lcITFs stimulated TLR2 stronger than scITFs. Cytokine patterns in PMBCs exposed to ITFs, showed a more immune-stimulating Th1-inducing effect of lcITFs, as TNFα production was higher compared with scITFs. A more immune-attenuated, Th1-inhibiting effect was found for scITFs, as the concentration of IL-6 was significantly lower in immune cells treated with this fiber. Not surprisingly the inulins had a different impact on antibody development after vaccination in young adults. The group of subjects who received lcITFs supplementation showed the highest HBsAg titers after day 35 compared with the group supplemented with scITFs and the placebo group. This finding was expected as the response to hepB vaccination is a Th1-dependent immune reaction. In summary, this work demonstrated for the first time the chain-length-dependent supportive effect of ITFs in human immunity (Abrams et al., 2005; Vogt et al., 2017).

3.3.4 Bone mineral metabolism

ITFs have much more beneficial effects on the host than having effects on the immune system. In a couple of studies by Abrams and colleagues, the effects of ITFs diet supplementation on calcium absorption and bone mineral accretion were assessed. The authors recruited 100 subjects aged 11 years and split them up in placebo group (supplementation with maltodextrin) or fructan treated group. The subjects consumed daily at breakfast an orange juice enriched with calcium and a mixture of scITFs and lcITFs (8 g/day) or maltodextrin during 1 year. Calcium absorption and bone mineralization were measured at the onset, 8 weeks, and after 1 year after the intervention. A blood sample was also collected for DNA analysis of vitamin D receptor polymorphisms. After 1 year, calcium absorption was significantly enhanced in the fructan group compared to the placebo group. This increase was accompanied by an increment in both whole-body bone mineral content and whole-body bone mineral density. The authors concluded that the inclusion of prebiotics such as ITFs in the daily diet enhances calcium absorption and bone mineralization in pubertal subjects. A possible mechanism underlying such effects was proposed. The authors proposed that calcium absorption was enhanced at the colon level. This hypothesis was based on the observation of enhancement of calcium solubility in the intestinal lumen, as the intestinal pH was decreased by the SCFAs produced by the fermentation of ITFs by intestinal microbiota (Abrams et al., 2005, 2007). The same group conducted a kinetic study of calcium absorption in healthy young adults aged 18−27 years. First, the subjects ingested 8 g/day of ITFs for 8 weeks. Afterward, calcium stable isotopes were orally and intravenously administered. Serum samples were collected during 26 h after the calcium administration. Isotope enrichment was measured in serum samples and also in 48h-pooled urine samples. All the subjects maintained diets with a calcium intake between 800 and 1000 mg/day during the study period. Eight subjects responded to the ITFs supplementation with an increased calcium absorption of at least 3%. Calcium colonic absorption represented 69% of the increase or it was equivalent to 49 mg/day. Thus, this study

demonstrated that supplementation with ITFs increased calcium absorption at the colon level. The authors underpinned the importance of ITFs benefits on the enhancement of colonic absorption. This finding would be of special interest to those patients with impairment of small intestine absorption (Abrams et al., 2007).

In summary, there have been made substantial advances in the elucidation of the immune mechanisms exerted by chicory and agave fructans that contribute to explain their health benefits. Beyond their extensively proven prebiotic effects, it has been documented that these dietary fibers, through direct contact, are sensed by receptors in different types of cells in the gut such as epithelial cells and DCs. Upon contact with fructans, specific components of immunity, such as TLRs and other PRRs, modestly trigger downstream cell signaling that leads to subsequent cytokine responses. These cytokine profiles can be of regulatory or stimulating nature (Fig. 13.2). Such effects are finally reflected in benefits, i.e., favoring of beneficial microbiota establishment, prevention of infections by avoiding the pathogenic adhesion to the intestinal epithelium, potentiation of immune stimulation during vaccination, or strengthening of the epithelial barrier. Moreover, it has been demonstrated that these direct beneficial effects of fructans are strongly dependent on their chemical structure and composition. All this scientific progress can be translated into the proposal of better-designed options for disease prevention according to the needs of specific life stages. In the following section, we will update the evidence about the immune-related aiding effect of chicory and agave fructans in the human disease state.

3.4 Effect of chicory and agave fructans on disease

3.4.1 Intestinal diseases

Functional bowel disorders comprise a group of inflammatory conditions of the gastrointestinal tract. Common examples of functional bowel disorders are IBS, Crohn's disease (CD), Ulcerative colitis (UC), and functional dyspepsia (Lacy et al., 2016). The functional bowel disorders etiology is complex, and it is believed to involve microbial dysbiosis and altered gut immune function. Patients with functional bowel disorders can present chronic recurrent episodes (with variable degree and duration) of symptoms such as abdominal pain, visceral hypersensitivity, bloating, distension, and abnormalities of bowel habits. In some cases, a psychological component, i.e., anxiety and depression, can also be involved due to disturbances in the gut − brain axis. Consequently, functional bowel disorders have a high impact on the quality of life of patients (Black et al., 2020).

Genetic predisposition and environmental factors such as unhealthy lifestyle but also Westernized-diet leading to dysbiosis do contribute to the ever-increasing frequency of functional bowel disorders (Wilson et al., 2019). Many of these factors contribute to alterations in gut microbiota or immune responses giving pathogenic bacteria a better chance to colonize and contribute to an inflammatory state of the gut. Such inflammatory state impairs the integrity of the intestinal epithelium, causing a more permeable, leaking gut which contributes to a further escalation of inflammatory processes (Del Fabbro et al., 2020). The inflammatory processes may become so severe that also enteric nerves become damaged which leads to visceral hypersensitivity and motility abnormalities (Talley, 2020).

Although there is not a curative medication yet, supplementation with dietary fibers such as ITFs has been proposed as a preventive or therapeutic option for many gastrointestinal disorders (Fransen et al., 2017). There are several trials where the effects of ITFs alone or in symbiotic combination with probiotics such as *Bifidobacterium* or *Lactobacillus* were studied (Ford et al., 2018; Man et al., 2020). In patients with CD, the supplementation of 15 g/d of ITFs for 3 weeks induced a significant reduction in the disease activity, increased fecal bifidobacteria, as well as an increased percentage of IL-10 positive regulatory DCs (Lindsay et al., 2006). In a follow-up study by Benjamin and colleagues, the supplementation of 15 g/d of ITFs during 4 weeks in patients with CD resulted in a reduction in the proportion of proinflammatory IL-6 positive DCs along with increased IL-10 regulatory positive DCs illustrating the regulatory effects of ITFs (Benjamin et al., 2011).

Not all ITF-related human trials have focused on immunological processes, but still found positive effects on bowel function (Closa-Monasterolo et al., 2013; Vandenplas et al., 2017). Micka et al. found improved stool frequency, consistency, and bowel function in healthy constipated subjects after supplementation with 12 g/d of ITFs (Micka et al., 2017). Moreover, in children with celiac disease ITFs supplementation alleviated symptoms of the disease (Drabińska, Jarocka-Cyrta et al., 2018; Drabińska, Krupa-Kozak et al., 2018; Drabińska et al., 2019; Krupa-Kozak et al., 2017). In another study it was also documented that doses of inulin up to 10 mg/mL can be well tolerated in healthy subjects (Bonnema et al., 2010).

Beneficial as well as negative effects of chicory inulin on intestinal bowel disorders have been reported in animal models. This might be due to the differences in the design of the experiments, the doses applied, and the duration as well as the types of fructans administered. In a study by Singh et al. (2019), aggravation of colonic inflammation was demonstrated after supplementation of the diet with either 7% scITFs or lcITFs in a mice colitis model. The exacerbation of colitis was

associated with the enrichment of butyrate-producing bacteria. The authors concluded that the severity of the disease should be considered and not be too far developed when supplementing colitis animals with dietary fibers (Singh et al., 2019).

In another study, the administration during 35 days with varying doses (5%−20%) of agave fructans was tested in a mice colitis model and demonstrated that not only disease severity but also the dose of fructans is important in providing beneficial effects on colitis. With supplementation of the diet with 12.5%, a higher production of butyric acid and other SCFAs was found. This had a direct beneficial impact on gut barrier function as demonstrated by enhanced epithelial cell proliferation and thickening of the mucosa in cecum and proximal colon. However, doses of 15% of fructans caused histological alteration of the cecum and colon which was characterized by disruption and loss of the mucus layer. This study clearly demonstrates that too high concentrations of fructans may have adverse effects on colitis and that in this specific colitis model a dose of 12.5% of agave fructans might be safe and beneficial in the prevention of gastrointestinal disorders (Castillo-Andrade et al., 2019).

In a recent study by Healey et al. (2021), the effect of ITFs supplementation in an animal model of colitis was studied. The authors found that mice fed with ITFs-enriched diet developed less colitis than the nonsupplemented group. The ITF-supplemented group had minimal colonic histopathological changes. The spleen weight was significantly lower in the ITF-supplemented group, which suggests reduced systemic inflammation. Moreover, in the ITF-supplemented group there were higher goblet cell numbers, but no significant reduction of the mucus layer thickness. Additionally, lower frequencies of the proinflammatory $Tbet^{+}IFN\gamma^{+}$ and $Tbet^{+}TNF^{+}$ $CD4^{+}$ T-cell subsets were observed in the spleen and mesenteric lymph nodes of the ITF-supplemented group, and a significant increase in frequency of regulatory $Foxp3^{+}IL\text{-}10^{+}$ and $Ror\gamma^{+}IL\text{-}22^{+}$ $CD4^{+}$ T-cells was found. Taken together these findings suggest that the consumption of ITF-enriched enteral diet can protect against immune activation and the development of colitis (Healey et al., 2021).

Based on all the evidence mentioned above, the therapeutic use of ITFs in patients with some gastrointestinal diseases looks promising, although it is important to consider and determine the effective dose, and the type of ITF to be supplemented. It has been documented that high doses (>15 g/d) of ITFs could induce adverse effects (Man et al., 2020). Furthermore, due to the fact that immunomodulatory effects of ITFs are chain-length dependent (Vogt et al., 2013) and can have opposite effects, the type of ITFs should receive more attention in future studies.

3.4.2 Obesity

The beneficial effect of the fructans extracted from chicory and agave has been exhaustively studied in the context of obesity in experimental animal models. Most of the research groups study the impact of dietary intervention with these fructans on metabolic markers such as body weight, serum glucose, cholesterol, triglycerides, and satiety-hormones such as glucagon-like peptide 1. The findings of these studies allow to conclude that chicory and agave fructans have potential beneficial effects on prevention of obesity and metabolic syndrome development, along with reducing effects on their comorbidities such as liver steatosis (Barbero-Becerra et al., 2021; Urías-Silvas et al., 2008). The proposed mechanisms underlying these effects include gut microbiota regulation and their metabolic products and regulation of signaling hormones for gastric satiety (Alvarado-Jasso et al., 2020).

In a recent study, Huazano-García et al. (2020) studied the effects of agavin in a mouse model of obesity and studied the impact of the agavin on gut microbiome, metabolic endotoxemia, and inflammatory state. The background is that obesity is related to a low-grade inflammatory state and gut dysbiosis, which might lead to a release of bacterial endotoxins such as LPS, a phenomenon also referred to as metabolic endotoxemia. In this study, mice were divided into groups for receiving a standard diet or high-fat diet alone or in combination with agavins. Agavin supplementation led to a microbiota composition more similar to those animals fed with standard diet. The high-fat group presented the highest LPS concentration, and the animals supplemented with agavins had a significant reduction of metabolic endotoxemia. Obese mice had increased serum proinflammatory cytokines (IL-1α, IL-1β, IL-6, and TNFα) combined with the lowest levels of regulatory cytokine IL-10. This could be prevented in obese animals supplemented with agavin. Obese animals on high-fat diet combined with agavin had a cytokine profile more similar to the standard-diet control and a significantly higher IL-10 level. The authors suggest that agavin supplementation attenuates the metabolic endotoxemia and low-grade inflammatory state in obesity (Huazano-Garcia et al., 2020). Similar findings were obtained with ITFs that also prevented high-fat-induced endotoxemia in mice (Li, Elmén, et al., 2020).

3.4.3 Antitumor effects of inulin

Many studies have demonstrated antitumor effects of inulin. It should be mentioned, however, that these studies mainly involve experimental models with chemically induced tumors in animal models (Allsopp et al., 2013; Gavresea et al.,

2018; Roller et al., 2004; Verma & Shukla, 2013), cell lines such as Caco-2 (Allsopp et al., 2013; Munjal et al., 2009; Sauer et al., 2007), or ex vivo experiments with samples of tumors (Kim et al., 2020; Mima et al., 2016; Richard et al., 2018). Clinical trials with cancer patients for studying antitumor effects of fructans are still scarce (Rafter et al., 2007; Roller et al., 2007). Despite this, some promising results have been obtained and some mechanistic insight into how inulin can reduce tumor growth has been generated.

In experimental animal models, it has been shown that a combination of ITFs in symbiosis with some probiotic lactobacillus or bifidobacterial strains can modulate responses against tumors. In a rat-study by Roller et al. (2004) supplementation with a prebiotic−probiotic symbiotic restored natural killer cell-like cytotoxicity to a colon cancer. Stimulation of the production of the regulatory cytokine IL-10 and the suppression of proliferative responses of lymphocytes from Peyer's Patches indicated that this was rather a stimulation of responses against the tumor than direct antiproliferative effects on the tumor itself (Roller et al., 2004).

In another study, the protective effect of inulin and lactulose against colon carcinogenesis was studied and was proposed to be due to direct effects of inulin on the production of carcinogenic metabolites such as secondary bile acids. To that end, male rats were pretreated with inulin and lactulose before colon carcinogenesis was induced by 1,2-dimethylhydrazine dihydrochloride injection. Aberrant crypt foci appearance was used as a marker for colon carcinogenesis and was significantly reduced in the groups treated with the inulin compared with the noninulin supplemented animals. The authors proposed that intervention with inulin could have a protective effect on induced carcinogenesis (Verma & Shukla, 2013).

The anticancer activity of agave fermentation products was studied by Allsopp and colleagues and was suggested to be caused by beneficial effects on gut epithelial cells. The Caco-2 cell line was exposed to agave fermentation products. An enhancement of epithelial barrier function was found. Moreover, no DNA damage or reduction in the proliferative activity of cells wase observed suggesting supportive effects of the agave fermentation products on epithelial function (Allsopp et al., 2013).

Also the effect of inulin on gut microbiota has been proposed as a mechanism for the antitumor effects of ITFs (Taghinezhad-S et al., 2020; Taper & Roberfroid, 2005; Theodoropoulos et al., 2016). This suggestion is based on two observations. The first is the current view that dysbiosis of gut microbiota is one of the main risk factors for colorectal cancer development (Drabińska, Jarocka-Cyrta et al., 2018; Drabińska, Krupa-Kozak et al., 2018; Drabińska et al., 2019), which can be prevented or corrected with inulin (Li, Elmén, et al., 2020; Li, Wang, et al., 2020; Liong, 2008). During dysbiosis, there are often more opportunistic bacteria such as *Escherichia coli, Clostridia, Bacteroides fragilis,* and *Enterococcus faecalis,* whose metabolic products have been proposed to act as potential genotoxic, carcinogenic, and tumorpromoting agents (Arthur et al., 2012; Chattopadhyay et al., 2021; de Vrese & Schrezenmeir, 2008; Ding et al., 2018; Liong, 2008; Richard et al., 2018). As inulin can shape the microbiota more toward genera such as *Bifidobacterium* and *Lactobacillus* it might overcome these risk factors (Li, Elmén, et al., 2020). The second route by which inulin might contribute via gut microbiota to the prevention of tumor development is by stimulation of production of beneficial fermentation products such as SCFAs. These SCFAs have been shown to prevent colon cancer development and can also act as inhibitors of the proliferative activity of cancer cells (Campos-Perez & Martinez-Lopez, 2021; Donohoe et al., 2014; Ohara & Suzutani, 2018; Sauer et al., 2007). However, studies that directly link chicory and agave fructans to clinical prevention or treatment of cancer are still needed. Also, more clinical trials that translate the current evidence available, for the design of better therapeutic options for the prevention and treatment of intestinal neoplasia remain to be performed.

4. Concluding remarks and future perspectives

During recent years, substantial advances have been made in understanding and determining the effects of chicory and agave fructans in health and disease as well as their underlying mechanisms. The *indirect* or prebiotic effects of these dietary fibers have been repeatedly and comprehensively demonstrated in vitro as well as in vivo and in clinical trials.

The *direct* immune effects of dietary fibers have become a major focus of research during the past decade. In the small intestine, there is amble opportunity for fibers to interact with gut epithelium and immune cells such as dendritic and intraepithelial lymphocytes which express pattern recognition receptors such as TLRs. Fructans have been proven to also act via this route and to contribute to gut homeostasis via triggering downstream signal transduction in gut immune cells that finally translates to a regulatory or tolerant effect. However, at the same time, it has been shown that not all fructans have the same efficacy, effects are very fructans' structure, type, chain-length, and dose-dependent. The use of modern technology such as metabolomics for a deeper characterization of the scopes of ITFs in human health and disease might be useful to gain more insight intohow fructans impact health (O'connell, 2020; Spacova et al., 2020).

Different areas in the world use fructans from different plant sources. As these fructans may differ to a great extent, it is essential not to generalize health benefits but to also study fructans that are not of chicory origin such as the structurally different agave fructans, commonly used in Latin America. These fructans might act differently and might also have different types of health benefits. Chapters 11 and 15 of this book refer to the potential of levan- and graminan-type fructans in terms of food and biomedical applications.

The knowledge generated on chicory and agave fructans contributes to the design of more personalized therapeutic options or food supplements in a prophylactic way (Reimer et al., 2020). Potential fields of application of fructans are to support healthy aging (Kiewiet et al., 2021), enhancement of effective vaccination (Vogt et al., 2017), or prevention of disease development and severity. It might even support the treatment of diseases such as inflammatory intestinal disorders, obesity, diabetes, and cancer (De Preter et al., 2013; Hiel et al., 2020; Li, Elmén, et al., 2020; Padilla-Camberos et al., 2018).

In this chapter, we have described the current insight into how fructans might impact health via changing gut microbiota, immune, or gut barrier function. During recent years, new insight has become available on mechanisms by which fructans can have such an effect but at the same time it has been demonstrated that effects highly depend on the structural characteristics of the fructans as well as on the age and health status of the host and probably even the gender of the consumer, e.g., differences between males and females have been observed in the effects of ITFs on mineral absorption (Roberfroid, 2005). For optimal dosing and maximal effects, it is necessary to gain more insight into which fructans should be applied for specific target groups allowing a more personalized approach to prevent disease. To illustrate the complexity, baby microbiota needs smaller DPs from chicory fructans to support fermentation processes but long chains are very much needed to support immune and gut barrier development. Giving exclusively smaller range DPs or longer DPs does not provide the needs of the infant at an early age. This is one of the many illustrations that to maximize the impact of fructans we need to tailor or mix fructans for specific target groups. Our expectation is that in the coming years we will learn more on specific needs of target groups and that science-based conclusions will be reached on which fructans should be given to specific individuals to maximize the impact on health and prevention of disease.

References

Abrams, S. A., Griffin, I. J., Hawthorne, K. M., Liang, L., Gunn, S. K., Darlington, G., & Ellis, K. J. (2005). A combination of prebiotic short- and long-chain inulin-type fructans enhances calcium absorption and bone mineralization in young adolescents. *American Journal of Clinical Nutrition, 82*(2), 471−476. https://doi.org/10.1093/ajcn.82.2.471

Abrams, S. A., Hawthorne, K. M., Aliu, O., Hicks, P. D., Chen, Z., & Griffin, I. J. (2007). An inulin-type fructan enhances calcium absorption primarily via an effect on colonic absorption in humans. *Journal of Nutrition, 137*(10), 2208−2212. https://doi.org/10.1093/jn/137.10.2208

Abreu, M. T. (2010). Toll-like receptor signalling in the intestinal epithelium: How bacterial recognition shapes intestinal function. *Nature Reviews Immunology, 10*(2), 131−143. https://doi.org/10.1038/nri2707

Ackerman, D. L., Craft, K. M., Doster, R. S., Weitkamp, J. H., Aronoff, D. M., Gaddy, J. A., & Townsend, S. D. (2018). Antimicrobial and antibiofilm activity of human milk oligosaccharides against *Streptococcus agalactiae, Staphylococcus aureus* and *Acinetobacter baumannii*. *ACS Infectious Diseases, 4*(3), 315−324. https://doi.org/10.1021/acsinfecdis.7b00183

Allsopp, P., Possemiers, S., Campbell, D., Oyarzábal, I. S., Gill, C., & Rowland, I. (2013). An exploratory study into the putative prebiotic activity of fructans isolated from *Agave angustifolia* and the associated anticancer activity. *Anaerobe, 22*, 38−44. https://doi.org/10.1016/j.anaerobe.2013.05.006

Alvarado-Jasso, G. M., Camacho-Díaz, B. H., Arenas-Ocampo, M. L., Jiménez-Ferrer, J. E., Mora-Escobedo, R., & Osorio-Díaz, P. (2020). Prebiotic effects of a mixture of agavins and green banana flour in a mouse model of obesity. *Journal of Functional Foods, 64*, 1−7.

Apolinário, A. C., De Lima Damasceno, B. P. G., De Macêdo Beltrão, N. E., Pessoa, A., Converti, A., & Da Silva, J. A. (2014). Inulin-type fructans: A review on different aspects of biochemical and pharmaceutical technology. *Carbohydrate Polymers, 101*(1), 368−378. https://doi.org/10.1016/j.carbpol.2013.09.081

Arslanoglu, S., Moro, G. E., Schmitt, J., Tandoi, L., Rizzardi, S., & Boehm, G. (2008). Early dietary intervention with a mixture of prebiotic oligosaccharides reduces the incidence of allergic manifestations and infections during the first two years of life. *Journal of Nutrition, 138*(6), 1091−1095. https://doi.org/10.1093/jn/138.6.1091

Arthur, J. C., Perez-Chanona, E., Mühlbauer, M., Tomkovich, S., Uronis, J. M., Fan, T. J., Campbell, B. J., Abujamel, T., Dogan, B., Rogers, A. B., Rhodes, J. M., Stintzi, A., Simpson, K. W., Hansen, J. J., Keku, T. O., Fodor, A. A., & Jobin, C. (2012). Intestinal inflammation targets cancer-inducing activity of the microbiota. *Science, 338*(6103), 120−123. https://doi.org/10.1126/science.1224820

Barbero-Becerra, V., Juárez-Hernández, E., Chávez-Tapia, N. C., & Uribe, M. (2021). Inulin as a clinical therapeutic intervention in metabolic associated fatty liver disease. *Food Reviews International*. https://doi.org/10.1080/87559129.2020.1867997

Barclay, T., Ginic-Markovic, M., Cooper, P., & Petrovsky, N. (2016). Inulin-a versatile polysaccharide with multiple pharmaceutical and food chemical uses. *Journal of Excipients and Food Chemicals, 1*(3), 27−50.

Benjamin, J. L., Hedin, C. R. H., Koutsoumpas, A., Ng, S. C., McCarthy, N. E., Hart, A. L., Kamm, M. A., Sanderson, J. D., Knight, S. C., Forbes, A., Stagg, A. J., Whelan, K., & Lindsay, J. O. (2011). Randomised, double-blind, placebo-controlled trial of fructo- oligosaccharides in active Crohn's disease. *Gut, 60*(7), 923−929. https://doi.org/10.1136/gut.2010.232025

Bermudez-Brito, M., Faas, M. M., & de Vos, P. (2016). Modulation of dendritic-epithelial cell responses against *Sphingomonas paucimobilis* by dietary fibers. *Scientific Reports, 6*. https://doi.org/10.1038/srep30277

Bermudez-Brito, M., Sahasrabudhe, N. M., Rösch, C., Schols, H. A., Faas, M. M., & de Vos, P. (2015). The impact of dietary fibers on dendritic cell responses in vitro is dependent on the differential effects of the fibers on intestinal epithelial cells. *Molecular Nutrition and Food Research, 59*(4), 698−710.

Black, C. J., Drossman, D. A., Talley, N. J., Ruddy, J., & Ford, A. C. (2020). Functional gastrointestinal disorders: Advances in understanding and management. *The Lancet, 396*(10263), 1664−1674. https://doi.org/10.1016/S0140-6736(20)32115-2

Bode, L. (2012). Human milk oligosaccharides: Every baby needs a sugar mama. *Glycobiology, 22*(9), 1147−1162. https://doi.org/10.1093/glycob/cws074

Bonnema, A. L., Kolberg, L. W., Thomas, W., & Slavin, J. L. (2010). Gastrointestinal tolerance of chicory inulin products. *Journal of the American Dietetic Association, 110*(6), 865−868. https://doi.org/10.1016/j.jada.2010.03.025

Borewicz, K., Suarez-Diez, M., Hechler, C., Beijers, R., de Weerth, C., Arts, I., Penders, J., Thijs, C., Nauta, A., Lindner, C., Van Leusen, E., Vaughan, E. E., & Smidt, H. (2019). The effect of prebiotic fortified infant formulas on microbiota composition and dynamics in early life. *Scientific Reports, 9*(1). https://doi.org/10.1038/s41598-018-38268-x

Camilleri, M., Madsen, K., Spiller, R., Van Meerveld, B., & Verne, G. (2012). Intestinal barrier function in health and gastrointestinal disease. *Neurogastroenterology & Motility, 24*(6), 503−512. https://doi.org/10.1111/j.1365-2982.2012.01921.x

Campos-Perez, W., & Martinez-Lopez, E. (2021). Effects of short chain fatty acids on metabolic and inflammatory processes in human health. *Biochimica et Biophysica Acta - Molecular and Cell Biology of Lipids, 1866*(5). https://doi.org/10.1016/j.bbalip.2021.158900

Carding, S., Verbeke, K., Vipond, D. T., Corfe, B. M., & Owen, L. J. (2015). Dysbiosis of the gut microbiota in disease. *Microbial Ecology in Health & Disease*. https://doi.org/10.3402/mehd.v26.26191

Castillo-Andrade, A. I., Bautista-Rivera, C., Ruiz-Cabrera, M. A., Soria-Guerra, R. E., García-Chávez, E., Fuentes-Ahumada, C., & Grajales-Lagunes, A. (2019). *Agave salmiana* fructans as gut health promoters: Prebiotic activity and inflammatory response in Wistar healthy rats. *International Journal of Biological Macromolecules, 136*, 785−795. https://doi.org/10.1016/j.ijbiomac.2019.06.045

Chambers, S. A., & Townsend, S. D. (2020). Like mother, like microbe: Human milk oligosaccharide mediated microbiome symbiosis. *Biochemical Society Transactions, 48*(3), 1139−1151. https://doi.org/10.1042/BST20191144

Chattopadhyay, I., Dhar, R., Pethusamy, K., Seethy, A., Srivastava, T., Sah, R., Sharma, J., & Karmakar, S. (2021). Exploring the role of gut microbiome in colon cancer. *Applied Biochemistry and Biotechnology*. https://doi.org/10.1007/s12010-021-03498-9

Chen, K., Chen, H., Faas, M. M., de Haan, B. J., Li, J., Xiao, P., Zhang, H., Diana, J., de Vos, P., & Sun, J. (2017). Specific inulin-type fructan fibers protect against autoimmune diabetes by modulating gut immunity, barrier function, and microbiota homeostasis. *Molecular Nutrition and Food Research, 61*(8). https://doi.org/10.1002/mnfr.201601006

Cheng, L., Akkerman, R., Kong, C., Walvoort, M. T. C., & de Vos, P. (2020). More than sugar in the milk: Human milk oligosaccharides as essential bioactive molecules in breast milk and current insight in beneficial effects. *Critical Reviews in Food Science and Nutrition*, 1−17. https://doi.org/10.1080/10408398.2020.1754756

Cheng, L., Kiewiet, M. B. G., Groeneveld, A., Nauta, A., & de Vos, P. (2019). Human milk oligosaccharides and its acid hydrolysate LNT2 show immunomodulatory effects via TLRs in a dose and structure-dependent way. *Journal of Functional Foods, 59*, 174−184. https://doi.org/10.1016/j.jff.2019.05.023

Cheng, L., Kiewiet, M. B. G., Logtenberg, M. J., Groeneveld, A., Nauta, A., Schols, H. A., Walvoort, M. T. C., Harmsen, H. J. M., & de Vos, P. (2020). Effects of different human milk oligosaccharides on growth of bifidobacteria in monoculture and co-culture with *Faecalibacterium prausnitzii*. *Frontiers in Microbiology, 11*. https://doi.org/10.3389/fmicb.2020.569700

Cheng, L., Kong, C., Wang, W., Groeneveld, A., Nauta, A., Groves, M. R., Kiewiet, M. B. G., & de Vos, P. (2021). The human milk oligosaccharides 3-FL, LNnT, and LDFT attenuate TNF-α induced inflammation in fetal intestinal epithelial cells in vitro through shedding or interacting with TNF receptor 1. *Molecular Nutrition & Food Research*. https://doi.org/10.1002/mnfr.202000425

Closa-Monasterolo, R., Gispert-Llaurado, M., Luque, V., Ferre, N., Rubio-Torrents, C., Zaragoza-Jordana, M., & Escribano, J. (2013). Safety and efficacy of inulin and oligofructose supplementation in infant formula: Results from a randomized clinical trial. *Clinical Nutrition, 32*(6), 918−927. https://doi.org/10.1016/j.clnu.2013.02.009

Collado, M. C., Cernada, M., Baüerl, C., Vento, M., & Pérez-Martínez, G. (2012). Microbial ecology and host-microbiota interactions during early life stages. *Gut Microbes, 3*(4). https://doi.org/10.4161/gmic.21215

Costalos, C., Kapiki, A., Apostolou, M., & Papathoma, E. (2008). The effect of a prebiotic supplemented formula on growth and stool microbiology of term infants. *Early Human Development, 84*(1), 45−49. https://doi.org/10.1016/j.earlhumdev.2007.03.001

Davis, E. C., Wang, M., & Donovan, S. M. (2017). The role of early life nutrition in the establishment of gastrointestinal microbial composition and function. *Gut Microbes, 8*(2), 143−171. https://doi.org/10.1080/19490976.2016.1278104

De Preter, V., Jossens, M., Ballet, V., Shkedy, Z., Rutgeerts, P., Vermeire, S., & Verbeke, K. (2013). Metabolic profiling of the impact of oligofructose-enriched inulin in Crohn's disease patients: A double-blinded randomized controlled trial. *Clinical and Translational Gastroenterology, 4*(1), e30.

Del Fabbro, S., Calder, P. C., & Childs, C. E. (2020). Microbiota-independent immunological effects of non-digestible oligosaccharides in the context of inflammatory bowel diseases. *Proceedings of the Nutrition Society, 79*(4), 468−478. https://doi.org/10.1017/S0029665120006953. Cambridge University Press.

Delzenne, N. M., Cani, P. D., Daubioul, C., & Neyrinck, A. M. (2005). Impact of inulin and oligofructose on gastrointestinal peptides. *British Journal of Nutrition, 93*, S157−S161. https://doi.org/10.1079/BJN20041342

Derrien, M., & van Hylckama Vlieg, J. E. T. (2015). Fate, activity, and impact of ingested bacteria within the human gut microbiota. *Trends in Microbiology, 23*(6), 354−366. https://doi.org/10.1016/j.tim.2015.03.002

Ding, C., Tang, W., Fan, X., & Wu, G. (2018). Intestinal microbiota: A novel perspective in colorectal cancer biotherapeutics. *OncoTargets and Therapy, 11*, 4797−4810. https://doi.org/10.2147/OTT.S170626

Donohoe, D. R., Holley, D., Collins, L. B., Montgomery, S. A., Whitmore, A. C., Hillhouse, A., Curry, K. P., Renner, S. W., Greenwalt, A., Ryan, E. P., Godfrey, V., Heise, M. T., Threadgill, D. S., Han, A., Swenberg, J. A., Threadgill, D. W., & Bultman, S. J. (2014). A gnotobiotic mouse model demonstrates that dietary fiber protects against colorectal tumorigenesis in a microbiota- and butyrate-dependent manner. *Cancer Discovery, 4*(12), 1387−1397. https://doi.org/10.1158/2159-8290.CD-14-0501

Drabińska, N., Jarocka-Cyrta, E., Markiewicz, L. H., & Krupa-Kozak, U. (2018). The effect of oligofructose-enriched inulin on faecal bacterial counts and microbiota-associated characteristics in celiac disease children following a gluten-free diet: Results of a randomized, placebo-controlled trial. *Nutrients, 10*(2). https://doi.org/10.3390/nu10020201

Drabińska, N., Jarocka-Cyrta, E., Złotkowska, D., Abramowicz, P., & Krupa-Kozak, U. (2019). Daily oligofructose-enriched inulin intake impacts bone turnover markers but not the cytokine profile in pediatric patients with celiac disease on a gluten-free diet: Results of a randomised, placebo-controlled pilot study. *Bone, 122*, 184−192. https://doi.org/10.1016/j.bone.2019.03.001

Drabińska, N., Krupa-Kozak, U., Abramowicz, P., & Jarocka-Cyrta, E. (2018). Beneficial effect of oligofructose-enriched inulin on vitamin d and e status in children with celiac disease on a long-term gluten-free diet: A preliminary randomized, placebo-controlled nutritional intervention study. *Nutrients, 10*(11). https://doi.org/10.3390/nu10111768

Dreher, M. L. (2018). Whole fruits and fruit fiber emerging health effects. *Nutrients, 10*(12). https://doi.org/10.3390/nu10121833

Dubois, B., Goubier, A., Joubert, G., & Kaiserlian, D. (2005). Oral tolerance and regulation of mucosal immunity. *Cellular and Molecular Life Sciences, 62*(12), 1322−1332. https://doi.org/10.1007/s00018-005-5036-0

Fan, C. H., Cao, J. H., & Zhang, F. C. (2016). The prebiotic inulin as a functional food - a review. *European Review for Medical and Pharmacological Sciences, 20*(15), 3262−3265. http://www.europeanreview.org/.

Figueroa-Lozano, S., & de Vos, P. (2019). Relationship between oligosaccharides and glycoconjugates content in human milk and the development of the gut barrier. *Comprehensive Reviews in Food Science and Food Safety, 18*(1), 121−139. https://doi.org/10.1111/1541-4337.12400

Flamm, G., Glinsmann, W., Kritchevsky, D., Prosky, L., & Roberfroid, M. (2001). Inulin and oligofructose as dietary fiber: A review of the evidence. *Critical Reviews in Food Science and Nutrition, 41*(5), 353−362. https://doi.org/10.1080/20014091091841

Ford, A. C., Harris, L. A., Lacy, B. E., Quigley, E. M., & Moayyedi, P. (2018). Systematic review with meta-analysis: The efficacy of prebiotics, probiotics, synbiotics and antibiotics in irritable bowel syndrome. *Alimentary Pharmacology and Therapeutics, 48*(10), 1044−1060. https://doi.org/10.1111/apt.15001

Fransen, F., Sahasrabudhe, N. M., Elderman, M., Bosveld, M., El Aidy, S., Hugenholtz, F., Borghuis, T., Kousemaker, B., Winkel, S., van der Gaast-de Jongh, C., de Jonge, M. I., Boekschoten, M. V., Smidt, H., Schols, H. A., & de Vos, P. (2017). β2→ 1-fructans modulate the immune system in vivo in a microbiota-dependent and-independent fashion. *Frontiers in Immunology, 8*, 154.

Fukuda, S., Toh, H., Hase, K., Oshima, K., Nakanishi, Y., Yoshimura, K., Tobe, T., Clarke, J. M., Topping, D. L., Suzuki, T., Taylor, T. D., Itoh, K., Kikuchi, J., Morita, H., Hattori, M., & Ohno, H. (2011). Bifidobacteria can protect from enteropathogenic infection through production of acetate. *Nature, 469*(7331), 543−549. https://doi.org/10.1038/nature09646

Gabriel, I., Olejek, A., Stencel-Gabriel, K., & Wielgoś, M. (2018). The influence of maternal vaginal flora on the intestinal colonization in newborns and 3-month-old infants. *Journal of Maternal-Fetal and Neonatal Medicine, 31*(11), 1448−1453. https://doi.org/10.1080/14767058.2017.1319352

Gavresea, F., Vagianos, C., Korontzi, M., Sotiropoulou, G., Dadioti, P., Triantafillidis, J. K., & Papalois, A. E. (2018). Beneficial effect of synbiotics on experimental colon cancer in rats. *Turkish Journal of Gastroenterology, 29*(4), 494−501. https://doi.org/10.5152/tjg.2018.17469

Gupta, N., Jangid, A. K., Pooja, D., & Kulhari, H. (2019). Inulin: A novel and stretchy polysaccharide tool for biomedical and nutritional applications. *International Journal of Biological Macromolecules, 132*, 852−863. https://doi.org/10.1016/j.ijbiomac.2019.03.188

Gutiérrez-Nava, Z. J., Jiménez-Aparicio, A. R., Herrera-Ruiz, M. L., & Jiménez-Ferrer, E. (2017). Immunomodulatory effect of *Agave tequilana* evaluated on an autoimmunity like-SLE model induced in Balb/c mice with pristane. *Molecules, 22*(6), 848.

Healey, G. R., Tsai, K., Lisko, D. J., Cook, L., Vallance, B. A., & Jacobson, K. (2021). An inulin-type fructan enriched exclusive enteral nutrition formula suppresses colitis through gut microbiome modulation and promoting expansion of anti-inflammatory T cell subsets. *bioRxiv*. https://doi.org/10.1101/2021.02.02.429403

He, Y., Wu, C., Li, J., Li, H., Sun, Z., Zhang, H., de Vos, P., Pan, L. L., & Sun, J. (2017). Inulin-type fructans modulates pancreatic-gut innate immune responses and gut barrier integrity during experimental acute pancreatitis in a chain length-dependent manner. *Frontiers in Immunology, 8*. https://doi.org/10.3389/fimmu.2017.01209

Hiel, S., Gianfrancesco, M. A., Rodriguez, J., Portheault, D., Leyrolle, Q., Bindels, L. B., Gomes da Silveira Cauduro, C., Mulders, M. D. G. H., Zamariola, G., Azzi, A. S., Kalala, G., Pachikian, B. D., Amadieu, C., Neyrinck, A. M., Loumaye, A., Cani, P. D., Lanthier, N., Trefois, P., Klein, O., … Delzenne, N. M. (2020). Link between gut microbiota and health outcomes in inulin -treated obese patients: Lessons from the Food4Gut multicenter randomized placebo-controlled trial. *Clinical Nutrition, 39*(12), 3618−3628. https://doi.org/10.1016/j.clnu.2020.04.005

Holscher, H. D., Bode, L., & Tappenden, K. A. (2017). Human milk oligosaccharides influence intestinal epithelial cell maturation *in vitro*. *Journal of Pediatric Gastroenterology and Nutrition, 64*(2), 296–301. https://doi.org/10.1097/MPG.0000000000001274

Holscher, H. D., Faust, K. L., Czerkies, L. A., Litov, R., Ziegler, E. E., Lessin, H., Hatch, T., Sun, S., & Tappenden, K. A. (2012). Effects of prebiotic-containing infant formula on gastrointestinal tolerance and fecal microbiota in a randomized controlled trial. *Journal of Parenteral and Enteral Nutrition, 36*(1). https://doi.org/10.1177/0148607111430087

Huazano-Garcia, A., Silva-Adame, M. B., Vázquez-Martínez, J., Gastelum-Arellanez, A., Sánchez-Segura, L., & López, M. G. (2020). Highly branched neo-fructans (agavins) attenuate metabolic endotoxemia and low-grade inflammation in association with gut microbiota modulation on high-fat diet-fed mice. *Foods, 9*, 1792.

Ivakhnenko, O. S., & Nyankovskyy, S. L. (2013). Effect of the specific infant formula mixture of oligosaccharides on local immunity and development of allergic and infectious disease in young children: Randomized study. *Pediatria Polska, 88*(5), 398–404. https://doi.org/10.1016/j.pepo.2013.07.002

Jantscher-Krenn, E., Lauwaet, T., Bliss, L. A., Reed, S. L., Gillin, F. D., & Bode, L. (2012). Human milk oligosaccharides reduce *Entamoeba histolytica* attachment and cytotoxicity in vitro. *British Journal of Nutrition, 108*(10), 1839–1846. https://doi.org/10.1017/S0007114511007392

Jeurink, P. V., Van Esch, B. C. A. M., Rijnierse, A., Garssen, J., & Knippels, L. M. J. (2013). Mechanisms underlying immune effects of dietary oligosaccharides. *American Journal of Clinical Nutrition, 98*(2). https://doi.org/10.3945/ajcn.112.038596

Johansson, C., & Kelsall, B. L. (2005). Phenotype and function of intestinal dendritic cells. *Seminars in Immunology, 17*(4), 284–294. https://doi.org/10.1016/j.smim.2005.05.010

Kanneganti, T. D. (2020). Intracellular innate immune receptors: Life inside the cell. *Immunological Reviews, 297*(1), 5–12. https://doi.org/10.1111/imr.12912

Kapiki, A., Costalos, C., Oikonomidou, C., Triantafyllidou, A., Loukatou, E., & Pertrohilou, V. (2007). The effect of a fructo-oligosaccharide supplemented formula on gut flora of preterm infants. *Early Human Development, 83*(5), 335–339. https://doi.org/10.1016/j.earlhumdev.2006.07.003

Kelly, G. (2008). Inulin-type prebiotics–a review: Part 1. *Alternative Medicine Review, 13*.

Kiewiet, M. B., Elderman, M. E., El Aidy, S., Burgerhof, J. G., Visser, H., Vaughan, E. E., Faas, M. M., & de Vos, P. (2021). Flexibility of gut microbiota in ageing individuals during dietary fiber long-chain inulin intake. *Molecular Nutrition & Food Research, 65*(4), 2000390. https://doi.org/10.1002/mnfr.202000390

Kim, Y. S., & Ho, S. B. (2010). Intestinal goblet cells and mucins in health and disease: Recent insights and progress. *Current Gastroenterology Reports, 12*(5), 319–330. https://doi.org/10.1007/s11894-010-0131-2

Kim, M. H., Kang, S. G., Park, J. H., Yanagisawa, M., & Kim, C. H. (2013). Short-chain fatty acids activate GPR41 and GPR43 on intestinal epithelial cells to promote inflammatory responses in mice. *Gastroenterology, 145*, 396–406. https://doi.org/10.1053/j.gastro.2013.04.056

Kim, M., Vogtmann, E., Ahlquist, D. A., Devens, M. E., Kisiel, J. B., Taylor, W. R., White, B. A., Hale, V. L., Sung, J., Chia, N., Sinha, R., & Chen, J. (2020). Fecal metabolomic signatures in colorectal adenoma patients are associated with gut microbiota and early events of colorectal cancer pathogenesis. *mBio, 11*(1). https://doi.org/10.1128/mBio.03186-19

Knol, J., Scholtens, P., Kafka, C., Steenbakkers, J., Groß, S., Helm, K., Klarczyk, M., Schöpfer, H., Böckler, H. M., & Wells, J. (2005). Colon microflora in infants fed formula with galacto- and fructo-oligosaccharides: More like breast-fed infants. *Journal of Pediatric Gastroenterology and Nutrition, 40*(1), 36–42. https://doi.org/10.1097/00005176-200501000-00007

Kong, C., Cheng, L., Krenning, G., Fledderus, J., de Haan, B. J., Walvoort, M. T. C., & de Vos, P. (2020). Human milk oligosaccharides mediate the crosstalk between intestinal epithelial Caco-2 cells and *Lactobacillus plantarum* WCFS1 in an *in vitro* model with intestinal peristaltic shear force. *Journal of Nutrition, 150*(8), 2077–2088. https://doi.org/10.1093/jn/nxaa162

Kong, C., Elderman, M., Cheng, L., de Haan, B. J., Nauta, A., & de Vos, P. (2019). Modulation of intestinal epithelial glycocalyx development by human milk oligosaccharides and non-digestible carbohydrates. *Molecular Nutrition and Food Research, 63*(17). https://doi.org/10.1002/mnfr.201900303

Kong, C., Faas, M. M., de Vos, P., & Akkerman, R. (2020). Impact of dietary fibers in infant formulas on gut microbiota and the intestinal immune barrier. *Food and Function, 11*(11), 9445–9467. https://doi.org/10.1039/d0fo01700k

Krupa-Kozak, U., Drabińska, N., & Jarocka-Cyrta, E. (2017). The effect of oligofructose-enriched inulin supplementation on gut microbiota, nutritional status and gastrointestinal symptoms in paediatric coeliac disease patients on a gluten-free diet: Study protocol for a pilot randomized controlled trial. *Nutrition Journal, 16*(1). https://doi.org/10.1186/s12937-017-0268-z

Lacy, B. E., Mearin, F., Chang, L., Chey, W. D., Lembo, A. J., Simren, M., & Spiller, R. (2016). Bowel disorders. *Gastroenterology, 150*(6), 1393–1407.e5. https://doi.org/10.1053/j.gastro.2016.02.031

Lambertz, J., Weiskirchen, S., Landert, S., & Weiskirchen, R. (2017). Fructose: A dietary sugar in crosstalk with microbiota contributing to the development and progression of non-alcoholic liver disease. *Frontiers in Immunology, 8*. https://doi.org/10.3389/fimmu.2017.01159

Lebeer, S., Vanderleyden, J., & De Keersmaecker, S. C. J. (2010). Host interactions of probiotic bacterial surface molecules: Comparison with commensals and pathogens. *Nature Reviews Microbiology, 8*(3), 171–184. https://doi.org/10.1038/nrmicro2297

Lépine, A., & de Vos, P. (2018). Synbiotic effects of the dietary fiber long-chain inulin and probiotic *Lactobacillus acidophilus* W37 can be caused by direct, synergistic stimulation of immune toll-like receptors and dendritic cells. *Molecular Nutrition and Food Research, 62*(15). https://doi.org/10.1002/mnfr.201800251

Lépine, A. F. P., de Wit, N., Oosterink, E., Wichers, H., Mes, J., & de Vos, P. (2018). *Lactobacillus acidophilus* attenuates Salmonella-induced stress of epithelial cells by modulating tight-junction genes and cytokine responses. *Frontiers in Microbiology, 9*. https://doi.org/10.3389/fmicb.2018.01439

Lépine, A. F. P., Konstanti, P., Borewicz, K., Resink, J. W., de Wit, N. J., de Vos, P., Smidt, H., & Mes, J. J. (2019). Combined dietary supplementation of long chain inulin and *Lactobacillus acidophilus* W37 supports oral vaccination efficacy against *Salmonella typhimurium* in piglets. *Scientific Reports, 9*(1). https://doi.org/10.1038/s41598-019-54353-1

Li, Y., Elmén, L., Segota, I., Xian, Y., Tinoco, R., Feng, Y., Fujita, Y., Segura Muñoz, R. R., Schmaltz, R., Bradley, L. M., Ramer-Tait, A., Zarecki, R., Long, T., Peterson, S. N., & Ronai, Z. A. (2020). Prebiotic-induced anti-tumor immunity attenuates tumor growth. *Cell Reports, 30*(6), 1753−1766.e6. https://doi.org/10.1016/j.celrep.2020.01.035

Lindsay, J. O., Whelan, K., Stagg, A. J., Gobin, P., Al-Hassi, H. O., Rayment, N., Kamm, M. A., Knight, S. C., & Forbes, A. (2006). Clinical, microbiological, and immunological effects of fructo-oligosaccharide in patients with Crohn's disease. *Gut, 55*(3), 348−355. https://doi.org/10.1136/gut.2005.074971

Liong, M. T. (2008). Roles of probiotics and prebiotics in colon cancer prevention: Postulated mechanisms and in-vivo evidence. *International Journal of Molecular Sciences, 9*(5), 854−863. https://doi.org/10.3390/ijms9050854

Li, L.-L., Wang, Y.-T., Zhu, L.-M., Liu, Z.-Y., Ye, C.-Q., & Qin, S. (2020). Inulin with different degrees of polymerization protects against diet-induced endotoxemia and inflammation in association with gut microbiota regulation in mice. *Scientific Reports, 10*(1), 1−12. https://doi.org/10.1038/s41598-020-58048-w

Logtenberg, M. J., Akkerman, R., An, R., Hermes, G. D. A., de Haan, B. J., Faas, M. M., Zoetendal, E. G., Schols, H. A., & de Vos, P. (2020). Fermentation of chicory fructo-oligosaccharides and native inulin by infant fecal microbiota attenuates pro-inflammatory responses in immature dendritic cells in an infant-age-dependent and fructan-specific way. *Molecular Nutrition and Food Research, 64*(13). https://doi.org/10.1002/mnfr.202000068

López-Velázquez, G., Díaz-García, L., Anzo, A., Parra-Ortiz, M., Llamosas-Gallardo, B., Ortiz-Hernández, A. A., Mancilla-Ramírez, J., Manuel Cruz-Rubio, J., & Gutiérrez-Castrellón, P. (2013). Safety of a dual potential prebiotic system from Mexican agave \Metlin® and Metlos®\, incorporated to an infant formula for term newborn babies: A randomized controlled trial. *Revista de Investigacion Clinica, 65*(6), 483−490. http://scielo-mx.bvs.br/scielo.php?script=sci_serial&lng=en&pid=0034-8376&nrm=iso.

López-Velázquez, G., Parra-Ortiz, M., De la Mora-De la Mora, I., García-Torres, I., Enríquez-Flores, S., Alcántara-Ortigoza, M. A., González-del Angel, A., Velázquez-Aragón, J., Ortiz-Hernández, R., Cruz-Rubio, J. M., Villa-Barragán, P., Jiménez-Gutiérrez, C., & Gutiérrez-Castrellón, P. (2015). Effects of fructans from Mexican agave in newborns fed with infant formula: A randomized controlled trial. *Nutrients, 7*(11), 8939−8951. https://doi.org/10.3390/nu7115442

López, M. G., Mancilla-Margalli, N. A., & Mendoza-Diaz, G. (2003). Molecular structures of fructans from *Agave tequilana* weber var. *azul*. *Journal of Agricultural and Food Chemistry, 51*(27), 7835−7840. https://doi.org/10.1021/jf030383v

López, M. G., & Urías-Silvas, J. E. (2007). Agave fructans as prebiotics. In S. Norio, B. Noureddine, & O. Shuichi (Eds.), *Recent advances in fructooligosaccharides research* (Issue 2, pp. 1−14). Research signpost.

Macia, L., Tan, J., Vieira, A. T., Leach, K., Stanley, D., Luong, S., Maruya, M., Ian McKenzie, C., Hijikata, A., Wong, C., Binge, L., Thorburn, A. N., Chevalier, N., Ang, C., Marino, E., Robert, R., Offermanns, S., Teixeira, M. M., Moore, R. J., … Mackay, C. R. (2015). Metabolite-sensing receptors GPR43 and GPR109A facilitate dietary fibre-induced gut homeostasis through regulation of the inflammasome. *Nature Communications, 6*. https://doi.org/10.1038/ncomms7734

MacPherson, G., Milling, S., Yrlid, U., Cousins, L., Turnbull, E., & Huang, F. P. (2004). Uptake of antigens from the intestine by dendritic cells. *Annals of the New York Academy of Sciences, 1029*, 75−82. https://doi.org/10.1196/annals.1309.010. New York Academy of Sciences.

Mancilla-Margalli, N. A., & Lopez, M. G. (2006). Water-soluble carbohydrates and fructan structure patterns from *Agave* and *Dasylirion* species. *Journal of Agricultural and Food Chemistry, 54*(20), 7832−7839. https://doi.org/10.1021/jf060354v

Man, S., Liu, T., Yao, Y., Lu, Y., Ma, L., & Lu, F. (2020). Friend or foe? The roles of inulin-type fructans. *Carbohydrate Polymers, 252*, 117155.

Martínez-Ortega, E. A., López-Briones, J. S., Rodríguez-Hernández, G., Ramírez-Orozco, R. E., & Franco-Robles, E. (2020). Antibacterial activity of agave fructans against *Salmonella typhimurium*. *Natural Product Research, 34*(18), 2639−2641. https://doi.org/10.1080/14786419.2018.1548446

Mellado-Mojica, E., & López, M. G. (2012). Fructan metabolism in *A. tequilana* Weber blue variety along its developmental cycle in the field. *Journal of Agricultural and Food Chemistry, 60*(47), 11704−11713. https://doi.org/10.1021/jf303332n

Micka, A., Siepelmeyer, A., Holz, A., Theis, S., & Schön, C. (2017). Effect of consumption of chicory inulin on bowel function in healthy subjects with constipation: A randomized, double-blind, placebo-controlled trial. *International Journal of Food Sciences and Nutrition, 68*(1), 82−89. https://doi.org/10.1080/09637486.2016.1212819

Mima, K., Cao, Y., Chan, A. T., Qian, Z. R., Nowak, J. A., Masugi, Y., Yan, S., Mingyang, S., Annacarolina, da S., Mancang, G., Wanwan, L., Tsuyoshi, H., Keisuke, K., Akiko, H., Li, L., D, K. A., Marios, G., Susan, B., Brennan, C. A., … Ogino, S. (2016). Fusobacterium nucleatum in colorectal carcinoma tissue according to tumor location. *Clinical and Translational Gastroenterology, 7*(11), e200. https://doi.org/10.1038/ctg.2016.53

Moreno-Vilet, L., Camacho-Ruiz, R. M., & Portales-Pérez, D. P. (2016). Prebiotic agave fructans and immune aspects. In *Probiotics, prebiotics, and synbiotics: Bioactive foods in health promotion* (pp. 165−179). Elsevier Inc. https://doi.org/10.1016/B978-0-12-802189-7.00011-3

Moreno-Vilet, L., Garcia-Hernandez, M. H., Delgado-Portales, R. E., Corral-Fernandez, N. E., Cortez-Espinosa, N., Ruiz-Cabrera, M. A., & Portales-Perez, D. P. (2014). *In vitro* assessment of agave fructans (*Agave salmiana*) as prebiotics and immune system activators. *International Journal of Biological Macromolecules, 63*, 181−187. https://doi.org/10.1016/j.ijbiomac.2013.10.039

Moro, G., Arslanoglu, S., Stahl, B., Jelinek, J., Wahn, U., & Boehm, G. (2006). A mixture of prebiotic oligosaccharides reduces the incidence of atopic dermatitis during the first six months of age. *Archives of Disease in Childhood, 91*(10), 814−819. https://doi.org/10.1136/adc.2006.098251

Mowat, A. M. I. (2003). Anatomical basis of tolerance and immunity to intestinal antigens. *Nature Reviews Immunology, 3*(4), 331−341. https://doi.org/10.1038/nri1057

Munjal, U., Glei, M., Pool-Zobel, B. L., & Scharlau, D. (2009). Fermentation products of inulin-type fructans reduce proliferation and induce apoptosis in human colon tumour cells of different stages of carcinogenesis. *British Journal of Nutrition, 102*(5), 663−671. https://doi.org/10.1017/S0007114509274770

O'connell, T. M. (2020). The application of metabolomics to probiotic and prebiotic interventions in human clinical studies. *Metabolites, 10*(3). https://doi.org/10.3390/metabo10030120

Ohara, T., & Suzutani, T. (2018). Intake of *Bifidobacterium longum* and fructooligosaccharides prevents colorectal carcinogenesis. *Euroasian Journal of Hepato-Gastroenterology, 8*(1), 11−17.

Ortega-Gonzalez, M. (2014). Fructooligosacharides reduce *Pseudomonas aeruginosa* PAO1 pathogenicity through distinct mechanisms. *PLoS One, 9*(1), e85772.

Padilla-Camberos, E., Barragán-Álvarez, C. P., Diaz-Martinez, N. E., Rathod, V., & Flores-Fernández, J. M. (2018). Effects of agave fructans (*Agave tequilana* weber var. azul) on body fat and serum lipids in obesity. *Plant Foods for Human Nutrition, 73*(1), 34−39. https://doi.org/10.1007/s11130-018-0654-5

Pérez-López, A. V., & Simpson, J. (2020). The sweet taste of adapting to the desert: Fructan metabolism in agave species. *Frontiers in Plant Science, 11*. https://doi.org/10.3389/fpls.2020.00324

Peshev, D., & Van den Ende, W. (2014). Fructans: Prebiotics and immunomodulators. *Journal of Functional Foods, 8*(1), 348−357. https://doi.org/10.1016/j.jff.2014.04.005

Pinto, D., & Clevers, H. (2005). Wnt control of stem cells and differentiation in the intestinal epithelium. *Experimental Cell Research, 306*(2), 357−363. https://doi.org/10.1016/j.yexcr.2005.02.022

Praznik, W., Löppert, R., Rubio, J. M., Zangger, K., & Huber, A. (2013). Structure of fructo-oligosaccharides from leaves and stem of *Agave tequilana* Weber, var. *azul*. *Carbohydrate Research, 381*, 64−73. https://doi.org/10.1016/j.carres.2013.08.025

Rafter, J., Bennett, M., Caderni, G., Clune, Y., Hughes, R., Karlsson, P. C., Klinder, A., O'Riordan, M., O'Sullivan, G. C., Pool-Zobel, B., Rechkemmer, G., Roller, M., Rowland, I., Salvadori, M., Thijs, H., Van Loo, J., Watzl, B., & Collins, J. K. (2007). Dietary synbiotics reduce cancer risk factors in polypectomized and colon cancer patients. *American Journal of Clinical Nutrition, 85*(2), 488−496. https://doi.org/10.1093/ajcn/85.2.488

Raveh, E., Wang, N., & Nobel, P. S. (1998). Gas exchange and metabolite fluctuations in green and yellow bands of variegated leaves of the monocotyledonous CAM species *Agave americana*. *Physiologia Plantarum, 103*(1), 99−106. https://doi.org/10.1034/j.1399-3054.1998.1030112.x

Rawi, M. H., Zaman, S. A., Pa'ee, K. F., Leong, S. S., & Sarbini, S. R. (2020). Prebiotics metabolism by gut-isolated probiotics. *Journal of Food Science and Technology, 57*(8), 2786−2799. https://doi.org/10.1007/s13197-020-04244-5

Reimer, R. A., Soto-Vaca, A., Nicolucci, A. C., Mayengbam, S., Park, H., Madsen, K. L., Menon, R., & Vaughan, E. E. (2020). Effect of chicory inulin-type fructan-containing snack bars on the human gut microbiota in low dietary fiber consumers in a randomized crossover trial. *American Journal of Clinical Nutrition, 111*(6), 1286−1296. https://doi.org/10.1093/ajcn/nqaa074

Richard, M. L., Liguori, G., Lamas, B., Brandi, G., da Costa, G., Hoffmann, T. W., Pierluigi Di Simone, M., Calabrese, C., Poggioli, G., Langella, P., Campieri, M., & Sokol, H. (2018). Mucosa-associated microbiota dysbiosis in colitis associated cancer. *Gut Microbes, 9*(2), 131−142. https://doi.org/10.1080/19490976.2017.1379637

Roberfroid, M. B. (2002). Global view on functional foods: European perspectives. *British Journal of Nutrition, 88*(2), S133−S138. https://doi.org/10.1079/bjn2002677. CAB International.

Roberfroid, M. B. (2005). Introducing inulin-type fructans. *British Journal of Nutrition, 93*, S13−S25. https://doi.org/10.1079/BJN20041350

Rodriguez-Herrera, A., Mulder, K., Bouritius, H., Rubio, R., Muñoz, A., Agosti, M., Lista, G., Corvaglia, L., Ludwig, T., Abrahamse-Berkeveld, M., & Perez-Navero, J. L. (2019). Gastrointestinal tolerance, growth and safety of a partly fermented formula with specific prebiotics in healthy infants: A double-blind, randomized, controlled trial. *Nutrients, 11*(7). https://doi.org/10.3390/nu11071530

Roller, M., Clune, Y., Collins, K., Rechkemmer, G., & Watzl, B. (2007). Consumption of prebiotic inulin enriched with oligofructose in combination with the probiotics *Lactobacillus rhamnosus* and *Bifidobacterium lactis* has minor effects on selected immune parameters in polypectomised and colon cancer patients. *British Journal of Nutrition, 97*(4), 676−684. https://doi.org/10.1017/S0007114507450292

Roller, M., Femia, A. P., Caderni, G., Rechkemmer, G., & Watzl, B. (2004). Intestinal immunity of rats with colon cancer is modulated by oligofructose-enriched inulin combined with *Lactobacillus rhamnosus* and *Bifidobacterium lactis*. *British Journal of Nutrition, 92*(6), 931−938. https://doi.org/10.1079/BJN20041289

Sato, A., & Iwasaki, A. (2005). Peyer's patch dendritic cells as regulators of mucosal adaptive immunity. *Cellular and Molecular Life Sciences, 62*(12), 1333−1338. https://doi.org/10.1007/s00018-005-5037-z

Sauer, J., Richter, K. K., & Pool-Zobel, B. L. (2007). Products formed during fermentation of the prebiotic inulin with human gut flora enhance expression of biotransformation genes in human primary colon cells. *British Journal of Nutrition, 97*(5), 928−937. https://doi.org/10.1017/S0007114507666422

Sáyago-Ayerdi, S. G., Zamora-Gasga, V. M., & Venema, K. (2020). Changes in gut microbiota in predigested *Hibiscus sabdariffa* L calyces and Agave (*Agave tequilana* weber) fructans assessed in a dynamic in vitro model (TIM-2) of the human colon. *Food Research International, 132*. https://doi.org/10.1016/j.foodres.2020.109036

Sestito, S., D'Auria, E., Baldassarre, M. E., Salvatore, S., Tallarico, V., Stefanelli, E., Tarsitano, F., Concolino, D., & Pensabene, L. (2020). The role of prebiotics and probiotics in prevention of allergic diseases in infants. *Frontiers in Pediatrics, 8*. https://doi.org/10.3389/fped.2020.583946

Shiou, S. R., Yu, Y., Guo, Y., He, S. M., Mziray-Andrew, C. H., Hoenig, J., Sun, J., Petrof, E. O., & Claud, E. C. (2013). Synergistic protection of combined probiotic conditioned media against neonatal necrotizing enterocolitis-like intestinal injury. *PLoS One, 8*(5). https://doi.org/10.1371/journal.pone.0065108

Shoaib, M., Shehzad, A., Omar, M., Rakha, A., Raza, H., Sharif, H. R., Shakeel, A., Ansari, A., & Niazi, S. (2016). Inulin: Properties, health benefits and food applications. *Carbohydrate Polymers, 147*, 444−454. https://doi.org/10.1016/j.carbpol.2016.04.020

Sims, I. M., & Tannock, G. W. (2020). Galacto-and fructo-oligosaccharides utilized for growth by cocultures of bifidobacterial species characteristic of the infant gut. *Applied and Environmental Microbiology, 86*(11), 1−11. https://doi.org/10.1128/AEM.00214-20

Singh, V., Yeoh, B. S., Walker, R. E., Xiao, X., Saha, P., Golonka, R. M., Cai, J., Bretin, A. C. A., Cheng, X., Liu, Q., Flythe, M. D., Chassaing, B., Shearer, G. C., Patterson, A. D., Gewirtz, A. T., & Vijay-Kumar, M. (2019). Microbiota fermentation-NLRP3 axis shapes the impact of dietary fibres on intestinal inflammation. *Gut, 68*(10), 1801−1812. https://doi.org/10.1136/gutjnl-2018-316250

Slizewska, K., & Chlebicz-Wójcik, A. (2020). The *in vitro* analysis of prebiotics to be used as a component of a synbiotic preparation. *Nutrients, 12*(5). https://doi.org/10.3390/nu12051272

Spacova, I., Dodiya, H. B., Happel, A. U., Strain, C., Vandenheuvel, D., Wang, X., & Reid, G. (2020). Future of probiotics and prebiotics and the implications for early career researchers. *Frontiers in Microbiology, 11*. https://doi.org/10.3389/fmicb.2020.01400

Stephen, A. M., & Phillips, G. O. (2006). *Food polysaccharides and their applications* (2nd ed.). CRC Press. https://doi.org/10.1201/9781420015164

Sundaram, B., & Kanneganti, T. D. (2021). Advances in understanding activation and function of the NLRC4 inflammasome. *International Journal of Molecular Sciences, 22*(3), 1−12. https://doi.org/10.3390/ijms22031048

Taghinezhad-S, S., Mohseni, A. H., & Fu, X. (2020). Intervention on gut microbiota may change the strategy for management of colorectal cancer. *Journal of Gastroenterology and Hepatology (Australia)*. https://doi.org/10.1111/jgh.15369

Takeda, K., & Akira, S. (2004). TLR signaling pathways. *Seminars in Immunology, 16*(1), 3−9. https://doi.org/10.1016/j.smim.2003.10.003

Talley, N. J. (2020). What causes functional gastrointestinal disorders? A proposed disease model. *American Journal of Gastroenterology, 115*(1), 41−48. https://doi.org/10.14309/ajg.0000000000000485

Taper, H. S., & Roberfroid, M. B. (2005). Possible adjuvant cancer therapy by two prebiotics - inulin or oligofructose. *Vivo, 19*(1), 201−204.

Theodoropoulos, G. E., Memos, N. A., Peitsidou, K., Karantanos, T., Spyropoulos, B. G., & Zografos, G. (2016). Synbiotics and gastrointestinal function-related quality of life after elective colorectal cancer resection. *Annals of Gastroenterology, 29*(1), 56−62. http://www.annalsgastro.gr/index.php/annalsgastro/article/download/2442/1665.

Theurich, M. A., Davanzo, R., Busck-Rasmussen, M., Díaz-Gómez, N. M., Brennan, C., Kylberg, E., Bærug, A., McHugh, L., Weikert, C., Abraham, K., & Koletzko, B. (2019). Breastfeeding rates and programs in europe: A survey of 11 national breastfeeding committees and representatives. *Journal of Pediatric Gastroenterology and Nutrition, 68*(3), 400−407. https://doi.org/10.1097/MPG.0000000000002234

Thurl, S., Munzert, M., Henker, J., Boehm, G., Mller-Werner, B., Jelinek, J., & Stahl, B. (2010). Variation of human milk oligosaccharides in relation to milk groups and lactational periods. *British Journal of Nutrition, 104*(9), 1261−1271. https://doi.org/10.1017/S0007114510002072

Ulluwishewa, D., Anderson, R. C., McNabb, W. C., Moughan, P. J., Wells, J. M., & Roy, N. C. (2011). Regulation of tight junction permeability by intestinal bacteria and dietary components. *Journal of Nutrition, 141*(5), 769−776. https://doi.org/10.3945/jn.110.135657

Urías-Silvas, J. E., Cani, P. D., Delmée, E., Neyrinck, A., López, M. G., & Delzenne, N. M. (2008). Physiological effects of dietary fructans extracted from *Agave tequilana* Gto. and *Dasylirion spp*. *British Journal of Nutrition, 99*(2), 254−261. https://doi.org/10.1017/S0007114507795338

Van den Abbeele, P., Taminiau, B., Pinheiro, I., Duysburgh, C., Jacobs, H., Pijls, L., & Marzorati, M. (2018). Arabinoxylo-oligosaccharides and inulin impact inter-individual variation on microbial metabolism and composition, which immunomodulates human cells. *Journal of Agricultural and Food Chemistry, 66*(5), 1121−1130. https://doi.org/10.1021/acs.jafc.7b04611

Vandenplas, Y., de Halleux, V., Arciszewska, M., Lach, P., Pokhylko, V., Klymenko, V., Schoen, S., Abrahamse-Berkeveld, M., Mulder, K. A., & Rubio, R. P. (2020). A partly fermented infant formula with postbiotics including 3′-GL, specific oligosaccharides, 2′-FL, and milk fat supports adequate growth, is safe and well-tolerated in healthy term infants: A double-blind, randomised, controlled, multi-country trial. *Nutrients, 12*(11), 1−17. https://doi.org/10.3390/nu12113560

Vandenplas, Y., Ludwig, T., Bouritius, H., Alliet, P., Forde, D., Peeters, S., Huet, F., & Hourihane, J. (2017). Randomised controlled trial demonstrates that fermented infant formula with short-chain galacto-oligosaccharides and long-chain fructo-oligosaccharides reduces the incidence of infantile colic. *Acta Paediatrica, International Journal of Paediatrics, 106*(7), 1150−1158. https://doi.org/10.1111/apa.13844

Vandeputte, D., Kathagen, G., D'Hoe, K., Vieira-Silva, S., Valles-Colomer, M., Sabino, J., Wang, J., Tito, R. Y., De Commer, L., Darzi, Y., Vermeire, S., Falony, G., & Raes, J. (2017). Quantitative microbiome profiling links gut community variation to microbial load. *Nature, 551*(7681), 507−511. https://doi.org/10.1038/nature24460

Van den Ende, W. (2013). Multifunctional fructans and raffinose family oligosaccharides. *Frontiers in Plant Science*. https://doi.org/10.3389/fpls.2013.00247

Verma, A., & Shukla, G. (2013). Administration of prebiotic inulin suppresses 1,2 dimethylhydrazine dihydrochloride induced procarcinogenic biomarkers fecal enzymes and preneoplastic lesions in early colon carcinogenesis in Sprague Dawley rats. *Journal of Functional Foods, 5*(2), 991−996. https://doi.org/10.1016/j.jff.2013.02.006

Victora, C. G., Bahl, R., Barros, A. J. D., França, G. V. A., Horton, S., Krasevec, J., Murch, S., Sankar, M. J., Walker, N., Rollins, N. C., Allen, K., Dharmage, S., Lodge, C., Peres, K. G., Bhandari, N., Chowdhury, R., Sinha, B., Taneja, S., Giugliani, E., … Richter, L. (2016). Breastfeeding in the 21st century: Epidemiology, mechanisms, and lifelong effect. *The Lancet, 387*(10017), 475−490. https://doi.org/10.1016/S0140-6736(15)01024-7

Vogt, L. M., Elderman, M. E., Borghuis, T., de Haan, B. J., Faas, M. M., & de Vos, P. (2017). Chain length-dependent effects of inulin-type fructan dietary fiber on human systemic immune responses against hepatitis-B. *Molecular Nutrition and Food Research, 61*(10). https://doi.org/10.1002/mnfr.201700171

Vogt, L. M., Meyer, D., Pullens, G., Faas, M. M., Venema, K., Ramasamy, U., Schols, H. A., & de Vos, P. (2014). Toll-like receptor 2 activation by β2→1-fructans protects barrier function of T84 human intestinal epithelial cells in a chain length-dependent manner. *Journal of Nutrition, 144*(7), 1002−1008. https://doi.org/10.3945/jn.114.191643

Vogt, L., Ramasamy, U., Meyer, D., Pullens, G., Venema, K., Faas, M. M., Schols, H. A., & de Vos, P. (2013). Immune modulation by different types of β2→1-fructans is toll-like receptor dependent. *PLoS One, 8*(7). https://doi.org/10.1371/journal.pone.0068367

de Vrese, M., & Schrezenmeir, J. (2008). Probiotics, prebiotics, and synbiotics. *Advances in Biochemical Engineering/Biotechnology, 111*, 1−66. https://doi.org/10.1007/10_2008_097

Walker, A. (2014). Intestinal colonization and programming of the intestinal immune response. *Journal of Clinical Gastroenterology, 48*, S8−S11. https://doi.org/10.1097/MCG.0000000000000230. Lippincott Williams and Wilkins.

Wernimont, S., Northington, R., Kullen, M. J., Yao, M., & Bettler, J. (2015). Effect of an α-lactalbumin-enriched infant formula supplemented with oligofructose on fecal microbiota, stool characteristics, and hydration status: A randomized, double-blind, controlled trial. *Clinical Pediatrics, 54*(4), 359−370. https://doi.org/10.1177/0009922814553433

Wiciński, M., Sawicka, E., Gebalski, J., Kubiak, K., & Malinowski, B. (2020). Human milk oligosaccharides: Health benefits, potential applications in infant formulas, and pharmacology. *Nutrients, 12*(1). https://doi.org/10.3390/nu12010266

Wilson, B., Rossi, M., Dimidi, E., & Whelan, K. (2019). Prebiotics in irritable bowel syndrome and other functional bowel disorders in adults: A systematic review and meta-analysis of randomized controlled trials. *American Journal of Clinical Nutrition, 109*(4), 1098−1111. https://doi.org/10.1093/ajcn/nqy376

CAPÍTULO 3

β(2→6)-Type fructans attenuate proinflammatory responses in a structure dependent fashion via Toll-like receptors.

C. Fernández-Lainez[a,b,c,*], R. Akkerman[a], M.M.P. Oerlemans[a], M.J. Logtenberg[d], H.A. Schols[d], L.A. Silva-Lagos[a], G. López-Velázquez[e], P. de Vos[a]

[a] Immunoendocrinology, Division of Medical Biology, Department of Pathology and Medical Biology, University of Groningen and University Medical Center Groningen, Hanzeplein 1, 9700 RB Groningen, The Netherlands.

[b] Laboratorio de Errores Innatos del Metabolismo y Tamiz, Instituto Nacional de Pediatría, Ciudad de México, México.

[c] Posgrado en Ciencias Biológicas, Universidad Nacional Autónoma de México UNAM, Ciudad de México, México.

[d] Laboratory of Food Chemistry, Wageningen University, Wageningen, The Netherlands.

[e] Laboratorio de Biomoléculas y Salud Infantil, Instituto Nacional de Pediatría, Ciudad de México, México.

Publicado en Carbohydrate Polymers 2022;277, 118893. https://doi.org/10.1016/j.carbpol.2021.118893.

Carbohydrate Polymers 277 (2022) 118893

Contents lists available at ScienceDirect

Carbohydrate Polymers

journal homepage: www.elsevier.com/locate/carbpol

β(2→6)-Type fructans attenuate proinflammatory responses in a structure dependent fashion via Toll-like receptors

C. Fernández-Lainez [a,b,c,*], R. Akkerman [a], M.M.P. Oerlemans [a], M.J. Logtenberg [d], H.A. Schols [d], L.A. Silva-Lagos [a], G. López-Velázquez [e], P. de Vos [a]

[a] Immunoendocrinology, Division of Medical Biology, Department of Pathology and Medical Biology, University of Groningen and University Medical Center Groningen, Hanzeplein 1, 9700 RB Groningen, the Netherlands
[b] Laboratorio de Errores Innatos del Metabolismo y Tamiz, Instituto Nacional de Pediatría, Ciudad de México, Mexico
[c] Posgrado en Ciencias Biológicas, Universidad Nacional Autónoma de México UNAM, Ciudad de México, Mexico
[d] Laboratory of Food Chemistry, Wageningen University, Wageningen, the Netherlands
[e] Laboratorio de Biomoléculas y Salud Infantil, Instituto Nacional de Pediatría, Ciudad de México, Mexico

ARTICLE INFO

Keywords:
Branched-chain fructans
Functional food
Immunomodulation
Non-digestible carbohydrates
Toll-like receptors

ABSTRACT

Graminan-type fructans (GTFs) have demonstrated immune benefits. However, mechanisms underlying these benefits are unknown. We studied GTFs interaction with Toll-like receptors (TLRs), performed molecular docking and determined their impact on dendritic cells (DCs). Effects of GTFs were compared with those of inulin-type fructans (ITFs). Whereas ITFs only contained β(2→1)-linked fructans, GTFs showed higher complexity as it contains additional β(2→6)-linkages. GTFs activated NF-κB/AP-1 through MyD88 and TRIF pathways. GTFs stimulated TLR3, 7 and 9 while ITFs activated TLR2 and TLR4. GTFs strongly inhibited TLR2 and TLR4, while ITFs did not inhibit any TLR. Molecular docking demonstrated interactions of fructans with TLR2, 3, and 4 in a structure dependent fashion. Moreover, ITFs and GTFs attenuated pro-inflammatory cytokine production of stimulated DCs. These findings demonstrate immunomodulatory effects of GTFs via TLRs and attenuation of cytokine production in dendritic cells by GTFs and long-chain ITF.

1. Introduction

Economic progress has led to spreading of the Western life style which has contributed to an increased risk for development of non-communicable diseases such as cardiovascular diseases, stroke, cancer, diabetes and respiratory diseases (Beaglehole et al., 2011; Patry & Nagler, 2021). These changes in lifestyle include less physical activity, higher intake of processed foods enriched with animal fats as well as lower intake of dietary fibers compared to more traditional diets (Health & Services, 2015; Temba et al., 2021). During recent years, especially enhanced intake of dietary fibers has been shown to be an effective strategy to reduce risk for developing chronic metabolic and immune diseases (Veronese et al., 2018). However, the mechanisms that underlie these health benefits are not completely understood. It has been shown that beneficial effects of dietary fiber intake might be associated with enhanced production of short-chain fatty acids (SCFAs) by intestinal microbiota (Van den Abbeele et al., 2021) but also other mechanisms such as direct interaction of dietary fibers with immune cells in the intestine have been suggested to be involved (Vogt et al., 2013).

An important family of dietary fibers are fructans which can be found in the cell wall of bacteria, fungi or in angiosperm plants (Flamm et al., 2001; Oerlemans et al., 2020; Pérez-López & Simpson, 2020). Fructans

Abbreviations: AP-1, activating-protein 1; DP, degree of polymerization; EU, endotoxin units; FLA-ST, flagellin from *S. typhimurium*; FSL-1, synthetic diacylated lipoprotein - TLR2/TLR6 ligand; GTF I, graminan-type fructan I; GTF II, graminan-type fructan II; G418, geneticin; HEK, human embryonic kidney cells; HPAEC, high performance anion exchange chromatography; HPSEC, high-pressure size exclusion chromatography; CL264, 2-(4-((6-amino-2-(butylamino)-8-hydroxy-9H_purin_9-yl) methyl)benzamido)acetic acid; ITF I, inulin-type fructan I; ITF II, inulin-type fructan II; LAL, limulus amebocyte lysate; MWD, molecular weight distribution; NF-κB, Nuclear factor kappa-light-chain-enhancer of activated B cells; ODN 2006, class B CpG synthetic oligonucleotide; Poly I:C, high molecular weight-synthetic analog of dsRNA; SEAP, Secreted Alkaline Phosphatase; ssRNA40/LyoVec, single-stranded GU-rich oligonucleotide complexed with the cationic lipid LyoVec™; THP1, Human monocytic cells; TLRs, Toll-like receptors.

* Corresponding author at: Immunoendocrinology, Division of Medical Biology, Department of Pathology and Medical Biology, University of Groningen and University Medical Center Groningen, Hanzeplein 1, 9700 RB Groningen, the Netherlands.
E-mail address: c.fernandez.lainez@umcg.nl (C. Fernández-Lainez).

https://doi.org/10.1016/j.carbpol.2021.118893
Received 31 July 2021; Received in revised form 25 October 2021; Accepted 11 November 2021
Available online 15 November 2021

are water soluble and energy-storing polysaccharides in plants (Van den Ende, 2013). Fructans are synthesized from glucose units to which a fructose unit is added. According to their composition, fructans are denoted as GF_n or F_n, where "G" corresponds to the terminal glucose unit, "F" corresponds to fructose, and "n" denotes the number of molecules that elongate the fructan chain (Roberfroid, 2005). Fructans are structurally diverse, and their composition depends on the metabolism present in the plant from which they are extracted (Versluys et al., 2018). Fructans can be classified in several groups according to the position of fructose carbon atoms that form the glycosidic bond for the elongation. Inulins are a type of fructans composed of β(2→1) bonds. These β(2→1) inulins have a linear structure and are different from the inulin neoseries that contain a glucose moiety between two fructose chains linked through β(2→1) bonds (Vijn & Smeekens, 1999). Another form of fructans are levans which are comprised of β(2→6) bonds and are also linear. Just like inulin, these levans also exist as neoseries containing a central sucrose molecule to which fructose chains are linked by β(2→6) bonds (Mancilla-Margalli & López, 2006; Vijn & Smeekens, 1999). These levans can be extracted from both bacteria and plants, where they have different biological functions (Young, et al. 2021). A third family of fructans are the graminans. These fructans consist of a mixture of both β(2→1) bonds and β(2→6) bonds and have a branched structure. All these fructans have a β-configuration of their chemical bonds which makes them mostly inaccessible to human digestive enzymes. Therefore, fructans are widely considered to be non-digestible carbohydrates (NDCs) (Roberfroid et al., 1998).

Graminan type fructans (GTFs) isolated from *Agave tequilana* (agave) are widely used in Latin America and recognized for their health benefits (López & Urías-Silvas, 2007). Because of these health benefits they have been applied as prebiotics in infant formula for newborns (López-Velázquez et al., 2015). Despite these recognized benefits, still there is poor knowledge about the effects of GTFs on immune health. On the other hand, inulin-type fructans (ITFs) are well recognized for their metabolic and immune health benefits (Vogt et al., 2013) and those isolated from *Cichorium intybus* (chicory), are widely used and consumed in Europe as food supplement. For some ITFs it has been shown that their beneficial effect on immune health occurs via binding to Toll-like receptors (TLRs) (Vogt et al., 2013). In humans, TLRs are a group of ten transmembrane proteins that participate in the immune response against pathogenic microorganisms (Abreu, 2010). Once TLRs recognize specific pathogenic molecules such as lipoproteins from bacterial cell wall or genetic material (RNA, DNA) signaling cascades are activated (Gay & Gangloff, 2007). These signaling cascades can follow either the Myeloid Differentiation primary-response protein 88 (MyD88) or the TIR domain-containing adaptor protein inducing IFN-β (TRIF) pathways for the production of inflammatory cytokines (Takeda & Akira, 2004). ITFs can activate TLRs and regulate inflammatory responses and effects are chain-length dependent (Bermudez-Brito et al., 2015). These immunomodulatory properties can be beneficial for gut and immune health as previously demonstrated in human studies (Bermudez-Brito et al., 2015; Kiewiet et al., 2021; Vogt et al., 2017).

We hypothesized that fructans from agave exert immunomodulation via TLRs, which might explain their health benefits. To determine this, we performed the current study in which we investigated the modulatory effect of GTFs on TLRs which was compared to that of ITFs of different chain lengths. Furthermore, as it is unknown for both GTFs and ITFs how and on which binding sites they interact with TLR we applied in silico docking studies to propose the specific binding sites of fructans on TLRs. This was performed on the TLRs that were most strongly regulated by fructans. Finally, the impact of these fructans on the cytokine responses from dendritic cells (DCs) was studied.

2. Materials and methods

2.1. Fructans

In order to study the effects of linear or branched structures of fructans on TLR signaling, two types of branched β(2→1) and β(2→6) linked graminan-type fructans were tested. One is a mixture of low DP chains (GTF I, Metlos™) and the other is a mixture of predominant higher DP (GTF II, Metlin™) fructan, both extracted from *Agave tequilana* Weber blue variety, were provided by Nekutli™, Guadalajara, México. These GTFs were studied and compared with two previously described linear β(2→1)-linked inulin-type fructans, ITF I (Frutafit™ CLR) and ITF II (Frutafit™TEX!). ITF I is short chain (DP range 3–10) and ITF II is long chain (DP range 10–60). Both β(2→1) fructans extracted from *Cichorium intybus* root, were provided by Sensus™ B. V., Roosendaal, The Netherlands (Vogt et al., 2013).

2.2. Chemical characterization of inulin and Graminan-type fructans

Chain length profile of GTF I and GTF II, as well as those of ITFs tested, were determined through HPAEC analysis, with a Dionex (Sunnyvale, CA, USA) Carbopac PA-1 column (2 × 250 mm) preceded by a Carbopac PA-1 guard column (2 × 25 mm). Samples were analyzed at a concentration of 50 μg/ml and introduced with a partial-loop injection of 10 μl. Carbohydrates were separated with a gradient elution: 0–400 mM NaOAc in 100 mM NaOH during 40 min, followed by a washing step of 5 min with 1 M NaOAc in 100 mM NaOH and column equilibration with 100 mM NaOH for 15 min. Pulsed amperometrics was used as detection system with a Dionex ISC5000 ED detector (Vogt et al., 2013). Data were acquired with Chromeleon software version 7.0 (Thermo Scientific, San Jose, CA, USA). Annotation of individual components present in GTF I and GTF II was accomplished by comparison of the elution profiles with the previously characterized ITFs (Vogt et al., 2013).

For determination of fructans MWD, HPSEC on an Ultimate 3000 HPLC system (Dionex) coupled to a Shodex RI-101 refractive index detector (Showa Denko, Tokyo, Japan) was used. For the analysis, 20 μl of sample (2.5 mg/ml) dissolved in water were injected at 55 °C. Three TSK-Gel columns connected in tandem (4000–3000–2500 SuperAW; 150 × 6 mm, Tosoh Bioscience, Tokyo, Japan), with the TSK Super AW-L guard column (35 × 4.6 mm, Tosoh Bioscience) were used and samples were eluted at 0.6 ml/min with $NaNO_3$ (0.2 M). Data were acquired with Chromeleon software version 7.0 (Thermo Scientific) and MWD was calculated by interpolation in a pullulan (Polymer Laboratories, Palo Alto, Ca, USA) standard curve in a range of 0.18–790 kDa.

2.3. Endotoxin measurement and removal

Endotoxin levels of all fructans were determined with the commercial Pierce LAL Chromogenic Endotoxin Quantitation Kit™ according to the manufacturer instructions. In case endotoxin levels were above 1 EU/ml, we applied the Pierce High-Capacity Endotoxin Removal Resin™. This resin decreased the endotoxin levels to less than 1 EU/ml (Table S1). These endotoxin concentrations have no influence on the studied cells (Lépine & de Vos, 2018; Vogt et al., 2013). Once fructans were endotoxin-free, they were freeze-dried and stored at −20 °C until use. To exclude any influence from possible endotoxin remnants, we additionally performed tests in which we added the fructans to the cells in the presence and absence of 100 μg/ml of the endotoxin-blocker polymyxin B (Invivogen, Toulouse, France). There were no significant differences between treated and non-treated cells (Fig. S1).

2.4. Reporter cell lines

THP1-XBlue™-MD2-CD14 human monocytes were used as reporter cell-line. This is a cell line which endogenously expresses all human

TLRs and has been genetically modified with the SEAP inducible reporter gene, under control of NF-κB and AP-1 promoters. It also has an extra insert for the expression of MD2 and CD14 accessory proteins which enhance TLR signaling (Cheng et al., 2019; Sahasrabudhe et al., 2018). Additionally, human embryonic kidney cells (HEK-Blue™) expressing either human TLRs 2, 3, 4, 5, 7, 8 or 9 were applied. Also, this cell-line has a SEAP reporter gene system. It is important to note that HEK-Blue™ TLR2 cell line, also expresses the TLRs 1 and 6. TLR2 forms active heterodimers with TLR1 and TLR6 (Sahasrabudhe et al., 2018). All these cell lines were acquired from Invivogen (Invivogen, Toulouse, France).

THP1-XBlue™-MD2-CD14 and HEK-Blue™ cell lines were cultured in RPMI-1640 medium with 2 mM glutamine and DMEM medium (Lonza, Basel, Switzerland), respectively. RPMI-1640 contained normocin 100 μg/ml (Invivogen, Toulouse, France) and DMEM medium penicillin/streptomycin 50 U/ml and 50 μg/ml. (Gibco, Leicestershire, UK). Both media were supplemented with 10% heat-inactivated fetal bovine serum (Sigma, St. Louis, MO, USA), sodium bicarbonate 1.5 g/l (Sigma, St. Louis, MO, USA) and sodium pyruvate 1 mM (Biowest, Nuaillé, France). Selection antibiotics (Invivogen, Toulouse, France) are indicated in Table S2. Cell lines were passaged twice a week and worked at 80% confluency, according to manufacturer's instructions.

2.5. TLR activation and inhibition assays with reporter cell lines

Assays for quantifying TLR activation were performed in THP1-XBlue™-MD2-CD14 and HEK-Blue™ cell lines by incubating 200 μl of the experimental sample in 96-well plates, at cell densities indicated in Table S2. This was done during 24 h at 37 °C, 5% CO_2, in presence of 0.5, 1 or 2 mg/ml of GTFs, as well as of ITFs at 2 mg/ml. These working concentrations were based on response curves from previous studies (Lépine & de Vos, 2018; Vogt et al., 2013).

Culture medium and agonists for each TLR, were included as positive and negative controls respectively (Table S2). TLR activation was determined by quantitation of SEAP secretion from the supernatant of cells which was diluted 1:10 with Quantiblue™ reagent (Invivogen, Toulouse, France). After incubation for 1 h at 37 °C, the change in absorbance was measured at 655 nm in a Bio-Rad™ Benchmark Plus microplate spectrophotometer reader (Bio-Rad Laboratories B.V, Veenendaal, Netherlands). Data were normalized relative to negative control, which were set to 1.

To assess whether fructans induce TLR signaling through the MyD88 or TRIF pathways, the synthetic peptides Pepinh-MYD™ and Pepinh-TRIF™ (Invivogen, Toulouse, France) were used. Pepinh-MYD™ and Pepinh-TRIF™ block these signaling pathways. THP1 -XBlue™-MD2-CD14 cells were pre-incubated with 50 μM of Pepinh-MYD™ or Pepinh-TRIF™ for 6 h at 37 °C, 5% CO_2. Afterwards the different fructans were added and cells were incubated during 24 h, followed by quantitation of SEAP production. The fold-change of NF-κB/AP-1 was calculated as mentioned above.

To assess the inhibitory effect of GTFs and ITFs on TLRs, HEK-Blue™ cells were pre-incubated for 1 h at 37 °C, 5% CO_2 with the fructans, followed by addition of the appropriate TLR ligands and incubation during 24 h. Next, SEAP production was determined as mentioned above. Positive controls were cells treated only with each individual TLR-specific agonist. The inhibition rate was calculated as the fold-change of NF-κB/AP-1 induction, compared to each specific TLR agonist positive control.

2.6. Prediction of fructans binding mode to TLRs by molecular docking

To predict the potential interaction sites of the different fructans with TLR2 or with TLR3 or with TLR4, molecular docking analyses were performed. We used the protein-small molecule docking web service, which is based on the docking software EADock DSS from the Molecular Modeling Group of the Swiss Institute of Bioinformatics, Lausanne, Switzerland (Grosdidier et al., 2011). For performing the docking analyses, TLRs were defined as protein targets and fructans were defined as ligands.

The crystallographic structure from human TLR2 in complex with Pam3CSK4 agonist available in the Protein Data Bank was used (PDB code 2Z7X) (Jin et al., 2007). The crystallographic structure of human TLR3 ligand binding domain was also applied (PDB code 2A0Z) (Bell et al., 2005). The crystallographic structure of TLR4 in complex with myeloid differentiation factor 2 (MD2) and lipopolysaccharide (LPS) agonist was also applied (PDB code 3FXI) (Park et al., 2009).

Since β(2→6) linkage is exclusive of GTFs, as a first approximation to determine potential interaction sites of these fructans with TLRs, we selected the simplest β(2→6) oligosaccharide found in GTFs, which is β-D-fructofuranosyl-(2→6)-β-D-fructofuranosyl α-D-glucopyranoside (6-kestose). Since ITFs only possess β(2→1) linkages, the fructan β-D-fructofuranosyl-(2→1)-β-D-fructofuranosyl α-D-glucopyranoside (1-kestose), was used to investigate whether it could have different binding sites to TLRs. Crystallographic structure of 1-kestose was extracted from Protein Data Bank and 6-kestose 3D-structure was obtained from its simplified molecular-input line-entry system (SMILES) notation deposited in PubChem data base (Table S3) (Berman et al., 2000; Kim et al., 2019).

Linear inulin and branched agavin, both constituted of GF_{10} series, were chosen as representative ligands of ITF II and GTF II, respectively (Table S4). Hereinafter called GF_{10}-inulin and GF_{10}-agavin. GF_{10}-inulin 3D-structure was obtained by modification of the PubChem structure (ID: 24763). Avogadro software version 1.2.0 was used for construction of the structure (Hanwell et al., 2012). GF_{10}-agavin structure was constructed based on the structure proposed by Mancilla-Margalli et al. (Mancilla-Margalli & López, 2006) by using the Optical Structure Recognition Software (OSRA) (Filippov & Nicklaus, 2009) and Avogadro software for structure refinement (Hanwell et al., 2012).

Prior to docking analyses, the energy of protein targets and ligands 3D-structures were minimized using Yasara minimization server or Avogadro (Filippov & Nicklaus, 2009; Hanwell et al., 2012; Krieger et al., 2009). The different protein-ligand models obtained from molecular docking, were evaluated and analyzed using UCSF Chimera software version 1.14 (Pettersen et al., 2004). The interaction measures and figures were generated with Pymol Molecular Graphics System version 2.3.5 Edu, Schrödinger, LLC (DeLano, 2002).

2.7. Stimulation of dendritic cells with agave and chicory fructans

Human dendritic cells (DCs) isolated from umbilical cord blood CD34+ progenitor cells (MatTek Corporation, Ashland, MA, USA), were used. DCs were defrosted and seeded in 96-well plates (3×10^5 cells/well), with maintenance culture medium containing cytokines (DC-MM; Mat Tek Corporation, Ashland, MA, USA), according to manufacturer's instructions. In order to get them attached to the wells DCs were incubated for 24 h at 37 °C and 5% CO_2 (normal conditions).

The influence of ITFs and GTFs on DCs cytokine release was investigated by incubating them for 48 h in the presence or absence of 500 μg/ml of ITFs and GTFs dissolved in DCs maintenance culture medium. In order to test the inhibitory effect of fructans on immune cells, DCs were pre-incubated for 1 h with 500 μg/ml of ITFs and GTFs, followed by the addition of TLR4 agonist (LPS), and a mixture of TLR2 agonists (FSL-1 and Pam3CSK4) at 10 ng/ml. Afterwards, DCs were incubated in presence of the agonists during 48 h under normal conditions. Cell supernatants were collected and stored at −80 °C until further use. Positive controls were DCs treated only with TLR4 and TLR2 agonists. Untreated controls were cells cultured only with DCs culture medium. The inhibition rate was calculated as the fold-change of cytokines production, compared to each TLR agonist positive control.

2.8. Determination of cytokine profile

Magnetic Luminex ® Assay (R&D systems, Biotechne, Minneapolis, USA) was used to quantify the DCs cytokine profile (MCP-1/CCL2, MIP-1α/CCL3, IL-1RA, IL-1β, IL-6, TNFα and IL-10). The manufacturer's protocol was followed. Briefly, 50 μl of DCs supernatants or standard solutions were mixed in 96-well plates with a mixture of magnetic beads containing antibodies for the different cytokines. The plates were incubated overnight at 4 °C under constant shaking. Afterwards, detection antibodies were added and the plate was incubated at RT for 30 min under constant shaking. Later, the plate was washed three times, followed by incubation with streptavidin for 30 min at RT under constant shaking. Then, after three-wash steps in which 100 μl of wash buffer was added per well, the plate was read in a Luminex 200 system. The data were analyzed with the Luminex xPOTENT software. At least five independent assays were performed for each test.

2.9. Statistical analyses

Data were analyzed with GraphPad Prism™ software (version 8.2.1 for Windows™, San Diego, CA, USA). Normal distribution of data was assessed with Shapiro-Wilk test. Normal distributed data were analyzed with one-way ANOVA followed by Dunnett's multiple comparisons adjustment. Non-parametric distributed data was analyzed with Mann-Whitney *U* test or Friedman test, followed by Dunn's multiple comparisons adjustment test. Results are expressed as mean ± SD or as median and interquartile range (IQR), for data with parametric and non-parametric distribution respectively. A p-value <0.05 was considered to be statistically significant ($^{*}p < 0.05$, $^{**}p < 0.01$, $^{***}p < 0.001$, $^{****}p < 0.0001$), p-values < 0.1 were considered as a trend.

3. Results

3.1. Characterization of inulin and graminan-type fructans

Inulin and graminan-type fructans were analyzed for determination of their molecular weight distribution profiles and the components that make up the mixtures. ITFs are inulin-type fructans with only β(2→1) linkages (Vogt et al., 2013). The DP of ITF I ranges from 3 to 10 (Fig. 1 a), but it also has chains with DP up to 25. These fructan is a fructooligosaccharide-enriched inulin, containing both GF_n and F_n type oligosaccharides, although the GF_n series is the most dominant over the F_n series in this fructan (Fig. 1b). ITF II consists only of GF_n units, with a broad range of chain lengths from DP9 to 60 (Fig. 1b). GTFs are a mixture of oligosaccharides linked by β(2→1) and β(2→6) (Lopez et al., 2003). DP 3 and 4 make up most of the GTF I mixture, although it has a very low amount of components in the range of DP 7–45 (Fig. 1a). GTFs contain F_n type oligosaccharides as well as GF_n series. The oligomer

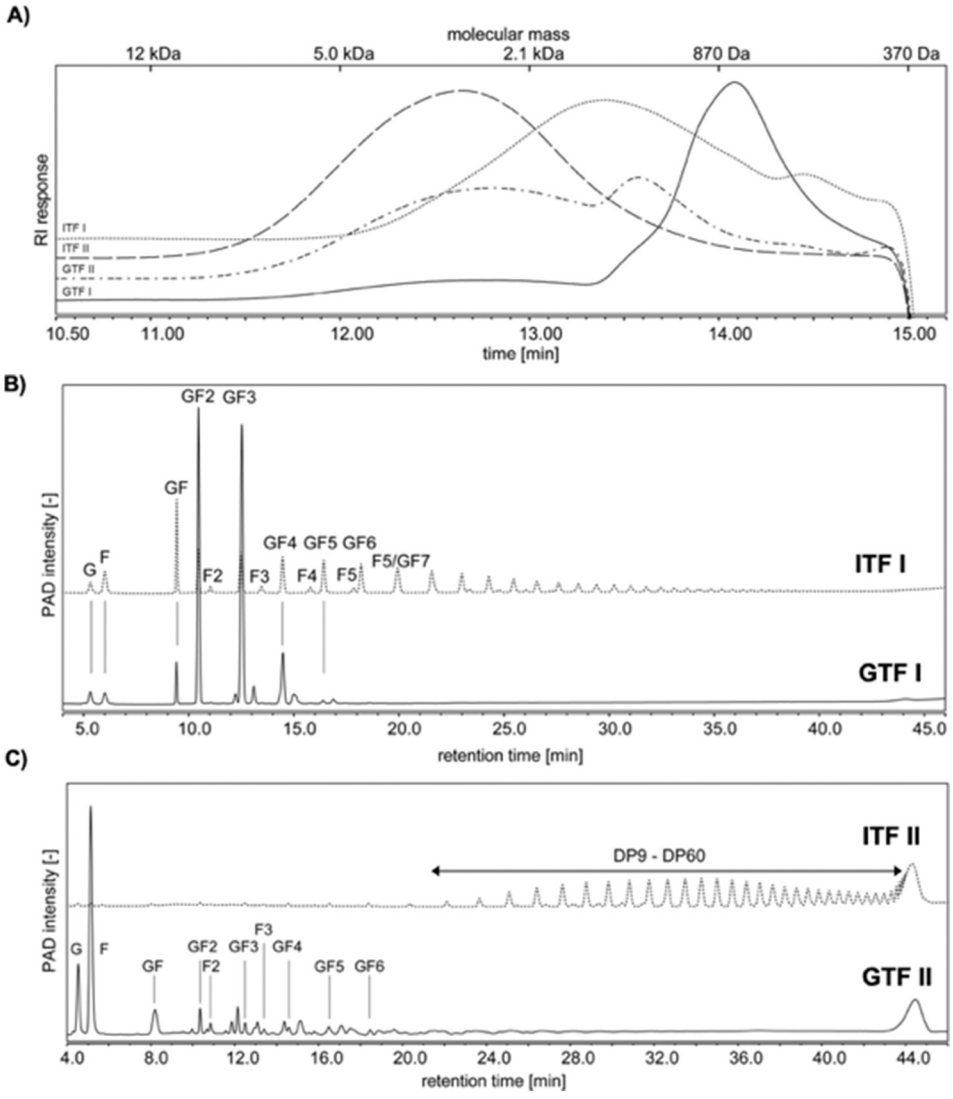

Fig. 1. HPSEC and HPAEC profiles of fructans from *Agave tequilana* and *Cychorium intybus*. (A) Molecular weight distribution profiles of ITFs and GTFs. GTF I molecular weight distribution is DP 3–4. ITF I has chains smaller than 10 DP. GTF II DP is around 17 with the presence of high molecular weight components. ITF II DP ranges between 9 and 60. Calibration of the system using pullulan standards is indicated. B) GTF I is composed of fructofuranosyl units with a terminal glucose. C) GTF II components belong to the GF series as well, and some others are of the Fn series. ITF II consists only of fructans of the GF_n type.

profile obtained from HPAEC demonstrates that GTF I is mainly composed of kestose (GF_2), nystose (GF_3) and fructosylnystose (GF_4) (Fig. 1b). GTFII contains in addition to these sugars, oligosaccharides F_2 and F_3 (Fig. 1c). GTF II has longer structures of which DP17 is the most abundant. Furthermore, in both GTFs, but specially in GTF I peaks that overlap with those of ITFs were detected. Additionally, in these studied GTFs, there were peaks detected which did not overlap with the ITFs profiles and hence, might represent the (neo-) levan or graminan type fructans.

3.2. GTFs are stronger stimulators of NF-kB activation in THP-1-MD2-CD14 cells than ITFs

ITFs and GTFs were tested for their capacity to induce NF-κB/AP-1 activation in a THP1-MD2-CD14 reporter cell line, which endogenously expresses all TLRs. NF-κB and AP-1 are essential transcription factors in signaling for cytokine release. ITFs were tested at a concentration of 2 mg/ml, as this was shown in a previous study to be an effective dose (Lépine & de Vos, 2018; Vogt et al., 2013). GTFs were tested at concentrations of 0.5, 1, and 2 mg/ml, as the concentration-dependent effects are unknown.

None of the ITFs were found to activate NF-κB/AP-1, except for ITF I in presence of MyD88 inhibitor (Fig. 2). This was different with GTF I and II that both activated NF-κB/AP-1. GTF I stimulated NF-κB/AP-1 only very mildly and only at a low concentration of 1 mg/ml (Fig. 2a). This was different with GTF II, as the fold change was of 1.59 ($p < 0.001$) compared with controls, and gradually increased with higher doses (Fig. 2b). Next, we determined whether the NF-κB/AP-1 activation observed with GTF I and II depends on the MyD88 signaling pathway, by repeating the experiments and adding the MyD88 inhibitor at 50 μM. MyD88 is the central transcription factor for all TLRs, with exception of TLR3 and endosomal TLR4. This MyD88 suppression resulted in complete loss of GTF I activation but, the effect was not MyD88-dependent with GTF II, as no reduction of NF-κB/AP-1 induced activation was observed in presence of Pepinh-MYD (Fig. 2c–d). As TLRs might also signal via TRIF pathway, we repeated the experiments with the TRIF inhibitor peptide, and also tested GTF I during TRIF inhibition. This resulted in a complete blockade of the GTF II induced activation of NF-κB/AP-1, and had no effect on GTF I (Fig. 2e–f).

3.3. TLR-activation is fructan type-dependent

The foregoing experiments demonstrate that the activating effect of GTFs and to a lesser extent the activating capacity of ITFs, are TLR dependent either via MyD88 or TRIF signaling. To identify which TLRs are activated, GTFs were also tested on reporter HEK-Blue cell lines which express either TLRs 2, 3, 4, 5, 7, 8 or 9. GTFs were tested at concentrations of 0.5, 1, and 2 mg/ml, while ITF I and II were included to allow comparison between β(2→1) and β(2→1)-β(2→6) fructans. To this end, we compared ITF I with GTF I as they are similar mixtures of chain-length values and we compared ITF II with GTF II because they share components with DP higher than 60.

ITF I only activated TLRs 2, 4 and 9. It exerted a stronger activation of TLRs 2 and 4, than of TLR 9 (Fig. 3a, c, g). Values were different with GTF I, which stimulated all TLRs. ITF I exerted a stronger activation of TLR2, which was 3.2 ($p < 0.0001$) fold enhanced and only 1.2 with GTF I ($p < 0.001$) (Fig. 3a). Also, TLR4 was strongly stimulated with ITF I which was 2.57-fold enhanced ($p < 0.0001$), and only 1.08-fold by GTF I (Fig. 3c). Effect on TLR5 by both fructans was similar and low, as it only induced a fold change of 1.05 for ITF I and 1.2 ($p < 0.05$) for GTF I (Fig. 3d).

ITF II only slightly stimulated TLRs 2 and 4 (Fig. 3h, j). While GTF II activated all TLRs in a dose-dependent manner, except on TLR4. The strongest stimulation observed with GTF II was on TLR9, with a 5.4-fold change ($p < 0.0001$), which was of 1.09 with ITF II (Fig. 3n). Also, GTF II induced a 4.05 ($p < 0.0001$) fold enhancement of TLR3 (Fig. 3i), which was of 1.04 with ITF II. Between GTF II and ITF II, a low and similar activating effect was observed on TLR4, which was 1.19 enhanced by GTF II, and 1.28 enhanced by ITF II ($p < 0.01$) (Fig. 3j).

3.4. Fructan-type influence the magnitude of inhibitory effect on individual TLRs

As the final effects of fructans on THP-1-MD2-CD14 cells may depend on the sum of activating and inhibiting effects of the fructans, we also studied and compared inhibitory effects of ITFs and GTFs on TLRs. To this end, all HEK-Blue™ cells were pre-incubated for 1 h with either 2 mg/ml of linear or 0.5, 1 and 2 mg/ml of branched fructans, followed by administration of the appropriate agonists to each cell line.

ITF I suppressed TLR5 and 9, with a fold change of 0.78 ($p < 0.001$) for TLR5 (Fig. 4c), and a fold change of 0.9 ($p < 0.0001$) for TLR9 (Fig. 4f). The other TLRs were unaffected by ITF I (Fig. 4). This was different with GTF I which strongly inhibited the activation of TLR 4, 8 and 9 in a dose dependent way (Fig. 4b, e, f). TLR4 activation was strongly inhibited by GTF I from 0.834 ($p < 0.0001$) to a 0.0.395-fold reduction ($p < 0.0001$), while the activation of TLR4 was not affected by ITF I (Fig. 4b). TLR9-activation was reduced from 1.006 to a fold change of 0.75 ($p < 0.0001$) by GTF I, while it was reduced to 0.9 ($p < 0.0001$) with ITF I (Fig. 4f). Interestingly, increasing the concentration of GTF I, did not inhibit but rather significantly enhanced TLR3 and 7 activation (both $p < 0.0001$), which did not occur with ITF I (Fig. 4a, d).

As TLR2 forms heterodimers with TLR1 and TLR6 to induce immune responses, we separately tested inhibition of TLR2-TLR1 by using the specific agonist Pam3CSK4, and for TLR2-TLR6 heterodimer by applying FSL-1. As shown in Fig. 5 a and c, the strongest inhibitory effect exerted by GTF I, was observed on TLR2-TLR6 activation, which was reduced from a fold change of 0.798 ($p < 0.05$) to 0.317 ($p < 0.0001$), and for TLR2-TLR1 the signaling was reduced from a fold change of 0.899 ($p < 0.05$) for 0.5 mg/ml of GTF I, to a fold change of 0.409 ($p < 0.0001$) for 2 mg/ml of GTF I. The activation of TLR2 was not inhibited by ITF I.

ITF II had no inhibitory effect on TLRs-activation, while GTF II strongly inhibited TLR2, 4 and 9 in a dose-dependent manner (Figs. 5b, d, 6b, f). TLR4 activation was strongly inhibited by GTF II, and such effect was proportional as the concentration increased, from a fold-change of 0.867 ($p < 0.001$) to 0.565 ($p < 0.001$) (Fig. 6b). To a lesser extent, GTF II inhibited TLR9 activation from 0.979 to a fold-change of 0.88 ($p < 0.0001$) (Fig. 6f).

In addition, the branched GTF II strongly inhibited TLR2-TLR1 activation in a dose-dependent way (Fig. 5b). This was mainly due to a strong reduction from 0.897 to a fold change of 0.421 ($p < 0.0001$). While the TLR2-TLR6 activation was reduced from 0.861 to 0.395 ($p < 0.0001$) with GTF II 0.5 mg/ml and 2 mg/ml respectively (Fig. 5d).

Instead of being inhibited, TLR3, 5, 7 and 8 were significantly increased with higher doses of GTF II. The largest increase observed was for TLR3 with a fold change of 2.1 ($p < 0.001$). This was not observed when cells were pre-treated with ITF II (Fig. 6a, c, d, e).

3.5. Docking predicts fructans bind differently to TLRs

In order to gain insight into the molecular mechanisms that drive the different activation and inhibitory effects exerted by ITFs and GTFs on TLRs, molecular docking analyses were performed. To that end, 1-kestose, 6-kestose, GF_{10}-inulin and GF_{10}-agavin were selected as one of the simplest structures that are present in the different fructans studied. From the aforementioned structures, ITF I can only have 1-kestose, GTF I and GTF II can have 6-kestose but neither of the ITFs can have it. ITF II can only have GF_{10}-inulin but cannot have GF_{10}-agavin, and GTF II can have both GF_{10}-inulin and GF_{10}-agavin. TLR2, TLR4 and TLR3 were chosen for these analyses as they were strongly influenced by the fructans and also because their crystal structure is well known.

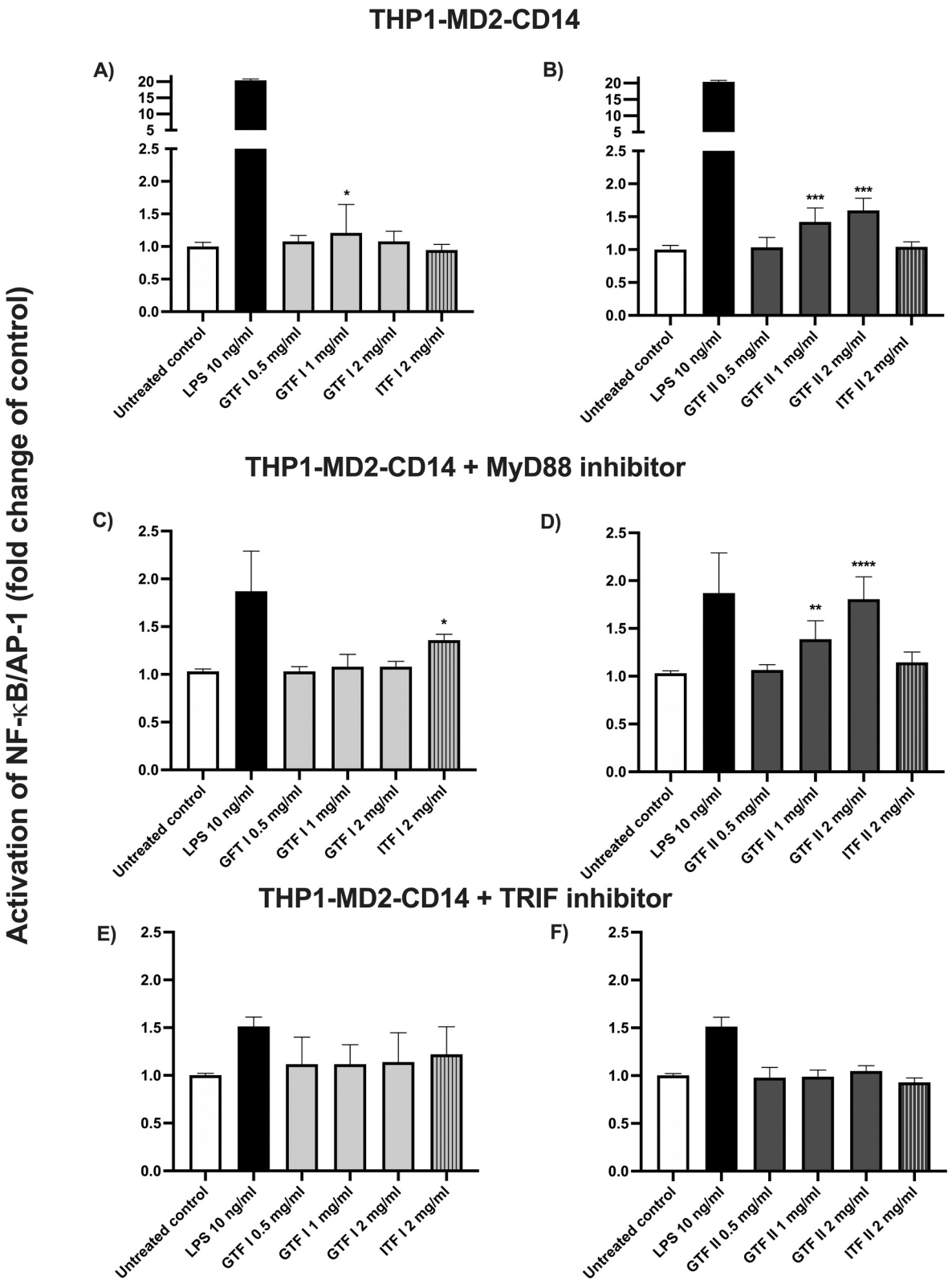

Fig. 2. NF-κB/AP-1 activation in THP1-MD2-CD14 reporter cells expressing all TLRs. A–B) THP1-MD2-CD14 cells. C–D) THP1-MD2-CD14 cells with Pepinh-MYD. E–F) THP1-MD2-CD14 cells with Pepinh-TRIF. Cells were pre-incubated in presence and absence of MyD88 inhibitor Pepinh-MYD, or TRIF inhibitor Pepinh-TRIF during 6 h before stimulation with 2 mg/ml of short and long linear chain fructans (ITF I and II) and 0.5, 1 and 2 mg/ml of short and long branched chain fructans (GTF I and II), after 24 h of incubation, NF-κB/AP-1 release was determined. Activation of NF-κB/AP-1 is presented as fold change of the untreated control. Results represent the median with interquartile range of at least three independent experiments, with three technical replicates. Statistical significance levels compared to the negative control were determined by Friedman test (non-parametric statistical test), followed by the Dunn's multiple comparisons test (post hoc test). A p-value <0.05 was considered to be statistically significant ($^{*}p < 0.05$, $^{**}p < 0.01$, $^{***}p < 0.001$, $^{****}p < 0.0001$), p-values < 0.1 were considered as a trend.

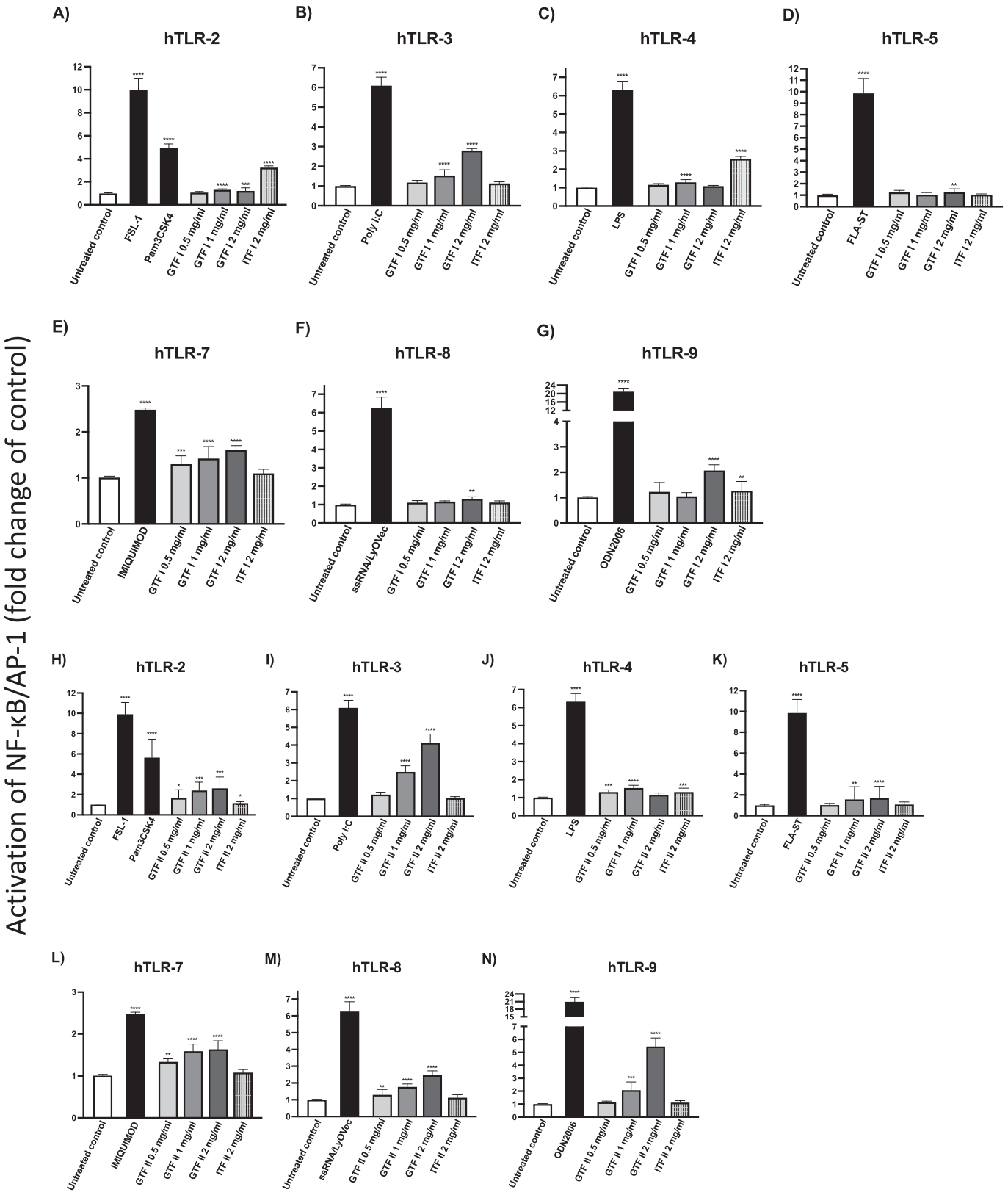

Fig. 3. Activation effects of ITFs and GTFs on HEK-Blue™ reporter cell lines. Each cell line was incubated during 24 h with 2 mg/ml of ITFs and 0.5, 1 and 2 mg/ml of GTFs. Next, NF-κB/AP-1 release was determined. Activation of NF-κB/AP-1 is presented as fold change of the untreated control. A–G) NF-κB/AP-1 activation effect of GTF I compared with ITF I. H–N) NF-κB/AP-1 activation effect of GTF II compared with ITF II. Appropriate agonists for each TLR served as positive controls. At least five independent assays, each one with three technical replicates. These data were normally distributed. Therefore, results are represented as the mean ± SD. Statistical significance levels compared to the negative control were determined by one-way ANOVA with Holm-Sidak's multiple comparisons test. A p-value <0.05 was considered to be statistically significant (*$p < 0.05$, **$p < 0.01$, ***$p < 0.001$, ****$p < 0.0001$), p-values < 0.1 were considered as a trend.

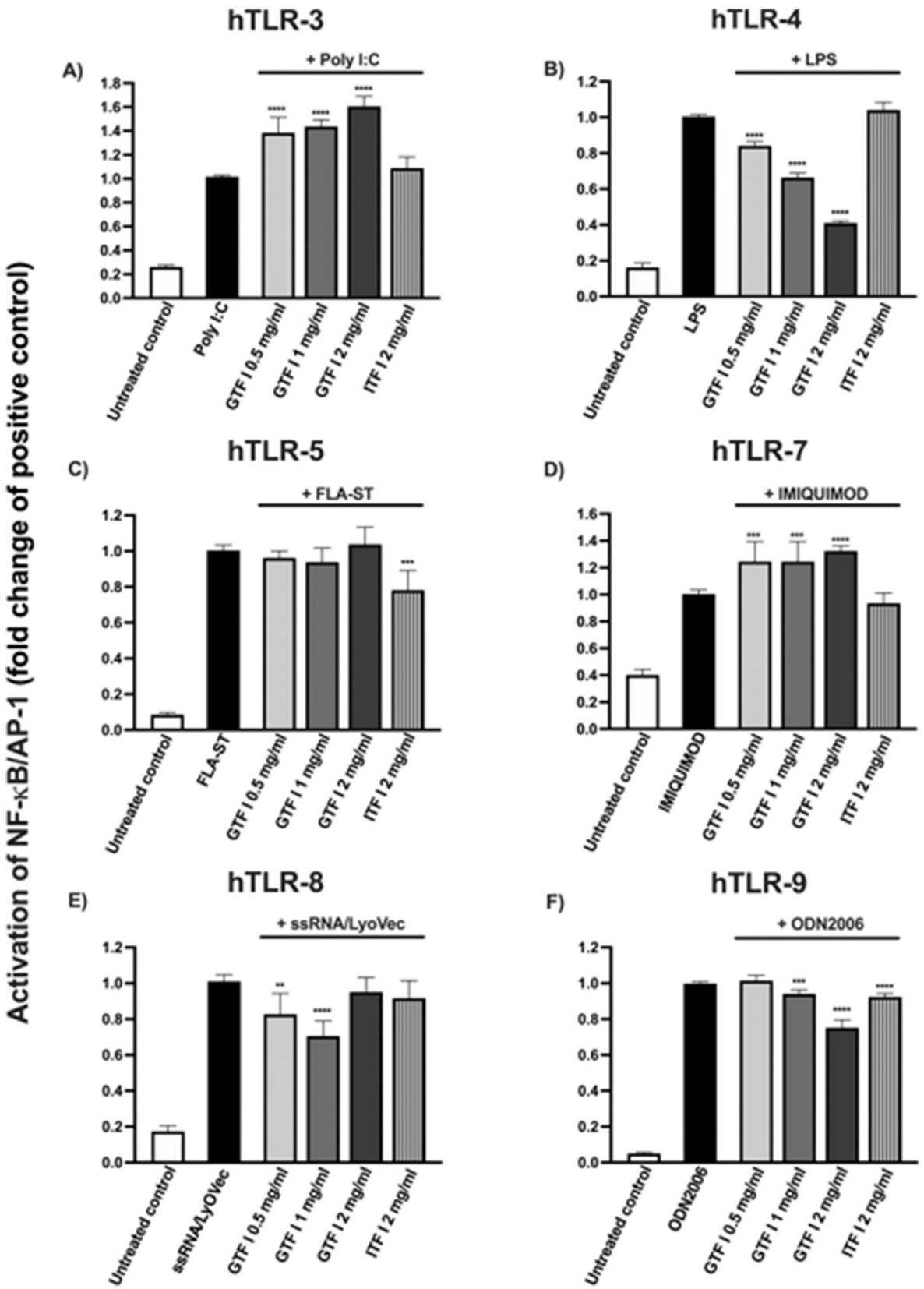

Fig. 4. Inhibitory effects of ITF I and GTF I on HEK-Blue™ reporter cell lines. Cells expressing TLR3 (A), TLR4 (B), TLR5 (C), TLR7 (D), TLR8 (E), and TLR9 (F), were pre-incubated during 1 h with short linear ITF I at 2 mg/ml and short branched GTF I at 0.5, 1 and 2 mg/ml, followed by the addition of the specific agonists for each TLR, and incubation of 24 h. Next, NF-κB/AP-1 release was determined. Panels A-F show inhibitory effect of GTF I and ITF I on TLRs activation, expressed as fold-change of NF-κB/AP-1 induction, compared to that of each specific TLR agonist. Results represent the mean ± SD of at least five independent assays, each with three technical replicates. Statistical comparisons were performed with one-way ANOVA and Geisser-Greenhouse correction, followed by Dunnett's multiple comparisons test. A p-value <0.05 was considered to be statistically significant (*$p < 0.05$, **$p < 0.01$, ***$p < 0.001$, ****$p < 0.0001$), p-values < 0.1 were considered as a trend.

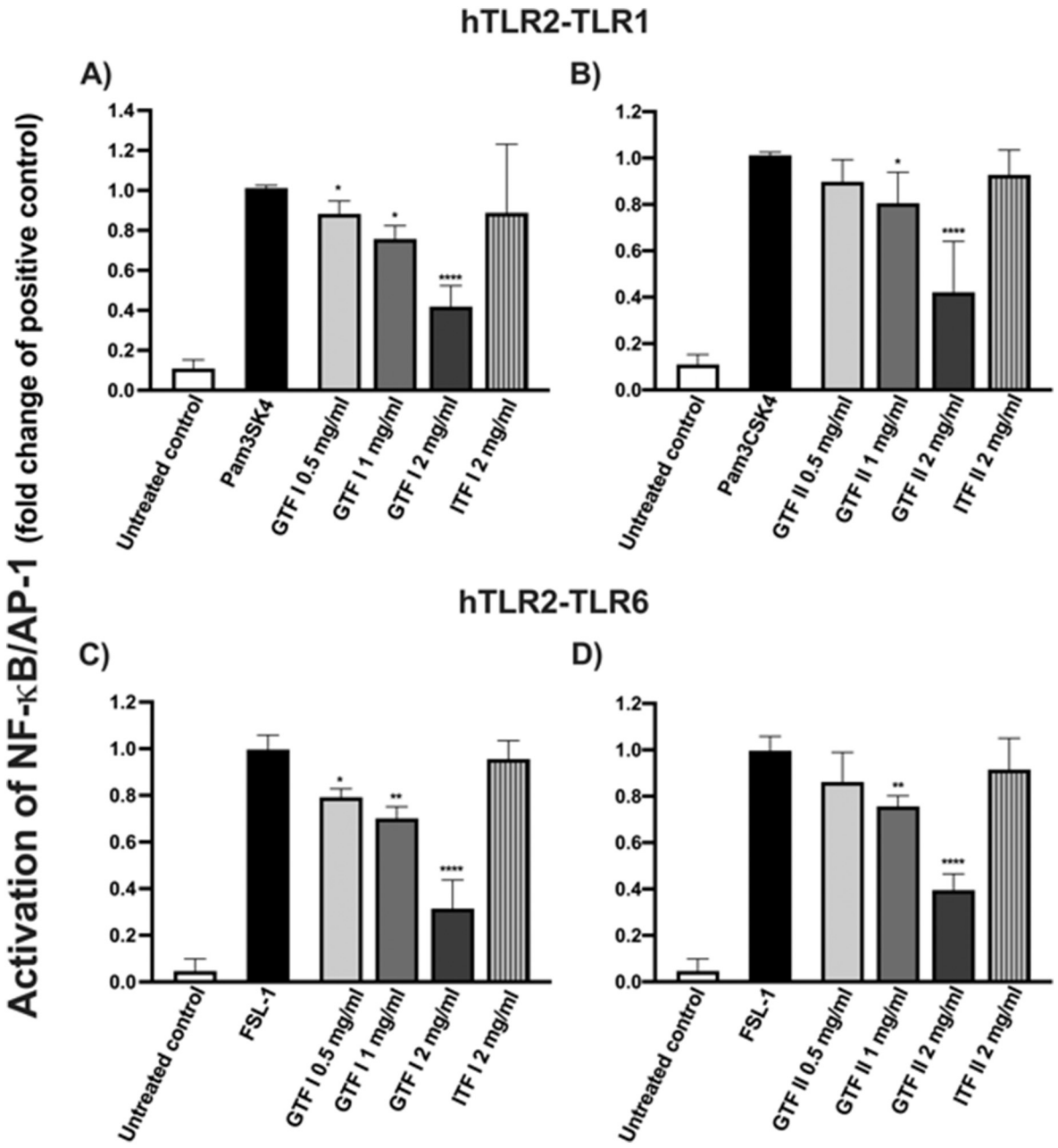

Fig. 5. Inhibitory effects of GTFs on HEK-Blue™ hTLR2 cells. Cells expressing TLR2-1 and TLR2-6 heterodimers, were pre-incubated during 1 h with 2 mg/ml of ITF I and ITF II, and 0.5, 1 and 2 mg/ml of GTF I and GTF II, followed by addition of the specific agonists Pam3CSK4 for TLR2-TLR1 heterodimer, and FSL-1 for TLR2-TLR6 heterodimer. After 24 h of incubation, NF-κB/AP-1 release was determined. Panels A–B show inhibitory effects of fructans on TLR2-TLR1 heterodimer activation, and panels C–D show inhibitory effect of fructans on TLR2-TLR6 heterodimer activation, expressed as fold-change of NF-κB/AP-1 induction, and compared to the positive control of each TLR2-heterodimer. Results represent the mean ± SD of at least five independent assays, each with three technical replicates. Statistical comparisons were performed with one-way ANOVA and Geisser-Greenhouse correction, followed by Dunnett's multiple comparisons test. A p-value <0.05 was considered to be statistically significant (*$p < 0.05$, **$p < 0.01$, ***$p < 0.001$, ****$p < 0.0001$), p-values < 0.1 were considered as a trend.

3.5.1. TLR2 docking predicted interactions

Molecular docking analysis of TLR2 with representative molecules of fructans, located them in different sites of this receptor. The best ranked pose of 1-kestose had a binding energy of −9.85 kcal/mol. 1-kestose established interactions with TLR2 residues at the central part of the ectodomain. Polar residues from TLR2 such as R447, S445 and K422 were interacting with 1-kestose (Fig. 7a–c). This was different with 6-kestose. The best ranked pose of 6-kestose had a binding energy of −8,22 kcal/mol and was found in a different region than the one found for 1-kestose. 6-kestose was located within the agonist binding pocket of TLR2. 6-kestose interacted with the 18 residues that conforms the pocket [27]. Most of amino acid residues interacting with 6-kestose were non-polar, such as leucine, isoleucine and valine. Three hydrogen bonds were formed between F322, F349 and L350 residues and 6-kestose (Fig. 7d–e).

1-kestose was found at the surface of TLR2 at the central ectodomain and at 19.2 Å from the entrance of the agonist binding site. GF_{10}-inulin was interacting with amino acid residues H238, L214, T236, Q209, D233 and K208 through hydrophobic interactions and hydrogen bonds (Fig. 7f–h).

GF_{10}-agavin was found located outside of the TLR2 pocket agonist entrance, exerting a partial blocking of this cavity, it was found

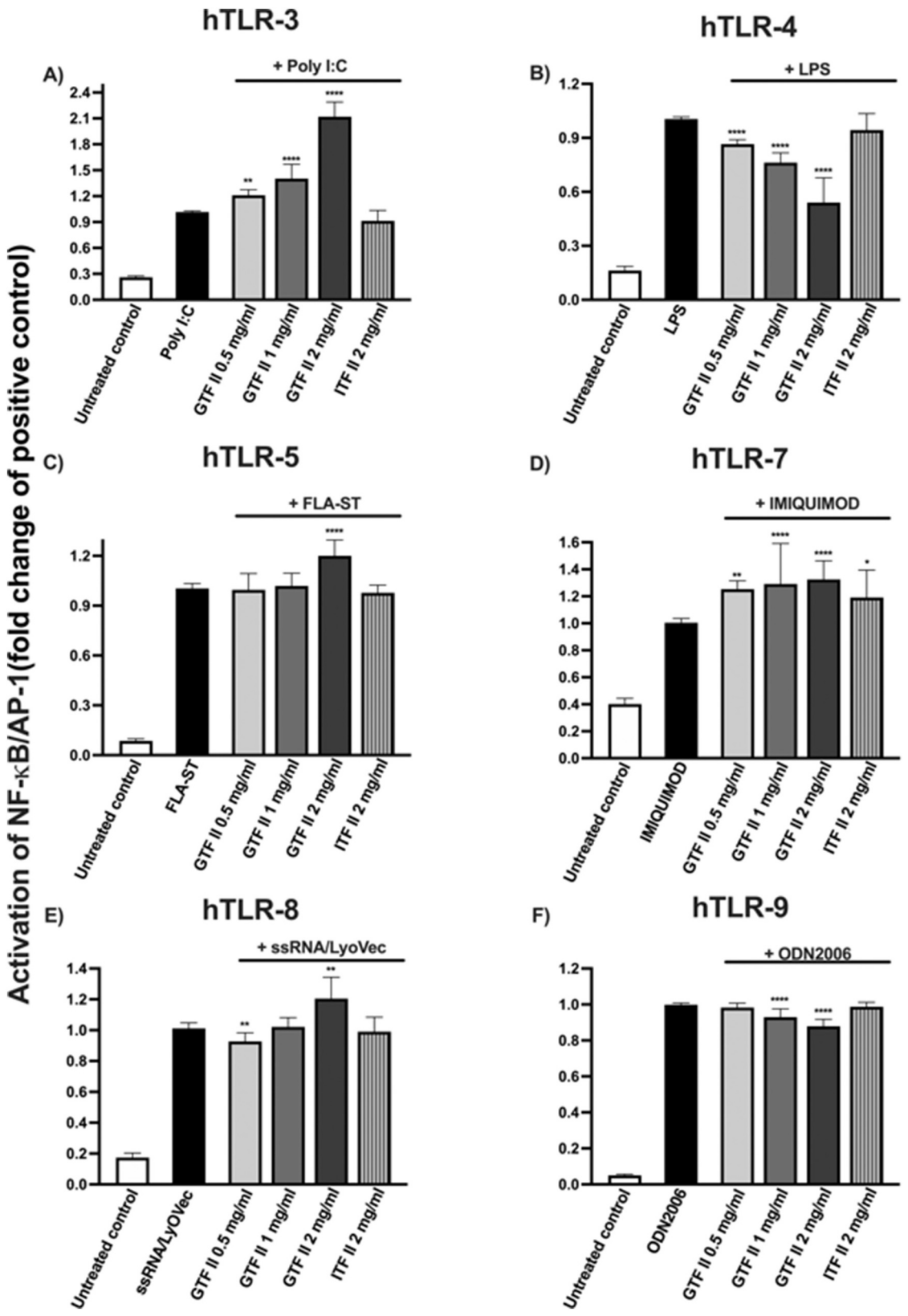

Fig. 6. Inhibitory effects of ITF II and GTF II on HEK-Blue™ reporter cell lines. Cells expressing TLR3 (A), TLR4 (B), TLR5 (C), TLR7 (D), TLR8 (E), and TLR9 (F), were pre-incubated during 1 h with ITF II at 2 mg/ml and GTF II at 0.5, 1 and 2 mg/ml, followed by the addition of the specific agonists for each TLR, and incubation of 24 h. Next, NF-κB/AP-1 release was determined. Panels A–F show inhibitory effect of GTF II and ITF II on TLRs activation, expressed as fold-change of NF-κB/AP-1 induction, compared to that of each specific TLR agonist. Results represent the mean ± SD of at least five independent assays, each with three technical replicates. Statistical comparisons were performed with one-way ANOVA and Geisser-Greenhouse correction, followed by Dunnett's multiple comparisons test. A p-value <0.05 was considered to be statistically significant ($^{*}p < 0.05$, $^{**}p < 0.01$, $^{***}p < 0.001$, $^{****}p < 0.0001$), p-values < 0.1 were considered as a trend.

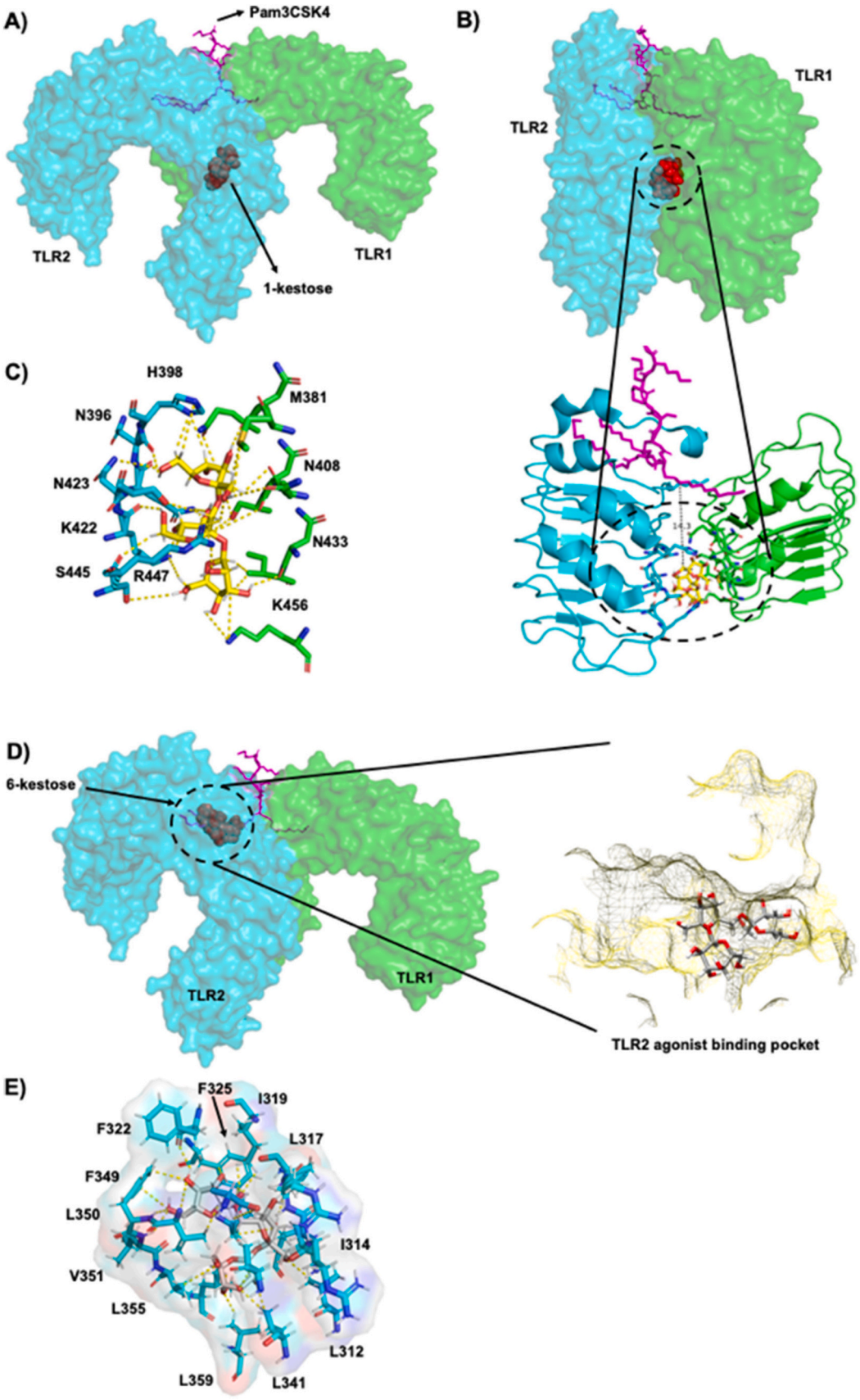

Fig. 7. Proposed binding site of fructans to TLR2-TLR1. Panels A–C demonstrates that 1-kestose binds to residues of the TLR2-TLR1 interface. Panels D–E indicates that 6-kestose has affinity to the Pam3CSK4 binding pocket of TLR2-TLR1. Panels F–H shows that GF_{10}-inulin interacts with the TLR2 surface. Panels I–J show GF_{10}-agavin established molecular interactions with amino acid residues of the agonist entrance pocket.

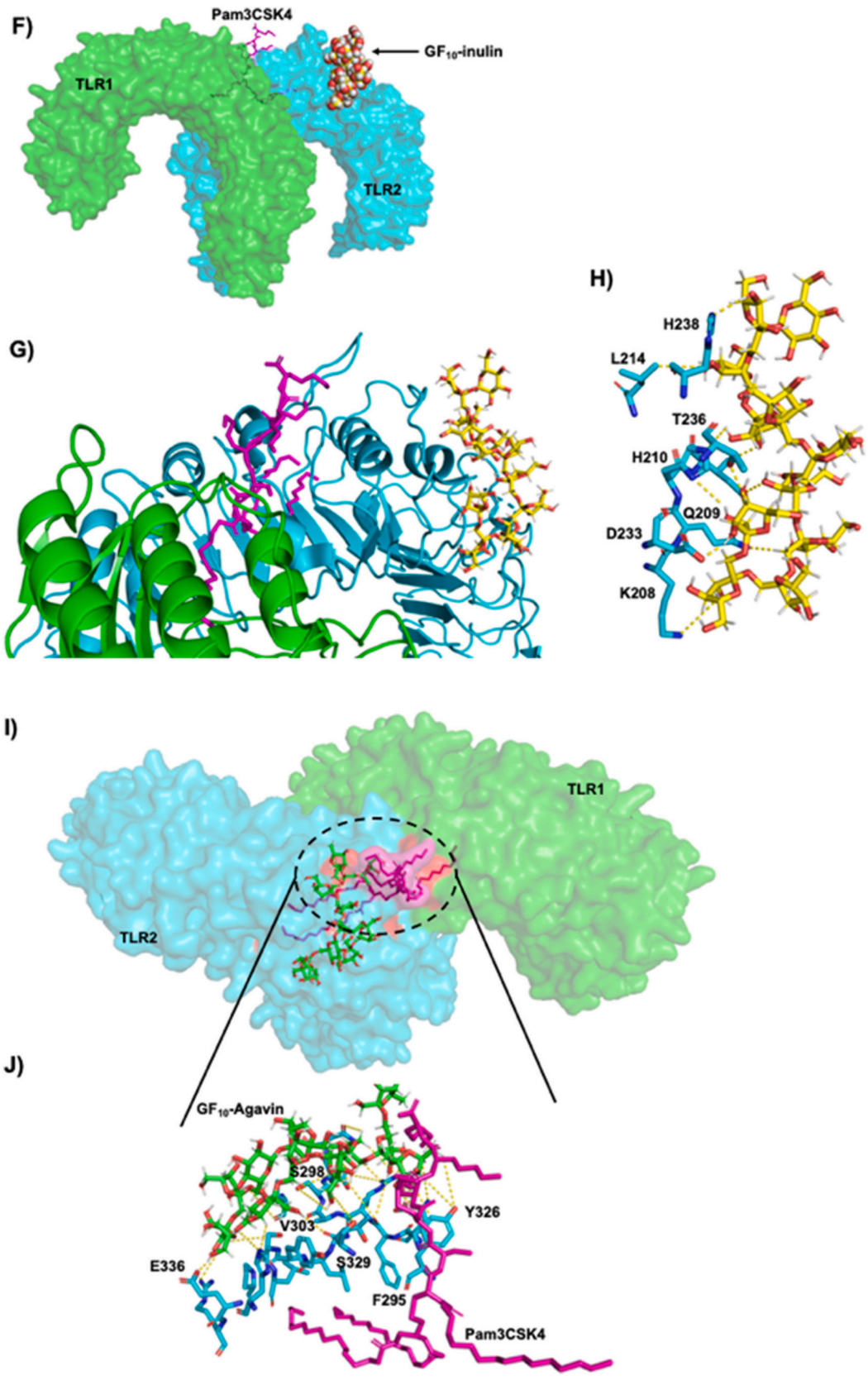

Fig. 7. (*continued*).

interacting with key amino acid residues of the binding site, such as Y326 and F325 (Fig. 7i–j).

3.5.2. TLR4 docking predicted interactions

As profound TLR4 inhibitory effects were observed for GTFs, docking analysis was performed to predict the potential binding sites of these

fructans. Docking analysis was made with the TLR4-MD2 complex with each of the four fructans. The functional unit of the TLR4-MD2 complex is formed by two TLR4 subunits, each forming a heterodimer with one MD-2 protein (Fig. 8a). The analysis predicts 1-kestose to bind within the MD-2 protein pocket (Fig. 8a). 1-kestose was found to interact only with MD-2 protein mainly through hydrophobic interactions with non-polar amino acid residues, such as I52, L61, L78, F147 and F151 (Fig. 8b–c). 6-kestose was also found within the MD-2 pocket (Fig. 8f), however the hydrophobic residues I32, I46, I94 and Y102 interacted with 6-kestose but not with 1-kestose (Fig. 8e–f). GF_{10}-inulin was found near the TLR4-MD2 interface (Fig. 8g). GF_{10}-inulin only interacted with amino acid residues of TLR4 such as H458 and G384, and those residues have not been described as key residues for interaction with LPS or for heterodimerization (Fig. 8h–i). Conversely, GF_{10}-agavin was found to interact with TLR4 as well as with MD-2 (Fig. 8j). GF_{10}-agavin established contact with some of the MD2 amino acid residues that participate in the interaction with LPS such as I124. Furthermore, GF_{10}-agavin interacted with 14 amino acid residues from MD-2 (Fig. 8k–l).

3.5.3. *TLR3 docking predicted interactions*

Enhancement of the activation instead of inhibition of TLR3 mediated by GTFs was found during the inhibition assays (Figs. 4a, 6a). In order to gain insight in the possible mechanism, docking analyses were performed with TLR3 and representative molecules of fructans. 1-kestose was located at the non-glycosylated side face of TLR3 (Fig. 9a, b), interacting with polar amino acid residues of TLR3, such as S160, K187 and E190 (Fig. 9c). 6-kestose was found located at N-terminal end of TLR3 (Fig. 9d–e). This molecule was interacting with key amino acids

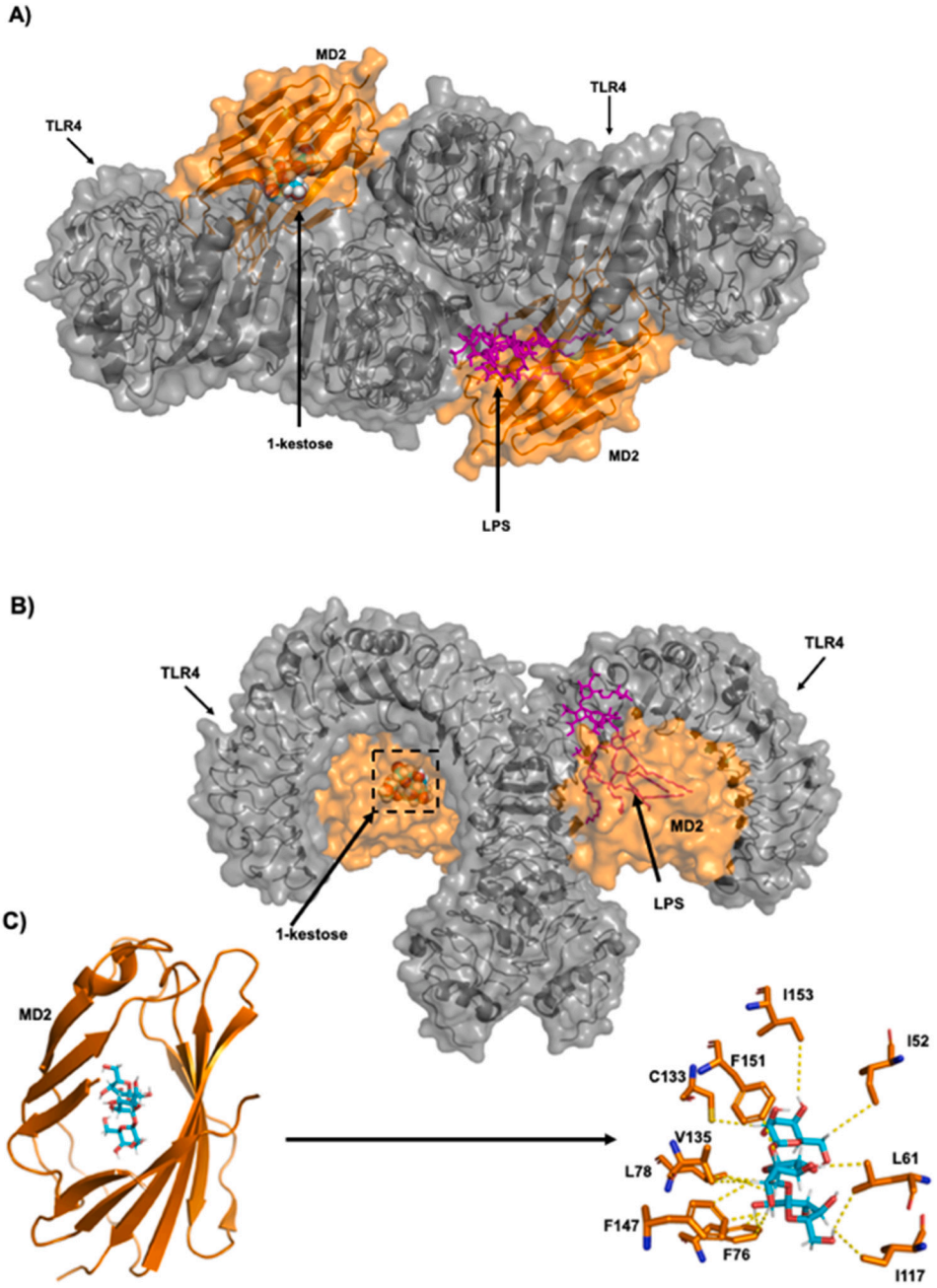

Fig. 8. Predicted sites of interaction between fructans and the TLR4-MD-2 heterodimer. The 1-kestose binding site was within the MD-2 pocket (A–C). 6-kestose established interactions with hydrophobic residues of the MD-2 pocket (D–F). GF_{10}-inulin only interacted with TLR4 amino acid residues (G–I). GF_{10}-agavin was found to interact with both TLR4 and MD-2 (J–L).

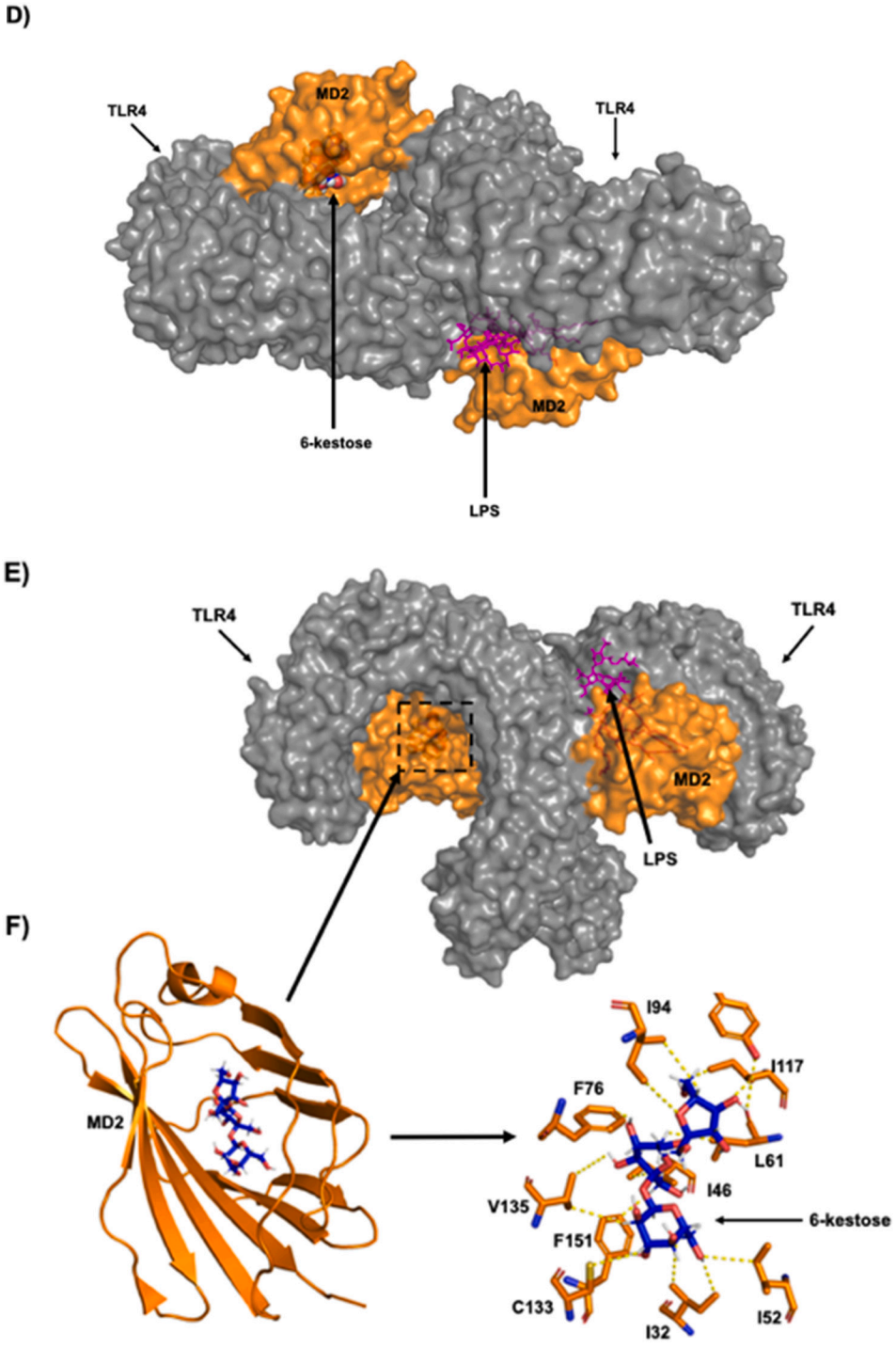

Fig. 8. (*continued*).

described for interaction with the natural agonist of TLR3, such as H39, H60, F84 and H108 (Fig. 9f) (Choe et al., 2005). On the other hand, GF_{10}-inulin, was located at the glycosylated face of TLR3 (Fig. 9g–h). GF_{10}-inulin was found interacting with polar amino acid residues such as E189 and R222, as well as hydrophobic amino acid residues such as I220, L243 and F217 (Fig. 9i). It was different GF_{10}-agavin, which was found at the N-terminal end of TLR3 (Fig. 9j–k), and the key arginine 64 was one of the amino acid residues which established an interaction with GF_{10}-agavin (Fig. 9l).

3.6. Fructans induce branching and structure-dependent inhibitory effects on cytokine production of TLR2 and TLR4 stimulated DCs

Dendritic cells are key players in the gut mucosal immune system and are distributed along the intestinal epithelium (Rescigno et al., 2001). We therefore investigated whether the fructans can also influence cytokine production of DCs. To that end, we incubated DCs for 48 h in the presence and absence of the fructans and determined cytokine release. However, as shown in Fig. S2, the fructans as such did not change cytokine production of DCs (Fig. S2). Since a strong inhibitory effect of the activation of TLR2 and TLR4 was found in HEK-cells, we

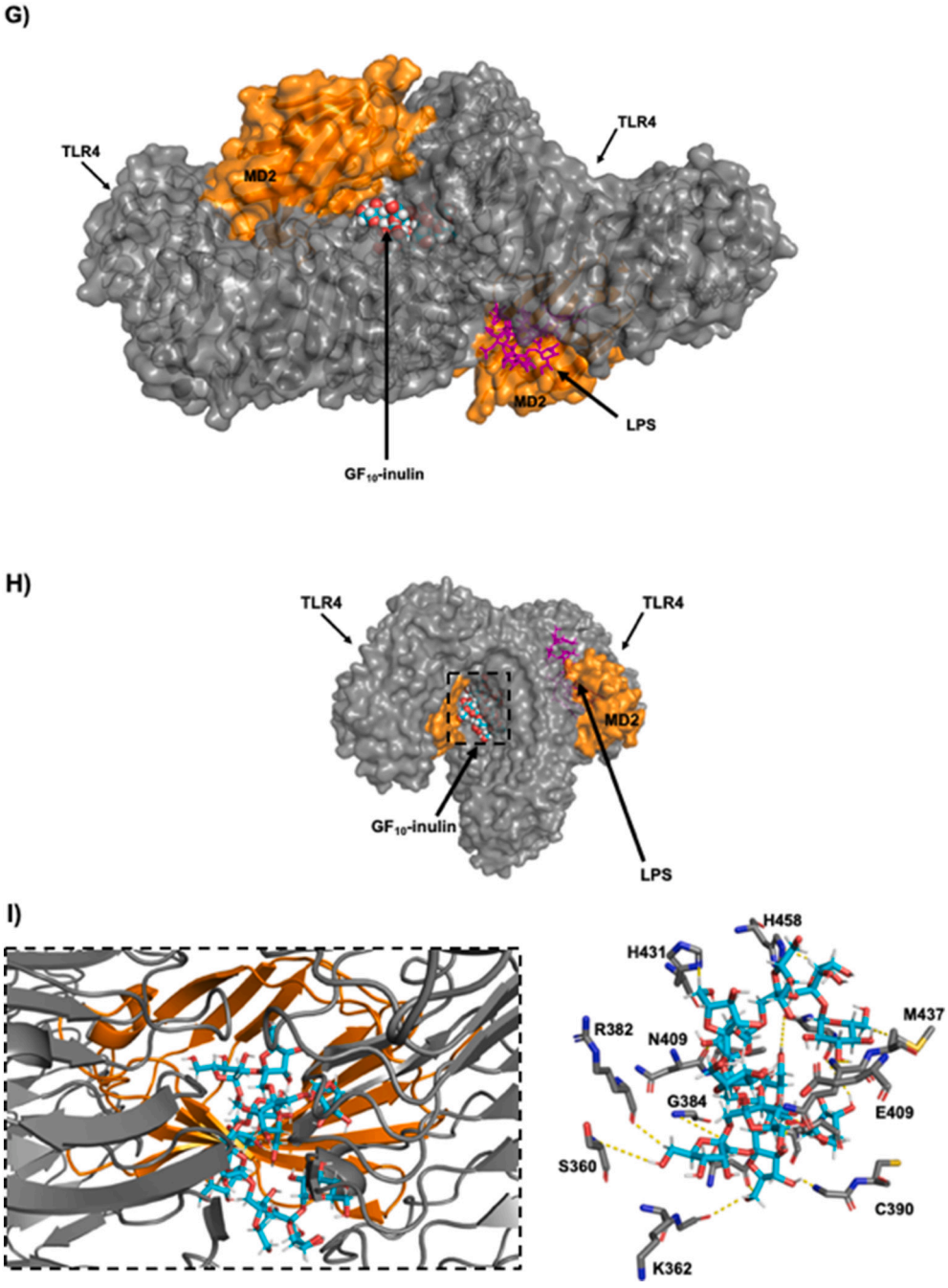

Fig. 8. (*continued*).

investigated in a next set of experiments whether fructans may reduce inflammatory responses induced by agonists for these two TLRs. Therefore, we pre-incubated DCs for 1 h with fructans followed by a stimulation with a combination of TLR2 agonists (FSL-1 and Pam3CSK4) and the TLR4 agonist LPS.

Pre-incubation of DCs with fructans caused attenuation of the inflammatory effect of the TLR2 agonist. ITF I only had a minor effect on the TLR2 induced release of TNFα by DCs (Fig. 10a). This was different for ITF II, which induced a 0.52-fold reduction ($p < 0.05$) in the TLR2 induced TNFα release. The pre-incubation of DCs with GTF I induced a 0.51-fold reduction ($p < 0.05$) in the production of TLR2 induced pro-inflammatory cytokine TNFα release. However, pre-incubation of DCs with GTF II did not induce a significant decrease of TLR2 induced TNFα production (Fig. 10a). No significant differences were found when DCs were preincubated with the fructans for production of MCP-1/CCL2, MIP-1α/CCL3, IL-1RA, IL-1β, IL-6 and IL-10 (Fig. S3a–f).

We also studied the effect of fructans on the cytokine production of DCs when stimulated with the TLR4 agonist LPS. ITF I had no significant effect on chemokine ligand of monocyte chemoattractant protein-1 (MCP-1)/CC (CCL2) (Fig. 10b). However, pre-incubation of ITF II followed by the addition of LPS, caused a decrease of 0.34-fold MCP-1/CC (CCL2) ($p < 0.001$) in TLR4 stimulated DCs. GTF I strongly attenuated MCP-1/CC (CCL2) in the TLR4 stimulated DCs with a 0.41-fold ($p < 0.0001$) reduction. Similar results were found for the pre-incubation of DCs with GTF II, which induced a 0.32-fold decrease ($p < 0.001$) in the TLR4 stimulated DCs (Fig. 10b).

The production of TNFα was not decreased when TLR4 stimulated DCs were pre-incubated with ITF I. This was different for GTF I, since the

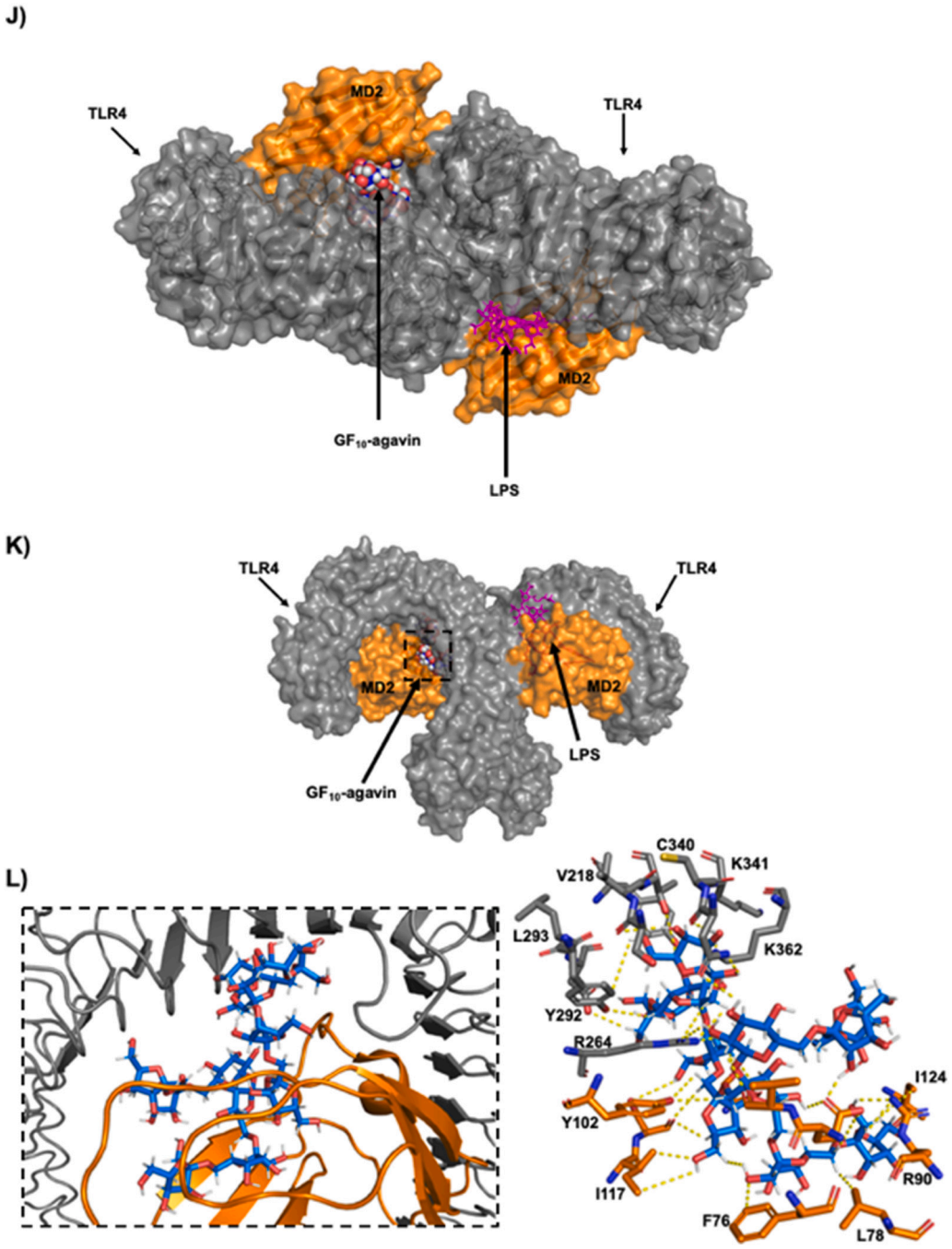

Fig. 8. (*continued*).

production of TNFα was 0.66-fold decreased ($p < 0.05$) in TLR4 stimulated DCs (Fig. 10c). A tendency to decrease the TNFα production was also observed in TLR4 stimulated DCs exposed to ITF II (0.73-fold, $p < 0.1$). This finding was different with GTF II, since no decrease in the production of TNFα was observed in TLR4 stimulated DCs (Fig. 10c). For IL6 we found no statistical lowered production in TLR4-stimulated DCs although GTF I showed a tendency to decrease with a fold change of 0.69 ($p < 0.1$) (Fig. S4d).

4. Discussion

The chemical structure and chain length of branched β(2→1)/β(2→6)-linked fructans from *Agave tequilana* and linear β(2→1)-linked fructans from *Cichorium intybus* were investigated and compared for immunomodulating effects via TLRs. We show that GTFs especially stimulate TLRs 3, 7 and 9 while they were also able to inhibit TLR2 and TLR4. Also, by performing in silico docking studies we identified the ligand binding sites for ITFs and GTFs on TLRs. To the best of our knowledge, this is the first study that demonstrates the direct effect of GTFs on human TLR signaling, their modes of interaction, as well as their influence on cytokine production in TLR2 and TLR4 stimulated dendritic cells.

In this study we investigated both the MyD88 and TRIF dependent pathways that might be influenced by fructans. MyD88 is involved in the signaling of all TLRs except TLR3 and endosomal TLR4 while TRIF signaling is involved in TLR3 and endosomal TLR4 activation (Yamamoto et al., 2003). When testing the stimulation of TLRs by GTFs, we found that in contrast to ITFs the downstream pathway followed for NF-

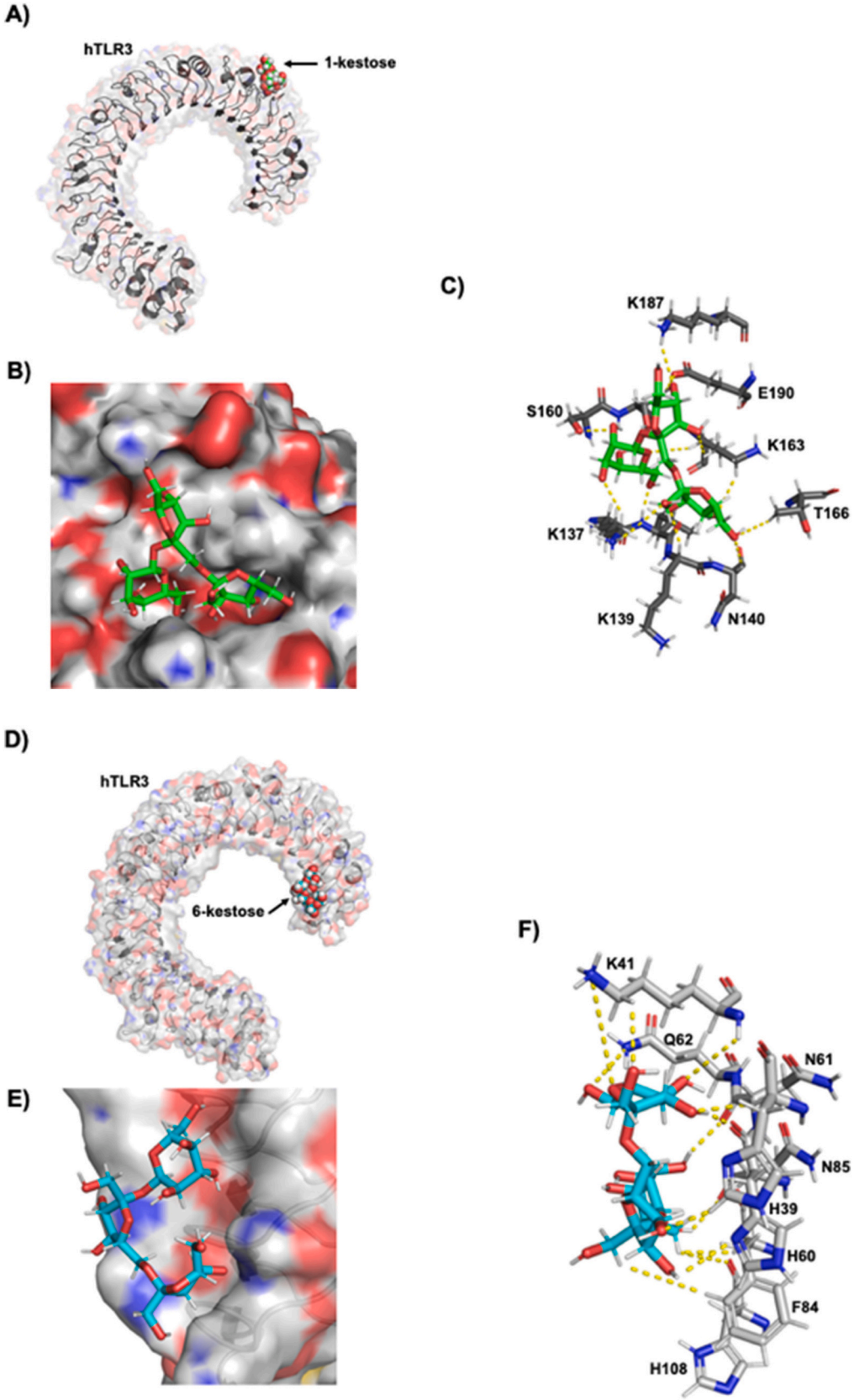

Fig. 9. Molecular interactions predicted between fructans and TLR3. 1-kestose was found to be located at the non-glycosylated side face of TLR3 (A–C). 6-kestose was located at the N-terminal end of TLR3 (D–F). GF_{10}-inulin was found located at the glycosylated face of TLR3 (G–I). GF_{10}-agavin was found at the N-terminal end of TLR3 (J–L).

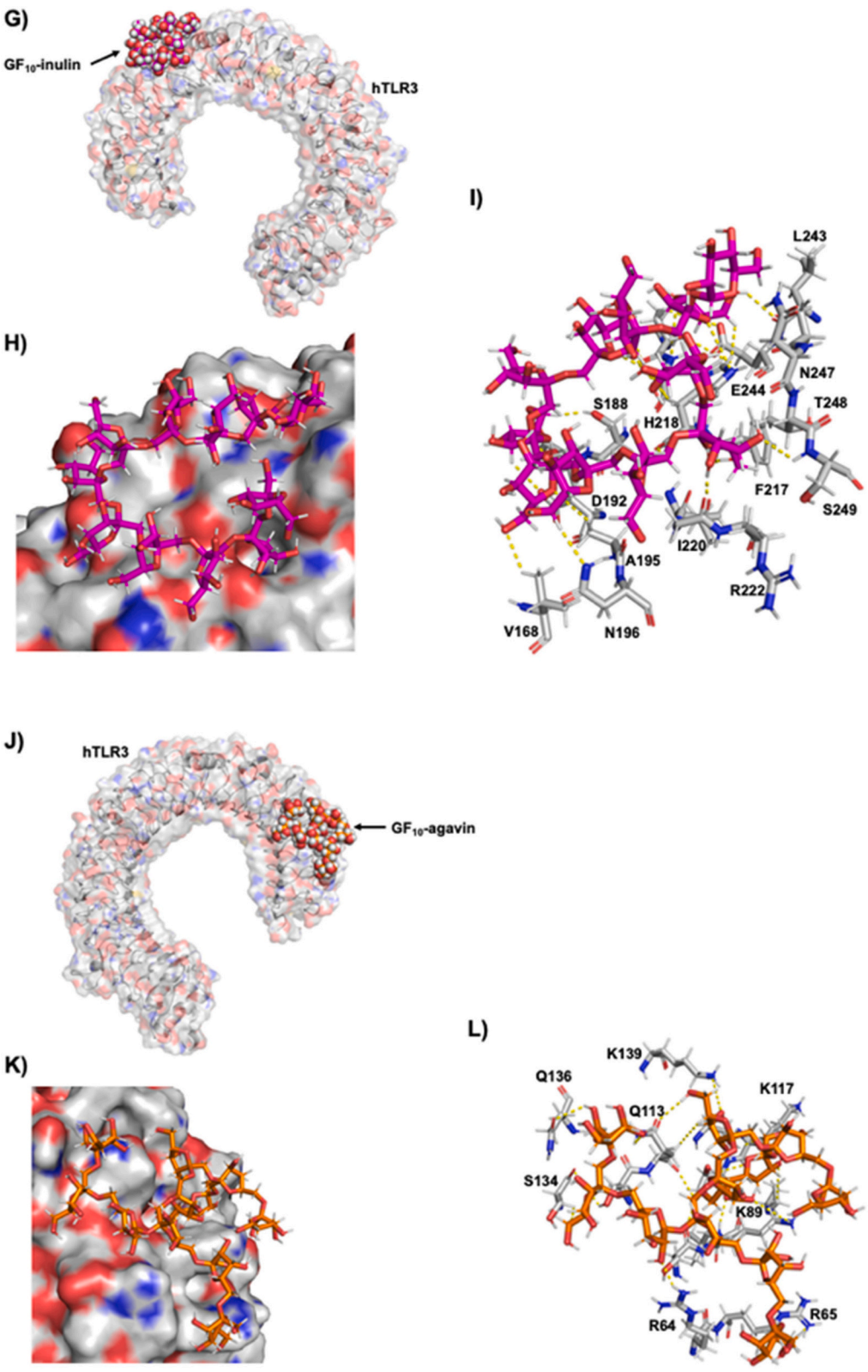

Fig. 9. (*continued*).

κB/AP-1 activation was different between both GTFs. When adding MyD88 inhibitor peptide to GTF I, the activation of NF-κB/AP-1 was completely lost which was different for GTF II where activation of NF-κB/AP-1 was only inhibited when adding the TRIF inhibitor. Thus, we show that GTF II not only depends on MyD88 but also on TRIF pathway for TLR signaling. As the main difference between GTFI and GTFII is the presence of molecules above DP 60 in GTF II, our data suggest that differences observed in the downstream signaling pathways of GTFs is dependent on the differences in structure between them.

Not only different pathways but also different TLRs were activated and inhibited by the fructans in a structure dependent way. The capacity to recognize a broad panel of ligands by TLRs is caused and determined

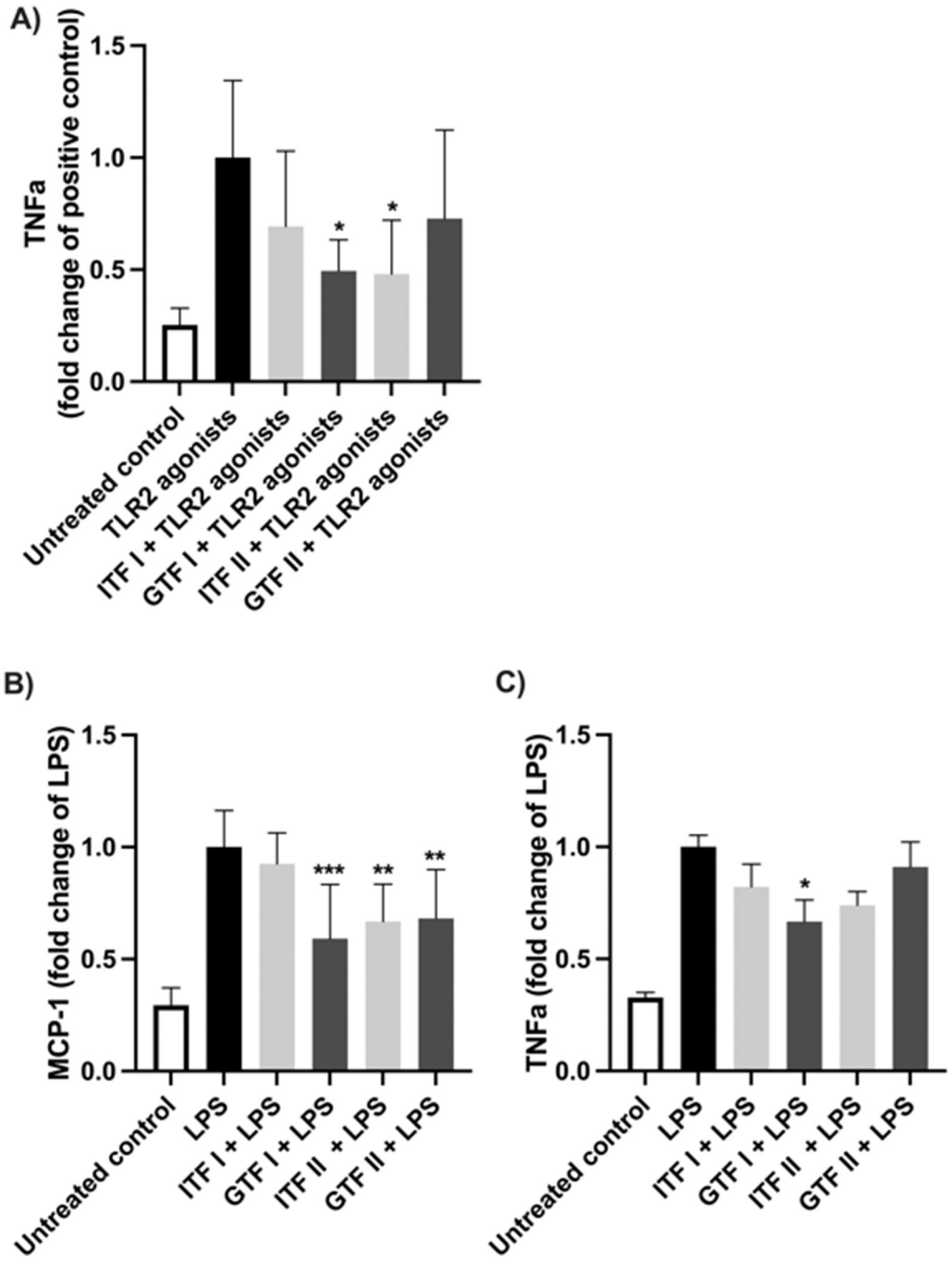

Fig. 10. Cytokine production (fold change of positive control) by dendritic cells pre-treated with GTFs and ITFs and stimulated with TLR2 and TLR4 agonists. * represent statistical differences between positive control and the different treatments (*$p < 0.05$, **$p < 0.01$, ***$p < 0.001$, ****$p < 0.0001$), p-values < 0.1 were considered as a trend.

by the leucine rich repeats (LRR) scaffold in TLRs which can accommodate a broad diversity of structures (Bell et al., 2005). When comparing the capacity of ITFs and GTFs to activate TLRs in HEK-Blue cell lines we found that ITFs and GTFs activate different TLRs. ITFs stimulated TLRs which were dependent on the MyD88 pathway such as TLR2 and 4 which corroborates our previous findings (Vogt et al., 2013) but a different and stronger activation was observed with GTFs that stimulated TRIF dependent TLRs such as TLR3, TLR7 and TLR9. This illustrated again the structure dependent immunomodulating effects of fructans.

Not only activation but also inhibition of TLR signaling was observed by GTFs. In several studies it has been shown that this capacity of food components is functional and can attenuate inflammatory responses (Kiewiet et al., 2018). Especially GTFs had a strong inhibitory effect on activation of TLR2 and TLR4. To gain insight in how GTFs can have such a strong inhibitory effect, we performed molecular docking studies to identify the site of interaction of representative molecules with TLRs. For TLR2, we studied how fructans can interact with binding to its heterodimer with TLR1 which is essential for TLR2 induced immune activation and cytokine release (Jin et al., 2007). This study demonstrates that 6-kestose can bind within the pocket of TLR2 where the natural agonist of its receptor Pam3CSK4 normally binds to the TLR2-1 heterodimer. This finding suggests that 6-kestose prevents binding of TLR2-1 ligands such as Pam3CSK4 to activate TLR2. GF_{10}-agavin was

found outside of the entrance for TLR2 agonist partially blocking this pocket. Moreover, this molecule established contact with Y326 residue, which has been described as a key residue for agonist binding to TLR2 (Jin et al., 2007). These findings suggest that both studied molecules possess the ability to avoid the binding of agonist to TLR2, although the site of binding is structure dependent.

Interaction of 1-kestose and GF_{10}-inulin with TLR2 was also observed but this was not in the ligand binding sites of TLR2-1 but in the heterodimer interface for 1-kestose, and in the central ectodomain for GF_{10}-inulin, which therefore could explain the observed lack of inhibitory effect but mild activating effects, which has been reported before (Vogt et al., 2013). These differences in the inhibition capacity between the studied fructans, might be related to the presence of β(2→6) bonds and the branched structure of GTFs, since GTFs' branched structure is more similar to the branched configuration of the lipid chains that normally fit in the TLR2 pocket (Jin et al., 2007).

GTFs also exerted a strong inhibitory effect on TLR4. Activation of TLR4 requires the formation of a heterodimer with MD2 protein (Park et al., 2009). The natural agonist of TLR4 is LPS (Kim et al., 2007) which binds to TLR4-MD2 complex through its acyl non-polar chains. Parts of these chains exert hydrophobic interactions with the TLR4-MD2 pocket which facilitates the dimerization. Our docking studies demonstrate the unique capacity of 6-kestose and GF_{10}-agavin to interact with key residues for the formation of the TLR4-MD2 complex or for the binding of LPS such as I32, I46 and I94 and I124, by which it can inhibit the TLR4 activation induced by LPS. 1-kestose and GF_{10}-inulin interacted differently with TLR4 and MD2. 1-kestose only interacted with MD2 residues such as L78 and F147, while GF_{10}-inulin only interacted with TLR4 residues such as H458 and G384. Moreover, none of these interactions were with key-amino acids involved in activation of the receptor or formation of the heterodimer. Again, this prediction could illustrate the characteristic properties of β(2→6) fructans to inhibit signaling of some proinflammatory TLRs.

Findings were different with TLR3. Preincubation with GTFs induced a stronger effect of the agonist for TLR3 rather than an inhibition illustrating the synergistic effect of the agonist and GTFs. Our docking studies revealed that 6-kestose and GF_{10}-agavin interacted with residues of TLR3 which have been previously described as key residues for interaction of this receptor with its natural agonist (Bell et al., 2005; Choe et al., 2005). The natural agonist of TLR3 is viral double stranded RNA (Bell et al., 2005; Choe et al., 2005). It has also been proposed that phosphate and ribose sugar moieties of RNA are responsible for interactions and activation of TLR3 (Bell et al., 2005). The structural similarities between ribose arrangement in RNA helix and the fructose units in GTFs with β(2→6) bonds and branched structure might explain the recognition of these polysaccharides by TLR3 and its over stimulation. This was different with 1-kestose and GF_{10}-inulin, since these molecules established interactions with amino acid residues located at the glycosylated face and the N-terminal end of TLR3. These glycosylated sites represent a steric hindrance for the binding of the agonist to TLR3 (Bell et al., 2005). Thus, this might be the explanation for the absence of interaction between ITFs and TLR3.

Dendritic cells are key players in the intestine immunity and are able to distinguish harmful from harmless antigens (Mowat, 2003; Rescigno et al., 2001; Sato & Iwasaki, 2005). They are equipped with TLRs and overactivation may lead to several intestinal and systemic disorders (Mowat, 2003). We therefore next tested whether ITFs are able to manage inflammatory responses by attenuating TLR2-1 and TLR4 induced responses in dendritic cells. As such the fructans did not change cytokines of unstimulated dendritic cells which corroborates previous findings (Bermudez-Brito et al., 2015). This was different in TLR2 and TLR4 stimulated dendritic cells. Both types of GTFs as well as ITFII had a profound inhibitory effect on TLR2 and TLR4 induced immune activation of dendritic cells. GTF I also exerted a reduction in the production of the chemokine ligand of monocyte chemoattractant protein-1 (MCP-1)/CC (CCL2) induced by TLR induced activation. This attenuation aligns with the findings of the docking studies and could possibly also be an explanation for the modulation in release of proinflammatory cytokines by immune cells described for other polysaccharides with prebiotic activity, such as galacto-oligo-saccharides, goat milk oligosaccharides and also fructooligosaccharides and inulins (Capitán-Cañadas et al., 2014).

In summary our findings may explain the mechanisms by which immunomodulating food ingredients such as agave fructans with β(2→6) bonds beneficially modulate immune responses (Bermudez-Brito et al., 2015; Vogt et al., 2013; Vogt et al., 2014). Agave plants are endemic in the Latin American region (López-Romero et al., 2018) and often used as an affordable source for obtaining fructans for food supplementation to support health. However, our data also suggest that the structure of fructans should be carefully determined and taken into consideration when intended to be used as food supplement as we show that the presence of linear or branched structure, the chain-length, as well as the dose of these molecules can exert differential responses. Further studies are needed in order to establish specifically in which disease state agave fructans could serve as an alternative or supplemental therapeutic option (Liu et al., 2004). As TLR2 and TLR4 signaling have been shown to be involved in mucositis and other intestinal disorders our data suggest that GTFs and ITF II have beneficial effects on these disorders. This suggestion is supported by a recent observation that ITF II supported gastrointestinal health in aged individuals (Kiewiet et al., 2021). Overall our study shows that beneficial immunomodulatory effects of GTFs may be explained by its impact on TLRs and attenuation of proinflammatory responses.

CRediT authorship contribution statement

C. Fernández-Lainez: Conceptualization, Methodology, Investigation, Formal analysis, Software, Writing – original draft. **R. Akkerman:** Methodology, Writing – review & editing. **M.M.P. Oerlemans:** Methodology, Writing – review & editing. **M.J. Logtenberg:** Methodology, Writing – review & editing. **H.A. Schols:** Conceptualization, Methodology, Formal analysis, Writing – review & editing. **L.A. Silva-Lagos:** Methodology, Writing – review & editing. **G. López-Velázquez:** Conceptualization, Methodology, Formal analysis, Software, Writing – review & editing. **P. de Vos:** Conceptualization, Writing – review & editing, Supervision, Project administration.

Declaration of competing interest

The authors declare no conflict of interest.

Acknowledgements

This study was partially financed by the "Programa de Recursos Fiscales para Investigación" from Instituto Nacional de Pediatría, Grant number 2019/062. C.F.L. was financially supported by Abel Tasman Talent Program Sandwich PhD from the University of Groningen-University Medical Center Groningen, UG/UMCG in collaboration with Universidad Nacional Autónoma de México, UNAM and CONACyT (#260625).

Appendix A. Supplementary data

Supplementary data to this article can be found online at https://doi.org/10.1016/j.carbpol.2021.118893.

References

Abreu, M. T. (2010). Toll-like receptor signalling in the intestinal epithelium: How bacterial recognition shapes intestinal function. *Nature Reviews Immunology, 10*, 131–144.

Beaglehole, R., Bonita, R., Horton, R., Adams, C., Alleyne, G., Asaria, P., & Casswell, S. (2011). Priority actions for the non-communicable disease crisis. *The Lancet, 377* (9775), 1438–1447.

Bell, J. K., Botos, I., Hall, P. R., Askins, J., Shiloach, J., Segal, D. M., & Davies, D. R. (2005). The molecular structure of the toll-like receptor 3 ligand-binding domain. *Proceedings of the National Academy of Sciences, 102*(31), 10976–10980.
Berman, H. M., Westbrook, J., Feng, Z., Gilliland, G., Bhat, T. N., Weissig, H., & Bourne, P. E. (2000). The protein data bank. *Nucleic Acids Research, 28*(1), 235–242.
Bermudez-Brito, M., Sahasrabudhe, N. M., Rösch, C., Schols, H. A., Faas, M. M., & de Vos, P. (2015). The impact of dietary fibers on dendritic cell responses in vitro is dependent on the differential effects of the fibers on intestinal epithelial cells. *Molecular Nutrition & Food Research, 59*(4), 698–710.
Capitán-Cañadas, F., Ortega-González, M., Guadix, E., Zarzuelo, A., Suárez, M. D., de Medina, F. S., & Martínez-Augustin, O. (2014). Prebiotic oligosaccharides directly modulate proinflammatory cytokine production in monocytes via activation of TLR 4. *Molecular Nutrition & Food Research, 58*(5), 1098–1110.
Cheng, L., Kiewiet, M. B., Groeneveld, A., Nauta, A., & de Vos, P. (2019). Human milk oligosaccharides and its acid hydrolysate LNT2 show immunomodulatory effects via TLRs in a dose and structure-dependent way. *Journal of Functional Foods, 59*, 174–184.
Choe, J., Kelker, M. S., & Wilson, I. A. (2005). Crystal structure of human toll-like receptor 3 (TLR3) ectodomain. *Science, 309*(5734), 581–585.
DeLano, W. L. (2002). Pymol: An open-source molecular graphics tool. *CCP4 Newsletter on Protein Crystallography, 40*(1), 82–92.
Filippov, I. V., & Nicklaus, M. C. (2009). Optical structure recognition software to recover chemical information: OSRA, an open source solution. *Journal of Chemical Information and Modeling, 49*(3), 740–743.
Flamm, G., Glinsmann, W., Kritchevsky, D., Prosky, L., & Roberfroid, M. (2001). Inulin and oligofructose as dietary fiber: A review of the evidence. *Critical Reviews in Food Science and Nutrition, 41*(5), 353–362.
Gay, N. J., & Gangloff, M. (2007). Structure and function of toll receptors and their ligands. *Annual Review of Biochemistry, 76*, 141–165.
Grosdidier, A., Zoete, V., & Michielin, O. (2011). SwissDock, a protein-small molecule docking web service based on EADock DSS. *Nucleic Acids Research, 39*(suppl_2), W270–W277.
Hanwell, M. D., Curtis, D. E., Lonie, D. C., Vandermeersch, T., Zurek, E., & Hutchison, G. R. (2012). Avogadro: An advanced semantic chemical editor, visualization, and analysis platform. *Journal of Cheminformatics, 4*(1), 1–17.
Health, U. D.o., & Services, H. (2015). *US Department of Agriculture. 2015–2020 dietary guidelines for Americans. Washington, DC*.
Jin, M. S., Kim, S. E., Heo, J. Y., Lee, M. E., Kim, H. M., Paik, S.-G., & Lee, J.-O. (2007). Crystal structure of the TLR1-TLR2 heterodimer induced by binding of a tri-acylated lipopeptide. *Cell, 130*(6), 1071–1082.
Kiewiet, M. B., Rodríguez, M. I. G., Dekkers, R., Gros, M., Ulfman, L. H., Groeneveld, A., & Faas, M. M. (2018). The epithelial barrier-protecting properties of a soy hydrolysate. *Food & Function, 9*(8), 4164–4172.
Kiewiet, M. B. G., Elderman, M. E., El Aidy, S., Burgerhof, J. G. M., Visser, H., Vaughan, E. E., & de Vos, P. (2021). Flexibility of gut microbiota in ageing individuals during dietary fiber long-chain inulin intake. *Molecular Nutrition & Food Research, 65*(4), 2000390.
Kim, H. M., Park, B. S., Kim, J.-I., Kim, S. E., Lee, J., Oh, S. C., & Yoo, O. J. (2007). Crystal structure of the TLR4-MD-2 complex with bound endotoxin antagonist eritoran. *Cell, 130*(5), 906–917.
Kim, S., Chen, J., Cheng, T., Gindulyte, A., He, J., He, S., & Yu, B. (2019). PubChem 2019 update: Improved access to chemical data. *Nucleic Acids Research, 47*(D1), D1102–D1109.
Krieger, E., Joo, K., Lee, J., Lee, J., Raman, S., Thompson, J., & Karplus, K. (2009). Improving physical realism, stereochemistry, and side-chain accuracy in homology modeling: Four approaches that performed well in CASP8. *Proteins: Structure, Function, and Bioinformatics, 77*(S9), 114–122.
Lépine, A., & de Vos, P. (2018). Synbiotic effects of the dietary fiber long-chain inulin and probiotic lactobacillus acidophilus W37 can be caused by direct, synergistic stimulation of immune toll-like receptors and dendritic cells. *Molecular Nutrition & Food Research, 62*(15), 1800251.
Liu, F., Liu, Y., Meng, Y., Yang, M., & He, K. (2004). Structure of polysaccharide from polygonatum cyrtonema hua and the antiherpetic activity of its hydrolyzed fragments. *Antiviral Research, 63*(3), 183–189.
López, M. G., & Urías-Silvas, J. E. (2007). Agave fructans as prebiotics. *Recent Advances in Fructooligosaccharides Research, 37*, 1–14.
Lopez, M. G., Mancilla-Margalli, N. A., & Mendoza-Diaz, G. (2003). Molecular structures of fructans from Agave tequilana Weber var. Azul. *Journal of Agricultural and Food Chemistry, 51*(27), 7835–7840.
López-Romero, J. C., Ayala-Zavala, J. F., González-Aguilar, G. A., Peña-Ramos, E. A., & González-Ríos, H. (2018). Biological activities of agave by-products and their possible applications in food and pharmaceuticals. *Journal of the Science of Food and Agriculture, 98*(7), 2461–2474.
López-Velázquez, G., Parra-Ortiz, M., de la Mora-de la Mora, I., García-Torres, I., Enríquez-Flores, S., Alcántara-Ortigoza, M. A., & Cruz-Rubio, J. M. (2015). Effects of fructans from Mexican agave in newborns fed with infant formula: a randomized controlled trial. *Nutrients, 7*(11), 8939–8951.
Mancilla-Margalli, N. A., & López, M. G. (2006). Water-soluble carbohydrates and fructan structure patterns from agave and dasylirion species. *Journal of Agricultural and Food Chemistry, 54*(20), 7832–7839.
Mowat, A. M. (2003). Anatomical basis of tolerance and immunity to intestinal antigens. *Nature Reviews Immunology, 3*(4), 331–341.
Oerlemans, M. M., Akkerman, R., Ferrari, M., Walvoort, M. T., & de Vos, P. (2020). Benefits of bacteria-derived exopolysaccharides on gastrointestinal microbiota, immunity and health. *Journal of Functional Foods, 104289*.
Park, B. S., Song, D. H., Kim, H. M., Choi, B.-S., Lee, H., & Lee, J.-O. (2009). The structural basis of lipopolysaccharide recognition by the TLR4–MD-2 complex. *Nature, 458*(7242), 1191–1195.
Patry, R. T., & Nagler, C. R. (2021). Fiber-poor Western diets fuel inflammation. *Nature Immunology*, 1–3.
Pérez-López, A. V., & Simpson, J. (2020). The sweet taste of adapting to the desert: Fructan metabolism in agave species. *Frontiers in Plant Science, 11*, 324.
Pettersen, E. F., Goddard, T. D., Huang, C. C., Couch, G. S., Greenblatt, D. M., Meng, E. C., & Ferrin, T. E. (2004). UCSF Chimera—a visualization system for exploratory research and analysis. *Journal of Computational Chemistry, 25*(13), 1605–1612.
Rescigno, M., Urbano, M., Valzasina, B., Francolini, M., Rotta, G., Bonasio, R., & Ricciardi-Castagnoli, P. (2001). Dendritic cells express tight junction proteins and penetrate gut epithelial monolayers to sample bacteria. *Nature Immunology, 2*(4), 361–367.
Roberfroid, M. B. (2005). Introducing inulin-type fructans. *British Journal of Nutrition, 93*(S1), S13–S25.
Roberfroid, M. B., Van Loo, J. A., & Gibson, G. R. (1998). The bifidogenic nature of chicory inulin and its hydrolysis products. *The Journal of Nutrition, 128*(1), 11–19.
Sahasrabudhe, N. M., Beukema, M., Tian, L., Troost, B., Scholte, J., Bruininx, E., & Schols, H. A. (2018). Dietary fiber pectin directly blocks toll-like receptor 2–1 and prevents doxorubicin-induced ileitis. *Frontiers in Immunology, 9*, 383.
Sato, A., & Iwasaki, A. (2005). Peyer's patch dendritic cells as regulators of mucosal adaptive immunity. *Cellular and Molecular Life Sciences, 62*(12), 1333–1338.
Takeda, K., & Akira, S. (2004). TLR signaling pathways. *Seminars in Immunology, 16*, 3–9. Elsevier.
Temba, G. S., Kullaya, V., Pecht, T., Mmbaga, B. T., Aschenbrenner, A. C., Ulas, T., & Kumar, V. (2021). Urban living in healthy tanzanians is associated with an inflammatory status driven by dietary and metabolic changes. *Nature Immunology, 22*(3), 287–300.
Van den Abbeele, P., Duysburgh, C., Ghyselinck, J., Goltz, S., Berezhnaya, Y., Boileau, T., & Marzorati, M. (2021). Fructans with varying degree of polymerization enhance the selective growth of bifidobacterium animalis subsp. Lactis BB-12 in the human gut microbiome in vitro. *Applied Sciences, 11*(2), 598.
Van den Ende, W. (2013). Multifunctional fructans and raffinose family oligosaccharides. *Frontiers in Plant Science, 4*, 247.
Veronese, N., Solmi, M., Caruso, M. G., Giannelli, G., Osella, A. R., Evangelou, E., & Tzoulaki, I. (2018). Dietary fiber and health outcomes: An umbrella review of systematic reviews and meta-analyses. *The American Journal of Clinical Nutrition, 107*(3), 436–444.
Versluys, M., Kirtel, O., Toksoy Öner, E., & Van den Ende, W. (2018). The fructan syndrome: Evolutionary aspects and common themes among plants and microbes. *Plant, Cell & Environment, 41*(1), 16–38.
Vijn, I., & Smeekens, S. (1999). Fructan: More than a reserve carbohydrate? *Plant Physiology, 120*(2), 351–360.
Vogt, L., Ramasamy, U., Meyer, D., Pullens, G., Venema, K., Faas, M. M., & de Vos, P. (2013). Immune modulation by different types of β2→ 1-fructans is toll-like receptor dependent. *PLoS One, 8*(7), Article e68367.
Vogt, L. M., Meyer, D., Pullens, G., Faas, M. M., Venema, K., Ramasamy, U., & de Vos, P. (2014). *Toll-Like Receptor 2 Activation by b2→ 1-Fructans Protects Barrier Function of T84 Human Intestinal Epithelial Cells in a Chain Length–Dependent Manner*.
Vogt, L. M., Elderman, M. E., Borghuis, T., de Haan, B. J., Faas, M. M., & de Vos, P. (2017). Chain length-dependent effects of inulin-type fructan dietary fiber on human systemic immune responses against hepatitis-B. *Molecular Nutrition & Food Research, 61*(10), 1700171.
Yamamoto, M., Sato, S., Hemmi, H., Hoshino, K., Kaisho, T., Sanjo, H., & Takeda, K. (2003). Role of adaptor TRIF in the MyD88-independent toll-like receptor signaling pathway. *Science, 301*(5633), 640–643.

CAPÍTULO 4

β(2→1) chicory and β(2→1)-β(2→6) agave fructans protect the human intestinal barrier function in vitro in a stressor-dependent fashion

Cynthia Fernández-Lainez,*[a,b,c] Madelon J. Logtenberg,[d] Xin Tang,[a] Henk A. Schols,[d] Gabriel López-Velázquez,[e] and Paul de Vos [a]

[a] Immunoendocrinology, Division of Medical Biology, Department of Pathology and Medical Biology, University Medical Centre Groningen, Hanzeplein 1, 9713 GZ, Groningen, The Netherlands.

[b] Laboratorio de Errores innatos del Metabolismo y Tamiz, Instituto Nacional de Pediatría, Av. Iman 1, 04530, Ciudad de México, México.

[c] Posgrado en Ciencias Biológicas, Universidad Nacional Autónoma de México. Edificio D, 1º Piso. Circuito de Posgrados, Ciudad Universitaria, 04510, Ciudad de México, México.

[d] Laboratory of Food Chemistry, Wageningen University, Bornse Weilanden 9, 6708 WG, Wageningen, The Netherlands.

[e] Laboratorio de Biomoléculas y Salud Infantil, Instituto Nacional de Pediatría, Av. Iman 1, 04530, Ciudad de México, México.

Publicado en Food & Function 2022, 13, 6737. DOI: 10.1039/d2fo00534.

Food & Function

ROYAL SOCIETY OF CHEMISTRY

PAPER

Cite this: *Food Funct.*, 2022, **13**, 6737

β(2→1) chicory and β(2→1)-β(2→6) agave fructans protect the human intestinal barrier function *in vitro* in a stressor-dependent fashion

Cynthia Fernández-Lainez, *[a,b,c] Madelon J. Logtenberg,[d] Xin Tang,[a] Henk A. Schols,[d] Gabriel López-Velázquez[e] and Paul de Vos[a]

Dietary fibers such as fructans can protect the intestinal epithelial barrier integrity, but the mechanisms underlying this protection are not completely understood. We aimed to study the protective effect of β(2→1)-β(2→6) branched graminan-type fructans (GTFs) on gut epithelial barrier function that was disrupted by three different agents which impact the barrier function *via* different cellular mechanisms. The effects of GTFs were compared with those of linear β(2→1) inulin-type fructans (ITFs). T84 intestinal epithelial monolayers were incubated with GTFs and ITFs. Afterwards, the monolayers were challenged with the barrier disruptors calcium ionophore A23187, 12-myristate 13-acetate (PMA) and deoxynivalenol (DON). Transepithelial resistance was measured with an electric cell–substrate impedance sensing system. All fructans studied prevented the barrier disruption induced by A23187. ITF II protected from the disruptive effects of PMA. However, none of the studied fructans influenced the disruption induced by DON. As a measure of disruption-induced inflammation, interleukin-8 (IL-8) production by the intestinal epithelium was determined by ELISA. The production of IL-8 induced by A23187 was decreased by all fructans, whereas IL-8 production induced by DON decreased only upon pre-treatment with ITF II. None of the studied fructans prevented PMA induced IL-8 production. GTFs just like ITFs can influence the barrier function and inflammatory processes in gut epithelial cells in a structure-dependent fashion. These distinct protective effects are dependent on the different signaling pathways that lead to gut barrier disruption.

Received 21st February 2022,
Accepted 20th May 2022

DOI: 10.1039/d2fo00534d

rsc.li/food-function

1. Introduction

The gastrointestinal epithelium is considered as the gatekeeper of the human body that separates and protects the host from the harsh conditions in the gut lumen.[1] To function as a barrier, the epithelial cells are linked by multiprotein complexes named tight junctions (TJs)[2] that avoid the entry of larger, possibly immunologically active macromolecules, or other agents such as pathogenic organisms that are harmful to the host.[3] These TJs allow the entry of molecules with radii between 3.5 and 6 Å[4] but can actively regulate their permeability in response to physiological stress.[5] Under normal barrier conditions, the transport of ions, water, and other molecules into the underlying lamina propria[6] is actively regulated by the epithelial intestinal cells to provide the host with the desired luminal molecules.[7]

Impairment of the intestinal barrier function has been proposed to be involved in the ever-growing list of Western diseases such as autoimmune diseases, allergies, some types of cancers, colitis, and inflammatory disorders.[8] The disruption has been attributed to not only the more frequent use of barrier disrupting medications such as nonsteroidal anti-inflammatory drugs (NSAIDs)[9] and proton pump inhibitors (PPIs)[10,11] but also the consumption of westernized diets rich in barrier disrupting food additives, high fat, or the absence or lower consumption of dietary fibers.[12,13] Although this emphasizes the importance of disrupted gut barrier function in

[a]*Immunoendocrinology, Division of Medical Biology, Department of Pathology and Medical Biology, University Medical Centre Groningen, Hanzeplein 1, 9713 GZ Groningen, The Netherlands. E-mail: c.fernandez.lainez@umcg.nl, lainezcynthia@hotmail.com, x.tang@umcg.nl, p.de.vos@umcg.nl; Fax: +3150-3611911; Tel: +3150-3618043*

[b]*Laboratorio de Errores innatos del Metabolismo y Tamiz, Instituto Nacional de Pediatría, Av. Iman 1, 04530 Ciudad de México, Mexico*

[c]*Posgrado en Ciencias Biológicas, Universidad Nacional Autónoma de México. Edificio D, 1° Piso. Circuito de Posgrados, Ciudad Universitaria, 04510 Ciudad de México, Mexico*

[d]*Laboratory of Food Chemistry, Wageningen University, Bornse Weilanden 9, 6708 WG Wageningen, The Netherlands. E-mail: madelon.logtenberg@wur.nl, henk.schols@wur.nl*

[e]*Laboratorio de Biomoléculas y Salud Infantil, Instituto Nacional de Pediatría, Av. Iman 1, 04530 Cuidad de México, Mexico. E-mail: glv_1999@ciencias.unam.mx*

disease development, it also opens venues to treat or prevent disease as many food molecules have been shown to stimulate gut barrier function.[14,15]

One such family of food molecules that have been shown to regulate the barrier function of gut epithelial cells are dietary fiber fructans.[16] Fructans are mostly plant-derived polysaccharides that can be categorized by the F_n type, where F indicates fructose units, and the GF_n type, where G indicates a glucose molecule linked to *n* number of fructose units.[17] Fructans can be linked by β(2→1) bonds rendering them a linear structure.[18] These fructans are of the inulin type[19] and often extracted from chicory. These inulin-type fructans (ITFs) are often used in infant formulas[20] and have been shown to protect the gut barrier function in a chain-length dependent fashion.[16] Another group of fructans that is used as a food additive in infant formulas is fructans linked by both β(2→1) and β(2→6) bonds.[21,22] These types of fructans are branched and known as graminans.[23–25] These graminan-type fructans (GTFs) are extracted from plants of the *Asparagaceae* family such as *Agave tequilana* and are one of the most complex fructans described to date.[26] It is unknown whether these branched fructans have any effect on gut barrier function.

Barrier disruption can occur *via* different cellular pathways in gut epithelial cells, but it is unknown by which pathways fructans protect epithelial cells from disruption. *In vitro*, barrier disruption can be induced by different agents and signaling mechanisms. Calcium ionophores, such as A23187, cause an increase of intracellular calcium leading to the disruption of the gut epithelial barrier.[27] Another agent, 12-myristate 13-acetate (PMA), is a tumor-promoting phorbol ester which has been shown to disrupt the gut barrier function *via* the activation of protein kinase C (PKC).[28] Another family of molecules that induce barrier disruption are trichothecenes such as the fungal toxin deoxynivalenol (DON) that act *via* MAPK signaling.[29,30] This toxin is produced by the members of the fungal genus *Fusarium*, which represents the most common source of mycotoxin contamination of crops worldwide.[31] As these agents disrupt the epithelial barrier *via* different mechanisms, they can be used to investigate the mechanisms underlying the protection against barrier disruption.

We aimed to determine whether and to what extent graminans of different molecular weights from agave could protect against gut barrier disruption. In addition, we compared the effects of GTFs with the barrier protective effect of ITFs from chicory. As it is unknown by which mechanisms fructans can protect against barrier disruption, we compared the effects induced by the calcium ionophore A23187, PMA and the fungal toxin DON which disrupt the epithelial integrity *via* different signaling pathways. Finally, interleukin-8 (IL-8) production by the intestinal epithelial cells was quantified as a measure of inflammatory stress induced by the above-mentioned disruptors and it was determined if fructans are able to protect from this inflammatory stress.

2. Materials & methods

2.1. Fructans

To study whether fructans with different structures and molecular sizes can protect against the disruption of the intestinal barrier of epithelial T84 cells, two formulations of β(2→1)-β(2→6)-linked graminan-type fructans from the *Agave tequilana* Weber blue variety (agave) and two formulations of β(2→1)-linked inulin-type fructans from *Cichorium intybus* (chicory) were included. Agave fructans GTF I (Metlos™) and GTF II (Metlin™) were provided by Nekutli™ (Guadalajara, México). Chicory fructans ITF I (Frutafit™ CLR) and ITF II (Frutafit™ TEX!) were provided by Sensus™ (B.V. Roosendaal, The Netherlands). These fructans have also been studied and analyzed in previous studies from our group.[32,33]

2.2. Cell lines

For determination of the potential protective effect of chicory and agave fructans on the barrier function of intestinal epithelial cells, we used colonic epithelial T84 cells (Sigma-Aldrich, Zwijndrecht, The Netherlands) between passages 28 and 34. Epithelial T84 cells were cultured in Dulbecco's modified Eagle's medium/nutrient mixture F-12 Ham with 15 mM HEPES and sodium bicarbonate (Sigma, Dorset, UK), supplemented with 10% heat-deactivated fetal bovine serum (Sigma-Aldrich, Dorset, UK) and gentamicin 50 mg ml^{-1} (Sigma-Aldrich, Dorset, UK) (complete medium). The epithelial T84 cells were cultured at 37 °C with 5% CO_2, until 80% confluence. The medium was refreshed twice a week. For maintenance, the cells were passaged after treatment with trypsin (Sigma-Aldrich, Dorset, UK).

2.3. Disruptors

The epithelial T84 monolayers were challenged using chemical compounds that disrupt the barrier function *via* different intracellular routes.[27–29] The barrier disruptors used herein were the calcium ionophore A23187, also known as calcimycin, the food-contaminant mycotoxin DON, and PMA. The concentrations used herein were previously demonstrated to induce epithelial barrier disruption.[14,16]

2.4. Transepithelial electrical resistance measurements

The T84 cell-intestinal epithelial barrier function was monitored in real time with an electric cell–substrate impedance sensing system (ECIS, Applied BioPhysics™ model Zθ). First, epithelial T84 cells were seeded at a density of 10 000 cells per well in a final volume of 300 μl, in a 96-well PET plate with gold electrodes (96W20idf PET, Applied Biophysics). To increase the electrical stability of measurements, the plates were pre-incubated at room temperature (R.T.) for 30 min with a PBS solution of L-cysteine (2 mg ml^{-1}) before seeding. Afterwards, the plates were washed with Dulbecco's modified Eagle's medium (DMEM) with 4.5 g L^{-1} glucose, 3.9 mM L-glutamine and 1 mM sodium pyruvate (Catalog number BE12-604F, Lonza, USA) and coated overnight at R.T. with a solution of 0.1% bovine serum albumin and 1% purified soluble collagen in DMEM. After washing the plates with com-

plete medium, epithelial T84 cells were seeded and cultured at 37 °C with 5% CO_2 for 21 days to allow the formation of a monolayer with stable transepithelial electrical resistance (TEER). The culture medium was refreshed every other day. For TEER measurements, the plates were placed in the ECIS equipment and the resistance was monitored for 5 hours at 400 Hz to ensure a stable measurement. Afterwards, the experiment was started. Epithelial T84 cells were pre-incubated for 24 hours with 10 mg ml^{-1} of the four studied fructans ITF I, ITF II, GTF I, and GTF II. This was followed by the addition of the disruptor calcium ionophore A23187 (4 μM, Sigma-Aldrich, UK), DON (8.4 μM, Sigma-Aldrich, UK), or PMA (1000 nM, Sigma-Aldrich, UK). After adding the disruptor, the TEER was monitored in the presence of the calcium ionophore A23187 for 3 hours, and with DON and PMA for 24 hours. The cells incubated only with the culture medium were used as untreated controls. The cells treated only with disruptors were included as positive controls. At least five independent experiments were performed with three technical replicates. To quantify the changes in the TEER after the different treatments, the area under the curve (AUC) was calculated. Untreated controls were set as 100% and the different conditions were related to the untreated controls.

2.5. Measurement of IL-8 production of epithelial T84 cells

To investigate whether disrupting molecules induce inflammation in T84 cells, the production of the pro-inflammatory cytokine IL-8 was measured. To that end, supernatants from the T84 cells were collected once the TEER experiments were finished. The supernatants were stored at −20 °C until further use. IL-8 was quantified with an ELISA kit (R&D Systems, Abingdon, UK) according to the manufacturer's protocol.

2.6. Statistical analyses

GraphPad software version 9.2 was used for statistical analyses. The Shapiro–Wilk test was performed to test for the normality distribution of the data. Since AUC and IL-8 data are normally distributed, such data were expressed as mean ± SD. The significance was assessed with one-way ANOVA with Dunnet's multiple comparison test. A p-value < 0.05 was considered as statistically significant, $*p < 0.05$, $**p < 0.01$, $***p < 0.001$, and $****p < 0.0001$.

3. Results

To study whether the differences in their chemical characteristics are important for their effects on the modulation of the induced-disruption of the epithelial barrier, four fructan formulations were used. The graminan-type fructans studied are oligosaccharides with β(2→1) and β(2→6) linkages, which confer them a branched structure. GTF I is a mixture of fructans enriched with DP 3–4, although oligosaccharides with DP 7–45 are also present in lower amounts. GTF II is a mixture of mainly longer fructans whose DP ranges between 3 and 60 with most components around DP 17, although some higher molecular weight molecules are present. Both GTFs are composed of fructan structures of the F_n and GF_n series of fructan structures (Table 1).[33] In addition, in these two mixtures, there are molecules that represent the neo-levan type, which are characteristic of fructans extracted from agave plants.[23] The inulin-type fructans included are oligosaccharides with only β(2→1) linkages, which confer them a linear structure. ITF I is a mixture of fructans with a DP range of 3–10, but it also possesses chains of DP up to 25. ITF II is a mixture of longer chain fructans with a DP of 10–60. ITF I contains both F_n and GF_n types of oligosaccharides, whereas ITF II is constituted only of GF_n units (Table 1).[32]

3.1. Agave and chicory fructans exert a protective effect on calcium ionophore-induced disruption of gut epithelial barrier function

To test the potential protective effect of branched graminan-type fructans on the intestinal barrier function, epithelial T84 cell monolayers were preincubated with GTFs before adding the barrier disruptor calcium ionophore A23187 after which the TEER was measured for three hours. Linear inulin-type fructans were also tested to compare the effects between branched and linear fructan structures. After pre-incubation with fructans for 24 hours, A23187 was added to the cells followed by TEER measurements for three more hours. Fig. 1A shows a representative example of TEER measurements. These TEER values were used for calculating AUC. As shown in Fig. 1B, the incubation of T84 cells with A23187 decreased their AUC to 27% ± 5.5 ($p < 0.001$) compared with that of the untreated control. This effect of A23187 was strongly attenuated when the cells were preincubated with GTFs or ITFs since the AUC of these cells was similar to that of the untreated control. ITF II was the fructan with the strongest protective capacity against the barrier function disruption as the AUC decreased only by 4.7% ± 3.7, followed by GTF I (7% ± 4), GTF II (8.2% ± 4) and ITF I (12.5% ± 5.4).

3.2. Linear long chain unbranched fructans exert protective effects against PMA-induced disruption of gut epithelial barrier function

PMA is a well-known barrier disruptor which acts *via* the activation of PKC.[28] We aimed to challenge the intestinal monolayers with this disruptor in order to study whether the protective effect exerted by chicory and agave fructans occurred *via* PKC. To that end, T84 monolayers were pre-incubated with fructans for 24 hours, followed by the addition of PMA and incubation for another 24 hours. A representative example of the TEER experiment is shown in Fig. 2A. These data were used for the calculation and plotting of the AUC percentage (Fig. 2B). Compared with the untreated control, PMA induced a reduction of 17% ± 1.5 ($p < 0.01$) in the AUC. This was lower in cells pre-incubated with ITF II where the AUC reduction was 10% ± 3.3 ($p < 0.05$) (Fig. 2B). The fructans ITF I, GTF I and GTF II did not influence the AUC reduction induced by PMA, since the AUC values obtained were 83.5% ± 1.8 for GTF II, 80% ± 2 for ITF I and 78% ± 2 for GTF I (Fig. 2B).

Table 1 Characteristics and comparison of the differences between linear and branched fructans[32,33]

Representative Haworth projections of fructans present in the mixture	Fructan mixture	Structure	DP range
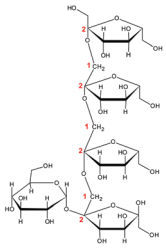	ITF I	Linear	3–10
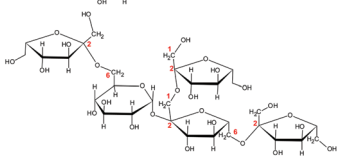	GTF I	Branched	3–45
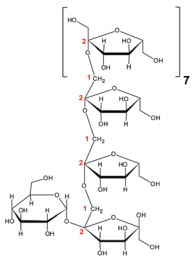	ITF II	Linear	9–60
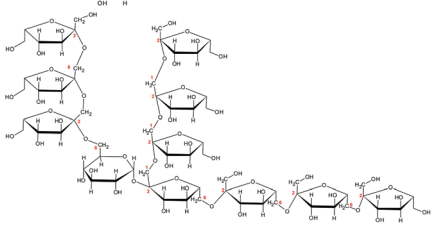	GTF II	Branched	3–60

3.3. No protective effect of fructans on DON induced disruption of gut epithelial barrier function

To investigate the ability of fructans to protect from epithelial barrier disruption exerted *via* MAPK signaling, epithelial T84 cells were also challenged with the fungal toxin DON. Monolayers of T84 cells were pre-incubated for 24 hours with the different fructans studied. Afterwards, DON was added followed by a subsequent incubation of another 24 hours. A representative example of the TEER measurements under different experimental conditions is shown in Fig. 3A. DON decreased the AUC significantly to 87.1% ± 1.3 ($p < 0.01$) compared to the control (Fig. 3B). This disruption could not be prevented with the fructans studied, since the AUC was 80.8% ± 2 for ITF I, 79.5% ± 1.9 for GTF I, 88.8% ± 0.24 for ITF II, and 86.7% ± 3.5 for GTF II (Fig. 3B).

3.4. Fructans protect T84 intestinal epithelial cells from the inflammatory effect induced by the calcium ionophore and DON but not by PMA

We aimed to investigate whether fructans could protect from the inflammation exerted by the different studied epithelial disruptors.

To that end, IL-8 secretion from T84 cells was measured at the end of TEER experiments. The calcium ionophore strongly increased the production of IL-8 by T84 cells from 182 ± 18 pg ml^{-1} to 1531 ± 96 pg ml^{-1} ($p < 0.001$). Interestingly, pre-incubation with all the tested fructans significantly decreased the production of IL-8. Compared with the effect of the positive control (set as 100%), ITF II caused a reduction in IL-8 production of 72% ± 3 ($p < 0.001$), GTF I attenuated it to 68% ± 3 ($p < 0.001$), followed by GTF II which decreased it to 66% ± 6 ($p < 0.001$), while ITF I reduced IL-8 production by T84 cells to 63% ± 3 ($p < 0.001$) (Fig. 4A).

Incubation with DON increased the IL-8 production from 182 ± 18 pg ml^{-1} to 1671 ± 131 pg ml^{-1} ($p < 0.0001$). Pre-incubation with linear fructans ITF I and ITF II significantly decreased the IL-8 production of T84 cells. ITF I reduced IL-8 production to 31% ± 2 ($p < 0.05$), and ITF II reduced it to 57.5% ± 4 ($p < 0.0001$). In contrast, branched chain fructans did not influence the inflammation induced by DON, since there were no statistical differences between the IL-8 production of the positive control and cells pre-treated with these agave fructans (Fig. 4B).

PMA significantly stimulated IL-8 production in T84 cells. Under these conditions, IL-8 increased 17-fold the untreated

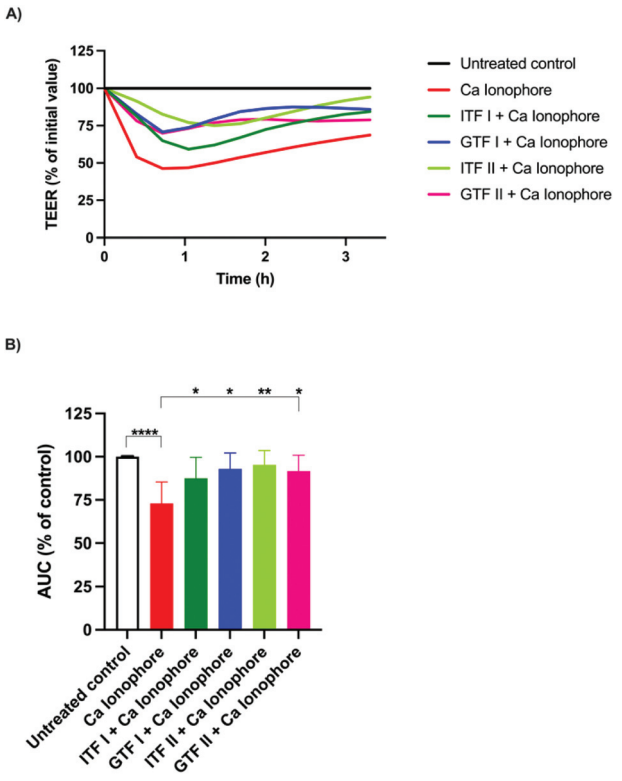

Fig. 1 The protective effect of β(2→1) and β(2→1)-β(2→6) fructans on T84 epithelial intestinal barrier disruption induced by the calcium ionophore A23187. Confluent monolayers of T84 cells were pre-incubated with 10 mg ml^{-1} of the linear fructans ITF I and ITF II and the branched fructans GTF I and GTF II for 24 hours. Afterwards, the calcium ionophore A23187 (4 μM) was added and the cells were incubated for three more hours. (A) The representative example of a TEER measurement with ECIS. (B) Calculated area under the curve (AUC). The % AUC of fructan pre-incubated epithelial cells was compared with that of the untreated controls. Statistical differences between the positive control and the different conditions were determined. Data from five independent experiments are presented as mean ± SD. ***$p < 0.001$.

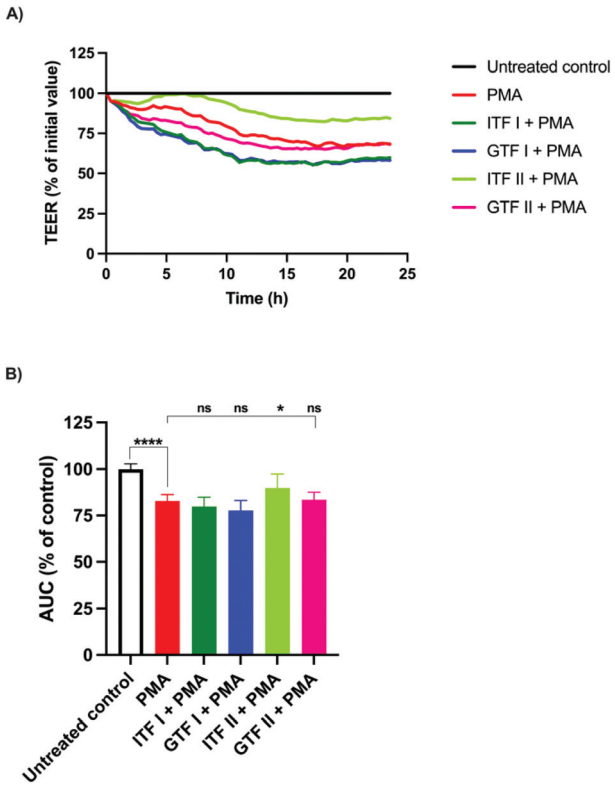

Fig. 2 The protective effect of β(2→1) and β(2→1)-β(2→6) fructans on T84 epithelial intestinal barrier disruption induced by the protein kinase C activator PMA. (A) Representative example of a TEER measurement with ECIS when preincubated with 10 mg ml^{-1} of agave and chicory fructans for 24 hours followed by the addition of 1000 nM PMA, and incubation for another 24 hours. (B) Calculated area under the curve (AUC). All the tested conditions were compared with the untreated control. Statistical differences between the positive control and cells pre-incubated with fructans were investigated. Data from five independent experiments are presented as mean ± SD. ****$p < 0.0001$.

control (from 182 ± 18 pg ml^{-1} to 3111 ± 118 pg ml^{-1}). However, none of the studied fructans attenuated the inflammatory effect exerted by PMA, since the production of IL-8 was similar to that of the positive control. In cells pre-incubated with ITF I, the IL-8 value was 3020 ± 62 pg ml^{-1}, 3321 ± 117 pg ml^{-1} for GTF I, 3034 ± 95 pg ml^{-1} for ITF II and 3136 ± 84 pg ml^{-1} for GTF II (Fig. 4C).

4. Discussion

Previous reports from our group and others have demonstrated the beneficial effects of inulin-type fructans on gut epithelial barrier function.[16,34] These studies have shown that for ITF, this protection is dependent on the chain length of the fructans. One of the new findings in this study is that the ITF induced protection was dependent on the applied disrupter and specific biochemical pathways. This is not known yet for ITFs. In addition, we studied for the first time the effects of GTFs which are different from those of ITF. The ITFs are composed of fructose units with only β-2→1 linkages, which confer them a linear structure. The GTFs are extracted from agave plants and are more complex than ITFs. Fructans from agave are a mixture of oligosaccharides with β-2→1 and β-2→6 linkages, also known as graminans or agavins. This gives them a branched structure. Moreover, fructans from the neo-series have also been found in the mixtures extracted from agave.[26] Their barrier-protective effects have never been studied. Since fructans from agave represent one of the most complex fructan types described to date, we compared their effects on gut epithelial barrier function with those of fructans with a linear structure and by which pathways they protect against barrier disruption. To the best of our knowledge, this is the first study where the protective effects of branched fructans from agave on gut epithelial barrier function are studied. The application of these fructans would be useful especially in regions where the agave plant is endemic, such as in the American continent, from the Canadian/United States border to the Northern region of South America.[35]

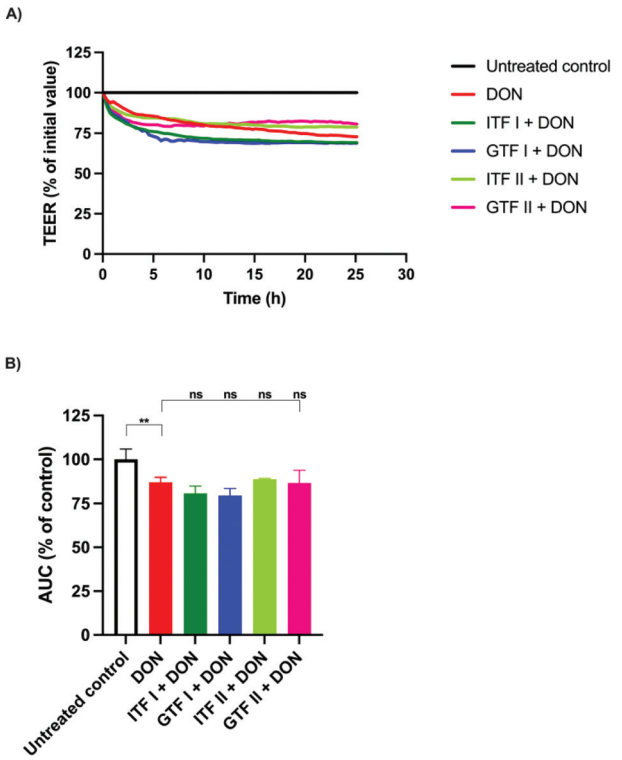

Fig. 3 No protective effect of β(2→1) and β(2→1)-β(2→6) fructans on T84 epithelial intestinal barrier disruption induced by the MAPK signaling disruptor DON. The TEER was monitored during a 24-hour pre-incubation of T84 monolayers with the studied fructans ITF I, ITF II GTF I and GTF II. Afterwards, DON 8.4 μM was added followed by TEER monitoring for another 24 hours. (A) Representative image of TEER measurements. (B) Calculated area under the curve (AUC) obtained from the TEER measurements. There was a non-statistical difference between the positive control and the cells pre-treated with fructans. The results are presented as mean ± SD of five independent experiments. $^{**}p < 0.01$.

To the best of our knowledge, this is the first study where it is investigated whether the protection of the intestinal barrier integrity exerted by fructans is dependent on the intracellular route by which the disruption is induced. To that end, three different disruptors which act *via* PKC or MAPK signaling were used. We found that the disruption induced *via* the PKC pathway was attenuated by ITF II, while the disruption induced by MAPK signaling was unaffected. Moreover, the protective effect of GTFs was not similar to that observed for ITFs, since ITF II was the only fructan that protected against the disruptive action of PMA, whereas the branched fructans did not influence the epithelial barrier impairment provoked by this molecule. This again illustrates that dietary fibers can attenuate barrier disruption depending on their chemical structure.

All fructans were effective in preventing barrier disruption induced by the calcium ionophore A23187. This effect was strongest with ITF II, followed by those with GTF I, GTF II, and ITF I. We hypothesize that the observed efficacy of fructans to attenuate A23187 induced barrier dysfunction is through a competition for the cell-binding site of the stressor on the cell membrane. Fructans possess a neutral charge. This neutral

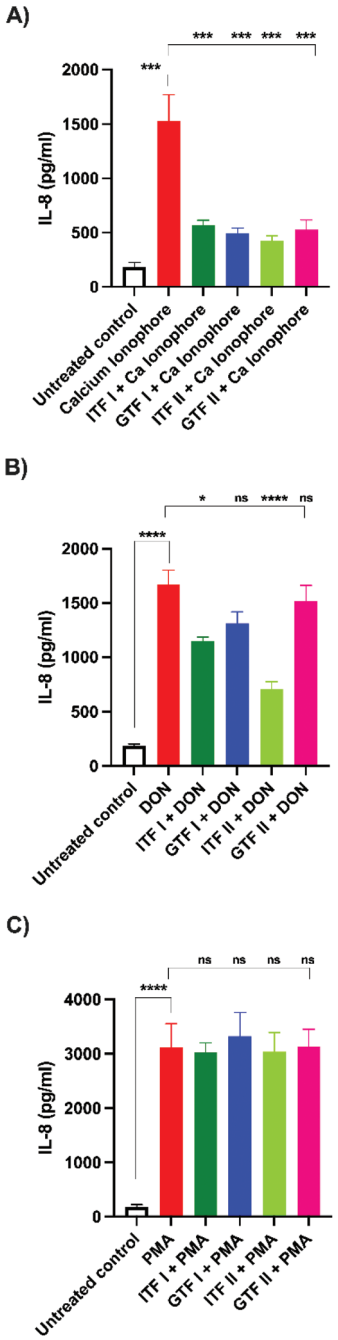

Fig. 4 Production of IL-8 by T84 epithelial intestinal cells stimulated with epithelial barrier disruptors in the presence or absence of β(2→1) and β(2→1)-β(2→6) fructans. T84 cells were pre-incubated with agave and chicory fructans, followed by the addition of the calcium ionophore A23187 (A), DON (B), or PMA (C) and 24 more hours of incubation. IL-8 production was quantified from cell supernatants collected at the end of the experiment. From five independent experiments a comparison between the positive control and tested conditions was performed to determine the influence of the studied fructans on the inflammatory effect induced by the barrier disruptors. Untreated cells served as negative controls. The results are presented as mean ± SD. $^{*}p < 0.05$, $^{**}p < 0.01$, $^{***}p < 0.001$, $^{****}p < 0.0001$.

charge allows fructans to interact with the lipidic bilayer of cell membranes by the establishment of non-polar interactions.[36–38] By this, fructans could occupy the binding sites of A23187, thus preventing, or reducing the binding of this disruptor. The binding mechanism of the calcium ionophore A23187 has been previously described. At physiological pH, the protonated form of A23187 prevails, and can strongly bind to the phospholipidic cellular membrane.[39] To induce barrier disruption, A23187 binds and transports divalent calcium ions across the cell membrane, with a concomitant increase of intracellular calcium.[40] Such an increase of intracellular calcium has been associated with changes in tight junctions and decreased resistance of T84 monolayers, a process ultimately mediated by PKC.[14,27,41] Fig. 5 schematically presents our proposed mechanism of protection of epithelial barrier function exerted by fructans.

The results were different with PMA induced barrier disruption. Only ITF II had a statistically significant effect on barrier disruption induced by PMA. Our findings indicate that protection against disruption by PMA is exclusive to linear structures of fructans and is chain-length dependent. The exclusive protection of ITF II from the disruptive action of PMA compared to those of other fructans could be explained by the long and linear structure of ITF II. Vereyken *et al.* studied the requirements for the establishment of interactions between inulins of different DP with mono- and bilayer lipidic systems. They found a strong dependency of the inulin chain length on the capacity to interact with lipid layers in favor of longer inulin that established the strongest interactions. In this study it was also proposed that the linearity and flexibility of furanose rings are the main characteristics responsible for the strong interaction between the long chain inulins and lipids.[38] This would be different for GTFs since their branched structure would provoke a more spatially disordered arrangement of their chains, which would decrease their physical contact with the cell membrane, leading to more free spaces for PMA for establishing interactions.

We found that the long chain fructan ITF II was the only fructan that exerted protection from the disruptive action of PMA. This finding seems to contradict the findings of Vogt *et al.*[16] where only non-statistical differences were found with long-chain inulins. Notably, however, differences in ITF dosing might be responsible for that, as Vogt *et al.* used a hundred-fold lower dose of fructans (0.1 mg

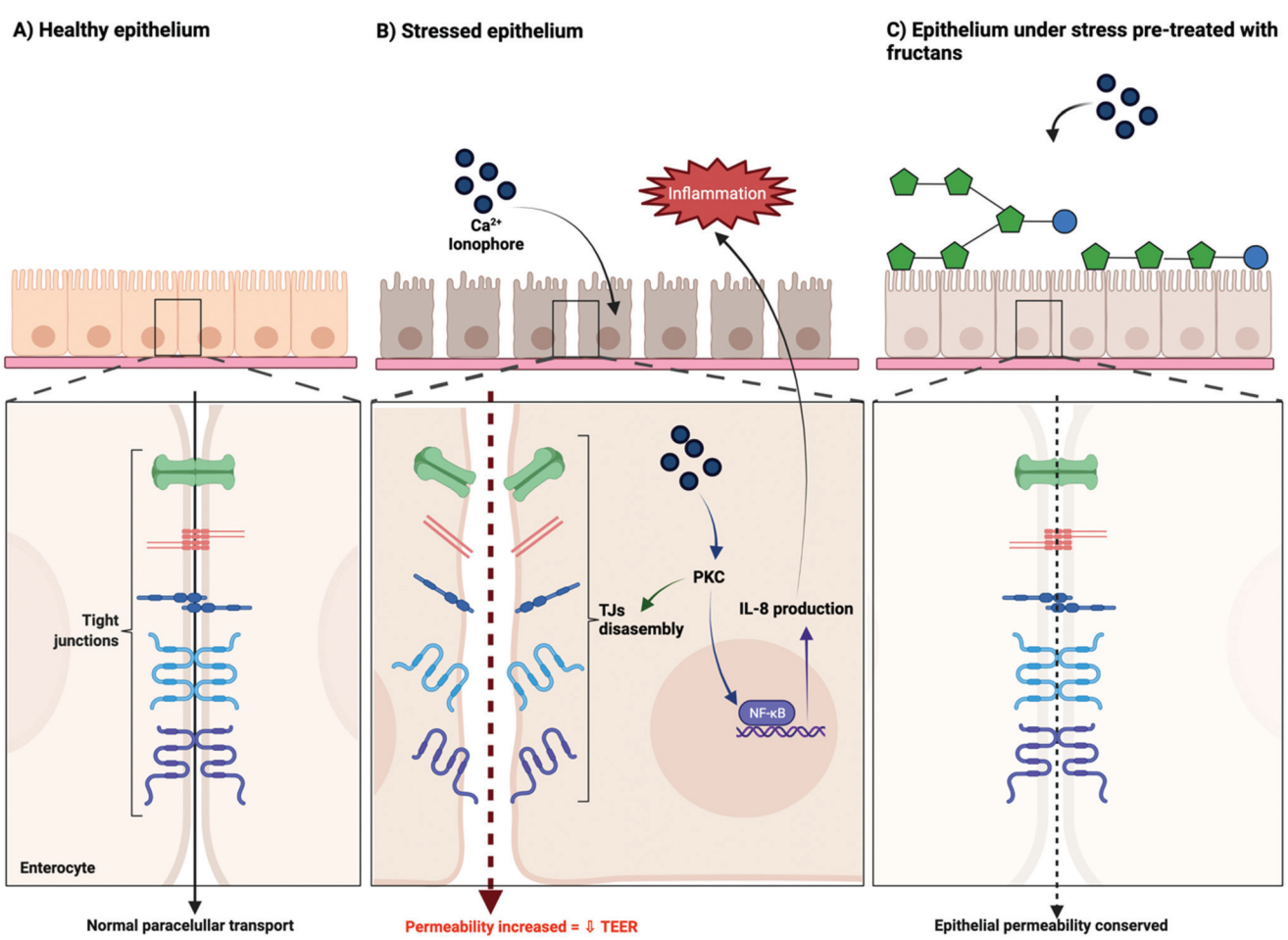

Fig. 5 Proposed mechanism of action of the protective effect of linear β(2→1) and branched β(2→1)-β(2→6) fructans on the intestinal epithelial barrier function.

ml^{-1}) for pre-treating T84 cells compared to the present study.

The disruptive effects of both PMA and the calcium ionophore A23187 are PKC-dependent[42] but the ways in which they lead to PKC-induced disruption are different. The intestinal barrier function depends on the assembly or disassembly of the proteins of the TJs. These TJs are regulated by the phosphorylation of the serine and threonine residues of their proteins. This regulation is achieved by protein kinases such as PKC. PKC is involved in TJ opening. At the cell membrane, PKC can phosphorylate TJ proteins such as occludin. This phenomenon has been observed when TJs are disassembled, and the barrier function is disrupted.[42] In the present study, A23187 was used as it facilitates the transport of calcium ions into the cytoplasm. This sudden calcium influx activates the calcium-dependent PKC, leading to the disassembly of the TJs. PMA works differently. PMA is an analogue of diacylglycerol, one of the natural activators of PKC. In contrast to A23187, PMA binds directly to a specific region of PKC which leads to activation.[43] This activation induces the translocation of PKC to the cell membrane and the disassembly of TJs.

At a structural level, A23187 and PMA also are different. A23187 is an antibiotic extracted from *Streptomyces chartreusensis*[44] composed of a carboxylic acid with a pyrrole ketone moiety, a substituted benzoxazole group and a spiroketal ring.[45] Two molecules of this compound chemically coordinate with a Ca^{2+} ion, which serves as a cation carrier into the cell.[46] However, PMA possesses a phorbol group that contains a long acyl chain, which confers it a highly hydrophobic nature (PubChem database, **https://pubchem.ncbi.nlm.nih.gov**, consulted on November 9th, 2021). Due to this property, PMA possesses a very high affinity for cellular lipid membranes[27] and probably a higher affinity than that of most fructans as fructans can only establish non-polar interactions with the cell membrane. This difference in affinity between A23187 and PMA for the cellular lipid membranes would likely be the reason for the differences in the effectiveness of fructans in protection from the barrier disruption induced by these agents.

We found that the long chain linear fructan ITF II had the strongest protective effect on epithelial barrier integrity when cells were challenged with A23187 and PMA. This confirms the findings of Wu *et al.* who showed that pre-incubation of Caco-2 Bbe1 monolayers or intestinal organoids exposed to short-chain and long-chain inulins protects the intestinal epithelial barrier from injury caused by enterohemorrhagic *Escherichia coli*. In addition, they also demonstrated that barrier function was reinforced through a PKC-dependent mechanism by a set of techniques that included the host-kinome with a 282-peptide immune array, gene enrichment analysis, and measurement of PKC isoform activities in the presence and absence of specific-isoform inhibitors.[41]

The epithelial barrier disruption provoked by the fungal toxin DON was not attenuated by the studied fructans. This toxin is known to decrease the transepithelial resistance *via* MAPK signaling.[30] Our findings, therefore, suggest that fructans cannot prevent the MAPK pathway induced epithelial barrier disruption. This is in accordance with a previous report where the microbiota-independent effects of galacto-oligosaccharides (GOS) on intestinal epithelial integrity and the release of IL-8 were studied and compared with those of FOS and inulin, in combination with GOS or alone. To that end, the different oligosaccharides were added to Caco-2 monolayers, and after 24 hours of incubation the fungal toxin DON was added to the cultures. Afterwards, the TEER and lucifer yellow permeability were quantified to determine the integrity of the intestinal barrier. Only GOS and not the fructans had protective effects on the impairment induced by DON.[34]

In addition to protecting against barrier disruption, the studied fructans have also been shown to have other health benefits. The prebiotic roles of inulin-type fructans and fructans from agave have been studied by our group and others.[22,47,48] These dietary fibers can exert an indirect beneficial effect on intestinal homeostasis by modifying the microbiota composition and supporting the production of its metabolic products such as short chain fatty acids (SCFAs).[49] The beneficial effect of SCFAs was demonstrated *in vitro* by Commane *et al.* These researchers found that the epithelial barrier of Caco-2 cells was strengthened by the fermentation products of Bifidobacterium Bb 12, which was exposed to ITFs of different molecular sizes.[50] This finding was later confirmed by Van den Abbeele *et al.* who demonstrated that the inulin-fermentation products from adult microbiota strengthened the gut barrier by increasing the TEER in Caco-2 cell monolayers *via* SCFA production.[51] Moreover, our group demonstrated that inulin-type fructans contribute to the maturation of the glycocalyx, which is an important component of the gut epithelium composed of glycans and proteins. The glycocalyx serves as a scaffold for the binding of intestinal commensal microbiota and it strengthens the gut barrier. By this, it avoids the adhesion of pathogen microorganisms. Kong *et al*. demonstrated that the incubation of Caco-2 cells with inulin-type fructans increased the glycocalyx development by enhancing its thickness and area of coverage of molecules that constitute the glycocalyx such as albumin, heparan sulphate and hyaluronic acid.[52]

The protection by the studied fructans from the disrupting action of A23187 was also reflected in the attenuation of the inflammatory state of T84 cells, since along with the protection from the epithelial barrier disruption, the concentration of the pro-inflammatory cytokine IL-8 decreased significantly. IL-8, also known as the chemotactic factor CXCL8, is considered an essential pro-inflammatory cytokine that is constitutively expressed by epithelial cells. This chemokine functions as an early warning signal to cells in the underlying lamina propria. When a potential danger is detected, it is released which subsequently leads to inflammatory responses by recruiting immune cells such as neutrophils to the site of injury.[53,54] Yu *et al.* previously demonstrated that A23187 stimulates IL-8 production in T84 cells following the release of intracellular calcium.[55] The exacerbated expression of this cytokine is also strongly associated with intestinal inflammatory disorders such as ulcerative colitis.[56]

The observed regulatory effect of the studied fructans on IL-8 production by T84 cells exposed to A23187 indicates that fructans not only protect from barrier disruption but also contribute to the lowering of inflammatory events as reported before.[16,57]

In the present study, a 17-fold increase of IL-8 production was observed when stimulating T84 monolayers with PMA. It is known that this epithelial disruptor activates PKC signaling which leads to the up-regulation of IL-8 gene expression in T84 cells.[55] The inflammatory effect observed was not influenced by the studied fructans. IL-8 production was also not attenuated by ITF II that protected from PMA induced barrier disruption, indicating that barrier disruption and regulation of inflammatory processes in epithelial cells might involve different pathways. A similar separate effect on barrier function inflammatory processes of fructans was observed for epithelial cells treated with DON. The production of IL-8 in T84 cells challenged with DON was significantly reduced by both studied ITFs in a chain-length dependent manner while barrier disruption was unaffected. These results suggest an MAPK-dependent regulatory role of ITFs on inflammatory processes but the absence of such an effect on the barrier function of gut epithelial cells.

5. Conclusions

To the best of our knowledge, this is the first study where the direct protective effects of GTFs on intestinal epithelial barrier function are addressed. We demonstrated that GTFs, just like ITFs, can prevent gut barrier disruption in a structure and size-dependent fashion. Their effect is most pronounced in calcium ionophore A23187-induced gut epithelial cell barrier disruption. This is different for ITFs that showed efficacy in not only A23187 but also PMA-induced gut barrier disruption. Specifically, the longer chain ITF II had such an effect. Linear ITFs in contrast to branched GTFs were able to reduce A23187 and DON-induced enhanced secretion of IL-8 by gut epithelial cells. These fructans were ineffective in reducing DON induced barrier dysfunction but efficacious in lowering inflammation, which suggest that different pathways are involved in how fructans can influence barrier function and inflammatory processes in gut epithelial cells.

Our results may lead to better and broader uses of agave fructans in areas where agave is endemic and chicory inulin is not available such as in Latin America.[35] There are several lines of applications of these fructans. They can be applied as a substitute for human milk oligosaccharides, which have health benefits in human milk. We show here that specific fructans might be used to protect against barrier disruption. Tailoring infant formulas supplemented with GTFs would be an option for babies with specific gastrointestinal issues such as premature babies.[58] In addition, in adults our findings may lead to new applications. Gastrointestinal discomfort and also barrier disruption are very common issues in adults.[59,60] Food with specific fructans may lead to lower frequencies of barrier disruption and lower discomfort. In the pharmaceutical sector, due to their non-digestible characteristics, ITFs have been used as drug stabilizers and carriers, improving drug dissolution and facilitation of controlled release of drugs to specific target sites such as the colon.[61] Overall, the present study contributes to a better understanding of the health promoting effects of fructans and their applications in specific chemistries to support specific health benefits.

Author contributions

C. F. L. and P. D. V. designed the study. C. F. L. performed cell-based experiments. X. T. assisted with the cell-based experiments. C. F. L., M. J. L., H. A. S., G. L. V., and P. D. V. wrote the manuscript. P. D. V. supervised and administered the project. All authors have revised, improved, and approved the manuscript.

Conflicts of interest

There are no conflicts to declare.

Acknowledgements

This study was partially financed by the "Programa de Recursos Fiscales para Investigación" of the Instituto Nacional de Pediatría (Grant number 2019/062). C. F. L. was financially supported by the Abel Tasman Talent Program Sandwich PhD from the University of Groningen-University Medical Center Groningen, UG/UMCG in collaboration with Universidad Nacional Autónoma de México, UNAM and CONACyT (#260625).

References

1 D. Ulluwishewa, R. C. Anderson, W. C. McNabb, P. J. Moughan, J. M. Wells and N. C. Roy, Regulation of tight junction permeability by intestinal bacteria and dietary components, *J. Nutr.*, 2011, **141**, 769–776.
2 C. Zihni, C. Mills, K. Matter and M. S. Balda, Tight junctions: from simple barriers to multifunctional molecular gates, *Nat. Rev. Mol. Cell Biol.*, 2016, **17**, 564.
3 M. Camilleri, K. Madsen, R. Spiller, B. Van Meerveld and G. Verne, Intestinal barrier function in health and gastrointestinal disease, *Neurogastroenterol. Motil.*, 2012, **24**, 503–512.
4 C. M. Van Itallie, J. Holmes, A. Bridges, J. L. Gookin, M. R. Coccaro, W. Proctor, O. R. Colegio and J. M. Anderson, The density of small tight junction pores varies among cell types and is increased by expression of claudin-2, *J. Cell Sci.*, 2008, **121**, 298–305.
5 T. Suzuki, Regulation of intestinal epithelial permeability by tight junctions, *Cell. Mol. Life Sci.*, 2013, **70**, 631–659.

6 S. Aijaz, M. S. Balda and K. Matter, Tight junctions: molecular architecture and function, *Int. Rev. Cytol.*, 2006, **248**, 261–298.

7 L. Shen, C. R. Weber, D. R. Raleigh, D. Yu and J. R. Turner, Tight junction pore and leak pathways: a dynamic duo, *Annu. Rev. Physiol.*, 2011, **73**, 283–309.

8 M. F. McCarty and A. Lerner, Perspective: Prospects for nutraceutical support of intestinal barrier function, *Adv. Nutr.*, 2021, **12**, 316–324.

9 F. Halter, Mechanisms of gastrointestinal toxicity of NSAIDS, *Scand. J. Rheumatol.*, 1988, **17**, 16–21.

10 J. L. Wallace, S. Syer, E. Denou, G. de Palma, L. Vong, W. McKnight, J. Jury, M. Bolla, P. Bercik and S. M. Collins, Proton pump inhibitors exacerbate NSAID-induced small intestinal injury by inducing dysbiosis, *Gastroenterology*, 2011, **141**, 1314–1322.

11 M. Vancamelbeke and S. Vermeire, The intestinal barrier: a fundamental role in health and disease, *Expert Rev. Gastroenterol. Hepatol.*, 2017, **11**, 821–834.

12 A. Lerner and T. Matthias, Changes in intestinal tight junction permeability associated with industrial food additives explain the rising incidence of autoimmune disease, *Autoimmun. Rev.*, 2015, **14**, 479–489.

13 M. Martinez-Medina, J. Denizot, N. Dreux, F. Robin, E. Billard, R. Bonnet, A. Darfeuille-Michaud and N. Barnich, Western diet induces dysbiosis with increased E coli in CEABAC10 mice, alters host barrier function favouring AIEC colonisation, *Gut*, 2014, **63**, 116–124.

14 M. B. Kiewiet, M. I. G. Rodríguez, R. Dekkers, M. Gros, L. H. Ulfman, A. Groeneveld, P. de Vos and M. M. Faas, The epithelial barrier-protecting properties of a soy hydrolysate, *Food Funct.*, 2018, **9**, 4164–4172.

15 L. Cheng, R. Akkerman, C. Kong, M. T. Walvoort and P. de Vos, More than sugar in the milk: human milk oligosaccharides as essential bioactive molecules in breast milk and current insight in beneficial effects, *Crit. Rev. Food Sci. Nutr.*, 2020, 1–17.

16 L. Vogt, D. Meyer, G. Pullens, M. M. Faas, K. Venema, U. Ramasamy, H. A. Schols and P. de Vos, Toll-Like Receptor 2 Activation by b2→ 1-Fructans Protects Barrier Function of T84 Human Intestinal Epithelial Cells in a Chain Length–Dependent Manner, *J. Nutr.*, 2014, **144**, 1002–1008.

17 M. B. Roberfroid, Introducing inulin-type fructans, *Br. J. Nutr.*, 2005, **93**, S13–S25.

18 G. Kelly, Inulin-type prebiotics–a review: part 1, *Altern. Med. Rev.*, 2008, **13**(4), 315–329.

19 G. T. C. Delgado, W. M. Tamashiro and G. M. Pastore, Immunomodulatory effects of fructans, *Food Res. Int.*, 2010, **43**, 1231–1236.

20 M. Wiciński, E. Sawicka, J. Gębalski, K. Kubiak and B. Malinowski, Human milk oligosaccharides: health benefits, potential applications in infant formulas, and pharmacology, *Nutrients*, 2020, **12**, 266.

21 G. López-Velázquez, L. Díaz-García, A. Anzo, M. Parra-Ortiz, B. Llamosas-Gallardo, A. A. Ortiz-Hernández, J. Mancilla-Ramírez, J. M. Cruz-Rubio and P. Gutiérrez-Castrellón, Safety of a dual potential prebiotic system from Mexican agave" Metlin® and Metlos®", incorporated to an infant formula for term newborn babies: A randomized controlled trial, *Rev. Invest. Clin.*, 2013, **65**, 483–490.

22 G. López-Velázquez, M. Parra-Ortiz, I. de la Mora-de la Mora, I. García-Torres, S. Enríquez-Flores, M. A. Alcántara-Ortigoza, A. González-del Angel, J. Velázquez-Aragón, R. Ortiz-Hernández and J. M. Cruz-Rubio, Effects of fructans from Mexican agave in newborns fed with infant formula: a randomized controlled trial, *Nutrients*, 2015, **7**, 8939–8951.

23 M. G. Lopez, N. A. Mancilla-Margalli and G. Mendoza-Diaz, Molecular structures of fructans from Agave tequilana Weber var. azul, *J. Agric. Food Chem.*, 2003, **51**, 7835–7840.

24 N. A. Mancilla-Margalli and M. G. López, Water-soluble carbohydrates and fructan structure patterns from Agave and Dasylirion species, *J. Agric. Food Chem.*, 2006, **54**, 7832–7839.

25 W. Praznik, R. Löppert, J. M. C. Rubio, K. Zangger and A. Huber, Structure of fructo-oligosaccharides from leaves and stem of Agave tequilana Weber, var. azul, *Carbohydr. Res.*, 2013, **381**, 64–73.

26 A. V. Pérez-López, J. Simpson, M. R. Clench, A. D. Gomez-Vargas and J. J. Ordaz-Ortiz, Localization and Composition of Fructans in Stem and Rhizome of Agave tequilana Weber var. azul, *Front. Plant Sci.*, 2021, **11**, 2309.

27 Y. H. Tai, J. Flick, S. A. Levine, J. L. Madara, G. W. Sharp and M. Donowitz, Regulation of tight junction resistance in T84 monolayers by elevation in intracellular Ca2+: a protein kinase C effect, *J. Membr. Biol.*, 1996, **149**, 71–79.

28 A. Y. Andreeva, J. Piontek, I. E. Blasig and D. I. Utepbergenov, Assembly of tight junction is regulated by the antagonism of conventional and novel protein kinase C isoforms, *Int. J. Biochem. Cell Biol.*, 2006, **38**, 222–233.

29 J. Lucioli, P. Pinton, P. Callu, J. Laffitte, F. Grosjean, M. Kolf-Clauw, I. P. Oswald and A. P. F. Bracarense, The food contaminant deoxynivalenol activates the mitogen activated protein kinases in the intestine: interest of ex vivo models as an alternative to in vivo experiments, *Toxicon*, 2013, **66**, 31–36.

30 T. Sergent, M. Parys, S. Garsou, L. Pussemier, Y.-J. Schneider and Y. Larondelle, Deoxynivalenol transport across human intestinal Caco-2 cells and its effects on cellular metabolism at realistic intestinal concentrations, *Toxicol. Lett.*, 2006, **164**, 167–176.

31 J. Van De Walle, B. Romier, Y. Larondelle and Y.-J. Schneider, Influence of deoxynivalenol on NF-κB activation and IL-8 secretion in human intestinal Caco-2 cells, *Toxicol. Lett.*, 2008, **177**, 205–214.

32 L. Vogt, U. Ramasamy, D. Meyer, G. Pullens, K. Venema, M. M. Faas, H. A. Schols and P. de Vos, Immune modulation by different types of β2→ 1-fructans is toll-like receptor dependent, *PLoS One*, 2013, **8**, e68367.

33 C. Fernández-Lainez, R. Akkerman, M. Oerlemans, M. Logtenberg, H. Schols, L. Silva-Lagos, G. López-

Velázquez and P. de Vos, β (2→ 6)-Type fructans attenuate proinflammatory responses in a structure dependent fashion via Toll-like receptors, *Carbohydr. Polym.*, 2022, **277**, 118893.
34 P. Akbari, J. Fink-Gremmels, R. H. Willems, E. Difilippo, H. A. Schols, M. H. Schoterman, J. Garssen and S. Braber, Characterizing microbiota-independent effects of oligosaccharides on intestinal epithelial cells: Insight into the role of structure and size, *Eur. J. Nutr.*, 2017, **56**, 1919–1930.
35 A. V. Pérez-López and J. Simpson, The Sweet Taste of Adapting to the Desert: Fructan Metabolism in Agave Species, *Front. Plant Sci.*, 2020, **11**, 324.
36 R. Demel, E. Dorrepaal, M. Ebskamp, J. Smeekens and B. De Kruijff, Fructans interact strongly with model membranes, *Biochim. Biophys. Acta, Biomembr.*, 1998, **1375**, 36–42.
37 I. J. Vereyken, V. Chupin, R. A. Demel, S. C. Smeekens and B. De Kruijff, Fructans insert between the headgroups of phospholipids, *Biochim. Biophys. Acta, Biomembr.*, 2001, **1510**, 307–320.
38 I. J. Vereyken, J. A. Van Kuik, T. H. Evers, P. J. Rijken and B. de Kruijff, Structural requirements of the fructan-lipid interaction, *Biophys. J.*, 2003, **84**, 3147–3154.
39 M. Kolber and D. Haynes, Fluorescence study of the divalent cation-transport mechanism of ionophore A23187 in phospholipid membranes, *Biophys. J.*, 1981, **36**, 369–391.
40 P. W. Reed and H. A. Lardy, A23187: a divalent cation ionophore, *J. Biol. Chem.*, 1972, **247**, 6970–6977.
41 R. Y. Wu, M. Abdullah, P. Määttänen, A. V. C. Pilar, E. Scruten, K. C. Johnson-Henry, S. Napper, C. O'Brien, N. L. Jones and P. M. Sherman, Protein kinase C δ signaling is required for dietary prebiotic-induced strengthening of intestinal epithelial barrier function, *Sci. Rep.*, 2017, **7**, 1–10.
42 L. González-Mariscal, R. Tapia and D. Chamorro, Crosstalk of tight junction components with signaling pathways, *Biochim. Biophys. Acta, Biomembr.*, 2008, **1778**, 729–756.
43 K. Kolczynska, A. Loza-Valdes, I. Hawro and G. Sumara, Diacylglycerol-evoked activation of PKC and PKD isoforms in regulation of glucose and lipid metabolism: a review, *Lipids Health Dis.*, 2020, **19**, 1–15.
44 Q. Wu, J. Liang, S. Lin, X. Zhou, L. Bai, Z. Deng and Z. Wang, Characterization of the biosynthesis gene cluster for the pyrrole polyether antibiotic calcimycin (A23187) in Streptomyces chartreusis NRRL 3882, *Antimicrob. Agents Chemother.*, 2011, **55**, 974–982.
45 M. O. Chaney, P. V. Demarco, N. D. Jones and J. L. Occolowitz, Structure of A23187, a divalent cation ionophore, *J. Am. Chem. Soc.*, 1974, **96**, 1932–1933.
46 G. Smith and W. Duax, Crystal and molecular structure of the calcium ion complex of A23187, *J. Am. Chem. Soc.*, 1976, **98**, 1578–1580.
47 M. J. Logtenberg, R. Akkerman, R. An, G. D. Hermes, B. J. de Haan, M. M. Faas, E. G. Zoetendal, H. A. Schols and P. de Vos, Fermentation of Chicory Fructo–Oligosaccharides and Native Inulin by Infant Fecal Microbiota Attenuates Pro–Inflammatory Responses in Immature Dendritic Cells in an Infant–Age–Dependent and Fructan–Specific Way, *Mol. Nutr. Food Res.*, 2020, **64**, 13.
48 R. Akkerman, M. J. Logtenberg, M. Beukema, B. J. De Haan, M. M. Faas, E. G. Zoetendal, H. A. Schols and P. De Vos, Chicory inulin enhances fermentation of 2′-fucosyllactose by infant fecal microbiota and differentially influences immature dendritic cell and T-cell cytokine responses under normal and Th2-polarizing conditions, *Food Funct.*, 2021, **12**, 9018–9029.
49 N. Gasaly, P. De Vos and M. A. Hermoso, Impact of bacterial metabolites on gut barrier function and host immunity: a focus on bacterial metabolism and its relevance for intestinal inflammation, *Front. Immunol.*, 2021, 1807.
50 D. M. Commane, C. T. Shortt, S. Silvi, A. Cresci, R. M. Hughes and I. R. Rowland, Effects of fermentation products of pro-and prebiotics on trans-epithelial electrical resistance in an in vitro model of the colon, *Nutr. Cancer*, 2005, **51**, 102–109.
51 P. Van den Abbeele, B. Taminiau, I. Pinheiro, C. Duysburgh, H. Jacobs, L. Pijls and M. Marzorati, Arabinoxylo-Oligosaccharides and Inulin Impact Inter-Individual Variation on Microbial Metabolism and Composition, Which Immunomodulates Human Cells, *J. Agric. Food Chem.*, 2018, **66**, 1121–1130.
52 C. Kong, M. Elderman, L. Cheng, B. J. de Haan, A. Nauta and P. de Vos, Modulation of intestinal epithelial glycocalyx development by human milk oligosaccharides and non–digestible carbohydrates, *Mol. Nutr. Food Res.*, 2019, **63**, 1900303.
53 Y. Yu, H. Zeng, S. Lyons, A. Carlson, D. Merlin, A. S. Neish and A. T. Gewirtz, TLR5-mediated activation of p38 MAPK regulates epithelial IL-8 expression via posttranscriptional mechanism, *Am. J. Physiol.: Gastrointest. Liver Physiol.*, 2003, **285**, G282–G290.
54 L. Eckmann, H. C. Jung, C. Schürer-Maly, A. Panja, E. Morzycka-Wroblewska and M. F. Kagnoff, Differential cytokine expression by human intestinal epithelial cell lines: regulated expression of interleukin 8, *Gastroenterology*, 1993, **105**, 1689–1697.
55 Y. Yu, C. De Waele and K. Chadee, Calcium-dependent interleukin-8 gene expression in T84 human colonic epithelial cells, *Inflammation Res.*, 2001, **50**, 220–226.
56 Y. Zhu, S. Yang, N. Zhao, C. Liu, F. Zhang, Y. Guo and H. Liu, CXCL8 chemokine in ulcerative colitis, *Biomed. Pharmacother.*, 2021, **138**, 111427.
57 X. Wang, Y. Li, X. Yang and J. Yao, Astragalus polysaccharide reduces inflammatory response by decreasing permeability of LPS-infected Caco2 cells, *Int. J. Biol. Macromol.*, 2013, **61**, 347–352.
58 R. Akkerman, M. M. Faas and P. de Vos, Non-digestible carbohydrates in infant formula as substitution for human milk oligosaccharide functions: Effects on microbiota and gut maturation, *Crit. Rev. Food Sci. Nutr.*, 2019, **59**, 1486–1497.

59 M. B. Kiewiet, M. E. Elderman, S. El Aidy, J. G. Burgerhof, H. Visser, E. E. Vaughan, M. M. Faas and P. de Vos, Flexibility of Gut Microbiota in Ageing Individuals during Dietary Fiber Long–Chain Inulin Intake, *Mol. Nutr. Food Res.*, 2021, **65**, 2000390.
60 R. An, E. Wilms, M. J. Logtenberg, M. P. van Trijp, H. A. Schols, A. A. Masclee, H. Smidt, D. M. Jonkers and E. G. Zoetendal, In vitro metabolic capacity of carbohydrate degradation by intestinal microbiota of adults and pre-frail elderly, *ISME Commun.*, 2021, **1**, 1–12.
61 X. Wan, H. Guo, Y. Liang, C. Zhou, Z. Liu, K. Li, F. Niu, X. Zhai and L. Wang, The physiological functions and pharmaceutical applications of inulin: A review, *Carbohydr. Polym.*, 2020, **246**, 116589.

CAPÍTULO 5

Branched graminan-type fructans and linear inulin-type fructans protect against impairment of intestinal tight junction gene expression and attenuate dendritic cell responses in a fructan dependent fashion

Cynthia Fernández-Lainez,[*,a,b,c] Myrthe aan de Stegge,[a] Luis Alfredo Silva-Lagos,[a] Gabriel López-Velázquez,[d] Paul de Vos[a]

[a] Immunoendocrinology, Division of Medical Biology, Department of Pathology and Medical Biology, University of Groningen, University Medical Center Groningen, Groningen, The Netherlands

[b] Laboratorio de Errores innatos del Metabolismo y Tamiz, Instituto Nacional de Pediatría, Ciudad de México, México.

[c] Posgrado en Ciencias Biológicas, Universidad Nacional Autónoma de México, Ciudad de México, México.

[d] Laboratorio de Biomoléculas y Salud Infantil, Instituto Nacional de Pediatría, Ciudad de México, México.

Submitted.

β(2→1)-β(2→6) and β(2→1) fructans protect from impairment of intestinal tight junction's gene expression and attenuate human dendritic cell responses in a fructan-dependent fashion

Cynthia Fernández-Lainez,[*,a,b,c] Myrthe aan de Stegge,[a] Luis Alfredo Silva-Lagos,[a] Gabriel López-Velázquez,[d] Paul de Vos[a]

[a] Immunoendocrinology, Division of Medical Biology, Department of Pathology and Medical Biology, University of Groningen, University Medical Center Groningen, Groningen, The Netherlands; Email: c.fernandez.lainez@umcg.nl, m.m.aan.de.stegge@student.rug.nl, l.a.silva.lagos@umcg.nl, p.de.vos@umcg.nl; Fax: +3150-3611911; Tel: +3150-3618043.

[b] Laboratorio de Errores innatos del Metabolismo y Tamiz, Instituto Nacional de Pediatría, Ciudad de México, México.

[c] Posgrado en Ciencias Biológicas, Universidad Nacional Autónoma de México, Cuidad de México, México.

[d] Laboratorio de Biomoléculas y Salud Infantil, Instituto Nacional de Pediatría, Cuidad de México, México. Email: glv_1999@ciencias.unam.mx

* Corresponding author: Fernández-Lainez Cynthia. Immunoendocrinology, Division of Medical Biology, Department of Pathology and Medical Biology, University of Groningen,

University Medical Center Groningen, Hanzeplein 1 (internal postal code EA11), 9713 GZ Groningen, The Netherlands. Email: c.fernandez.lainez@umcg.nl

Abbreviations: β-actin gene, *ACTB*; Caco-2, human colon carcinoma cell line; Caco-spent medium, CSM; calcium ionophore A23187, A23187; claudin-1 gene, *CLDN-1*; claudin-2 gene, *CLDN-2*; claudin-3 gene, *CLDN-3*; Dulbecco Modified Eagle Medium, DMEM; degree of polymerization, DP; enterohemorrhagic *Escherichia coli*, EHEC; epithelial cadherin, E-cadherin; E-cadherin gene , *CDH1*; dendritic cells, DCs; deoxynivalenol, DON; glyceraldehyde-3-phosphate dehydrogenase gene, *GAPDH*; graminan-type fructans, GTFs; intestinal epithelial cells, IECs; interleukin IL-1β; interleukin IL-1RA ; interleukin 6, IL-6; interleukin 8, IL-8; interleukin 10, IL-10; inulin-type fructans, ITFs; mitogen-activated protein kinase, MAPK; monocyte chemoattractant protein-1, MCP-1/CCL2; macrophage inflammatory protein-1 alpha, MIP-1α/CCL3; Nuclear factor kappa-light-chain-enhancer of activated B cells, NF-κB; occludin gene, *OCLN*; tight junctions, protein kinase C, PKC; quantitative reverse transcription polymerase chain reaction, RT-qPCR; TJs; tumor necrosis factor alpha, TNFα; zonula occludens, transepithelial electrical resistance, TEER; ZO-1; ZO-1 gene, *TJP1*.

HIGHLIGHTS

- Higher DP fructans decrease expression of the intestinal tight junction protein claudin-2.
- Only graminan-type fructans prevent DON-induced dysregulation of claudin-1.
- Claudin-3 DON-induced overexpression was regulated only by short chain fructans.
- Graminan-type fructans attenuate pro-inflammatory cytokines in dendritic cells.
- Cell culture medium from gut cells exposed to graminan- and inulin-type fructans attenuates inflammatory responses in dendritic cells.
- Graminan- and inulin-type fructans might contribute to prevention of intestinal inflammation.

ABSTRACT

β(2→1)-β(2→6) branched graminan-type fructans (GTFs) and β(2→1) linear fructans (ITFs) possess immunomodulatory properties and protect human intestinal barrier function, however the mechanisms underlying these effects are not well studied. Herein, GTFs and ITFs effects with different degree of polymerization (DP) values on tight junctions (TJs) genes *CLDN-1, -2* and *-3*, *CDH1*, *OCLN* and *TJP1* were studied in Caco-2 gut epithelial cells, under homeostatic and inflammatory conditions. Also, cytokine production in dendritic cells (DCs) was studied. Higher DP fructans decreased the expression of the pore forming *CLDN-2*. Higher DP GTFs enhanced *CLDN-3, OCLN,* and *TJP-1*. Fructans prevented mRNA dysregulation of *CLDN-1*, *-2* and *-3* induced by the barrier disruptors A23187 and deoxynivalenol in a fructan-type dependent fashion. The production of pro-inflammatory cytokines MCP-1/CCL2, MIP-1α/CCL3 and TNFα by DCs was also attenuated in a fructan-type dependent manner and was strongly attenuated by DCs cultured with medium of Caco-2 cells which were pre-exposed to fructans. Our data show that specific fructans have TJs and DCs modulating effects and contribute to gut homeostasis. This might serve to design effective dietary means to prevent intestinal inflammation.

Keywords

Tight junctions, non-digestible carbohydrates, inflammatory bowel disease, nutraceuticals, functional foods, intestinal and immune cells crosstalk.

1 Introduction

The intestinal epithelial cells (IECs) form a highly dynamic barrier between the human host and the luminal environment of the gut. These IECs are joined by multi protein complexes such as tight junctions (TJs) (Garcia-Hernandez, Quiros, & Nusrat, 2017). TJs are composed of transmembrane proteins mainly claudins, and occludin, although other cytoplasmic proteins such as the zonula occludens (ZO-1) are associated to these TJ complexes (Tsukita, Furuse, & Itoh, 2001). All these proteins together regulate the passage of solutes by the so-called paracellular pathway (Garcia-Hernandez et al., 2017). TJ-proteins between the epithelial cells function as a dynamic barrier as the epithelial layer should be permeable to ions, nutrients of certain size, and water, while simultaneously they should block the passage of harmful substances such as toxins, allergens, and pathogens to the bloodstream (Matter & Balda, 2003). The TJ-protein expression is regulating this semipermeability.

To maintain intestinal homeostasis and gut barrier function, the gene expression of TJs proteins is strictly regulated (Shen, 2012). The mechanisms of regulation of TJs gene expression are complex and cell-type dependent (Günzel & Yu, 2013; Shen, 2012). It is known that impaired abundance, arrangement, and expression of TJs play a pivotal role in the pathogenesis of many intestinal disorders such as in inflammatory bowel disease (Camilleri, Madsen, Spiller, Van Meerveld, & Verne, 2012; Pastorelli, De Salvo, Mercado, Vecchi, & Pizarro, 2013; Vanuytsel, Tack, & Farre, 2021).

Several molecules have been used to induce barrier disruption and TJ dysregulation in gut epithelial cells. The calcium ionophore A23187 is commonly used for the induction of gut barrier disruption (Forstner, Zhang, McCool & Forstner 1993; González-Mariscal, Tapia, & Chamorro 2008; Kiewiet et al., 2018; Figueroa-Lozano et al.,

2021). A23187 induces an increase of intracellular calcium, which activates protein kinase C (PKC) pathway. This PKC disassembles the TJs, and disrupts the intestinal barrier (Tai et al., 1996). Another disruptive molecule is the fungal toxin deoxynivalenol (DON). This toxin is produced by fungus of the *Fusarium* genus, which is the most common global cause of mycotoxin contamination of crops (Van de Walle, Romier, Larondelle, & Schneider 2008). This molecule acts via activating the mitogen-activated protein kinase (MAPK) signaling pathway, that concomitantly enhance permeability of the intestinal epithelial barrier by dysregulation of TJs (Sergent et al., 2006; Lucioli et al., 2013; Pestka, 2008).

Many efforts have been undertaken during recent years to regulate the gene expression of TJs by e.g., nutraceuticals. One of these nutraceuticals that might aid in maintaining gut barrier function are fructans (Peters, Dijkstra, & Campmans-Kuijpers, 2022; Salinas et al., 2021; Yang, Zhao, Li, Guo, & Gao, 2022). Fructans are water soluble, fructose-based oligo and polysaccharides synthesized by specific microorganisms, fungus, and plants (Young, Latousakis, & Juge, 2021).

Fructans extracted from *Cichorium intybus* (chicory) roots, among other plants from the *Asteraceae* family are widely used in Europe and other world regions for food supplementation (Li et al., 2020; Perović et al., 2021; Wan et al., 2020). The chemical structure of fructans is diverse (Versluys, Kirtel, Toksoy Öner, & Van den Ende, 2018). Fructans extracted from chicory are composed of linear chains of fructose residues linked by $\beta(2\rightarrow1)$ bonds. These linear fructans with $\beta(2\rightarrow1)$ bonds are named inulin-type fructans (ITFs) (Kelly, 2008). In regions where ITFs-producing plants are unavailable, such as in Latin America, endemic plants from the *Asparagaceae* family, such as agave, are used for fructan harvesting and application in foods (López & Urías-Silvas, 2007; Pérez-López & Simpson, 2020). These fructans are different from ITFs and contain both $\beta(2\rightarrow1)$ and

β(2→6) bonds, which confers them a more complex branched structure. This type of β(2→1)-β(2→6) fructans are named graminan-type fructans (GTFs) (Pérez-López, Simpson, Clench, Gomez-Vargas, & Ordaz-Ortiz, 2021). Besides GTFs, agave fructans also contain neoseries fructans, which have a glucose molecule between two fructose units (Mancilla-Margalli & López, 2006). The structural diversity of agave fructans makes them the most complex fructan structure described to date (Pérez-López, Simpson, Clench, Gomez-Vargas & Ordaz-Ortiz, 2021). ITFs are well studied for health benefits and known to have some protective effect on gut barrier function (Bermudez-Brito et al., 2015; Vogt et al., 2014), but whether GTFs have such an effect is unknown.

ITFs can protect the integrity of the intestinal barrier function by direct interaction with IECs, an effect dependent on the fructans chain-length (Vogt et al., 2014). Moreover, we previously demonstrated that the beneficial effects of fructans go beyond the intestinal epithelium and can even reach immune cells located in the underlying lamina propria such as dendritic cells (DCs), producing a regulatory effect (Bermudez-Brito et al., 2015). We hypothesized that fructans from agave and chicory have beneficial effects on the intestinal TJs gene expression, as well as on DCs responses. Therefore, the aim of the present study was to determine *in vitro* whether GTFs and ITFs can influence the expression of epithelial intestinal TJs genes in the presence and absence of well-known disruptor molecules impacting TJs. Also, we studied whether ITFs and GTFs are protective against epithelial intestinal barrier disruption-induced inflammation. To that end, the pro-inflammatory cytokine IL-8 was measured as a marker of epithelial inflammation in the presence and absence of TJ disrupting molecules. Finally, to investigate if fructans could also have beneficial effects on specific underlying immune cells that are in constant crosstalk with the intestinal epithelium, we studied the impact of the fructans on DCs cytokine responses.

2. Experimental section

2.1 Fructans

The effect of fructans with different structures, linear or branched, as well as the effect of their chain length was studied on the TJs mRNA expression in gut epithelial cells. To that end, we included one mixture of short chain and one mixture of long chain β(2→1)-β(2→6)-linked graminan-type fructans (GTFs), as well as one mixture of short chain and one mixture of long chain β(2→1)-linked inulin-type fructans (ITFs). Branched GTFs were extracted from *Agave tequilana* Weber blue variety and were provided by Nekutli™, Guadalajara, Mexico. Linear ITFs Frutafit™ CLR and Frutafit™ TEX! were studied as well. Both ITFs were provided by Sensus™ (B.V. Roosendaal, The Netherlands). It is important to note that the chemical characteristics of these four mixtures of fructans have been previously studied and reported by our group (Fernández-Lainez et al., 2022a).

2.2 Culture of Caco-2 cells

To study the effects of fructans on the mRNA expression of gut epithelial TJs genes, the human colon carcinoma Caco-2 cell line was used. Caco-2 cells were cultured in T-75 flasks at 37ºC in humidified air and 5% CO_2, and cultured in Dulbecco Modified Eagle Medium (DMEM, Lonza, MD, USA) with glucose (4.5 g/L) and L-glutamine, supplemented with 10% heat-deactivated fetal bovine serum (Sigma-Aldrich, Zwijndrecht, The Netherlands), 1% non-essential amino acids (Gibco, Paisley, UK), 10 mM HEPES buffer (Sigma-Aldrich, Zwijndrecht, The Netherlands) and penicillin/streptomycin 50 U/mL and 50 µg/mL (Gibco, Paisley, UK). The medium was refreshed twice a week and cells were passaged when they reached confluency. Cells used in experiments were between passages 22-36 (Fig. 1A).

2.3 Effect of GTFs and ITFs on the expression of intestinal tight junction genes

Confluent cultures of Caco-2 cells were detached from the flask bottom by trypsinization (Sigma-Aldrich, Zwijndrecht, The Netherlands). Afterwards, cells were seeded in 24-well plates (Corning, NY, USA) at a density of 3 x 10^4 cells/mL in 1 mL of culture medium for 21 days until they reached a transepithelial electrical resistance (TEER) of 300 $\Omega \cdot cm^2$ (Fig. 1A). TEER was measured as previously described (Bermudez-Brito et al., 2015). Culture medium was exchanged at the day of the experiment with medium containing 10 mg/mL of endotoxin-free branched GTFs and linear ITFs, followed by incubation for 24 hours (Fig. 1B) (Fernández-Lainez et al., 2022a). Working concentration of both GTFs and ITFs was established after determination of a dose-effector pilot study (Fig. S1). Untreated cells (only culture medium) served as controls.

2.3.1 RNA extraction, cDNA synthesis and quantitative PCR (qPCR)

To study the relative mRNA expression of the tight junction genes *CLDN-1* (claudin-1), *CLDN-2* (claudin-2), *CLDN-3* (claudin-3), *CDH1* (epithelial cadherin, E-cadherin), *OCLN* (occludin), and *TJP1* (ZO-1), quantitative reverse transcription polymerase chain reaction (RT-qPCR) was performed (for nucleotide sequence of the primers used see Table S1) (Kiewiet et al., 2018). To that end, after incubation under the different experimental conditions, cells were washed twice with cold (4ºC) phosphate buffer solution (PBS) (Fig. 1B). For RNA isolation, cells were extracted from the plates by the addition of 500 μL of TRIzol™ reagent (Life Technologies, Bleiswijk, The Netherlands) following manufacturer's instructions. Total RNA was dissolved in nuclease-free diethylpyrocarbonate (DEPC) treated-water (Life Technologies, Bleiswijk, The Netherlands). RNA concentration and integrity were determined by spectrophotometry using a NanoDrop device (Thermo Fisher Scientific, USA) and by performing gel electrophoresis on a 2% agarose gel, respectively.

RNA samples were stored at -80ºC until use. Using 500 ng of total RNA, cDNA synthesis was performed with SuperScript II™ reverse transcriptase (Life Technologies, Bleiswijk, The Netherlands) according to the manufacturer's instructions. Briefly, RNA samples were pre-treated with DNAse I (Thermo Fisher Scientific, USA) at 37ºC for 30 minutes. This was followed by deactivation of DNAse I with EDTA at 50 mM at 65ºC for 10 minutes. This mixture was used for a retro-transcription reaction. To that end, 300 ng of random hexamer primers (Life Technologies, Bleiswijk, The Netherlands) and 10 mmol/L of dDNTPs (Thermo Fisher Scientific, USA) were incubated with the mix for 10 min at 65ºC. Afterwards, 5x first strand buffer, 0.1 mM of DTT, 40 units/μL of recombinant ribonuclease inhibitor (Thermo Fisher Scientific, USA) and 200 units of SuperScript II™ reverse transcriptase were added to the mix. This was followed by incubation at 25ºC for 10 minutes, 42ºC for 50 minutes and 70ºC for 15 minutes using a TProfessional Basic Thermocycler (Biometra, Göttingen, Germany). Total cDNA obtained from retro-transcription (approximately 25 ng/mL) was diluted 20x with DEPC treated-water (Life Technologies, Bleiswijk, The Netherlands) and 5 μL of this dilution were mixed with 5 μL of FastStart Universal SYBR Green Master (ROX) qPCR Master Mix 2x concentrated (Roche Diagnostics, Basel, Switzerland) including specific primers. Forward and reverse primers were used at a final concentration of 300 nmol/L. The qPCR for tight junction genes was performed in a Viia 7 Real-Time PCR System (Applied Biosystems, CA, USA) with the cycling protocol shown in Table S2. The primer annealing temperature and the primer efficiency was determined using a 5-point standard curve, which was prepared with a pool of all cDNA samples diluted 5-80x. A reaction efficiency of 90-110 % was considered acceptable. *GAPDH* (glyceraldehyde-3-phosphate dehydrogenase) and *ACTB* (β-actin) were used as housekeeping genes (Piana et al., 2008). mRNA fold-change was calculated relative to untreated controls or relative to cells treated only with disruptors, which were set

to 1. The relative $2^{-\Delta\Delta Ct}$ method was used for gene expression calculations (Livak & Schmittgen, 2001). At least five independent assays were performed.

2.4 Protective effect of fructans from induced barrier disruption in Caco-2 cells

To test if fructans can protect intestinal barrier against disruptor molecules, Caco-2 cells were challenged with the epithelial barrier disruptors calcium ionophore A23187 (hereinafter called A23187) at a concentration of 2 μM (Sigma-Aldrich, Zwijndrecht, The Netherlands) and the fungal toxin DON 6.3 μM (Sigma-Aldrich, Zwijndrecht, The Netherlands) (Fig. 1C). Our group and others have previously demonstrated that the applied doses impair the epithelial barrier of intestinal cells *in vitro (*Akbari et al., 2014; Akbari et al., 2017; Figueroa-Lozano et al., 2021; Kiewiet et al., 2018; Ren et al., 2020*)*. These molecules are known to dysregulate the expression of tight junctions at the epithelial barrier by different cellular pathways (Arunachalam & Doohan, 2013; González-Mariscal, Tapia, & Chamorro, 2008). Caco-2 cells were pre-incubated with 10 mg/mL of fructans for 24 hours, followed by an additional incubation of 6 hours in presence of the barrier disrupting stressors (Fig. 1C). Untreated cells (only culture medium) were used as negative controls. To calculate the fold-change in these experiments, cells treated only with disruptors were set as 1. At least five independent experiments were performed.

2.5 Measurement of IL-8 production by Caco-2 cells

For determination of the inflammatory effect of the disruptor molecules on Caco-2 cells, IL-8 secretion was quantified from the cell supernatants after exposure to A23187. Cells incubated only with culture medium were used as controls. IL-8 concentration was determined using an ELISA kit (R&D Systems, Biotechne, Minneapolis, USA) according to manufacturer's instructions (Fig. 1).

2.6 Effect of ITFs and GTFs on the cytokine production by dendritic cells

To test if the beneficial effects of branched fructans on the intestinal epithelial barrier function is extended to immune cells that reside underneath and between the epithelial barrier, dendritic cells were exposed to ITFs and GTFs. DCs isolated from human umbilical cord blood (MatTek Corporation, Ashland, MA, USA) were seeded in 96-well plates at a density of 3 x10^5 cells/well in maintenance culture medium containing cytokines (DC-MM; Mat Tek Corporation, Ashland, MA, USA). To let DCs recover from freezing and to allow the cells to attach to the wells, DCs were incubated for 24 hours in a humidified incubator at 37ºC under a 5% CO_2 atmosphere. Afterwards, ITFs and GTFs were dissolved in DCs-maintenance culture medium to a final concentration of 500 μg/mL and were added to DCs. DCs were incubated under these conditions for 48 hours at 37ºC and 5% CO_2. Cell supernatants were collected and stored at -80ºC for later determination of cytokine production. Untreated DCs served as controls (Fig.1E). At least five independent assays were performed.

2.7 Effect of ITFs and GTFs-Caco-2-spent medium on the cytokine production by dendritic cells

Also, Caco-2 spent medium was generated to investigate if intestinal epithelial cells (IECs), when in contact with branched fructans produce some signal that facilitate DCs to produce cytokines as has been reported before (Bermudez-Brito et al., 2015). To that end, Caco-2 cells (3 x 10^3 cells/mL in 200 μL of culture medium) were seeded in permeable (3 μm pore size) polyester membranes at the apical side of 24-transwell plates (Corning, NY, USA). Caco-2 cells were incubated at 37ºC and 5% CO_2, during 21 days until they reached a transepithelial electrical resistance of 300 $\Omega \cdot cm^2$. Medium was refreshed every other day. Afterwards, cells were incubated in the presence of 5 mg/mL of GTFs, for 24

hours at 37ºC and 5% CO_2. Caco-spent medium (CSM) was collected from the basolateral side of the transwells and stored at -80ºC for further experiments. ITFs were included in the study to investigate the differences of effects between linear and branched fructans. DCs were incubated in presence of ITF-CSM and GTF-CSM diluted 1:10 for 48 hours at 37ºC and 5% CO_2. Finally, DCs supernatants were collected and stored at -80ºC for later determination of cytokine production. DCs treated with CSM coming from non-treated Caco-2 cells were used as controls (Fig. 1D). At least five independent assays were performed.

2.8 Determination of dendritic cells cytokine production

Cytokine production by DCs (MCP-1/CCL2, MIP-1α/CCL3, IL-1RA, IL-1β, IL-6, TNFα and IL-10) was measured using the Magnetic Luminex Assay (R&D systems, Biotechne, Minneapolis, USA) according to manufacturer's instructions. Briefly, 50 μL of magnetic microparticle cocktail containing antibodies for the studied cytokines, were mixed with 50 μL of DCs supernatant in the presence or absence of CSM or standard solutions in 96-well plates overnight at 4ºC with constant shaking. After 3-washing steps, the plate was incubated at room temperature for 30 min under constant shaking in the presence of a biotin-antibody cocktail, followed by streptavidin-phycoerythrin conjugate for cytokines detection. Then, after another 3-washing steps, and after the addition of 100 μL of wash buffer to each well, the plate was read in a Luminex 200 system (Luminex, Den Bosch, The Netherlands). Obtained data was analyzed with the Luminex xPOTENT software (Luminex, Den Bosch, The Netherlands). Untreated cells served as controls. Data was expressed as fold-change compared to controls. At least five independent assays were performed.

2.9 Statistical analyses

Statistical analyses were performed with GraphPad Prism version 9.2. Outliers were identified using the ROUT method. Normal distribution of data was demonstrated by the Kolmogorov-Smirnov test. Data are expressed as mean ± standard deviation (SD). At least five independent assays were performed for each experiment. Statistical significance was determined using one-way ANOVA with Dunnett's multiple comparison test. A *p*-value <0.05 was considered significant. * or † (p <0.05), ** or †† (p <0.01), *** or ††† (p <0.001), **** or †††† (p <0.0001).

3. Results

3.1 Chemical characteristics of studied fructans

Two mixtures of GTFs and two mixtures of ITFs were included to study the effect of fructans with different structure and size on the expression of intestinal epithelial TJ genes. As previously described, GTFs contain β(2→1) and β(2→6) linkages which confers them a complex branched structure (Lopez, Mancilla-Margalli, & Mendoza-Diaz, 2003). GTF I is a mixture with predominantly short chain fructans with a degree of polymerization (DP) of 3-4 but also contains fructans of DP 7-45. GTF II contains a mixture of longer chain fructans with a DP of 17, but it also contains fructans with longer chains. Both GTFs contain oligosaccharides of the fructose (F_n) and glucose-fructose (GF_n) series. ITFs contain only β(2→1) linkages which confers them a linear structure. ITF I is a short chain mixture with a DP range of 3-10. It contains fructans of the F_n and GF_n series. ITF II is a long chain mixture of fructans with a DP range of 10-60 and only contains fructans of the GF_n series (Fig. 2) (Fernández-Lainez et al., 2022a).

3.2. Longer chain fructans decreased the expression of the pore-forming *CLDN-2*

To study the effect of branched and linear fructans on the expression of intestinal tight junction genes, Caco-2 cells were incubated for 24 hours in presence of GTFs and ITFs. Relative to the untreated control, this had an impact on tight junction expression in a fructan-specific manner (Fig. 3). None of the fructans had an impact on *CLDN-1* expression (Fig. 3A). This was different for *CLDN-2*, where a reduction of the expression of 0.58 ± 0.3-fold ($p < 0.01$) and 0.41 ± 0.8-fold ($p < 0.05$) with the longer fructans ITF II and GTF II respectively, was observed (Fig. 3B). The longer agave fructan GTF II increased *CLDN-3* expression 0.45 ± 0.12-fold ($p < 0.05$) (Fig. 3C). *CDH1* expression was 0.3 ± 0.7-fold decreased by GTF I ($p < 0.01$) and 0.32 ± 0.4-fold decreased by ITFII ($p <$

0.01) (Fig. 3D). GTF II significantly increased the expression of *OCLN* by 1.1 ± 0.27-fold ($p < 0.05$) (Fig. 3E), and it also increased *TJP1* expression 0.93 ± 0.22-fold ($p < 0.001$) (Fig. 3F).

3.3 Linear and branched fructans prevent A23187-induced dysregulation of expression of *CLDN-1*, *-2* and *-3* in Caco-2 cells

The protective role of fructans on the expression of intestinal tight junction genes in Caco-2 cells when exposed to tight junction stressor agents was also investigated. A23187 induces an increase of intracellular calcium, which leads to disruption of the intestinal barrier (Tai et al., 1996). To study the possible prevention of this disruption, cells were pre-incubated with fructans for 24 hours before being challenged with A23187. This disruptor induced a significant increase in the expression of *CLDN-1* of 0.36 ± 0.03-fold relative to the untreated control ($p < 0.01$) (Fig. 4A). The expression of *CLDN-1* in cells pre-exposed to the branched GTF I attenuated this increase 0.31 ± 0.06-fold relative to cells stressed with A23187 ($p < 0.05$). The other fructans did not significantly modify the expression of *CLDN-1*.

Relative to the untreated control, A23187 significantly increased *CLDN-2* expression 0.46 ± 0.03-fold ($p < 0.001$), which codes the pore-forming protein claudin-2 (Fig. 4B). This elevation of *CLDN-2* was prevented by ITF I but not by the longer ITF II. Both GTF I and II were able to prevent the A23187-induced effect on *CLDN-2*. The expression in cells pre-exposed to GTF II was 0.69 ± 0.03-fold lower ($p < 0.0001$) and in cells exposed to GTF I 0.59 ± 0.03-fold lower ($p < 0.0001$) relative to the A23187 exposed cells.

CLDN-3 expression was enhanced 0.59 ± 0.02-fold by A23187 treatment ($p < 0.0001$) relative to the untreated control (Fig. 4C). This enhancement was prevented in the cells by all the four tested fructans. Relative to the A23187 treated cells, ITF I pre-treated cells had a 0.41 ± 0.03-fold lower expression of *CLDN-3* ($p < 0.0001$). For the longer ITF II this was similarly lower (0.46 ± 0.02-fold, $p < 0.0001$). For the branched GTF I, the expression was 0.42 ± 0.03-fold ($p < 0.0001$) lower, and for its longer chain variant GTF II it was 0.44 ± 0.03-fold ($p < 0.0001$) lower.

Relative to the untreated control, the expression of *CDH1* in Caco-2 cells treated with A23187 was not affected (Fig. 4D). This was the same for cells pre-incubated with ITF II. However, ITF I, GTF I and GTF II decreased the expression of this protein 0.37 ± 0.05-fold ($p < 0.05$), 0.41 ± 0.06-fold ($p < 0.01$) and 0.36 ± 0.06-fold ($p < 0.05$) respectively.

OCLN expression was 0.64 ± 0.03-fold ($p < 0.05$) enhanced by A23187 relative to the untreated control, but none of the fructans could prevent this (Fig. 4E). Also, *TJP-1* expression was enhanced 0.5 ± 0.04-fold ($p < 0.05$) by A23187 (Fig. 4F) but also, *TJP-1* overexpression could not be prevented by any of the fructans.

3.3 Fructans prevent the DON-induced overexpression of *CLDN-1* and *CLDN-3* in Caco-2 cells in a fructan- and chain length-dependent manner

Next, we studied the preventive effect of the different fructans on Caco-2 intestinal cells that were exposed to the barrier disrupting fungal toxin DON. This toxin disturbs TJs expression via mitogen-activated protein kinase (MAPK) signaling (Lucioli et al., 2013). To study possible prevention of this disruption, Caco-2 cells were pre-incubated with ITFs and GTFs for 24 hours, followed by addition of DON and incubation for 6 more hours. As shown in Fig. 5A, relative to the untreated control, *CLDN-1* expression was 0.55 ± 0.02-

fold ($p < 0.0001$) increased by DON. This DON-induced increase in *CLDN-1* expression was prevented by GTF I and GTF II by 0.34 ± 0.06-fold ($p < 0.01$) and 0.3 ± 0.03-fold respectively ($p < 0.05$).

Relative to the untreated control, *CLDN-2* was not enhanced by DON or any of the tested fructans (Fig. 5B). Conversely, the expression of *CLDN-3* was significantly increased by DON by 0.77 ± 0.01-fold relative to the untreated control ($p < 0.0001$) (Fig 5C). This DON-induced increase in *CLDN-3* expression was prevented by short chain ITF I and GTF I, since the expression of this gene in cells pre-incubated with both ITF I and GTF I was 0.28 ± 0.04-fold lower than cells treated with DON ($p < 0.05$).

Relative to the untreated control, there was no difference in the expression of *CDH1* when cells were exposed to DON. Neither a difference was found when cells were pre-incubated with the studied fructans followed by the addition of DON (Fig. 5D).

OCLN was increased 0.73 ± 0.02-fold by DON ($p < 0.01$) relative to the untreated control. However, this increase was not attenuated by any of the pre-treatments with fructans (Fig. 5E).

Relative to the untreated control, *TJP-1* overexpression of 0.69 ± 0.02-fold was observed when Caco-2 cells were treated with DON ($p < 0.05$) (Fig 5F). This overexpression could however not be attenuated by any of the studied fructans.

3.4 Fructans do not prevent A23187- or DON-induced IL-8 increase

Next, we tested the effect of fructans on the production of IL-8 by gut epithelial cells. To this end, Caco-2 cells were incubated with fructans for 24 hours. As shown in Fig. 6, both branched fructans significantly increased the IL-8 production from 24.3 ± 1.7 pg/mL to 37.5

± 1.3 pg/mL in cells treated with GTF I ($p < 0.01$), and to 38.5 ± 3 pg/mL in cells treated with GTF II ($p < 0.01$). This was different for cells treated with linear fructans where no differences were observed (Fig. 6A).

Later, the potential protective role of fructans on IL-8 production from Caco-2 cells exposed to A23187 and DON was investigated. To that end, Caco-2 cells were pretreated with fructans for 24 hours, followed by the addition of either A23187 or DON for 6 hours followed by IL-8 quantification in the supernatant. When Caco-2 cells were incubated in presence of A23187, the concentration of IL-8 increased from 24.3 ± 1.7 pg/mL (untreated control) to 42.1 ± 1.7 pg/mL ($p < 0.001$). This IL-8 production was not influenced by any of the studied fructans, since the IL-8 concentration in cells pre-incubated with ITF I was 39 ± 1.3 pg/mL, for GTF I 36.3 ± 3.8 pg/mL, for ITF II 40 ± 3.4 pg/mL, and for GTF II it was 37.7 ± 2.1 pg/mL (Fig. 6B).

DON in contrast to A23187 did not influence the IL-8 production by Caco-2 cells (Fig. 6C). However, ITF II preexposure followed by DON challenge significantly increased IL-8 production from 24.3 ± 1.7 pg/mL to 59.3 ± 6.2 pg/mL ($p < 0.001$). Pre-incubating cells with the other fructans before the addition of DON, did not influence the production of IL-8 compared with cells treated with DON.

3.5 Fructans attenuate cytokine production in DCs in a fructan-dependent way

As cytokine production in epithelial cells was influenced by the fructans, we questioned whether this might also have an impact on DCs that are located between and underneath gut epithelial cells. To that end, DCs were incubated in the presence or absence of either GTF I, GTF II, ITF I or ITF II. Afterwards, DCs cytokine production was measured. The chemokine ligand of monocyte chemoattractant protein-1 (MCP-1/CCL2) was attenuated

by all fructans except by ITF I (Fig. 7A). A 0.3 ± 0.07-fold decrease (p <0.01) was observed for MCP-1/CCL2 in cells treated with GTF I. This attenuation was independent of the fructan size as it was 0.33 ± 0.07-fold (p <0.01) and 0.26 ± 0.07-fold (p <0.05) attenuated by the longer chain ITF II and GTF II. MIP-1α/CCL3 was also attenuated by the fructans but this only reached statistical significance with ITF II (0.5 ± 0.01-fold decrease (p <0.05) (Fig. 7B). IL-1β was not statistically significant influenced by any of the fructans (Fig. 7C). However, the anti-inflammatory cytokine IL-1RA was specifically reduced by the shorter branched GTF I which induced a 0.45 ± 0.07-fold reduction (p >0.05) in production by DCs (Fig. 7D). IL-6 production was not influenced by either fructans (Fig. 7E). However, the proinflammatory TNF-α was 0.26 ± 0.09-fold reduced by the longer chain ITF II (p >0.05). The IL-10 levels were not influenced by the studied fructans (Fig. 7G).

3.6 Intestinal epithelial spent medium enhanced the anti-inflammatory effects of fructans in dendritic cells

Previous studies have shown that medium of epithelial cells pre-exposed to specific fructans enhanced and potentiated the responses of DCs (Bermudez-Brito et al., 2015; Lépine & de Vos, 2018). Therefore, we performed experiments in which we first exposed epithelial cells to either GTF I, GTF II, ITF I or ITF II for 24 hours. The supernatants were harvested for coincubation with DCs and will be referred to as Caco-2-spent medium (CSM). CSM was used to potentiate DCs (Fig. 1) as previously described (Bermudez-Brito et al., 2015). As shown in Fig. 8, CSM had a profound effect on cytokine production by DCs and effects of the fructans was more pronounced but very fructan specific. MCP-1/CCL2 production was strongly attenuated by ITF I (0.48 ± 0.04-fold, p <0.0001) but not by the longer chain ITF II. The production of this MCP-1/CCL2 was reduced by the

branched GTF I by 0.37 ± 0.12-fold (p <0.01), while its production was also attenuated by the longer chain GTF II 0.49 ± 0.11-fold (p <0.001) (Fig. 8A).

The production of pro-inflammatory MIP-1α/CCL3 was strongly decreased by all fructan-conditions except by the longer linear ITF II (Fig. 8B). The branched GTF II-CSM exerted the strongest reduction with a 0.67 ± 0.04-fold decrease (p <0.001), followed by GTF I-CSM which reduced MIP-1α/CCL3 production 0.62 ± 0.03-fold (p <0.001), and by linear short chain ITF I-CSM which reduced MIP-1α/CCL3 0.5 ± 0.05-fold (p <0.01).

For the pro-inflammatory cytokine IL-1β this was different. CSM did not enhance IL-1β production nor did any of the fructans-CSM (Fig. 8C).

The production of the regulatory IL-1RA was strongly enhanced by all the fructan-CSM (Fig 8D). The linear longer chain ITF II-CSM caused the strongest enhancement of IL-1RA production by 1.7 ± 0.2-fold (p <0.01). This was followed by ITF I-CSM that induced a 1.3 ± 0.2-fold enhancement (p <0.01) of IL-1RA while both branched fructans GTF I-CSM and GTF II-CSM caused a 1.21 ± 0.4-fold increase and 1.21 ± 0.3-fold increase respectively (p <0.05).

The production of the pro-inflammatory cytokine IL-6 was strongly prevented in cells treated with all the fructan-CSM (Fig. 8E). The strongest effect was observed in cells treated with short chain linear ITF I-CSM which induced a 0.51 ± 0.07-fold reduction in IL-6 (p <0.01). This was similar for branched GTF I-CSM treated cells, since a 0.48 ± 0.05-fold decrease in IL-6 was observed (p <0.05). The longer fructans, GTF II-CSM and ITF II-CSM induced a 0.43 ± 0.09-fold and a 0.42 ± 0.1-fold (p <0.05) reduction in IL-6.

The production of the pro-inflammatory cytokine TNFα was strongly reduced in DCs by all fructan-CSM, except by the longer linear ITF II-CSM (Fig. 8F). ITF I-CSM decreased its production 0.52 $\pm$ 0.03-fold (p <0.0001) while the branched GTF II-CSM decreased it 0.51 $\pm$ 0.15-fold (p <0.01) and GTF I-CSM decreased it 0.47 $\pm$ 0.18-fold (p <0.01).

The production of the regulatory cytokine IL-10 was influenced only by treatment with ITF II-CSM (Fig. 8G). This ITF II-CSM enhanced IL-10 production 2.5 $\pm$ 1.2-fold (p <0.01).

4. Discussion

To the best of our knowledge, this is the first report where the effects of GTFs on the gene expression of intestinal TJs is studied under physiological and inflammatory conditions and is compared with that of ITFs. It was unknown whether GTFs can protect against TJs mRNA dysregulation induced by the well-known disruptors A23187 and DON. Herein we demonstrate that both GTFs and ITFs can directly influence TJs gene expression and protect from disruption induced by A23187 and DON. Also, we show that GTFs, just like ITFs, can modulate responses of DCs that are in between or are situated under the gut epithelial layer and that effects are stronger in presence of CSM. All these effects are fructan-structure and size dependent as will be discussed in more detail below.

CLDN-1 expression was not influenced by any of the studied fructans. This is in line with the findings of Wu et al (Wu et al., 2017), who studied the effect of linear, β(2→1), short-chain fructooligosaccharide and a long-chain inulin on the expression of this gene. We demonstrate that neither the branched GTFs nor the linear ITFs induced a change in *CLDN-1* expression. Thus, the lack of influence of the studied fructans on the expression of *CLDN-1* as well as findings of others (Wu et al., 2017) made us conclude that this lack of effect is independent of their structure.

The gene expression of *CLDN-2* was strongly decreased when intestinal epithelial cells were incubated in presence of the long-chain fructans GTF II and ITF II. *CLDN-2* is responsible for TJs that form paracellular pores which allow the diffusion of cations, water, and molecules with a molecular radius < 4 Å (Van Itallie et al., 2008). Since the decrease in the expression of *CLDN*-2 is related to an increased epithelial barrier function (Furuse, Furuse, Sasaki, & Tsukita, 2001), the long chain fructans studied herein might be strengthening the epithelial barrier by preventing the increase of intestinal permeability.

The branched fructan GTF II enhanced the expression of *CLDN-3*, *OCLN*, and *TJP-1*, while none of the linear ITFs modified their expression. This illustrates that effects on TJ-regulation are dependent on the structure and size of the fructans. *CLDN-3* functions as a barrier-forming protein, and its overexpression induces an increase in transepithelial resistance (Milatz et al., 2010). *OCLN* and *TJP-1* code for occludin and ZO-1 proteins respectively, which form part of the large protein complexes that regulate the TJs by recruiting other cytosolic components such as protein kinases, GTPases and transcription factors (Matter & Balda, 2003). The up-regulated expression of these genes has been associated with a strengthened barrier function (Pastorelli et al., 2013).

The branched GTF I and the long chain linear ITF II decreased the expression of *CDH1*. This seems to oppose the findings of Uerlings et al., who found an enhanced expression of this gene after incubation of intestinal piglet cells with inulin (Uerlings et al., 2020). The differences observed might be due to the working concentration of inulin, the type of inulin and the type of cell studied, as well as an inulin pre-digestion step which changed the inulin-sample composition (Uerlings et al., 2020). While Uerlings et al., stimulated a piglet cell line instead of a human cell, they also used a low concentration of 0.5 mg/mL of inulin while we needed 10 mg/mL of short chain and long chain ITFs and branched GTFs to obtain significant effects. Another key factor is likely the structural differences of the inulins used. The inulin applied by Uerlings et al., was pre-digested with enzymes before its application to piglet intestinal cells. This might have changed the composition of the inulin and the preparation might have contained proteins and contaminants which were not present in our fructans samples.

We not only studied the effects of the fructans under homeostatic conditions but also in presence of the disruptors A23187 and DON. A23187 does disrupt barrier function by inducing a sudden increase in intracellular calcium which activates the calcium-

dependent PKC. This kinase participates in TJs disassembly (Tai et al., 1996). DON acts via a different route and stimulates MAPK signaling (Li et al., 2022). It is known that this MAPK signaling is involved in the regulation of TJs structure, expression, and function (Arunachalam et al., 2010). We show here that the effects of fructans were not only dependent on the structure but also on the pathways by which TJ regulation was disturbed by the two disruptors.

None of the studied linear ITFs prevented *CLDN-1* overexpression caused by exposure of Caco-2 cells to A23187. This is in line with the findings of Wu et al., who studied the protective effect of a short-chain fructooligosaccharide and a long-chain inulin on the barrier integrity of Caco-2 cell monolayers exposed to another disruptor agent i.e. enterohemorrhagic *Escherichia coli* (EHEC). In this study, ITFs did not prevent EHEC-induced *CLDN-1* dysregulation nor any other TJ gene (Wu et al., 2017). However, we found that the branched GTF I prevented A23187-induced *CLDN-1* overexpression. This again illustrates that the chemical structure of fructans is important for its protective effect on barrier disruption.

A23187 caused an up-regulated expression of *CLDN-2* and *CLDN-3* in Caco-2 cells. Imbalances in the expression of these genes can lead to the development of intestinal disorders, such as ulcerative colitis and Crohn´s disease (Garcia-Hernandez et al., 2017; Günzel & Yu, 2013; Pastorelli et al., 2013; Weber, Nalle, Tretiakova, Rubin, & Turner, 2008; Zeissig et al., 2007), as well as to enhanced sensitivity to bacterial infection (Zhang, Wu, Xia, & Sun, 2013). This A23187-induced increased expression of *CLDN-2* was prevented by pre-incubation of the cells with all fructans except by ITF II. *CLDN-3* over-expression was prevented by all tested fructans. This positive impact of the tested fructans support our suggestion that supplementation of food with these TJ-regulating

dietary fibers might contribute to homeostasis in claudin expression and therewith to prevention of intestinal disease.

In the present study we also investigated the protective effect of fructans on the DON-induced TJ dysregulation. Food contamination with this fungal toxin has been considered a public health issue and was therefore studied here as well (Akbari et al., 2015). Treating Caco-2 cells with the fungal toxin DON caused an overexpression of *CLDN-1*, *CLDN-3*, *OCLN*, and *TJP1*. This coincides with previous findings of Akbari et al (Akbari et al., 2015). In our study, both tested branched GTFs prevented the increase in expression of *CLDN-1*, while the up-regulation of *CLDN-3* by DON was prevented only by the short chain fructans ITF I and GTF I. None of the studied fructans influenced the upregulation of *OCLN* and *TJP1* induced by DON.

The intestinal barrier function is directly influenced by TJs gene expression (Laukoetter, Nava & Nusrat, 2008). To investigate the protective effect of GTFs and ITFs on the barrier function, we previously performed transepithelial resistance (TEER) studies in T84 gut epithelial cells instead of in Caco2 cells which are used here. To that end, we also disrupted the barrier in T84 cells with A23187 and DON. We found that pre-incubation of cells with both ITFs and GTFs, protected for A23187-induced epithelial disruption. However, the gut epithelial barrier disruption provoked by DON was not prevented by any of these fructans (Fernández-Lainez et al., 2022b). Taking together the current findings in Caco2 cells and our previous functional TEER studies in T84 cells, confirm that the protective effects of fructans on the intestinal epithelial barrier integrity, is very dependent on the pathway that drives to the disruption. All studied fructans protect from both disruption and TJs gene dysregulation induced by A23187, which is exerted via PKC. However, when the disruption was exerted by DON via MAPK, fructans prevented only

dysregulation of a few TJs gene as shown here and none of them protected from the barrier disruption (Fernández-Lainez et al., 2023b).

Our current study on Caco2 cells and their TJs expression also provides a new mechanism by which the fructans can contribute to protection for A23187-induced barrier disruption. In our previous TEER study, we suggested that ITF and GTFs might compete for the cell-binding site of A23187 on the cell membrane in a structure and chain length dependent manner (Fernández-Lainez et al., 2022b). However, the current findings of the impact of preexposure of Caco2 cells to ITFs and GTFs, on prevention of TJs dysregulation, provides another mechanism that might explain the protective effects of fructans for A23187-induced barrier disruption. In this study, we used Caco2 instead of T84 cells as the experiments were designed to study the impact of Caco2 spent medium on DCs cytokine responses. This model was previously established with supernatant of Caco2 cells (Bermudez-Brito et al., 2015).

Taken together, all these findings indicate a structure- and size-dependent effect of the studied fructans. We hypothesize that long chain fructans could exert a stronger and longer lasting interaction with the cell membrane of intestinal epithelial cells, compared to interactions that short chain fructans could have. It is known that due to their neutral charge, fructans can stablish non-polar interactions with the cell membrane (Demel et al., 1998, Vereyken et al., 2001, Vereyken et al., 2003). However, further studies are needed to corroborate this suggestion.

Since dysregulation of TJs can lead to intestinal inflammation (Pastorelli et al., 2013), we also determined whether fructans can influence the production of the chemotactic factor IL-8 in Caco-2 cells in presence and absence of A23187 or DON. As such, the branched fructans GTF I and GTF II caused enhanced production of IL-8. This however should not be considered as a negative finding as the chemotactic properties of

IL-8 (Yu et al., 2003) could serve to combat or prevent intestinal infections with pathogenic organisms such as *Salmonella typhimurium* (Lépine & de Vos, 2018) or EHEC (Johnson-Henry et al., 2014). This is also suggested by findings of Lepine et al, where an increase in IL-8 was observed when dendritic cells were exposed to ITF II alone or in symbiotic combination with *Lactobacillus* LaW37 or to ITF II-CSM or CSM coming from Caco-2 cells pre-exposed to *S. typhimurium* (Lépine & de Vos, 2018).

We found that the branched GTFs were capable to induce IL-8 production in Caco-2 cells, while the linear ITFs did not stimulate IL-8 production. This differential result provides evidence for structure-dependent effect of the fructans. Notably, however, the production of IL-8 is a complex phenomenon that is regulated at several levels, such as by NF-κB and protein kinase C (PKC) signaling pathways, but also at transcriptional and translational levels (Yu de Waele & Chadee 2001). In our previous studies, we found that IL-8 production and its regulation by fructans is complex and probably cell type-dependent. In T-84 cells we found that the four fructans protected from the inflammatory action of ionophore A23187 and induced a reduction in IL-8 production (Fernández-Lainez et al., 2022b). In goblet like cells, we found that only the short chain fructans, both linear and branched, caused a decrease in the production of IL-8 (Fernández-Lainez et al., 2023). The mechanisms that explain the different findings in different cells will be subject of future studies with *i.e.* organoids that might provide an integral overview of the final effect of these fibers and their potential protective and anti-inflammatory properties when these cells are combined.

The treatment of Caco-2 cells with A23187 also caused an increase in IL-8 production but none of the studied fructans prevented this IL-8 increase. In our previous TEER study with T84-cells, we observed that fructans did protect for IL-8 release induced by A23187 (Fernández-Lainez et al., 2022b). Besides the difference in cell-type studied, T84 cells vs. Caco-2 cells, this difference could be explained by a difference in

susceptibility for A23187 between the cell-lines. In T84-cells A23187 caused an increase in IL-8 production of 8.4-fold (from 182 ± 18 pg/mL in the untreated control to 1531 ± 96 pg/mL in A23187-treated cells). However, in the current study with Caco2-cells, A23187 induced a less intense increase of 1.7-fold of IL-8 production (from 24.3 ± 1.7 pg/mL in the untreated controls to 42.1 ± 1.7 pg/mL in A23187-treated cells). It might be that fructans protective effect is not that strong when the A23187-induced increase in IL-8 production is not that profound.

To the best of our knowledge, this is the first study where the effect of branched GTFs on cytokine production by DCs is studied. DCs might be located in between or underneath the intestinal epithelial cells. In these DCs, all studied fructans, except the short chain linear ITF I caused a decrease of the pro-inflammatory cytokine MCP-1/CCL2. ITF II was the only fructan that decreased the production of MIP-1α/CCL3 and TNFα. The short chain branched GTF I decreased the production of the neutralizing and regulatory cytokine IL-RA. None of the fructans influenced IL-1β, IL-6, and IL-10 production. These effects were even more pronounced with application of CSM from intestinal epithelial cells which were pre-exposed to the studied fructans. CSM alone had a profound effect on the production of the pro-inflammatory cytokines MIP-1α/CCL3 and TNF-α and reduced the production of the regulatory cytokine IL-10 (Bermudez-Brito et al., 2015; Lépine & de Vos, 2018). All studied fructans, with exception of ITF II-CSM exerted a profound attenuation of this enhanced cytokine production. Notably, the extent to which this attenuation was accomplished was very fructan-size dependent, since the long-chain ITF II-CSM had a lesser attenuating effect on cytokines produced by DCs than the shorter version. However, only ITFII-CSM significantly increased the regulatory IL-10.

Conclusions

The previously proposed role of specific fructans as supportive therapy for the treatment or prevention of inflammatory gut disorders (Del Fabbro, Calder, & Childs, 2020) is supported by the findings of the present study. We demonstrate for the first time the protective and immunomodulatory effect of GTFs on intestinal TJs gene expression, which is GTFs-structure and -size dependent. Effects were compared to that of ITFs. Both GTFs and ITFs can directly modulate TJs in gut epithelial cells but also modulate DC responses. This seems to be mediated via crosstalk with epithelial cells as previously reported (Bermudez-Brito et al., 2015) as DCs exposed to CSM of epithelial cells pre-exposed to the fructans, potentiated the DC-effects of fructans. Therefore, the regulatory effect observed from the studied fructans and the fructan-derived intestinal factors on DCs provide more evidence for chemistry dependent beneficial effects of these non-digestible carbohydrates on intestinal homeostasis and their potential prophylactic use on the attenuation of inflammation in intestinal disorders. Fig. 9 summarizes the effects of fructans observed on intestinal epithelial cells and DCs.

CRediT authorship contribution statement

C. Fernández-Lainez: Conceptualization, Methodology, Investigation, Formal analysis, Software, Writing – original draft. **M. aan de Stegge**: Methodology, Writing – review & editing. **L.A. silva-Lagos:** Formal analysis, Writing – review & editing. **G. López-Velázquez**: Formal analysis, Writing – review & editing. **P. de Vos**: Conceptualization, Writing – review & editing, Supervision, Project administration.

Declaration of competing interest

The authors declare no conflict of interest.

Acknowledgements

This study was partially financed by the “Programa de Recursos Fiscales para Investigación” from Instituto Nacional de Pediatría, Grant number 2019/062. C.F.L. was financially supported by Abel Tasman Talent Program Sandwich PhD from the University of Groningen-University Medical Center Groningen, UG/UMCG in collaboration with Universidad Nacional Autónoma de México, UNAM and CONACyT (#260625).

Appendix A. Supplementary data

Supplementary data to this article (Tables S1, and S2, Fig. S1) can be found online.

References

Akbari, P., Braber, S., Alizadeh, A., Verheijden, K. A., Schoterman, M. H., Kraneveld, A. D., Garssen, J., & Fink-Gremmels, J. (2015). Galacto-oligosaccharides protect the intestinal barrier by maintaining the tight junction network and modulating the inflammatory responses after a challenge with the mycotoxin deoxynivalenol in human Caco-2 cell monolayers and B6C3F1 mice. *The Journal of Nutrition, 145*(7), 1604-1613. https://doi.org/10.3945/jn.114.209486

Akbari, P., Braber, S., Gremmels, H., Koelink, P. J., Verheijden, K. A., Garssen, J., & Fink-Gremmels, J. (2014). Deoxynivalenol: a trigger for intestinal integrity breakdown. *The FASEB Journal, 28*(6), 2414-2429. https://doi.org/10.1096/fj.13-238717

Akbari, P., Fink-Gremmels, J., Willems, R. H., Difilippo, E., Schols, H. A., Schoterman, M. H., Garssen, J., & Braber, S. (2017). Characterizing microbiota-independent effects of oligosaccharides on intestinal epithelial cells: Insight into the role of structure and size. *European Journal of Nutrition, 56*(5), 1919-1930. https://doi.org/10.1007/s00394-016-1234-9

Arunachalam, C., & Doohan, F. M. (2013). Trichothecene toxicity in eukaryotes: Cellular and molecular mechanisms in plants and animals. *Toxicology Letters, 217*(2), 149-158. https://doi.org/10.1016/j.toxlet.2012.12.003

Bermudez-Brito, M., Sahasrabudhe, N. M., Rösch, C., Schols, H. A., Faas, M. M., & de Vos, P. (2015). The impact of dietary fibers on dendritic cell responses in vitro is dependent on the differential effects of the fibers on intestinal epithelial cells. *Molecular Nutrition and Food Research, 59*(4), 698-710. https://doi.org/10.1002/mnfr.201400811

Camilleri, M., Madsen, K., Spiller, R., Van Meerveld, B., & Verne, G. (2012). Intestinal barrier function in health and gastrointestinal disease. *Neurogastroenterology & Motility, 24*(6), 503-512. https://doi.org/10.1111/j.1365-2982.2012.01921.x

Del Fabbro, S., Calder, P. C., & Childs, C. E. (2020). Microbiota-independent immunological effects of non-digestible oligosaccharides in the context of inflammatory bowel diseases. *Proceedings of the Nutrition Society, 79*(4), 468-478. https://doi.org/10.1017/S0029665120006953

Demel, R. A., Dorrepaal, E., Ebskamp, M. J. M., Smeekens, J. C. M., & De Kruijff, B. (1998). Fructans interact strongly with model membranes. *Biochimica et Biophysica Acta (BBA)-Biomembranes*, *1375*(1-2), 36-42. https://doi.org/10.1016/S0005-2736(98)00138-2

Fernández-Lainez, C., Akkerman, R., Oerlemans, M., Logtenberg, M., Schols, H., Silva-Lagos, L., López-Velázquez, G., & de Vos, P. (2022a). β (2→ 6)-Type fructans attenuate proinflammatory responses in a structure dependent fashion via Toll-like receptors. *Carbohydrate Polymers, 277*, 118893. https://doi.org/10.1016/j.carbpol.2021.118893

Fernández-Lainez, C., Logtenberg, M. J., Tang, X., Schols, H. A., López-Velázquez, G., & de Vos, P. (2022b). β (2→ 1) chicory and β (2→ 1)-β (2→ 6) agave fructans protect the human intestinal barrier function in vitro in a stressor-dependent fashion. *Food & Function*, *13*(12), 6737-6748. 10.1039/d2fo00534d

Fernández-Lainez, C., aan de Stegge, M., Silva-Lagos, L. A., López-Velázquez, G., & de Vos, P. (2023). β (2→ 1)-β (2→ 6) branched graminan-type fructans and β (2→ 1) linear fructans impact mucus-related and endoplasmic reticulum stress-related

genes in goblet cells and attenuate inflammatory responses in a fructan dependent fashion. *Food & Function*, *14*(3), 1338-1348. https://doi.org/10.1039/d2fo02710k

Figueroa-Lozano, S., Akkerman, R., Beukema, M., van Leeuwen, S. S., Dijkhuizen, L., & de Vos, P. (2021). 2′-Fucosyllactose impacts the expression of mucus-related genes in goblet cells and maintains barrier function of gut epithelial cells. *Journal of Functional Foods, 85*, 104630. https://doi.org/10.1016/j.jff.2021.104630

Forstner, G., Zhang, Y., McCool, D., & Forstner, J. (1993). Mucin secretion by T84 cells: stimulation by PKC, Ca2+, and a protein kinase activated by Ca2+ ionophore. *American Journal of Physiology-Gastrointestinal and Liver Physiology*, 264(6), G1096-G1102. DOI: 10.1152/ajpgi.1993.264.6.G1096.

Furuse, M., Furuse, K., Sasaki, H., & Tsukita, S. (2001). Conversion of zonulae occludentes from tight to leaky strand type by introducing claudin-2 into Madin-Darby canine kidney I cells. *The Journal of Cell Biology, 153*(2), 263-272. https://doi.org/10.1083/jcb.153.2.263

Garcia-Hernandez, V., Quiros, M., & Nusrat, A. (2017). Intestinal epithelial claudins: expression and regulation in homeostasis and inflammation. *Annals of the New York Academy of Sciences, 1397*(1), 66-79. https://doi.org/10.1111/nyas.13360

González-Mariscal, L., Tapia, R., & Chamorro, D. (2008). Crosstalk of tight junction components with signaling pathways. *Biochimica et Biophysica Acta (BBA)-Biomembranes, 1778*(3), 729-756. doi: 10.1016/j.bbamem.2007.08.018

Günzel, D., & Yu, A. S. (2013). Claudins and the modulation of tight junction permeability. *Physiological Reviews, 93*(2), 525-569. https://doi.org/10.1152/physrev.00019.2012

Johnson-Henry, K. C., Pinnell, L. J., Waskow, A. M., Irrazabal, T., Martin, A., Hausner, M., & Sherman, P. M. (2014). Short-chain fructo-oligosaccharide and inulin modulate inflammatory responses and microbial communities in Caco2-bbe cells and in a mouse model of intestinal injury. *The Journal of Nutrition, 144*(11), 1725-1733. https://doi.org/10.3945/jn.114.195081

Kelly, G. (2008). Inulin-type prebiotics--a review: part 1. [Review]. *Alternative Medicine Review, 13*(4), 15.

Kiewiet, M. B., Rodríguez, M. I. G., Dekkers, R., Gros, M., Ulfman, L. H., Groeneveld, A., de Vos, P., & Faas, M. M. (2018). The epithelial barrier-protecting properties of a soy hydrolysate. *Food and function, 9*(8), 4164-4172.10.1039/C8FO00913A

Laukoetter, M. G., Nava, P., & Nusrat, A. (2008). Role of the intestinal barrier in inflammatory bowel disease. *World journal of gastroenterology*, 14(3): 401–407. 10.3748/wjg.14.401

Lépine, A., & de Vos, P. (2018). Synbiotic effects of the dietary fiber long-chain inulin and probiotic lactobacillus acidophilus W37 can be caused by direct, synergistic stimulation of immune toll-like receptors and dendritic cells. *Molecular Nutrition and Food Research, 62*(15), 1800251. https://doi.org/10.1002/mnfr.201800251

Li, J., Wang, Y., Deng, Y., Wang, X., Wu, W., Nepovimova, E., Wu, Q., & Kuca, K. (2022). Toxic mechanisms of the trichothecenes T-2 toxin and deoxynivalenol on protein synthesis. *Food and Chemical Toxicology*, 113044. https://doi.org/10.1016/j.fct.2022.113044

Li, L.-L., Wang, Y.-T., Zhu, L.-M., Liu, Z.-Y., Ye, C.-Q., & Qin, S. (2020). Inulin with different degrees of polymerization protects against diet-induced endotoxemia and

inflammation in association with gut microbiota regulation in mice. *Scientific Reports, 10*(1), 1-12. https://doi.org/10.1038/s41598-020-58048-w

Livak, K. J., & Schmittgen, T. D. (2001). Analysis of relative gene expression data using real-time quantitative PCR and the 2− ΔΔCT method. *methods, 25*(4), 402-408. https://doi.org/10.1006/meth.2001.1262

Lopez, M. G., Mancilla-Margalli, N. A., & Mendoza-Diaz, G. (2003). Molecular structures of fructans from Agave tequilana Weber var. azul. *Journal of Agricultural and Food Chemistry, 51*(27), 7835-7840. https://doi.org/10.1021/jf030383v

López, M. G., & Urías-Silvas, J. E. (2007). Agave fructans as prebiotics. *Recent Advances in Fructooligosaccharides Research, 37*, 1-14.

Lucioli, J., Pinton, P., Callu, P., Laffitte, J., Grosjean, F., Kolf-Clauw, M., Oswald, I. P., & Bracarense, A. P. F. (2013). The food contaminant deoxynivalenol activates the mitogen activated protein kinases in the intestine: interest of ex vivo models as an alternative to in vivo experiments. *Toxicon, 66*, 31-36. https://doi.org/10.1016/j.toxicon.2013.01.024

Man, S., Liu, T., Yao, Y., Lu, Y., Ma, L., & Lu, F. (2020). Friend or foe? The roles of inulin-type fructans. Carbohydrate Polymers, 252:117155. https://doi.org/10.1016/j.carbpol.2020.117155

Mancilla-Margalli, N. A., & López, M. G. (2006). Water-soluble carbohydrates and fructan structure patterns from Agave and Dasylirion species. *Journal of Agricultural and Food Chemistry, 54*(20), 7832-7839. https://doi.org/10.1021/jf060354v

Matter, K., & Balda, M. S. (2003). Signalling to and from tight junctions. *Nature Reviews Molecular Cell Biology, 4*(3), 225-237. https://doi.org/10.1038/nrm1055

Milatz, S., Krug, S. M., Rosenthal, R., Günzel, D., Müller, D., Schulzke, J.-D., Amasheh, S., & Fromm, M. (2010). Claudin-3 acts as a sealing component of the tight junction for ions of either charge and uncharged solutes. *Biochimica et Biophysica Acta (BBA)-Biomembranes, 1798*(11), 2048-2057. https://doi.org/10.1016/j.bbamem.2010.07.014

Pastorelli, L., De Salvo, C., Mercado, J. R., Vecchi, M., & Pizarro, T. T. (2013). Central role of the gut epithelial barrier in the pathogenesis of chronic intestinal inflammation: lessons learned from animal models and human genetics. *Frontiers in Immunology, 4*, 280. https://doi.org/10.3389/fimmu.2013.00280

Pérez-López, A. V., & Simpson, J. (2020). The Sweet Taste of Adapting to the Desert: Fructan Metabolism in Agave Species. *Frontiers in Plant Science, 11*, 324. https://doi.org/10.3389/fpls.2020.00324

Pérez-López, A. V., Simpson, J., Clench, M. R., Gomez-Vargas, A. D., & Ordaz-Ortiz, J. J. (2021). Localization and Composition of Fructans in Stem and Rhizome of Agave tequilana Weber var. azul. *Frontiers in Plant Science, 11*, 2309. https://doi.org/10.3389/fpls.2020.608850

Perović, J., Šaponjac, V. T., Kojić, J., Krulj, J., Moreno, D. A., García-Viguera, C., Bodroza-Solarov, M., & Ilić, N. (2021). Chicory (Cichorium intybus L.) as a food ingredient–Nutritional composition, bioactivity, safety, and health claims: A review. *Food Chemistry, 336*, 127676. https://doi.org/10.1016/j.foodchem.2020.127676

Pestka, J. J. (2008). Mechanisms of deoxynivalenol-induced gene expression and apoptosis. *Food Additives and Contaminants*, 25(9), 1128-1140. https://doi.org/10.1080/02652030802056626.

Peters, V., Dijkstra, G., & Campmans-Kuijpers, M. J. (2022). Are all dietary fibers equal for patients with inflammatory bowel disease? A systematic review of randomized controlled trials. *Nutrition Reviews, 80*(5), 1179-1193. https://doi.org/10.1093/nutrit/nuab062

Piana, C., Wirth, M., Gerbes, S., Viernstein, H., Gabor, F., & Toegel, S. (2008). Validation of reference genes for qPCR studies on Caco-2 cell differentiation. *European Journal of Pharmaceutics and Biopharmaceutics, 69*(3), 1187-1192. doi: 10.1016/j.ejpb.2008.03.008

Pinton, P., Braicu, C., Nougayrede, J.-P., Laffitte, J., Taranu, I., & Oswald, I. P. (2010). Deoxynivalenol impairs porcine intestinal barrier function and decreases the protein expression of claudin-4 through a mitogen-activated protein kinase-dependent mechanism. *The Journal of Nutrition, 140*(11), 1956-1962. https://doi.org/10.3945/jn.110.123919

Ren, C., Zhang, Q., de Haan, B. J., Faas, M. M., Zhang, H., & de Vos, P. (2020). Protective effects of lactic acid bacteria on gut epithelial barrier dysfunction are Toll like receptor 2 and protein kinase C dependent. *Food and Function, 11*(2), 1230-1234. 10.1039/C9FO02933H

Salinas, E., Reyes-Pavón, D., Cortes-Perez, N. G., Torres-Maravilla, E., Bitzer-Quintero, O. K., Langella, P., & Bermúdez-Humarán, L. G. (2021). Bioactive Compounds in Food as a Current Therapeutic Approach to Maintain a Healthy Intestinal

Epithelium. *Microorganisms, 9*(8), 1634. https://doi.org/10.3390/microorganisms9081634

Sergent, T., Parys, M., Garsou, S., Pussemier, L., Schneider, Y. J., & Larondelle, Y. (2006). Deoxynivalenol transport across human intestinal Caco-2 cells and its effects on cellular metabolism at realistic intestinal concentrations. *Toxicology Letters*, 164(2), 167-176. https://doi.org/10.1016/j.toxlet.2005.12.006.

Shen, L. (2012). Tight junctions on the move: molecular mechanisms for epithelial barrier regulation. *Annals of the New York Academy of Sciences, 1258*(1), 9-18.

https://doi.org/10.1111/j.1749-6632.2012.06613.x

Tai, Y. H., Flick, J., Levine, S. A., Madara, J. L., Sharp, G. W., & Donowitz, M. (1996). Regulation of tight junction resistance in T84 monolayers by elevation in intracellular Ca2+: a protein kinase C effect. *The Journal Membrane Biology, 149*(1), 71-79. doi: 10.1007/s002329900008

Tsukita, S., Furuse, M., & Itoh, M. (2001). Multifunctional strands in tight junctions. *Nature Reviews Molecular Cell Biology, 2*(4), 285-293. https://doi.org/10.1038/35067088

Uerlings, J., Schroyen, M., Willems, E., Tanghe, S., Bruggeman, G., Bindelle, J., & Everaert, N. (2020). Differential effects of inulin or its fermentation metabolites on gut barrier and immune function of porcine intestinal epithelial cells. *Journal of Functional Foods, 67*, 103855. https://doi.org/10.1016/j.jff.2020.103855

Van De Walle, J., Romier, B., Larondelle, Y., & Schneider, Y. J. (2008). Influence of deoxynivalenol on NF-κB activation and IL-8 secretion in human intestinal Caco-2

cells. *Toxicology Letters*, 177(3), 205-214. https://doi.org/10.1016/j.toxlet.2008.01.018

Van Itallie, C. M., Holmes, J., Bridges, A., Gookin, J. L., Coccaro, M. R., Proctor, W., Colegio, O. R., & Anderson, J. M. (2008). The density of small tight junction pores varies among cell types and is increased by expression of claudin-2. *Journal of Cell Science, 121*(3), 298-305. https://doi.org/10.1242/jcs.021485

Vanuytsel, T., Tack, J., & Farre, R. (2021). The Role of Intestinal Permeability in Gastrointestinal Disorders and Current Methods of Evaluation. *Frontiers in Nutrition*, 585. https://doi.org/10.3389/fnut.2021.717925

Vereyken, I. J., Chupin, V., Demel, R. A., Smeekens, S. C., & De Kruijff, B. (2001). Fructans insert between the headgroups of phospholipids. *Biochimica et Biophysica Acta (BBA)-Biomembranes*, *1510*(1-2), 307-320. https://doi.org/10.1016/S0005-2736(00)00363-1

Vereyken, I. J., Van Kuik, J. A., Evers, T. H., Rijken, P. J., & de Kruijff, B. (2003). Structural requirements of the fructan-lipid interaction. *Biophysical journal*, *84*(5), 3147-3154. https://doi.org/10.1016/S0006-3495(03)70039-3

Versluys, M., Kirtel, O., Toksoy Öner, E., & Van den Ende, W. (2018). The fructan syndrome: evolutionary aspects and common themes among plants and microbes. *Plant, Cell and Environment, 41*(1), 16-38. https://doi.org/10.1111/pce.13070

Vogt, L., Meyer, D., Pullens, G., Faas, M. M., Venema, K., Ramasamy, U., Schols, H. A., & de Vos, P. (2014). Toll-Like Receptor 2 Activation by b2→ 1-Fructans Protects Barrier Function of T84 Human Intestinal Epithelial Cells in a Chain Length–

Dependent Manner. *The Journal of Nutrition, 144*, 1002-1008. doi: 10.3945/jn.114.191643

Wan, X., Guo, H., Liang, Y., Zhou, C., Liu, Z., Li, K., Niu, F., Zhai, X., & Wang, L. (2020). The physiological functions and pharmaceutical applications of inulin: A review. *Carbohydrate Polymers, 246*, 116589. https://doi.org/10.1016/j.carbpol.2020.116589

Weber, C. R., Nalle, S. C., Tretiakova, M., Rubin, D. T., & Turner, J. R. (2008). Claudin-1 and claudin-2 expression is elevated in inflammatory bowel disease and may contribute to early neoplastic transformation. *Laboratory Investigation, 88*(10), 1110-1120. https://doi.org/10.1038/labinvest.2008.78

Wu, R. Y., Abdullah, M., Määttänen, P., Pilar, A. V. C., Scruten, E., Johnson-Henry, K. C., Napper, S., O'Brien, C., Jones, N. L., & Sherman, P. M. (2017). Protein kinase C δ signaling is required for dietary prebiotic-induced strengthening of intestinal epithelial barrier function. *Scientific Reports, 7*(1), 1-10. https://doi.org/10.1038/srep40820

Yang, W., Zhao, P., Li, X., Guo, L., & Gao, W. (2022). The potential roles of natural plant polysaccharides in inflammatory bowel disease: A review. *Carbohydrate Polymers, 277*, 118821. https://doi.org/10.1016/j.carbpol.2021.118821

Young, I. D., Latousakis, D., & Juge, N. (2021). The immunomodulatory properties of β-2, 6 fructans: a comprehensive review. *Nutrients, 13*(4), 1309. https://doi.org/10.3390/nu13041309

Yu, Y., Zeng, H., Lyons, S., Carlson, A., Merlin, D., Neish, A. S., & Gewirtz, A. T. (2003). TLR5-mediated activation of p38 MAPK regulates epithelial IL-8 expression via

posttranscriptional mechanism. *American Journal of Physiology-Gastrointestinal and Liver Physiology, 285*(2), G282-G290. https://doi.org/10.1152/ajpgi.00503.2002

Yu, Y., C. De Waele, C., & K. Chadee. (2001). Calcium-dependent interleukin-8 gene expression in T84 human colonic epithelial cells. *Inflammation Research*, *50*, 220–226. https://doi.org/10.1007/s000110050747

Zeissig, S., Bürgel, N., Günzel, D., Richter, J., Mankertz, J., Wahnschaffe, U., Kroesen, A. J., Zeitz, M., Fromm, M., & Schulzke, J. D. (2007). Changes in expression and distribution of claudin 2, 5 and 8 lead to discontinuous tight junctions and barrier dysfunction in active Crohn's disease. *Gut, 56*(1), 61-72. http://dx.doi.org/10.1136/gut.2006.094375

Zhang, Y.-g., Wu, S., Xia, Y., & Sun, J. (2013). Salmonella infection upregulates the leaky protein claudin-2 in intestinal epithelial cells. *PloS One, 8*(3), e58606. https://doi.org/10.1371/journal.pone.0058606

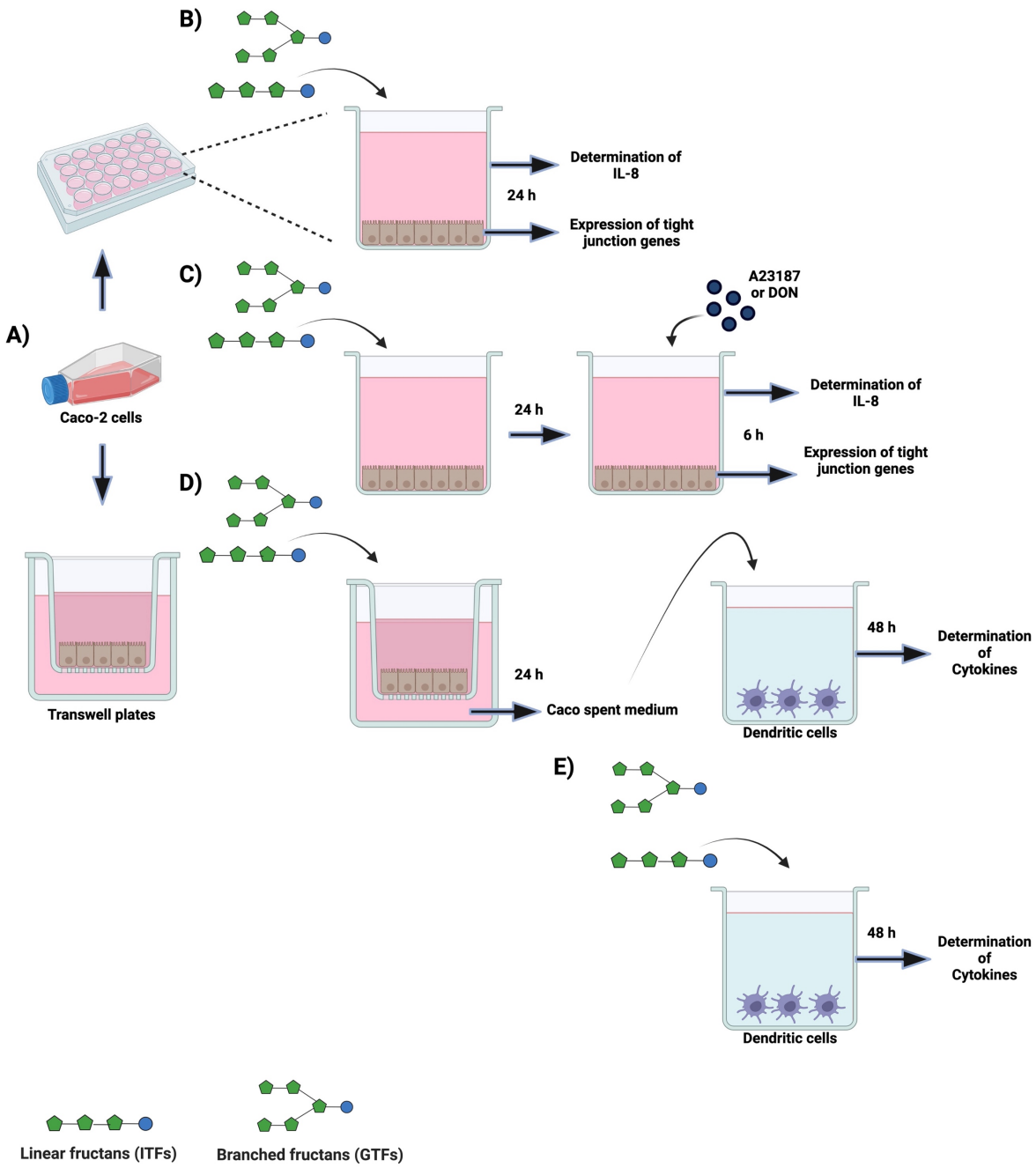

Fig. 1. Design of experiments. A) Confluent Caco-2 cells were seeded in 24-well plates and transwells. B) Expression of tight junction genes was determined after incubation of cells with ITFs or GTFs. Production of IL-8 was determined from Caco-2 supernatant. C) Cells were incubated in presence of ITFs or GTFs, followed by the addition of the barrier disruptors A23187 or DON. Afterwards, expression of tight junction genes and IL-8 production were determined. D) Caco-spent medium (CSM) was obtained after incubation of Caco-2 cells in presence of ITFs or GTFs. This CSM was added to DCs. After

incubation for 48 hours, cytokine profile was determined in DCs supernatants. E) DCs were incubated in presence of ITFs or GTFs for 48 hours, followed by determination of cytokine profile from supernatants. The schemes of fructans were made following the standardized symbol nomenclature for glycans (National Institute of Biotechnology, https://www.ncbi.nlm.nih.gov/glycans/snfg.html, consulted on November 4th, 2022)

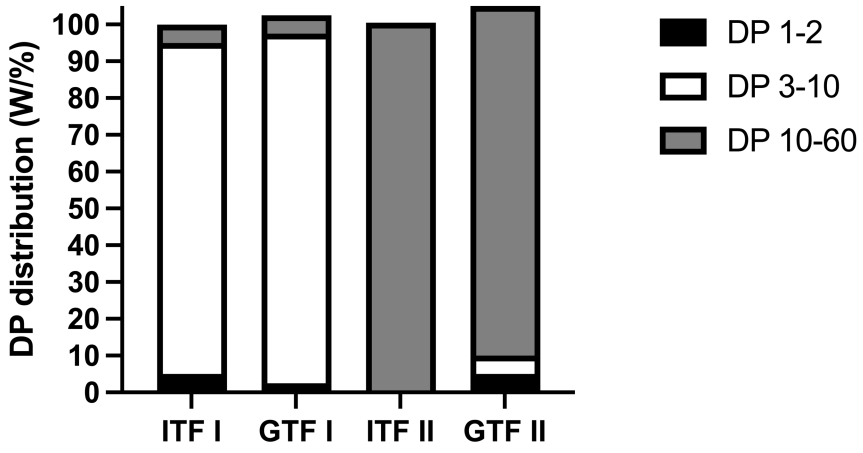

Fig. 2. Chain length distribution of ITF and GTF. Most of ITF I chains are smaller than 10 DP, although chains with DP up to 25 are also present. The DP of GTF I is predominantly 3-4, however a small proportion of chains with DP between 7-45 also form part of this mixture. ITF II is composed of longer chains with a DP that ranges between 10-60. The most abundant chains of GTF II have a DP of 17, although it also contains shorter as well as longer chains. (Fernández-Lainez et al., 2022a).

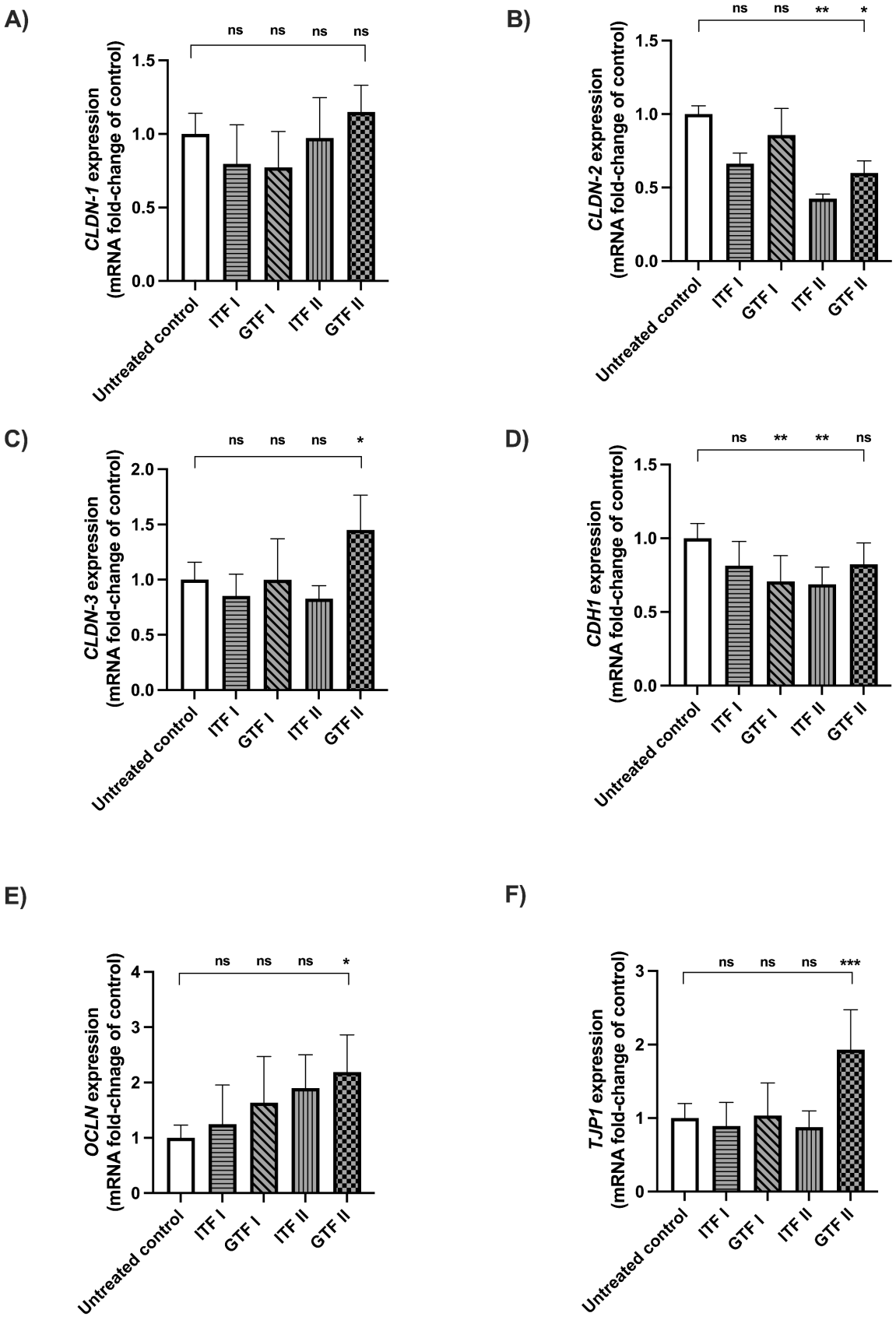
A)
ns ns ns ns
CLDN-1 expression (mRNA fold-change of control)
1.5
1.0
0.5
0.0
Untreated control
ITF I
GTF I
ITF II
GTF II
B)
ns ns ** *
CLDN-2 expression (mRNA fold-change of control)
1.5
1.0
0.5
0.0
Untreated control
ITF I
GTF I
ITF II
GTF II
C)
ns ns ns *
CLDN-3 expression (mRNA fold-change of control)
2.0
1.5
1.0
0.5
0.0
Untreated control
ITF I
GTF I
ITF II
GTF II
D)
ns ** ** ns
CDH1 expression (mRNA fold-change of control)
1.5
1.0
0.5
0.0
Untreated control
ITF I
GTF I
ITF II
GTF II
E)
ns ns ns *
OCLN expression (mRNA fold-chnage of control)
4
3
2
1
0
Untreated control
ITF I
GTF I
ITF II
GTF II
F)
ns ns ns ***
TJP1 expression (mRNA fold-change of control)
3
2
1
0
Untreated control
ITF I
GTF I
ITF II
GTF II

Fig. 3. Effect of chicory inulin type fructans (ITFs) and agave graminan type fructans (GTFs) of different molecular weight on the expression of intestinal tight junction genes in gut epithelial Caco-2 cells. Caco-2 cells were incubated for 24hours in presence or absence of 10 mg/mL of the studied fructans. Afterwards, changes in expression of tight junction genes *CLDN-1* (A), *CLDN-2* (B), *CLDN-3* (C), *CDH1* (D), *OCLN* (E), and *TJP1* (F) were determined by qPCR. Data are expressed as mean ± SD. Statistical differences between untreated control and cells incubated with fructans were calculated.

* (p <0.05), ** (p <0.01), *** (p <0.001), **** (p <0.0001).

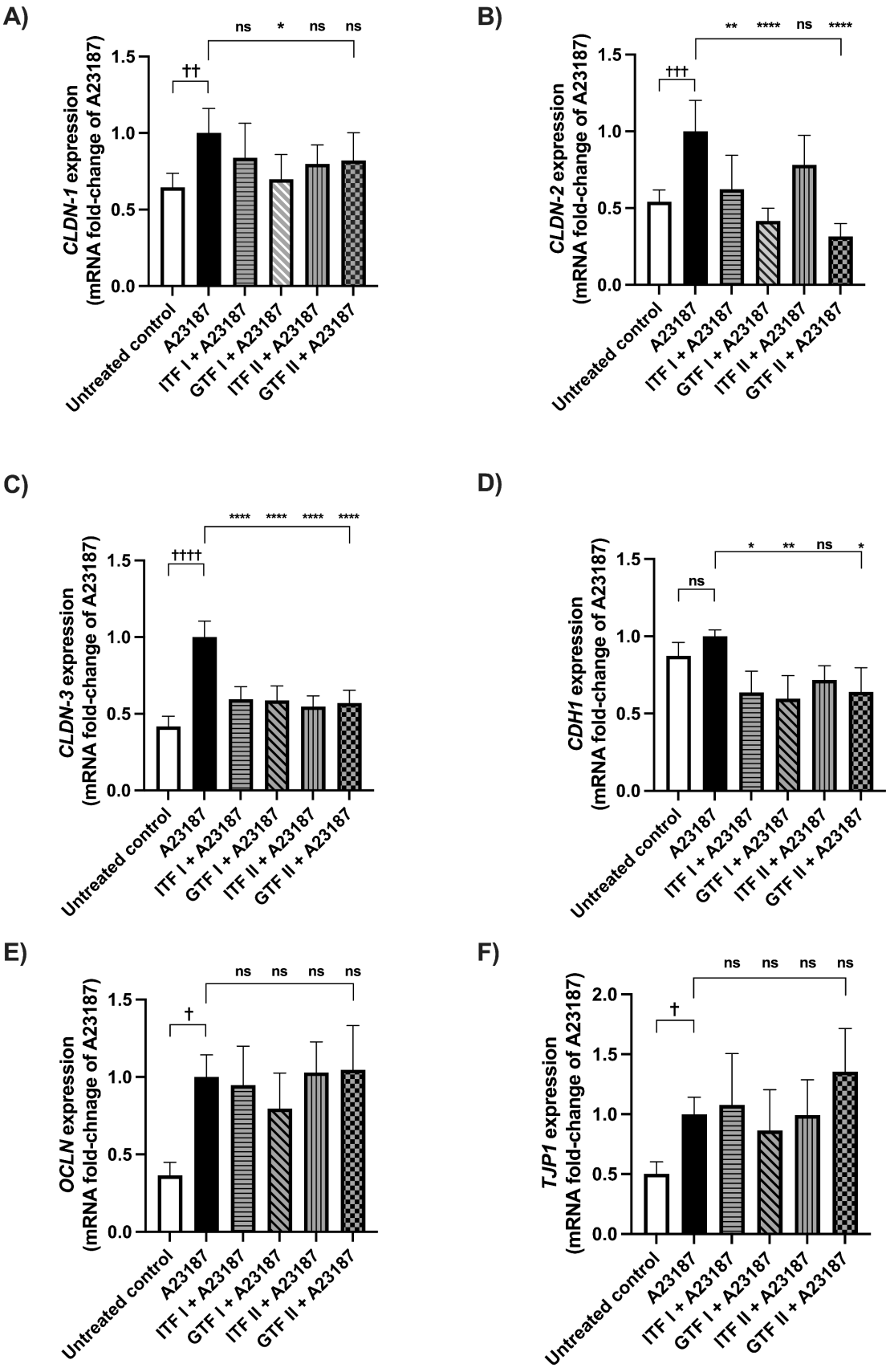
A)
B)
C)
D)
E)
F)
CLDN-1 expression (mRNA fold-change of A23187)
CLDN-2 expression (mRNA fold-change of A23187)
CLDN-3 expression (mRNA fold-change of A23187)
CDH1 expression (mRNA fold-change of A23187)
OCLN expression (mRNA fold-chnage of A23187)
TJP1 expression (mRNA fold-change of A23187)
Untreated control
A23187
ITF I + A23187
GTF I + A23187
ITF II + A23187
GTF II + A23187
ns
*
**
****
†
††
†††
††††

Fig. 4. Prevention of tight-junction dysregulation induced by A23187 by ITFs and GTFs in Caco-2 cells. Caco-2 cells were incubated in presence of 10 mg/mL of fructans, followed by the addition of A23187. Expression of tight junction genes *CLDN-1* (A), *CLDN-2* (B), *CLDN-3* (C), *CDH1* (D), *OCLN* (E), and *TJP1* (F) was determined by qPCR. Data are expressed as mean ± SD. Statistical differences between untreated control and cells treated with A23187 were calculated. Cells treated with A23187 and those pre-treated with fructans were compared. * or † (p <0.05), ** or †† (p <0.01), *** or ††† (p <0.001), **** or †††† (p <0.0001).

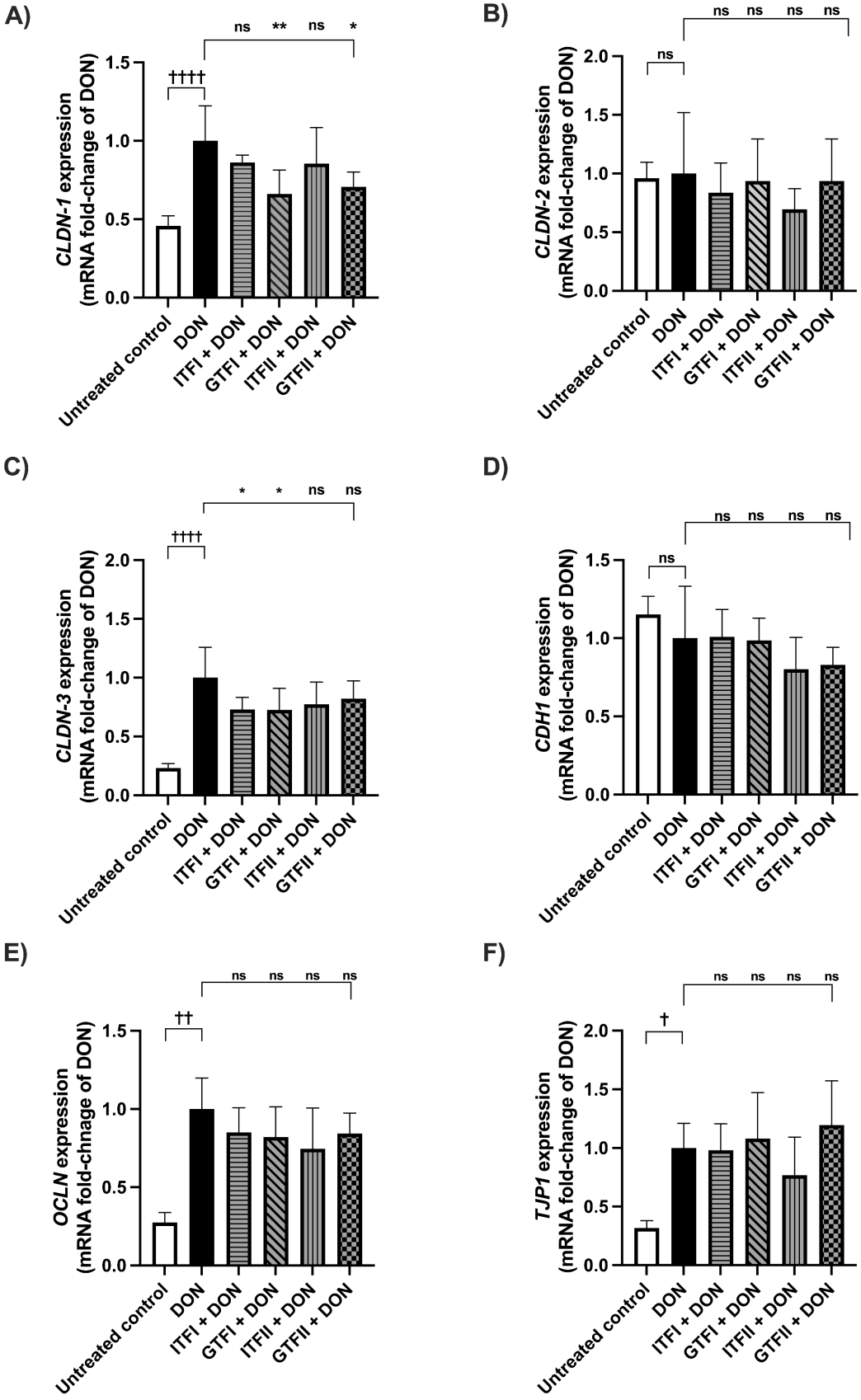
A)
CLDN-1 expression (mRNA fold-change of DON)
ns ** ns *
††††
B)
CLDN-2 expression (mRNA fold-change of DON)
ns ns ns ns
ns
C)
CLDN-3 expression (mRNA fold-change of DON)
* * ns ns
††††
D)
CDH1 expression (mRNA fold-change of DON)
ns ns ns ns
ns
E)
OCLN expression (mRNA fold-chnage of DON)
ns ns ns ns
††
F)
TJP1 expression (mRNA fold-change of DON)
ns ns ns ns
†
Untreated control
DON
ITFI + DON
GTFI + DON
ITFII + DON
GTFII + DON

Fig. 5. Prevention of tight-junction dysregulation induced by DON by ITFs and GTFs in Caco-2 cells. After incubation of cells with ITFs and GTFs for 24 hours, DON was added followed by 6 more hours of incubation. The expression of tight junction genes *CLDN-1* (A), *CLDN-2* (B), *CLDN-3* (C), *CDH1* (D), *OCLN* (E), and *TJP1* (F) was determined by qPCR. Data are expressed as mean ± SD. Statistical differences between untreated control and cells treated with DON were calculated. Cells treated with DON and those pre-treated with fructans were compared. * or † (p <0.05), ** or †† (p <0.01), *** or ††† (p <0.001), **** or †††† (p <0.0001).

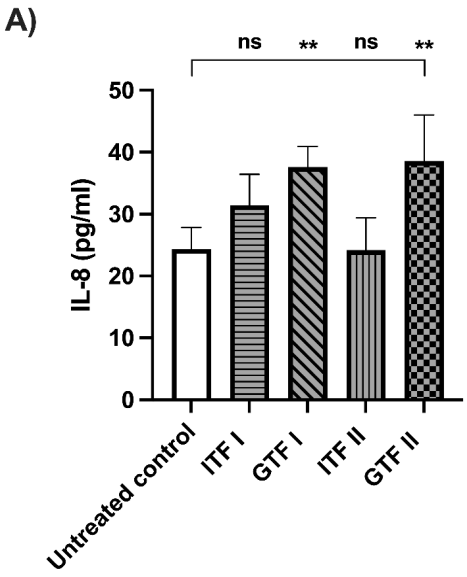
A)
ns
**
ns
**
IL-8 (pg/ml)
50
40
30
20
10
0
Untreated control
ITF I
GTF I
ITF II
GTF II

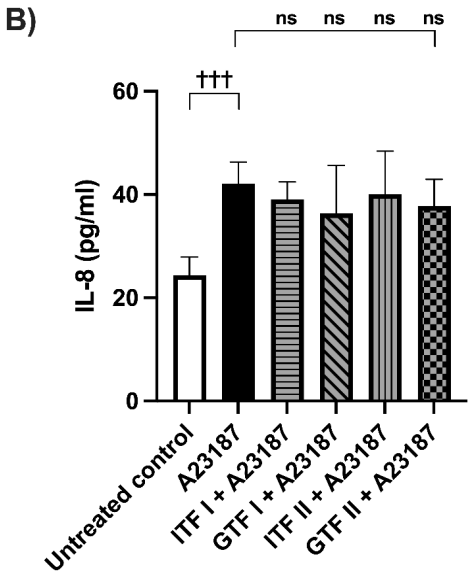
B)
ns
ns
ns
ns
†††
IL-8 (pg/ml)
60
40
20
0
Untreated control
A23187
ITF I + A23187
GTF I + A23187
ITF II + A23187
GTF II + A23187

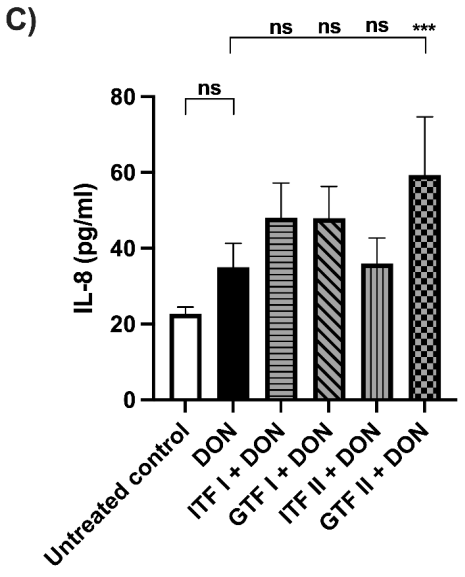
C)
ns
ns
ns
***
ns
IL-8 (pg/ml)
80
60
40
20
0
Untreated control
DON
ITF I + DON
GTF I + DON
ITF II + DON
GTF II + DON

Fig. 6. Production of IL-8 by Caco-2 cells after fructans exposure in presence and absence of A23187 or DON. All data are expressed as mean ± SD. A) Cells were incubated with either ITF I, ITF I, GTF I and GTF II for 24 hours, followed by quantification of IL-8 production. Statistical differences between untreated control and cells incubated with fructans were calculated. In a second set of experiments, Caco-2 cells were pre-incubated with fructans for 24 hours. Afterwards, A23187 (B) and DON (C) were added, and the cultures were incubated 6 more hours. Finally, the production of IL-8 was quantified from cell supernatants. Statistical differences between untreated control and cells treated with A23187 or DON were calculated. Cells treated with A23187 or DON, and those pre-treated with fructans were compared. * or † (p <0.05), ** or †† (p <0.01), *** or ††† (p <0.001), **** or †††† (p <0.0001).

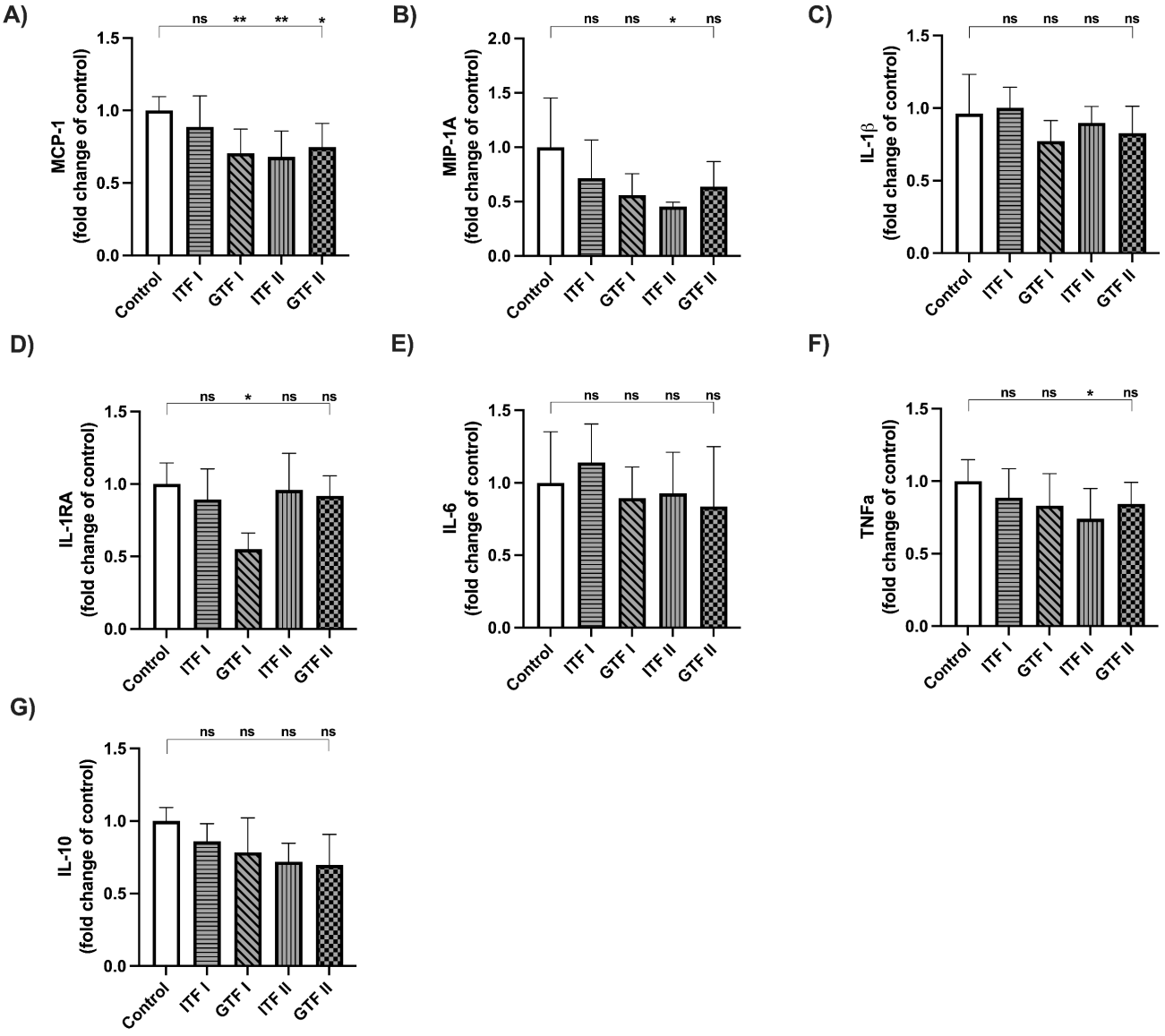

Fig. 7. Cytokine production by dendritic cells treated with chicory inulin type fructans (ITFs) and agave graminan type fructans (GTFs). Dendritic cells were incubated with ITF I, GTFI, ITF II and GTF II for 48 hours. The production of MCP-1/CCL2 (A), MIP-1α/CCL3 (B), IL-1β (C), IL-1RA (D), IL-6 (E), TNFα (F) and IL-10 (G) was quantified in DCs supernatants by Luminex assay and the fold-change compared to untreated controls was calculated. Data are expressed as mean ± SD. Statistical differences between untreated control and cells incubated with fructans were calculated. * (p <0.05), ** (p <0.01), *** (p <0.001), **** (p <0.0001).

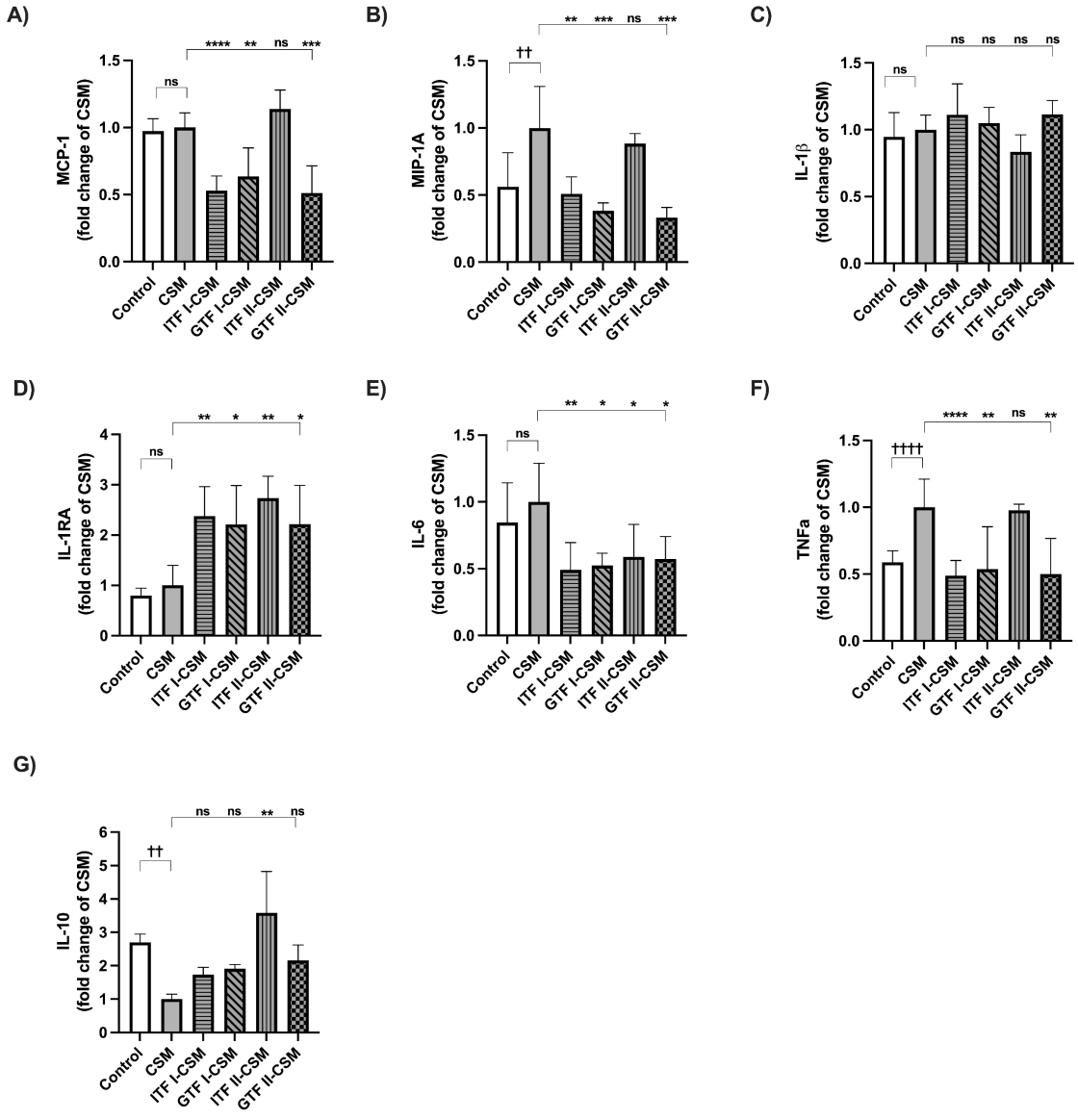

Fig. 8. Cytokine production (fold-change of CSM) of dendritic cells exposed to fructan-Caco-spent medium. Dendritic cells were incubated for 48 hours in presence of CSM. Afterwards, supernatants were collected for determination of the cytokine profile that included MCP-1/CCL2 (A), MIP-1α/CCL3 (B), IL-1RA (C), IL-1β (D), IL-6 (E), TNFα (G) and IL-10 (G). Data are expressed as mean ± SD. Statistical differences between untreated control and cells treated with CSM were calculated. Cells treated with CSM and either ITF I-CSM, GTF I-CSM, ITF II-CSM or GTF II-CSM were compared. * or † (p <0.05), ** or †† (p <0.01), *** or ††† (p <0.001), **** or †††† (p <0.0001).

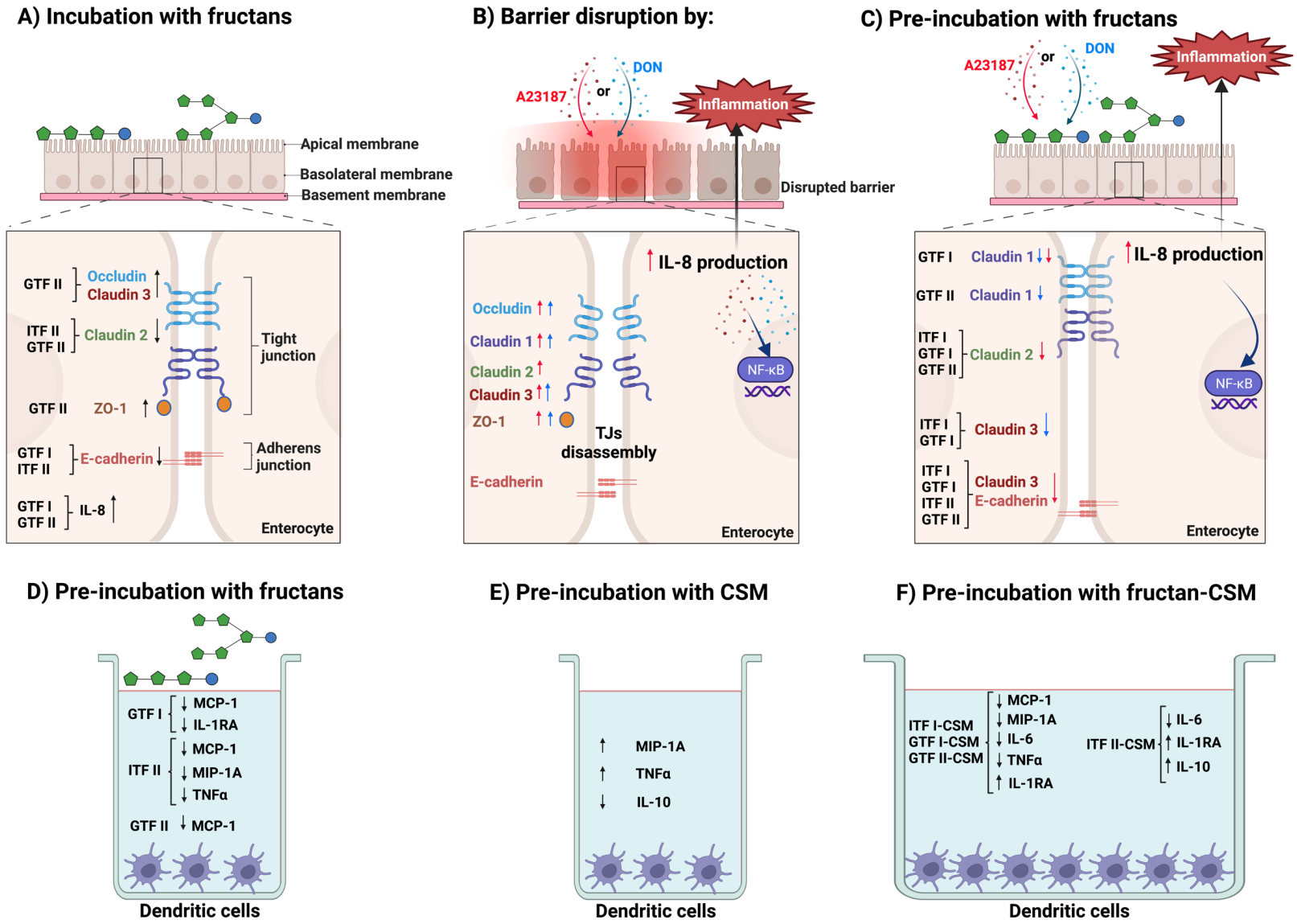
A) Incubation with fructans
Apical membrane
Basolateral membrane
Basement membrane
GTF II
Occludin
Claudin 3
ITF II
GTF II
Claudin 2
Tight junction
GTF II
ZO-1
GTF I
ITF II
E-cadherin
Adherens junction
GTF I
GTF II
IL-8
Enterocyte
B) Barrier disruption by:
A23187
or
DON
Inflammation
Disrupted barrier
IL-8 production
Occludin
Claudin 1
Claudin 2
Claudin 3
ZO-1
TJs disassembly
NF-κB
E-cadherin
Enterocyte
C) Pre-incubation with fructans
A23187
or
DON
Inflammation
IL-8 production
GTF I
Claudin 1
GTF II
Claudin 1
ITF I
GTF I
GTF II
Claudin 2
NF-κB
ITF I
GTF I
Claudin 3
ITF I
GTF I
ITF II
GTF II
Claudin 3
E-cadherin
Enterocyte
D) Pre-incubation with fructans
GTF I
MCP-1
IL-1RA
ITF II
MCP-1
MIP-1A
TNFα
GTF II
MCP-1
Dendritic cells
E) Pre-incubation with CSM
MIP-1A
TNFα
IL-10
Dendritic cells
F) Pre-incubation with fructan-CSM
ITF I-CSM
GTF I-CSM
GTF II-CSM
MCP-1
MIP-1A
IL-6
TNFα
IL-1RA
ITF II-CSM
IL-6
IL-1RA
IL-10
Dendritic cells

Fig. 9. Schematic illustration of the effect of branched graminan-type and linear inulin-type fructans on Caco-2 cells tight junctions gene expression (A-C) and on dendritic cells cytokine production (D-F).

Supplementary material.

Table S1. Nucleotide sequence of primers used for qPCR of tight junction genes in Caco-2 cells (Kiewiet et al., 2018).

TJ protein	Gene	Forward	Reverse
β-actin	*ACTB*	5'-AGAAAATCTGGCACCACACC	5'-TAGCACAGCCTGGATAGCAA
Glyceraldehyde-3-phosphate dehydrogenase	*GAPDH*	5'-ATGGACTGTGGTCATGAGTCCTTC	5'-AAGATCATCAGCAATGCCTCCTGC
Claudin-1	*CLDN-1*	5'-GATGAGGTGCAGAAGATGAG	5'-GGACAGGAACAGCAAAGTAG
Claudin-2	*CLDN-2*	5'-CTGCTCATCCAGAGAAATC	5'-CTGTCAGGCTGTAGGAATTG
Claudin-3	*CLDN-3*	5'-CTGCTCTGCTGCTCGTGTC	5'-CGTAGTCCTTGCGGTCGTAG
E-cadherin	*CDH1*	5'-GGTTATTCCTCCCATCAGCT	5'-CTTGGCTGAGGATGGTGTA
Occludin	*OCLN*	5'-CTATAAATCCACGCCGGTTC	5'-TATTCCTGTAGGCCAGTGTC
Zonula occludens 1 (ZO-1)	*TJP1*	5'-CGGTCCTCTGAGCCTGTAAG	5'-GGATCTACATGCGACGACAA

Table S2. Cycling protocol for qPCR of tight junction genes in Caco-2 cells.

Step	Time and temperature	
Denaturalization	15 sec at 95 ºC	40 cycles
Primer annealing	30 sec at 55 ºC	
Extension	30 sec at 72 ºC	

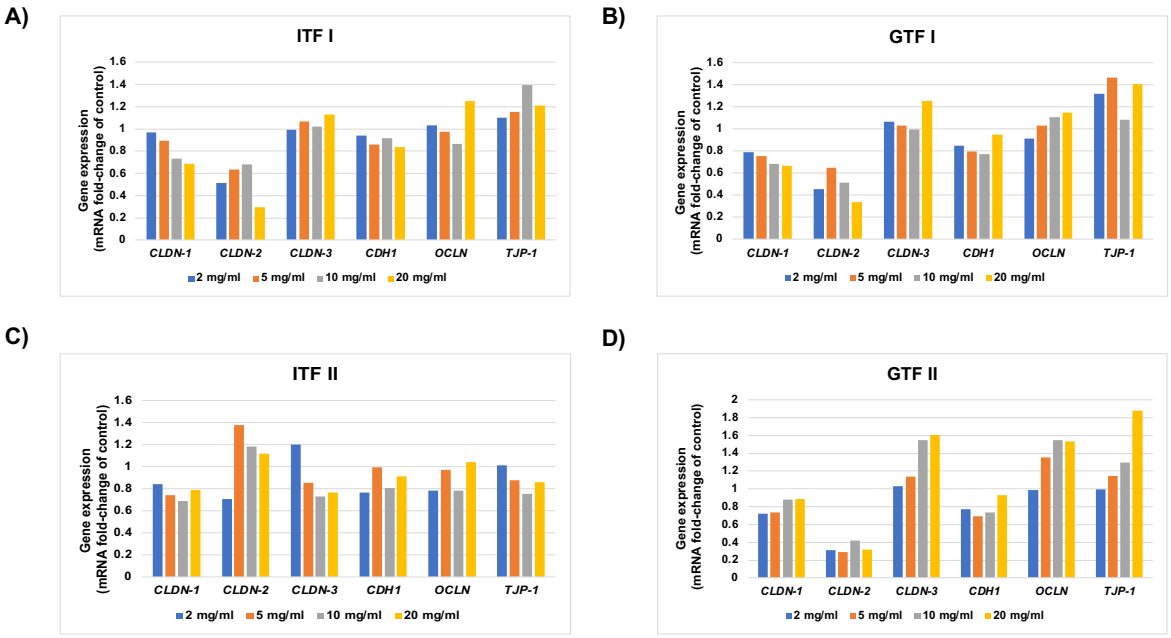

Fig. S1. Dose-effector pilot study for selection of fructans working concentration. Confluent Caco-2 cell cultures were exposed to increasing concentration of ITF I, GTF I, ITF II, and GTF II during 24 hours. Afterwards, mRNA expression of *CLDN-1*, *CLDN-2*, *CLDN-3*, *CDH1*, *OCLN*, and *TJP-1* was measured by qPCR. Expression is presented as fold-change of the untreated control. Results are expressed as the mean of a duplicate.

CAPÍTULO 6

β(2→1)-β(2→6) branched graminan-type fructans and β(2→1) linear fructans impact mucus-related and endoplasmic reticulum stress-related genes in goblet cells and attenuate inflammatory responses in a fructan dependent fashion

Cynthia Fernández-Lainez,[*,a,b,c] Myrthe aan de Stegge,[a] Luis Alfredo Silva-Lagos,[a] Gabriel López-Velázquez,[d] Paul de Vos[a]

[a] Immunoendocrinology, Division of Medical Biology, Department of Pathology and Medical Biology, University of Groningen, University Medical Center Groningen, Groningen, The Netherlands

[b] Laboratorio de Errores innatos del Metabolismo y Tamiz, Instituto Nacional de Pediatría, Ciudad de México, México.

[c] Posgrado en Ciencias Biológicas, Universidad Nacional Autónoma de México, Ciudad de México, México.

[d] Laboratorio de Biomoléculas y Salud Infantil, Instituto Nacional de Pediatría, Ciudad de México, México.

Publicado en Food & Function 2023, DOI: 10.1039/D2FO02710K.

Food & Function

ROYAL SOCIETY OF CHEMISTRY

COMMUNICATION

View Article Online
View Journal | View Issue

Cite this: *Food Funct.*, 2023, **14**, 1338

β(2 → 1)-β(2 → 6) branched graminan-type fructans and β(2 → 1) linear fructans impact mucus-related and endoplasmic reticulum stress-related genes in goblet cells and attenuate inflammatory responses in a fructan dependent fashion†

Received 13th September 2022,
Accepted 13th January 2023

DOI: 10.1039/d2fo02710k

rsc.li/food-function

Cynthia Fernández-Lainez, *[a,b,c] Myrthe aan de Stegge, [a] Luis Alfredo Silva-Lagos, [a] Gabriel López-Velázquez[d] and Paul de Vos [a]

Dietary fibers such as fructans have beneficial effects on intestinal health but it is unknown whether they impact goblet cells (GCs). Here we studied the effects of inulin-type fructans (ITFs) and graminan-type fructans (GTFs) with different molecular weights on mucus- and endoplasmic reticulum (ER) stress-related genes in intestinal GCs. To that end, GCs were incubated in the presence of ITFs or GTFs, or ITFs and GTFs + TNFα or the *N*-glycosylation inhibitor tunicamycin (Tm). IL-8 production by GCs was studied as a marker of inflammation. Effects between ITFs and GTFs were compared. We found a beneficial impact of GTFs especially on the expression of *RETNLB*. GTF II protects from the TNFα-induced gene expression dysregulation of *MUC2*, *TFF3*, *GAL3ST2*, and *CHST5*. Also, all the studied fructans prevented Tm-induced dysregulation of *GAL3ST2*. Interestingly, only the short chain fructans ITF I and GTF I have anti-inflammatory properties on GCs. All the studied fructans except ITF I decreased the expression of the ER stress-related *HSPA5* and *XBP1*. All these benefits were fructan-structure and chain length dependent. Our study contributes to a better understanding of chemical structure-dependent beneficial effects of ITFs and GTFs on gut barrier function, which could contribute to prevention of gut inflammatory disorders.

[a]*Immunoendocrinology, Division of Medical Biology, Department of Pathology and Medical Biology, University Medical Centre Groningen, Hanzeplein 1, 9713 GZ Groningen, The Netherlands. E-mail: c.fernandez.lainez@umcg.nl, myrtheads@gmail.com, l.a.silva.lagos@umcg.nl, p.de.vos@umcg.nl; Fax: +3150-3611911; Tel: +3150-3618043*

[b]*Laboratorio de Errores innatos del Metabolismo y Tamiz, Instituto Nacional de Pediatría, Av. Iman 1, 04530 Ciudad de México, Mexico*

[c]*Posgrado en Ciencias Biológicas, Universidad Nacional Autónoma de México. Edificio D, 1° Piso. Circuito de Posgrados, Ciudad Universitaria, 04510 Ciudad de México, Mexico*

[d]*Laboratorio de Biomoléculas y Salud Infantil, Instituto Nacional de Pediatría, Av. Iman 1, 04530 Cuidad de México, Mexico. E-mail: glv_1999@ciencias.unam.mx*

† Electronic supplementary information (ESI) available. See DOI: https://doi.org/10.1039/d2fo02710k

1. Introduction

The intestinal epithelium is covered by a mucus layer which serves as the first barrier against the harmful content of the lumen.[1] This mucus is formed by a film mainly constituted by mucins.[2] Mucin-2 (encoded by *MUC2*) is the most abundant mucin in the gut. This large multimeric protein undergoes posttranslational modifications such as *O*- and *N*-glycosylation and sulfation, conferring MUC2 a highly viscous gel-like consistency.[3,4] MUC2, along with proteins such as trefoil factor-3 (encoded by *TFF3*),[5] resistin-like molecule β (encoded by *RETNLB*)[6] and other antimicrobial peptides form an organized structure similar to a net and provide a semi-permeable barrier between the intestinal epithelium and the lumen which allows the passage of small molecules while it hampers the translocation of microorganisms.[7]

Interweaved between enterocytes and the other components of the intestinal epithelium are goblet cells (GCs), which are mucus-synthesizing specialized cells.[8] Due to MUC2 dual expression (constitutive and regulated), GCs possess and require a highly active protein trafficking from the endoplasmic reticulum (ER) where its folding occurs, and where glycosylation and sulfation occurs, to its final site of action.[9] In these last posttranslational sulfation modifications galactose-3-*O*-sulfotransferase (encoded by *GAL3ST2*), and carbohydrate sulfotransferase (encoded by *CHST5*) are implicated.[10,11]

In GCs under stress, unfolded protein response (UPR) activation might occur due to inefficient protein folding in the ER.[12] The activation of this group of intracellular signaling pathways can drive GCs to stress responses or toward apoptosis when malfunction is irreversible.[13,14] Genes such as *HSPA5* and *XBP1* participate in this UPR.[15] *HSPA5* codes for the ER chaperone BiP, member 5 of the heat shock protein 70 (Hsp70) family. BiP acts mainly as a sensor of unfolded proteins activating the UPR and the subsequent downstream signaling.[16] The

XBP1 gene codes for the X-box binding protein 1, a transcription factor that belongs to the inositol-requiring enzyme 1α(IRE1α)-signaling axis.[17] Inflammation can also activate ER stress.[18] Intestinal inflammatory disorders such as inflammatory bowel disease (IBD) have been related to ER stress.[19] Under these inflammatory conditions, impairment of GCs function such as aberrant mucin folding has been observed.[20]

Chronic consumption of Western diet, characterized by low intake of dietary fibers, favor the development of intestinal inflammatory disorders,[21–24] whereas, regular consumption of dietary fibers has been associated to a low inflammatory state and to a strengthened barrier function of the mucus layer.[25–27]

An important group of dietary fibers are fructans. Fructans are mainly plant-derived water-soluble oligo and polysaccharides.[28,29] Fructans from chicory plant are broadly used in Europe in the food industry.[30] Chicory fructans are composed of fructofuranose molecules linked by β(2 → 1) bonds with a glucose moiety at the reducing end, which confers them a linear structure.[31] These chicory fructans are known as inulin-type fructans (ITFs).[32] In Latin America, fructans from agave plants are used as fiber supplements in foods.[33,34] These agave fructans are structurally different from ITFs since besides β(2 → 1) fructose chains, they also contain fructose units linked by β(2 → 6) bonds.[35] These β(2 → 1)-β(2 → 6) bonds gives them a branched complex structure.[36,37] This type of fructans are named graminan-type fructans (GTFs).[38]

It is unknown whether ITFs and GTFs have an impact in GCs on mucus-related genes in presence and absence of inflammatory or ER-stress. Therefore, in this study we aimed to determine whether ITFs and GTFs have an influence on the expression of mucus-related and ER stress-related genes in GCs. We also tested if ITFs and GTFs were capable to protect, and attenuate inflammatory responses of GCs exposed to disruptor agents.

2. Materials & methods

2.1 Fructans

To study the effect of fructans of different sizes with a branched or linear structure, on the expression of mucus-related and ER stress-related genes in gut GCs, β(2 → 1)–β(2 → 6) GTFs and β(2 → 1) ITFs were used. GTFs were extracted from *Agave tequilana* Weber blue variety and were provided by Nekutli™, Guadalajara, Mexico. ITFs Frutafit™ CLR and Frutafit™ TEX! were studied as well. Both ITFs were provided by Sensus™ (B.V. Roosendaal, The Netherlands). These fructans have been previously studied by our group.[39–42]

2.2 Cell culture

To study the effects of fructans on the expression of mucus-related and ER stress-related genes in gut GCs, the human colorectal adenocarcinoma-derived LS174T cell line, which exhibits a GC-like phenotype (ATCC® CL188™, Manassas, USA) was used. GCs were maintained in T-75 flasks at 37 °C in humidified air and 5% CO_2 and cultured in Eagle Minimum Essential Medium (EMEM, Lonza, MD, USA) supplemented with 10% heat-inactivated fetal bovine Serum (Sigma-Aldrich, Zwijndrecht, The Netherlands), 2 mM L-glutamine (Lonza, MD, USA) and penicillin/streptomycin 50 U mL^{-1} and 50 μg mL^{-1} (Gibco, Paisley, UK). When reached ~80% confluency and after treatment with 10% trypsin-EDTA (Sigma-Aldrich, Zwijndrecht, The Netherlands), GCs were passaged. GCs were used for experiments between passages 30–40.

2.3 Effect of ITFs and GTFs on the expression of intestinal mucus- and ER stress-related genes

Freshly resuspended GCs were seeded at a cell density of 3×10^5 cells per mL in standard 24-well plates (Corning, NY, USA) and cultured at 37 °C and 5% CO_2 until they reached ~80% confluency (2–3 days) (Fig. 1A). At the experiment day, the medium was replaced with 1 mL medium containing 10 mg mL^{-1} of endotoxin-free GTFs and ITFs, followed by incubation for 72 hours under homeostatic conditions (without any stressor) (Fig. 1B). This incubation time was selected based on previous observations by our group and others that the expression of the studied genes on GCs increased with incubation time up to 72 hours.[43,44] Untreated cells (only medium) were used as untreated controls. At the end of experiments, the morphology of controls as well as the cells under the different treatments were studied at light microscope to exclude possible morphological changes.

2.4 Protective effect of fructans from induced inflammation, mucus barrier disruption and ER stress on GCs

To study whether fructans can protect from induced inflammation, mucus barrier disruption and ER stress, GCs were exposed to 10 ng mL^{-1} of the pro-inflammatory cytokine TNFα

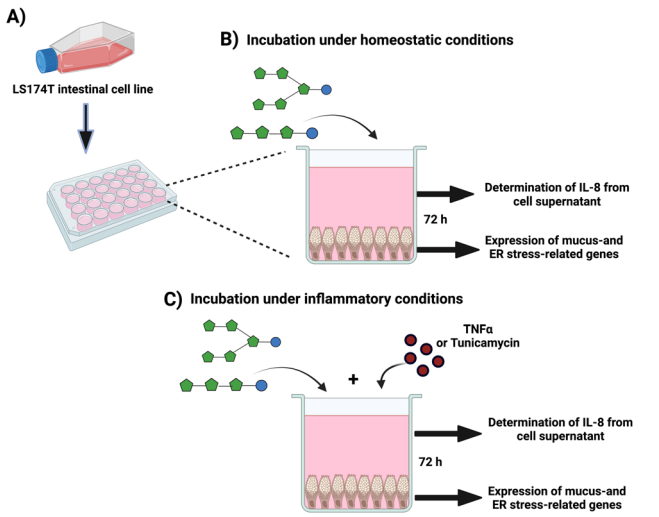

Fig. 1 Experimental design. (A) Confluent goblet cells were seeded in 24-well plates. (B) After a 72-hour incubation of cells in presence of ITFs or GTFs the expression of mucus- and ER stress-related genes was determined by qPCR. The production of IL-8 was quantified from GCs supernatants. (C) GCs were incubated for 72 hours with TNFα or Tm in presence of ITFs or GTFs. Afterwards, expression of mucus- and ER stress-related genes, as well as IL-8 production were determined.

(Immunotools, Friesoythe, Germany), or to 1 μg mL^{-1} of the *N*-glycosylation inhibitor tunicamycin (Tm) (Sigma-Aldrich, Zwijndrecht, The Netherlands) for 72 hours, according to the previously standardized and described by our group.[44,45] These molecules are known to dysregulate the expression of mucus- as well as ER-stress related genes in gut GCs.[46,47] In a second set of experiments, GCs were incubated for 72 hours with TNFα or Tm in presence of 10 mg mL^{-1} of fructans (Fig. 1C). Untreated cells (only culture medium) were used as negative controls. To calculate the fold-change in these experiments, cells treated with disruptor (*i.e.*, Tm or TNF) where used as reference, thus data was normalized using the disruptors as reference conditions. At least five independent experiments were performed. After the experiments, cells were prepared for RNA isolation with trizol reagent.

2.5 RNA extraction, and quantitative reverse-transcription polymerase chain reaction PCR (qPCR)

We studied the relative mRNA expression of the mucus-related genes *MUC2*, *TFF3*, and *RETNLB*. We also studied the *CHST5* and *GAL3ST2* genes which are associated to posttranslational modification of mucin. Finally, on these GCs we studied the expression of the genes *HSPA5* and *XBP1*, which are related to control of protein maturation, ER-stress, and UPR.[48,49] After incubation under the different experimental conditions, RNA was isolated from GCs by the addition of 500 μL of TRIzol™ reagent (Life Technologies, Bleiswijk, The Netherlands) following the manufacturer's instructions. Followed by RNA quantitation, which was performed by spectrophotometry (Thermo Fisher Scientific, USA). The RNA integrity was determined by gel electrophoresis on a 2% agarose gel. Afterwards, 500 ng of total RNA were used for cDNA synthesis, which was performed with SuperScript II™ reverse transcriptase (Life Technologies, Bleiswijk, The Netherlands) according to the manufacturer's instructions. Briefly, after pre-treatment with DNAse I, RNA samples were used for a retro-transcription reaction with 300 ng of random hexamer primers (Life Technologies, Bleiswijk, The Netherlands),10 mmol L^{-1} of DNTPs (Thermo Fisher Scientific, USA), 5× first strand buffer, 0.1 mM of DTT, 40 units per μL of recombinant ribonuclease inhibitor (Thermo Fisher Scientific, USA) and 200 units of SuperScript II™ reverse transcriptase. This was followed by incubation at 25 °C for 10 minutes, 42 °C for 50 minutes and 70 °C for 15 minutes using a TProfessional Basic Thermocycler (Biometra, Göttingen, Germany). The total cDNA obtained was diluted 20x with DEPC-treated water (Life Technologies, Bleiswijk, The Netherlands) and 5 μL of this dilution were mixed with 5 μL of FastStart Universal SYBR Green Master (ROX) qPCR Master Mix 2× concentrated (Roche Diagnostics, Basel, Switzerland) including gene specific primers at a final concentration of 300 nmol L^{-1} (Table S1†).[44,45,50] The qPCRs were performed in a Viia 7 Real-Time PCR System (Applied Biosystems, CA, USA). The cycling protocol used is shown in Table S2.† The primer annealing temperature and efficiency were determined with a 5-point standard curve, which was prepared with a pool of all cDNA samples diluted 5–80×. A reaction efficiency of 90–110% was considered acceptable. B2M (beta-2-microglobulin) was used as housekeeping gene.[43,46] mRNA fold-change was calculated against untreated controls or against cells treated only with disruptors using the $2^{-\Delta\Delta Ct}$ method.[51]

2.6 Measurement of GCs IL-8 production

Interleukin-8 (IL-8) from cell supernatants was considered as a marker of inflammation of GCs challenged with the disruptor molecules TNFα and Tm. After the incubation of GCs under the above-mentioned conditions, cells supernatants were collected and centrifuged for removing death cells and cell debris. The IL-8 was quantitated by ELISA from GCs supernatants according to manufacturer's instructions (R&D Systems, Biotechne, Minneapolis, USA). Controls were those GCs without any treatment.

2.7 Statistical analyses

GraphPad Prism version 9.2 was used for statistical analyses. Normal distribution of data was examined by the Shapiro–Wilk test. These data were normally distributed. Therefore, data are expressed as mean ± standard deviation (SD) from least five independent assays. Untreated control and those cells incubated with fructans were compared. Untreated control and cells treated with TNFα or Tm were also compared. Finally, cells treated with TNFα alone and those treated with TNFα in presence of fructans were compared. In all experiments statistical significance was determined using ordinary one-way ANOVA with Dunnett's multiple comparison test. A p-value < 0.05 was considered significant. * or † ($p < 0.05$), ** or †† ($p < 0.01$), *** or ††† ($p < 0.001$), **** or †††† ($p < 0.0001$).

3. Results

3.1 Chemical characteristics of studied fructans

To investigate the effect of fructans with different structure and size on the expression of mucus-related and USP-related GCs genes, GTFs and ITFs were included. The presence of β(2 → 1) and β(2 → 6) linkages in GTFs confers them a complex branched structure.[37] GTF I is a mixture with mostly short chain fructans with a degree of polymerization (DP) between 3–4 but it also has fructans of DP 7–45. GTF II contains a mixture of longer chain fructans with an average DP of 17, but it also has longer chain fructans. These GTFs possess oligosaccharides of fructose (F_n) and glucose-fructose (GF_n) series.[41] ITFs are constituted only of fructans linked by β(2 → 1) bonds, this gives them a linear structure. ITF I is a short chain fructan mixture with a DP range of 3–10. It has fructans of the F_n and GF_n series. ITF II possess a mixture composed of longer chain fructans with a DP range of 10–60 and it only has fructans of the GF_n series (Table 1).[39]

3.2 Graminan-type fructans enhance mucus-related genes in GCs

To study the effects of ITFs and GTFs on the expression of mucus-related genes, GCs were incubated in presence of these

Table 1 Chemical and structural characteristics of fructans included in the study[39,41]

	Branched graminan-type fructan	Linear inulin-type fructan	DP range
ITF I	Absent	Present	3–10
ITF II	Absent	Present	10–60
GTF I	Present	Present	3–45
GTF II	Present	Present	3–60

● = glucose, ⬟ = fructose, *n* = number of fructose units. The schemes of fructans were made following the standardized symbol nomenclature for glycans (National Institute of Biotechnology, **https://www.ncbi.nlm.nih.gov/glycans/snfg.html**, consulted on December 16th, 2021).

fructans for 72 hours. This provoked a differential gene expression in a fructan structure dependent manner (Fig. 2). The expression of *MUC2* was 0.38 ± 0.3-fold decreased (p > 0.01) and 0.48 ± 0.1-fold decreased (p > 0.001) by ITF I and ITF II, while none of the GTFs influenced *MUC2* expression (Fig. 2A). This was different for *TFF3*, where an enhancement of 0.52 ± 0.3-fold (p < 0.05) and 0.52 ± 0.4-fold (p < 0.05) was observed in GCs treated with ITF I and GTF II, respectively (Fig. 2B). The *RETNLB* expression was strikingly enhanced only by the branched fructans. GTF I enhanced it 6.3 ± 2-fold (p < 0.01) and GTF II enhanced it 9.37 ± 1-fold (p < 0.0001) (Fig. 2C). The *CHST5* expression was only enhanced 0.25 ± 0.4-fold (p < 0.05) by GTF II (Fig. 2E). Conversely, the expression of *HSPA5* and *XBP1* were significantly reduced by all fructans except by ITF I (Fig. 2F and G).

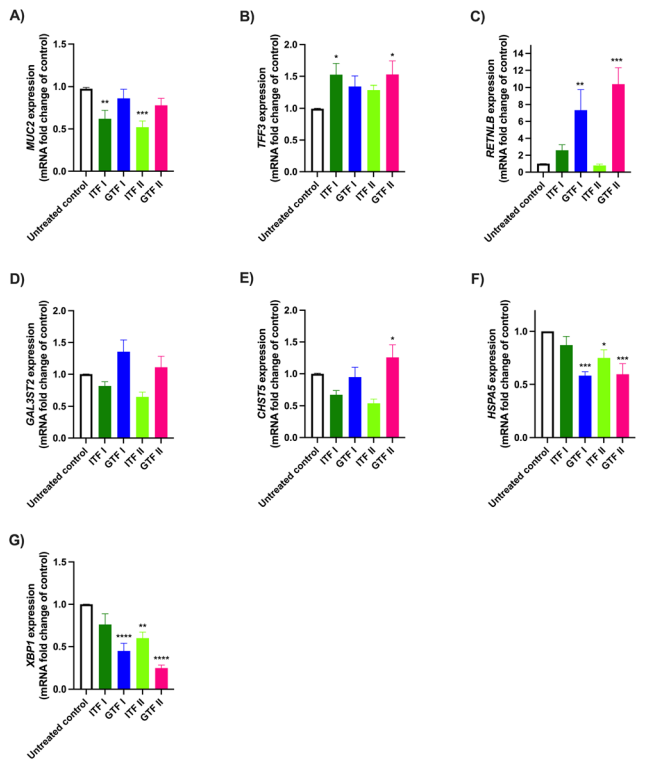

Fig. 2 Effect of ITFs and GTFs with different molecular weight on the expression of mucus- and ER stress-related genes in goblet intestinal cells. GCs were incubated for 72 hours with 10 mg mL^{-1} of ITFs and GTFs, followed by the determination of mRNA production of *MUC2* (A), *TFF3* (B), *RETNLB* (C), *GAL3ST2* (D), *CHST5* (E), *HSPA5* (F), and *XBP1* (G) by qPCR. At least five independent experiments were performed. These data were normally distributed. Therefore, data are expressed as mean ± SD. Statistical differences between untreated control and cells incubated with fructans were calculated by ordinary one-way ANOVA with Dunnett's multiple comparison test. * (p < 0.05), ** (p < 0.01), *** (p < 0.001), **** (p < 0.0001).

3.3 Long chain GTF prevents TNFα-induced dysregulation of mucus-related genes in GCs

We investigated the potential protective effect of ITFs and GTFs on mucus- and ER stress-related genes in GCs exposed to TNFα. It is known that TNFα alters the expression of secretory proteins in GCs.[46] To study the prevention of this impairment, GCs were incubated with TNFα in presence of the studied fructans for 72 hours. Compared with the untreated control *MUC2* expression was 1.7 ± 0.7-fold decreased by TNFα (p < 0.01) (Fig. 3A). In cells incubated with TNFα in presence of GTF II this increase was 0.3 ± 1.5-fold attenuated compared with cells challenged with TNFα (p < 0.05). The remaining fructans did not significantly prevent the reduction of *MUC2* expression.

Compared with the untreated control, TNFα significantly decreased the expression of *TFF3* 1.5 ± 0.9-fold (p < 0.01) (Fig. 3B). This decrease was 0.3 ± 0.9-fold lower and thus partly prevented by GTF II (p < 0.05). The other studied fructans did not prevent the reduction of *TFF3* expression.

The *RETNLB* expression was 4.6 ± 0.7-fold decreased in cells treated with TNFα compared with the untreated control (p < 0.001). All the studied fructans except ITF II prevented this decrease and they even enhanced *RETNLB* expression. Cells incubated with TNFα in presence of GTF II had a better prevention of TNFα-induced decrease of *RETNLB* expression as it was 13.2 ± 3-fold higher compared with cells challenged with TNFα (p < 0.0001) (Fig. 3C).

TNFα decreased the expression of *GAL3ST2* and *CHST5* 0.4 ± 0.1-fold (p < 0.01) and 2.8 ± 0.9-fold (p < 0.001) respectively (Fig. 3D and E). These genes are related to mucin posttranslational modifications. The only fructan that significantly prevented this decrease was GTF II. Neither GTF I nor ITFs prevented the decreased production of *GAL3ST2* and *CHST5* mRNA.

The expression of the ER stress-related genes *HSPA5* and XBP1 was significantly decreased in cells treated with TNFα 1.4 ± 0.5-fold (p < 0.0001) and 1.8 ± 0.4-fold compared with the untreated control (p < 0.0001) (Fig. 3F and G). None of the studied fructans prevented this induced decrease.

3.4 ITFs and GTFs do not prevent Tm-induced changes in mucus-related genes in GCs

The preventive effect of fructans from the deleterious action of the *N*-glycosylation inhibitor Tm was studied. To that end, GCs

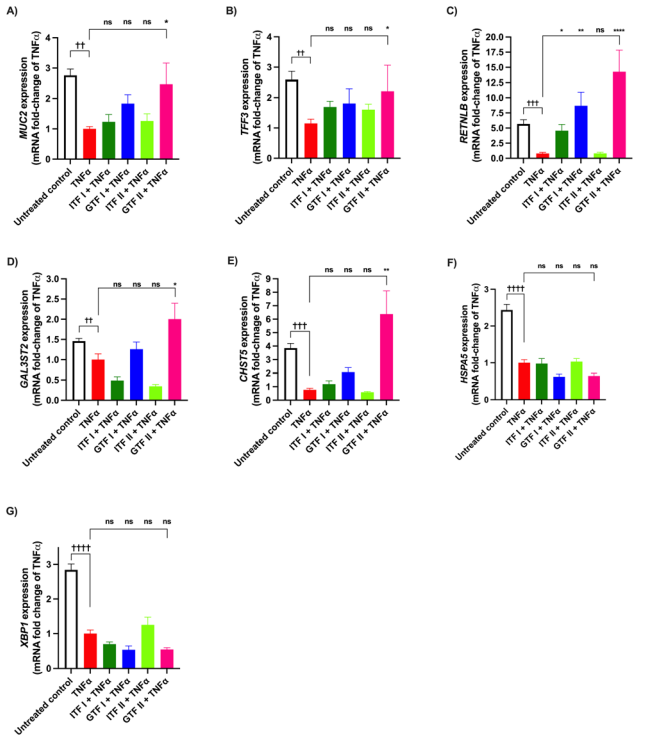

Fig. 3 Prevention by ITFs and GTFs of TNFα-induced mucus- and ER stress-related gene dysregulation in goblet cells. GCs were incubated for 72 hours with TNFα in presence of 10 mg mL^{-1} of ITFs or GTFs. Expression of *MUC2* (A), *TFF3* (B), *RETNLB* (C), *GAL3ST2* (D), *CHST5* (E), *HSPA5* (F), and *XBP1* (G) was determined by qPCR. At least five independent experiments were performed. These data were normally distributed. Therefore, data are expressed as mean ± SD. Statistical differences between untreated control and cells treated with TNFα were calculated by ordinary one-way ANOVA with Dunnett's multiple comparison test. Cells treated with TNFα alone and those treated with TNFα in presence of fructans were compared and statistical differences were calculated by ordinary one-way ANOVA with Dunnett's multiple comparison test. * or † ($p < 0.05$), ** or †† ($p < 0.01$), *** or ††† ($p < 0.001$), **** or †††† ($p < 0.0001$).

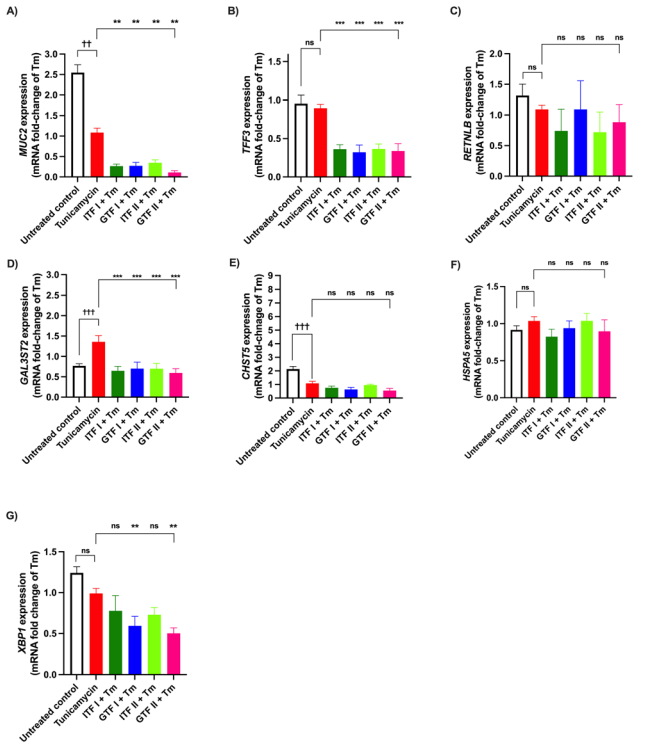

Fig. 4 Prevention by ITFs and GTFs of Tm-induced mucus- and ER stress-related gene dysregulation in goblet cells. GCs were incubated for 72 hours with Tm in presence of 10 mg mL^{-1} of ITFs or GTFs. Expression of *MUC2* (A), *TFF3* (B), *RETNLB* (C), *GAL3ST2* (D), *CHST5* (E), *HSPA5* (F), and *XBP1* (G) was determined by qPCR. At least five independent experiments were performed. These data were normally distributed. Therefore, data are expressed as mean ± SD. Statistical differences between untreated control and cells treated with Tm were calculated by ordinary one-way ANOVA with Dunnett's multiple comparison test. Cells treated with Tm alone and those treated with Tm in presence of fructans were compared. Statistical differences were calculated by ordinary one-way ANOVA with Dunnett's multiple comparison test. * or † ($p < 0.05$), ** or †† ($p < 0.01$), *** or ††† ($p < 0.001$), **** or †††† ($p < 0.0001$) (Tm = Tunicamycin).

were incubated with Tm for 72 hours in presence of fructans (Fig. 4). The *MUC2* expression was 1.5 ± 0.6-fold decreased compared with the untreated control ($p < 0.01$) (Fig. 4A). None of the studied fructans prevented this decrease.

Compared with the untreated control the expression of *TFF3* and *RETNLB* was not influenced by the Tm challenge (Fig. 4B and C).

Tm treatment provoked a 0.6 ± 0.1-fold increase of the *GAL3ST2* expression, compared with the untreated control ($p < 0.001$) (Fig. 4D). All of the studied fructans provoked a *GAL3ST2* expression more likely to that of the untreated control.

Compared with the untreated control a 1.0 ± 0.5-fold decrease of the *CHST5* expression was observed in cells treated with Tm ($p < 0.001$) (Fig. 4E). None of the studied fructans influenced this decrease.

The mRNA production of *HSPA5* remained without significant changes after the Tm challenge. The same occurred when incubating GCs with Tm in presence of fructans (Fig. 4F).

Compared with the untreated control the *XBP1* expression was not influenced by the Tm challenge alone or in presence of fructans (Fig. 4G).

3.5 GTF I prevent TNFα-induced IL-8 increase in GCs

Next, the effect of fructans on the IL-8 production by GCs was investigated. To that end, GCs were incubated with fructans for 72 hours. Fig. 5A shows that ITF I as well as GTF I significantly decreased the IL-8 production by GCs compared with the untreated control, from 1322 ± 107 pg mL^{-1} to 885 ± 176 pg mL^{-1} ($p < 0.05$) for those cells treated with ITF I and to 888 ± 278 pg mL^{-1} for GTF I treated cells ($p < 0.05$).

Next the protective effect of fructans on IL-8 production by GCs exposed to TNFα or Tm was studied. To this end, GCs were incubated for 72 hours with TNFα or Tm in presence of 10 mg mL^{-1} of fructans. The IL-8 production was quantified from the GCs supernatant. The presence of TNFα alone increased IL-8 production from 1322 ± 107 pg mL^{-1} in the

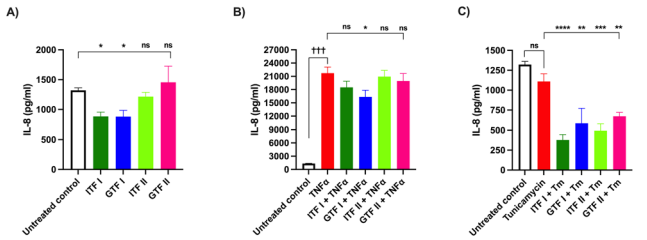

Fig. 5 Production of IL-8 by goblet cells. (A) Cells were incubated with either ITF I, ITF II, GTF I or GTF II for 72 hours, followed by quantification of IL-8 production from cell supernatants. At least five independent experiments were performed. These data were normally distributed. Therefore, data are expressed as mean ± SD. Statistical differences between untreated control and cells incubated with fructans were calculated by ordinary one-way ANOVA with Dunnett's multiple comparison test. (B and C) In a second set of experiments, GCs were incubated for 72 hours with TNFα or tunicamycin alone or with TNFα or tunicamycin in presence of 10 mg mL^{-1} of ITFs or GTFs. At least five independent experiments were performed. These data were normally distributed. Therefore, data are expressed as mean ± SD. Statistical differences between cells treated only with disruptors and cells incubated with TNFα or tunicamycin in presence of 10 mg mL^{-1} of ITFs or GTFs were calculated by ordinary one-way ANOVA with Dunnett's multiple comparison test. * or † ($p < 0.05$), ** or †† ($p < 0.01$), *** or ††† ($p < 0.001$), **** or †††† ($p < 0.0001$) (Tm = tunicamycin).

untreated control to 21 716 ± 3100 pg mL^{-1} ($p < 0.001$) (Fig. 5B). This increased IL-8 production was decreased to 16 336 ± 3383 pg mL^{-1} ($p < 0.05$) by GTF I. The other studied fructans did not influence the over IL-8 production of GCs under TNFα challenge.

The challenge of GCs with Tm did not influence the IL-8 concentration (Fig. 5C). However, incubation of cells with Tm in presence of fructans caused a significant decrease in IL-8 production to values even lower than those of the untreated control. The production of IL-8 decreased from 1109 ± 192 pg mL^{-1} in cells treated with Tm to 378 ± 135 ($p < 0.0001$), 588 ± 316 ($p < 0.01$), 499 ± 174 ($p < 0.001$) and 671 ± 97 ($p < 0.01$) in cells pre-incubated with ITF I, GTF I, ITF II and GTF II, respectively.

4. Discussion

In the present study we present, to the best of our knowledge, for the first time the *in vitro* effect of ITFs and GTFs on the expression of mucus- and ER stress-related genes under homeostatic and inflammatory conditions and their regulatory capacities in gut GCs. We found a remarkable beneficial impact of GTFs especially on the expression of *RETNLB*. It was unknown whether and to what extend these fructans could protect from the action of TNFα and Tm. Here we demonstrate that the branched long chain GTF II can protect from the gene expression dysregulation induced by TNFα. We also show that all the studied fructans prevent the Tm-induced dysregulation of *GAL3ST2*. Interestingly, only the short chain fructans have anti-inflammatory properties on GCs under homeostatic conditions. All these benefits found are fructan-structure and chain length dependent.

When tested under homeostatic conditions, ITF I and GTF II significantly increased the *TFF3* expression. TFF3 belongs to the trefoil family of secretory peptides whose main function is mucosal protection and repairment of damaged epithelium.[52] This integral and constituent mucus protein has shown to possess therapeutic potential, since its interaction with protease activator receptors (PAR) cause downregulation of proinflammatory cytokines such as IL-6 and IL-8 and upregulation of defensin expression in intestinal epithelial cells.[53] Moreover, when GCs were challenged with TNFα, the expression of *TFF3* significantly decreased. This effect, which is in line with others,[54] was prevented by GTF II. Therefore, the prevention of *TFF3* downregulation by GTF II could have an application under inflammatory conditions, such as IBD or gastrointestinal infections. Additionally, due to its protective and reparative functions, TFF3 has been proposed as a therapeutic agent for intestinal inflammatory disorders such as colitis and IBD.[54,55] Furthermore, the anti-inflammatory capacity of TFF3 goes beyond the gut since it has been found in microglia.[56]

Interestingly, the expression of *RETNLB* was the most up regulated among the studied genes, and this was observed only with the branched fructans GTF I and GTF II under homeostatic conditions. When GCs were stimulated with TNFα *RETNLB* expression downregulation was observed. This was prevented by all fructans, except ITF II. *RETNLB* codes for RELMβ protein which belongs to the wide repertory of intestinal antimicrobial peptides.[57] The intestinal secretion of this cysteine-rich 12.5 kDa protein increases in animal models during helminth infection[58,59] and other enteric pathogens[60] to promote their expulsion.[59] It is also known that RELMβ can inhibit parasite chemotaxis and interferes with their nutrition by directly binding to their chemosensory constituents.[61,62] Therefore, the increased *RETNLB* expression caused by GTFs could be considered as a defensive factor to aid during intestinal infections.

Under homeostatic conditions the *CHST5* expression was increased only by GTF II. This is one of the proteins that participate in the decoration of the mucin protein core by *O*-glycosylations.[63] The increased expression of *CHST5* has been previously associated with enhancement of the mucosal barrier function in LS174T cells.[10] Also, this may imply that cells with higher expression of *CHST5* may be able to deal better with ER stress, since an increase in this enzyme may help to relieve the proteins that, due to poor folding or altered posttranslational modifications, got stuck in the ER. This might explain too why cells challenged with Tm in presence of GTF II have lower markers of ER stress. Thus, GTF II could represent a potential molecule for strengthening mucus barrier function.

The expression of the ER stress-related gene HSPA5 was decreased only by GTFs under homeostatic conditions. During homeostasis the protein product of *HSPA5* BiP acts as a repressor of the UPR signal transducers inositol-requiring protein-1

(IRE1) and protein kinase RNA (PKR)-like ER kinase (PERK) by forming a complex. Upon ER stress BiP dissociates from the complex, provoking activation of the UPR with subsequent downstream signaling to restore ER homeostasis.[49,64] Since the activation of the UPR signal depends on the repressor action of BiP, then BiP overexpression keeps UPR repressed, whereas reduced BiP levels activate the UPR.[64] Thus, the decreased expression of *HSPA5* that we observed would be indicating a more efficient capacity of counteraction of ER stress. However, herein we are presenting preliminary data about the influence of GTFs on UPR at mRNA level, and additional assessments of BiP protein might further support a complete insight into the role of GTFs in this pathway.

Under homeostatic conditions the expression of the ER stress-related gene *XBP1* was decreased by all fructans, except ITF I. The downregulation of these ER-stress- and UPR-related gene has been previously reported by Engevik *et al.*, as an ER-stress modulatory beneficial effect, which was observed when incubating T84 human colonic cells with a probiotic organism.[65]

The same was observed by Xiong *et al.* when incubating GCs with a flavonoid molecule.[66] It is known that UPR activation is associated with inflammation[18] and to failure in immunotolerance with the concomitant development of autoimmune disorders such as IBD and rheumatoid arthritis.[67–69] Moreover, genetic sequencing of IBD patients revealed several *XBP1* variants as factors of susceptibility for IBD development.[19] Thus, the use of these fructans for the prevention of UPR activation could be valuable for the design of therapeutics against these disorders.

Incubation of GCs with Tm and TNFα-induced downregulation of the *XBP1* mRNA. Upon ER stress, *XBP1* mRNA suffers unconventional splicing to obtain an active *XBP1* spliced form.[17] Previous studies from Xue *et al.*, who studied the expression of *XBP1* on the murine fibrosarcoma L929 cell line, demonstrated that under homeostatic conditions there is a basal expression of both the unspliced and spliced forms of *XBP1*. When cells are exposed to ER stress by the action of the Tm, then the proportion of the spliced form increases until practically a complete predominance of this spliced form. This leads to the disappearance of the unspliced *XBP1* form.[70]

These findings of Xue, *et al.*, let us hypothesize that in our study we indirectly found that the *XBP1* spliced form increases as the observed unspliced form decreases. In other words, under homeostatic conditions we could expect the *XBP1* spliced form in the same proportion as the unspliced form (untreated control), and in those cells challenged with Tm we would expect the double proportion of the *XBP1* spliced form than the observed unspliced form. Finding the spliced form in major proportion would indicate a more efficient counteraction of ER stress. As to the cells challenged with TNFα, again based on Xue, *et al.* findings, the predominance of the unspliced and spliced forms of *XBP1* change practically in the same manner as the challenge with Tm. Therefore, our findings indicate a more efficient manner to counteract the ER stress induced by TNFα.

It is known that TNFα can induce the UPR in a reactive oxygen species (ROS)-dependent fashion.[70] In the present study the measurement of ROS was not determined, however, since it is known that fructans from chicory and from agave possess ROS scavenging capacities,[71–73] assessment of ROS after exposure to fructans, in presence or absence of TNFα, along with other inflammatory stressors deserves further studies.

Incubation of GCs in presence of Tm significantly downregulated the expression of *MUC2* and *CHST5 and* increased the expression of *GAL3ST2*. This is in line with our previous studies.[44,45] Tm is a well-known glycosylation inhibitor which induces ER stress.[47] None of the fructans protected GCs from the downregulating effect of Tm. This could be indicative of the null capacity of these fructans to protect from the deregulatory effects of Tm under the studied experimental conditions.

The production of IL-8 was considered to be an indicator of inflammation in GCs. When GCs were incubated in presence of fructans, the short chain ITF I and GTF I significantly decreased this IL-8 production. Thus, these fructans could be protecting GCs from inflammation. We have previously observed this protective effect in gut epithelial cells.[42] The challenge with TNFα alone caused a 16-fold increase of IL-8 production, while this TNFα challenge in presence of GTF I significantly decreased this elevation. IL-8 is a chemoattractant molecule for immune cells such as neutrophiles, whose excessive production is related to inflammatory disorders.[66] This, allow us to suggest that GTF I possess a potential anti-inflammatory effect, that could contribute to lowering symptoms of intestinal inflammatory disorders.

A possible explanation of all these findings (Fig. 6) could be related to the establishment of an interaction between the fructans applied and GCs just as observed in our previous studies,[41,42] which may lead to lowering permeability of the mucus layer, due to the saccharide nature of fructans, which resembles the glycans that are added to mucins.

However, a deeper study of the mechanisms by which the studied fructans influence GCs biology is guaranteed. In line with this is the fact that LS174T cells compared to normal GCs synthesize glycans that are truncated compared to normal MUC2 glycosylation.[74] This might make these cells prone to enteropathogenic infection, as has been reported in these cells.[75] Thus, we speculate that the studied fructans could have a beneficial influence on the barrier function of mucins with truncated glycosylation by replacing the lack of glycans.

Besides the direct protecting and regulatory effects of the studied fructans on GCs presented herein, it is important to acknowledge that there may also be substantial effects that are mediated by the intestinal microbiota and the metabolites they produce from fructans fermentation. This well-known prebiotic effect[76–78] remains to be elucidated on GCs.

One limitation of the present study is the absence of complementary assessment of the proteins coded by the studied genes. However, since the influence of fructans derived from agave on intestinal goblet cells has never been studied, we consider our preliminary data on mRNA data is still of value,

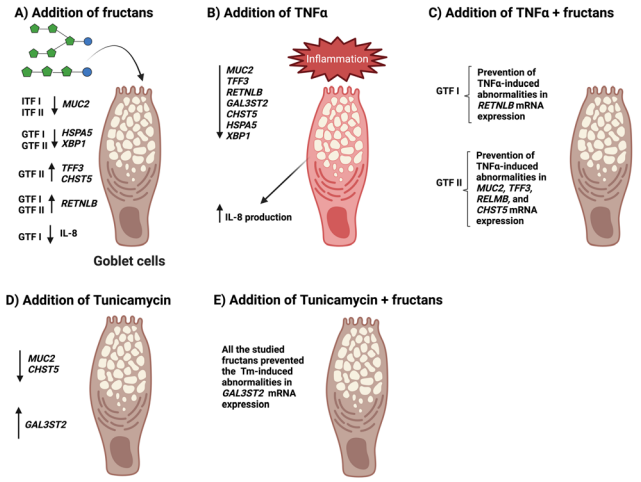

Fig. 6 Schematic summary of the observed effects of ITFs and GTFs and of fructans + disruptors on mucus- and ER stress-related GCs genes.

although further additional assessments of the protein products of the studied genes might provide a wider understanding of the potential beneficial effects of these dietary fibers on cellular homeostasis in GCs. Another limitation is the lack of assessment of the expression of other mucin coding genes than MUC2, such as MUC5AC, MUC6 and MUC1, MUC4 and MUC13, since LS174T cells do produce these mucins which also represent challenges for the ER secretory pathway.[20,79]

5. Conclusions

Findings of the present study contribute to enhanced knowledge on beneficial effects that dietary fibers such as ITFs and GTFs can exert on the preservation of GC-homeostasis. It is shown that the beneficial effects are dependent on the structure and chain length of the fructan applied. This, knowledge combined with finding from our previous studies[39–42] allow us to propose specific fructan molecules as potential candidates for the design of therapies for the reestablishment of health in gut inflammatory disorders.

Author contributions

C.F.L. and P.D.V. designed the study. C.F.L. and M.A.D.S. performed the experiments. L.A.S.L. conceptualization and assisted in the qPCR data analysis. G.L.V. revised and edited the manuscript. P.D.V. Supervised and Administered the project. C.F.L. and P.D.V. wrote the manuscript. All authors have revised and improved the manuscript.

Conflicts of interest

There are no conflicts to declare.

Acknowledgements

This study was partially financed by the "Programa de Recursos Fiscales para Investigación" from Instituto Nacional de Pediatría, Grant Number 2019/062. C. F. L. was financially supported by Abel Tasman Talent Program Sandwich PhD from the University of Groningen-University Medical Center Groningen, UG/UMCG in collaboration with Universidad Nacional Autónoma de México, UNAM and CONACyT (#260625).

References

1 M. E. Johansson and G. C. Hansson, Immunological aspects of intestinal mucus and mucins, *Nat. Rev. Immunol.*, 2016, **16**, 639–649.
2 E. E. Nyström, B. Martinez-Abad, L. Arike, G. M. Birchenough, E. B. Nonnecke, P. A. Castillo, F. Svensson, C. L. Bevins, G. C. Hansson and M. E. Johansson, An intercrypt subpopulation of goblet cells is essential for colonic mucus barrier function, *Science*, 2021, **372**(6539), 1–29.
3 T. Pelaseyed, J. H. Bergström, J. K. Gustafsson, A. Ermund, G. M. Birchenough, A. Schütte, S. van der Post, F. Svensson, A. M. Rodríguez-Piñeiro and E. E. Nyström, The mucus and mucins of the goblet cells and enterocytes provide the first defense line of the gastrointestinal tract and interact with the immune system, *Immunol. Rev.*, 2014, **260**, 8–20.
4 Y. Tobisawa, Y. Imai, M. Fukuda and H. Kawashima, Sulfation of colonic mucins by N-acetylglucosamine 6-O-sulfotransferase-2 and its protective function in experimental colitis in mice, *J. Biol. Chem.*, 2010, **285**, 6750–6760.
5 L. Thim and F. May, Trefoil factors, *Cell. Mol. Life Sci.*, 2005, **62**, 2956–2973.
6 D. Artis, M. L. Wang, S. A. Keilbaugh, W. He, M. Brenes, G. P. Swain, P. A. Knight, D. D. Donaldson, M. A. Lazar and H. R. Miller, RELMβ/FIZZ2 is a goblet cell-specific immune-effector molecule in the gastrointestinal tract, *Proc. Natl. Acad. Sci. U. S. A.*, 2004, **101**, 13596–13600.
7 J. J. Kim and W. I. Khan, Goblet cells and mucins: role in innate defense in enteric infections, *Pathogens*, 2013, **2**, 55–70.
8 K. A. Knoop and R. D. Newberry, Goblet cells: multifaceted players in immunity at mucosal surfaces, *Mucosal Immunol.*, 2018, **11**, 1551–1557.
9 S. Cornick, A. Tawiah and K. Chadee, Roles and regulation of the mucus barrier in the gut, *Tissue Barriers*, 2015, **3**(1–2), e982426.
10 N. P. Ponnuraj, S. Bhatia, J. Chow, S. Davis, M. J. Miller and H. R. Gaskins, Direct modulation of goblet cell function by galacto-oligosaccharides, *FASEB J.*, 2013, **27**, lb388–lb388.
11 K. Honke, M. Tsuda, S. Koyota, Y. Wada, N. Iida-Tanaka, I. Ishizuka, J. Nakayama and N. Taniguchi, Molecular cloning and characterization of a human β-Gal-3′-sulfotransferase that acts on both type 1 and type 2 (Galβ1–3/

1–4GlcNAc-R) oligosaccharides, *J. Biol. Chem.*, 2001, **276**, 267–274.
12 M. H. Smith, H. L. Ploegh and J. S. Weissman, Road to ruin: targeting proteins for degradation in the endoplasmic reticulum, *Science*, 2011, **334**, 1086–1090.
13 S. E. Bettigole and L. H. Glimcher, Endoplasmic reticulum stress in immunity, *Annu. Rev. Immunol.*, 2015, **33**, 107–138.
14 L. Zhou, H. Shen, X. Li and H. Wang, Endoplasmic Reticulum Stress in Innate Immune Cells-A Significant Contribution to Non-Alcoholic Fatty Liver Disease, *Front. Immunol.*, 2022, 3902.
15 J. Grootjans, A. Kaser, R. J. Kaufman and R. S. Blumberg, The unfolded protein response in immunity and inflammation, *Nat. Rev. Immunol.*, 2016, **16**, 469–484.
16 M. C. Kopp, N. Larburu, V. Durairaj, C. J. Adams and M. M. Ali, UPR proteins IRE1 and PERK switch BiP from chaperone to ER stress sensor, *Nat. Struct. Mol. Biol.*, 2019, **26**, 1053–1062.
17 H. Yoshida, T. Matsui, A. Yamamoto, T. Okada and K. Mori, XBP1 mRNA is induced by ATF6 and spliced by IRE1 in response to ER stress to produce a highly active transcription factor, *Cell*, 2001, **107**, 881–891.
18 A. Shkoda, P. A. Ruiz, H. Daniel, S. C. Kim, G. Rogler, R. B. Sartor and D. Haller, Interleukin-10 blocked endoplasmic reticulum stress in intestinal epithelial cells: impact on chronic inflammation, *Gastroenterology*, 2007, **132**, 190–207.
19 A. Kaser, A.-H. Lee, A. Franke, J. N. Glickman, S. Zeissig, H. Tilg, E. E. Nieuwenhuis, D. E. Higgins, S. Schreiber and L. H. Glimcher, XBP1 links ER stress to intestinal inflammation and confers genetic risk for human inflammatory bowel disease, *Cell*, 2008, **134**, 743–756.
20 C. K. Heazlewood, M. C. Cook, R. Eri, G. R. Price, S. B. Tauro, D. Taupin, D. J. Thornton, C. W. Png, T. L. Crockford and R. J. Cornall, Aberrant mucin assembly in mice causes endoplasmic reticulum stress and spontaneous inflammation resembling ulcerative colitis, *PLoS Med.*, 2008, **5**, e54.
21 M. Martinez-Medina, J. Denizot, N. Dreux, F. Robin, E. Billard, R. Bonnet, A. Darfeuille-Michaud and N. Barnich, Western diet induces dysbiosis with increased E coli in CEABAC10 mice, alters host barrier function favouring AIEC colonisation, *Gut*, 2014, **63**, 116–124.
22 I. A. Myles, Fast food fever: reviewing the impacts of the Western diet on immunity, *Nutr. J.*, 2014, **13**, 1–17.
23 A. Agus, J. Denizot, J. Thévenot, M. Martinez-Medina, S. Massier, P. Sauvanet, A. Bernalier-Donadille, S. Denis, P. Hofman and R. Bonnet, Western diet induces a shift in microbiota composition enhancing susceptibility to Adherent-Invasive E. coli infection and intestinal inflammation, *Sci. Rep.*, 2016, **6**, 1–14.
24 V. Peters, G. Dijkstra and M. J. Campmans-Kuijpers, Are all dietary fibers equal for patients with inflammatory bowel disease? A systematic review of randomized controlled trials, *Nutr. Rev.*, 2022, **80**, 1179–1193.
25 N. Veronese, M. Solmi, M. G. Caruso, G. Giannelli, A. R. Osella, E. Evangelou, S. Maggi, L. Fontana, B. Stubbs and I. Tzoulaki, Dietary fiber and health outcomes: an umbrella review of systematic reviews and meta-analyses, *Am. J. Clin. Nutr.*, 2018, **107**, 436–444.
26 E. Salinas, D. Reyes-Pavón, N. G. Cortes-Perez, E. Torres-Maravilla, O. K. Bitzer-Quintero, P. Langella and L. G. Bermúdez-Humarán, Bioactive Compounds in Food as a Current Therapeutic Approach to Maintain a Healthy Intestinal Epithelium, *Microorganisms*, 2021, **9**, 1634.
27 W. Yang, P. Zhao, X. Li, L. Guo and W. Gao, The potential roles of natural plant polysaccharides in inflammatory bowel disease: A review, *Carbohydr. Polym.*, 2022, **277**, 118821.
28 M. Shoaib, A. Shehzad, M. Omar, A. Rakha, H. Raza, H. R. Sharif, A. Shakeel, A. Ansari and S. Niazi, Inulin: Properties, health benefits and food applications, *Carbohydr. Polym.*, 2016, **147**, 444–454.
29 D. C. Mudannayake, D. D. Jayasena, K. M. Wimalasiri, C. S. Ranadheera and S. Ajlouni, Inulin fructans–food applications and alternative plant sources: a review, *Int. J. Food Sci. Technol.*, 2022, **57**, 5764–5780.
30 R. Singh, T. Singh and C. Larroche, Biotechnological applications of inulin-rich feedstocks, *Bioresour. Technol.*, 2019, **273**, 641–653.
31 L. Vogt, D. Meyer, G. Pullens, M. Faas, M. Smelt, K. Venema, U. Ramasamy, H. A. Schols and P. De Vos, Immunological properties of inulin-type fructans, *Crit. Rev. Food Sci. Nutr.*, 2015, **55**, 414–436.
32 G. Kelly, Inulin-type prebiotics–a review: part 1, *Altern. Med. Rev.*, 2008, **13**, 15.
33 H. Espinosa-Andrews, J. E. Urias-Silvas and N. Morales-Hernández, The role of agave fructans in health and food applications: A review, *Trends Food Sci. Technol.*, 2021, **114**, 585–598.
34 W. G. García-Villalba, R. Rodríguez-Herrera, L. A. Ochoa-Martínez, O. M. Rutiaga-Quiñones, J. A. Gallegos-Infante and S. M. González-Herrera, Agave fructans: a review of their technological functionality and extraction processes, *J. Food Sci. Technol.*, 2022, 1–9.
35 E. Mellado-Mojica, L. E. González de la Vara and M. G. López, Fructan active enzymes (FAZY) activities and biosynthesis of fructooligosaccharides in the vacuoles of Agave tequilana Weber Blue variety plants of different age, *Planta*, 2017, **245**, 265–281.
36 M. G. Lopez, N. A. Mancilla-Margalli and G. Mendoza-Diaz, Molecular structures of fructans from Agave tequilana Weber var. azul, *J. Agric. Food Chem.*, 2003, **51**, 7835–7840.
37 A. V. Pérez-López, J. Simpson, M. R. Clench, A. D. Gomez-Vargas and J. J. Ordaz-Ortiz, Localization and Composition of Fructans in Stem and Rhizome of Agave tequilana Weber var. azul, *Front. Plant Sci.*, 2021, **11**, 2309.
38 N. A. Mancilla-Margalli and M. G. López, Water-soluble carbohydrates and fructan structure patterns from Agave and Dasylirion species, *J. Agric. Food Chem.*, 2006, **54**, 7832–7839.

39 L. Vogt, U. Ramasamy, D. Meyer, G. Pullens, K. Venema, M. M. Faas, H. A. Schols and P. de Vos, Immune modulation by different types of β2→ 1-fructans is toll-like receptor dependent, *PLoS One*, 2013, **8**(7), e68367.

40 L. Vogt, D. Meyer, G. Pullens, M. M. Faas, K. Venema, U. Ramasamy, H. A. Schols and P. de Vos, Toll-Like Receptor 2 Activation by b2→ 1-Fructans Protects Barrier Function of T84 Human Intestinal Epithelial Cells in a Chain Length–Dependent Manner, *J. Nutr.*, 2014, **144**, 1002–1008.

41 C. Fernández-Lainez, R. Akkerman, M. Oerlemans, M. Logtenberg, H. Schols, L. Silva-Lagos, G. López-Velázquez and P. de Vos, β (2→ 6)-Type fructans attenuate proinflammatory responses in a structure dependent fashion via Toll-like receptors, *Carbohydr. Polym.*, 2022, **277**, 118893.

42 C. Fernández-Lainez, M. J. Logtenberg, X. Tang, H. A. Schols, G. López-Velázquez and P. de Vos, β (2→ 1) chicory and β (2→ 1)-β (2→ 6) agave fructans protect the human intestinal barrier function in vitro in a stressor-dependent fashion, *Food Funct.*, 2022, **13**, 6737–6748.

43 S. Bhatia, P. N. Prabhu, A. C. Benefiel, M. J. Miller, J. Chow, S. R. Davis and H. R. Gaskins, Galacto–oligosaccharides may directly enhance intestinal barrier function through the modulation of goblet cells, *Mol. Nutr. Food Res.*, 2015, **59**, 566–573.

44 L. Cheng, C. Kong, M. T. Walvoort, M. M. Faas and P. de Vos, Human milk oligosaccharides differently modulate goblet cells under homeostatic, proinflammatory conditions and ER stress, *Mol. Nutr. Food Res.*, 2020, **64**, 1900976.

45 C. Ren, J. Dokter-Fokkens, S. Figueroa Lozano, Q. Zhang, B. J. de Haan, H. Zhang, M. M. Faas and P. de Vos, Lactic acid bacteria may impact intestinal barrier function by modulating goblet cells, *Mol. Nutr. Food Res.*, 2018, **62**, 1700572.

46 J. A. Croix, S. Bhatia and H. R. Gaskins, Inflammatory cues modulate the expression of secretory product genes, Golgi sulfotransferases and sulfomucin production in LS174T cells, *Exp. Biol. Med.*, 2011, **236**, 1402–1412.

47 I. Das, C. W. Png, I. Oancea, S. Z. Hasnain, R. Lourie, M. Proctor, R. D. Eri, Y. Sheng, D. I. Crane and T. H. Florin, Glucocorticoids alleviate intestinal ER stress by enhancing protein folding and degradation of misfolded proteins, *J. Exp. Med.*, 2013, **210**, 1201–1216.

48 A. S. Lee, The ER chaperone and signaling regulator GRP78/BiP as a monitor of endoplasmic reticulum stress, *Methods*, 2005, **35**, 373–381.

49 O. I. Coleman and D. Haller, ER stress and the UPR in shaping intestinal tissue homeostasis and immunity, *Front. Immunol.*, 2019, **10**, 2825.

50 S. Figueroa-Lozano, R. Akkerman, M. Beukema, S. S. van Leeuwen, L. Dijkhuizen and P. de Vos, 2′-Fucosyllactose impacts the expression of mucus-related genes in goblet cells and maintains barrier function of gut epithelial cells, *J. Funct. Foods*, 2021, **85**, 104630.

51 K. J. Livak and T. D. Schmittgen, Analysis of relative gene expression data using real-time quantitative PCR and the 2− ΔΔCT method, *Methods*, 2001, **25**, 402–408.

52 N. B. Emidio, W. Hoffmann, S. M. Brierley and M. Muttenthaler, Trefoil factor family: Unresolved questions and clinical perspectives, *Trends Biochem. Sci.*, 2019, **44**, 387–390.

53 G. Barrera and G. S. Tortolero, Trefoil factor 3 (TFF3) from human breast milk activates PAR-2 receptors, of the intestinal epithelial cells HT-29, regulating cytokines and defensins, *Bratisl. Lek. Listy*, 2016, **117**, 332–339.

54 M. Loncar, E. Al-Azzeh, P. S. Sommer, M. Marinovic, K. Schmehl, M. Kruschewski, N. Blin, R. Stohwasser, P. Gött and T. Kayademir, Tumour necrosis factor α and nuclear factor κB inhibit transcription of human TFF3 encoding a gastrointestinal healing peptide, *Gut*, 2003, **52**, 1297–1303.

55 B.-H. Zhang, H.-G. Yu, Z.-X. Sheng, H.-S. Luo and J.-P. Yu, The therapeutic effect of recombinant human trefoil factor 3 on hypoxia-induced necrotizing enterocolitis in immature rat, *Regul. Pept.*, 2003, **116**, 53–60.

56 P. Arnold, U. Rickert, A.-K. Helmers, J. Spreu, J. Schneppenheim and R. Lucius, Trefoil factor 3 shows anti-inflammatory effects on activated microglia, *Cell Tissue Res.*, 2016, **365**, 3–11.

57 D. C. Propheter, A. L. Chara, T. A. Harris, K. A. Ruhn and L. V. Hooper, Resistin-like molecule β is a bactericidal protein that promotes spatial segregation of the microbiota and the colonic epithelium, *Proc. Natl. Acad. Sci. U. S. A.*, 2017, **114**, 11027–11033.

58 D. B. R. Herbert, J.-Q. Yang, S. P. Hogan, K. Groschwitz, M. Khodoun, A. Munitz, T. Orekov, C. Perkins, Q. Wang and F. Brombacher, Intestinal epithelial cell secretion of RELM-β protects against gastrointestinal worm infection, *J. Exp. Med.*, 2009, **206**, 2947–2957.

59 G. Chen, S. H. Wang, J. C. Jang, J. I. Odegaard and M. G. Nair, Comparison of RELMα and RELMβ single-and double-gene-deficient mice reveals that RELMα expression dictates inflammation and worm expulsion in hookworm infection, *Infect. Immun.*, 2016, **84**, 1100–1111.

60 K. S. Bergstrom, V. Morampudi, J. M. Chan, G. Bhinder, J. Lau, H. Yang, C. Ma, T. Huang, N. Ryz and H. P. Sham, Goblet cell derived RELM-β recruits CD4 + T cells during infectious colitis to promote protective intestinal epithelial cell proliferation, *PLoS Pathog.*, 2015, **11**, e1005108.

61 Y. S. Kim and S. B. Ho, Intestinal goblet cells and mucins in health and disease: recent insights and progress, *Curr. Gastroenterol. Rep.*, 2010, **12**, 319–330.

62 N. Ahmed, E. Heitlinger, N. Affinass, A. A. Kühl, N. Xenophontos, V. H. Jarquin, J. Jost, S. Steinfelder and S. Hartmann, A novel non-invasive method to detect RELM beta transcript in gut barrier related changes during a gastrointestinal nematode infection, *Front. Immunol.*, 2019, **10**, 445.

63 J. K. Lee, A. Bistrup, A. Van Zante and S. D. Rosen, Activities and expression pattern of the carbohydrate sulfotransferase GlcNAc6ST-3 (I-GlcNAc6ST): functional implications, *Glycobiology*, 2003, **13**, 245–254.

64 D. Ron and P. Walter, Signal integration in the endoplasmic reticulum unfolded protein response, *Nat. Rev. Mol. Cell Biol.*, 2007, **8**, 519–529.

65 M. A. Engevik, B. Herrmann, W. Ruan, A. C. Engevik, K. A. Engevik, F. Ihekweazu, Z. Shi, B. Luck, A. L. Chang-Graham and M. Esparza, Bifidobacterium dentium-derived y-glutamylcysteine suppresses ER-mediated goblet cell stress and reduces TNBS-driven colonic inflammation, *Gut Microbes*, 2021, **13**, 1902717.

66 W. Xiong, H. Ma, Z. Zhang, M. Jin, J. Wang, Y. Xu and Z. Wang, The protective effect of icariin and phosphorylated icariin against LPS-induced intestinal goblet cell dysfunction, *Innate Immun.*, 2020, **26**, 97–106.

67 I. Kim, W. Xu and J. C. Reed, Cell death and endoplasmic reticulum stress: disease relevance and therapeutic opportunities, *Nat. Rev. Drug Discovery*, 2008, **7**, 1013–1030.

68 S. S. Cao and R. J. Kaufman, Unfolded protein response, *Curr. Biol.*, 2012, **22**, R622–R626.

69 A. Kaser, T. E. Adolph and R. S. Blumberg, The unfolded protein response and gastrointestinal disease, *Semin. Immunopathol.*, 2013, **35**, 307–319.

70 X. Xue, J.-H. Piao, A. Nakajima, S. Sakon-Komazawa, Y. Kojima, K. Mori, H. Yagita, K. Okumura, H. Harding and H. Nakano, Tumor necrosis factor α (TNFα) induces the unfolded protein response (UPR) in a reactive oxygen species (ROS)-dependent fashion, and the UPR counteracts ROS accumulation by TNFα, *J. Biol. Chem.*, 2005, **280**, 33917–33925.

71 S. G. Sayago-Ayerdi, V. M. Zamora-Gasga and K. Venema, Changes in gut microbiota in predigested Hibiscus sabdariffa L calyces and Agave (Agave tequilana weber) fructans assessed in a dynamic in vitro model (TIM-2) of the human colon, *Food Res. Int.*, 2020, **132**, 109036.

72 W. Van den Ende, D. Peshev and L. De Gara, Disease prevention by natural antioxidants and prebiotics acting as ROS scavengers in the gastrointestinal tract, *Trends Food Sci. Technol.*, 2011, **22**, 689–697.

73 J. r. m. Busserolles, E. Gueux, E. Rock, C. Demigne, A. Mazur and Y. Rayssiguier, Oligofructose protects against the hypertriglyceridemic and pro-oxidative effects of a high fructose diet in rats, *J. Nutr.*, 2003, **133**, 1903–1908.

74 K. Lavrsen, S. Dabelsteen, S. Y. Vakhrushev, A. M. Levann, A. D. Haue, A. Dylander, U. Mandel, L. Hansen, M. Frödin and E. P. Bennett, De novo expression of human polypeptide N-acetylgalactosaminyltransferase 6 (GalNAc-T6) in colon adenocarcinoma inhibits the differentiation of colonic epithelium, *J. Biol. Chem.*, 2018, **293**, 1298–1314.

75 C. B. Amat, J.-P. Motta, E. Fekete, F. Moreau, K. Chadee and A. G. Buret, Cysteine protease–dependent mucous disruptions and differential mucin gene expression in Giardia duodenalis infection, *Am. J. Pathol.*, 2017, **187**, 2486–2498.

76 A. Kapiki, C. Costalos, C. Oikonomidou, A. Triantafyllidou, E. Loukatou and V. Pertrohilou, The effect of a fructo-oligosaccharide supplemented formula on gut flora of preterm infants, *Early Hum. Dev.*, 2007, **83**, 335–339.

77 R. Closa-Monasterolo, M. Gispert-Llaurado, V. Luque, N. Ferre, C. Rubio-Torrents, M. Zaragoza-Jordana and J. Escribano, Safety and efficacy of inulin and oligofructose supplementation in infant formula: results from a randomized clinical trial, *Clin. Nutr.*, 2013, **32**, 918–927.

78 G. López-Velázquez, M. Parra-Ortiz, I. D. l. M.-D. l. Mora, I. García-Torres, S. Enríquez-Flores, M. A. Alcántara-Ortigoza, A. G.-d. Angel, J. Velázquez-Aragón, R. Ortiz-Hernández and J. M. Cruz-Rubio, Effects of fructans from Mexican agave in newborns fed with infant formula: a randomized controlled trial, *Nutrients*, 2015, **7**, 8939–8951.

79 A. Tawiah, S. Cornick, F. Moreau, H. Gorman, M. Kumar, S. Tiwari and K. Chadee, High MUC2 mucin expression and misfolding induce cellular stress, reactive oxygen production, and apoptosis in goblet cells, *Am. J. Pathol.*, 2018, **188**, 1354–1373.

CAPÍTULO 7

The giardial arginine deiminase participates in giardia-host immunomodulation in a structure dependent fashion via Toll-like receptors

Cynthia Fernández-Lainez [a,b,c], Ignacio de la Mora-de la Mora [d], Sergio Enríquez-Flores [d], Itzhel García-Torres [d], Luis A. Flores-López [d,e], Pedro Gutiérrez-Castrellón [f], Paul de Vos [b], Gabriel López-Velázquez [d,*]

[a] Laboratorio de Errores Innatos del Metabolismo y Tamiz, Instituto Nacional de Pediatria, Ciudad de México 04530, Mexico.
[b] Immunoendocrinology, Division of Medical Biology, Department of Pathology and Medical Biology, University of Groningen and University Medical Center Groningen, 9700 Groningen, The Netherlands.
[c] Posgrado en Ciencias Biológicas, Universidad Nacional Autónoma de México, Ciudad de México 04510, Mexico.
[d] Laboratorio de Biomoleculas y Salud Infantil, Instituto Nacional de Pediatria, Ciudad de México 04530, Mexico.
[e] CONACYT-Instituto Nacional de Pediatria, Secretaria de Salud, Ciudad de México 04530, Mexico.
[f] Hospital General Dr. Manuel Gea González, Ciudad de México 14080, Mexico.

Publicado en International Journal of Molecular Sciences 2022, 23, 11552. https://doi.org/ 10.3390/ijms231911552

International Journal of
Molecular Sciences

MDPI

Article

The Giardial Arginine Deiminase Participates in *Giardia*-Host Immunomodulation in a Structure-Dependent Fashion via Toll-like Receptors

Cynthia Fernández-Lainez [1,2,3], Ignacio de la Mora-de la Mora [4], Sergio Enríquez-Flores [4], Itzhel García-Torres [4], Luis A. Flores-López [4,5], Pedro Gutiérrez-Castrellón [6], Paul de Vos [2] and Gabriel López-Velázquez [4,*]

1 Laboratorio de Errores Innatos del Metabolismo y Tamiz, Instituto Nacional de Pediatria, Ciudad de México 04530, Mexico
2 Immunoendocrinology, Division of Medical Biology, Department of Pathology and Medical Biology, University of Groningen and University Medical Center Groningen, 9700 Groningen, The Netherlands
3 Posgrado en Ciencias Biológicas, Universidad Nacional Autónoma de México, Ciudad de México 04510, Mexico
4 Laboratorio de Biomoleculas y Salud Infantil, Instituto Nacional de Pediatria, Ciudad de México 04530, Mexico
5 CONACYT-Instituto Nacional de Pediatria, Secretaria de Salud, Ciudad de México 04530, Mexico
6 Hospital General Dr. Manuel Gea González, Ciudad de México 14080, Mexico
* Correspondence: glv_1999@ciencias.unam.mx; Tel.: +52-5510840900 (ext. 1726)

check for updates

Citation: Fernández-Lainez, C.; de la Mora-de la Mora, I.; Enríquez-Flores, S.; García-Torres, I.; Flores-López, L.A.; Gutiérrez-Castrellón, P.; de Vos, P.; López-Velázquez, G. The Giardial Arginine Deiminase Participates in *Giardia*-Host Immunomodulation in a Structure-Dependent Fashion via Toll-like Receptors. *Int. J. Mol. Sci.* **2022**, *23*, 11552. https://doi.org/10.3390/ijms231911552

Academic Editor: Mohammad Hassan Baig

Received: 22 August 2022
Accepted: 19 September 2022
Published: 30 September 2022

Publisher's Note: MDPI stays neutral with regard to jurisdictional claims in published maps and institutional affiliations.

Abstract: Beyond the problem in public health that protist-generated diseases represent, understanding the variety of mechanisms used by these parasites to interact with the human immune system is of biological and medical relevance. *Giardia lamblia* is an early divergent eukaryotic microorganism showing remarkable pathogenic strategies for evading the immune system of vertebrates. Among various multifunctional proteins in *Giardia*, arginine deiminase is considered an enzyme that plays multiple regulatory roles during the life cycle of this parasite. One of its most important roles is the crosstalk between the parasite and host. Such a molecular "chat" is mediated in human cells by membrane receptors called Toll-like receptors (TLRs). Here, we studied the importance of the 3D structure of giardial arginine deiminase (GlADI) to immunomodulate the human immune response through TLRs. We demonstrated the direct effect of GlADI on human TLR signaling. We predicted its mode of interaction with TLRs two and four by using the AlphaFold-predicted structure of GlADI and molecular docking. Furthermore, we showed that the immunomodulatory capacity of this virulent factor of *Giardia* depends on the maintenance of its 3D structure. Finally, we also showed the influence of this enzyme to exert specific responses on infant-like dendritic cells.

Keywords: giardiasis; immune response; inflammation; protein–protein interactions; 3D structure

1. Introduction

Human giardiasis is caused by the flagellated protist *Giardia lamblia* and is responsible for diarrheal disease and chronic postinfectious illnesses such as irritable bowel syndrome [1]. Most infections are asymptomatic or mildly symptomatic, such as cramps and mild chronic diarrhea, even though severe complications associated with intestinal malabsorption are also frequent. Resultant diarrhea is thought to be due to nutrient malabsorption, epithelial barrier defects, and ion secretion [2]. However, the mechanisms by which *G. lamblia* causes disease and different symptoms severity are poorly understood.

This parasite has developed many mechanisms to escape from the immune system for growing in the intestine. Although giardiasis is commonly asymptomatic, symptoms such as diarrhea, abdominal pain, nausea, intestinal malabsorption, and weight loss can occur along a broad spectrum. Especially in children, *Giardia* may cause issues as they

show a high prevalence of giardiasis. In some cases, it may lead to malnutrition, failure to thrive, stunting, and cognitive impairment [3,4]. Nutrient depletion of the host, caused by the feeding of *Giardia* and secreted cargo by the parasite, might be reasons for these symptoms [5].

Alongside other giardial proteins, the arginine deiminase from *G. lamblia* (GlADI) can be found extracellularly in the absence of a signal sequence by a mechanism termed unconventional protein secretion (UPS) [6]. Moonlighting functions (multiple functions for a protein) are often present in UPS cargoes, suggesting that these characteristics are directly linked to each other, as posttranslational modifications seem to influence the function and transport of a protein [5]. GlADI belongs to the arginine dihydrolase pathway for ATP generation in *Giardia* [7,8], which is highly efficient due to the giardial arginine transport system that is 10- to 20-fold higher maximal transport capacity than that of the intestinal epithelial cells (IECs) [9].

Along with such a canonical function, GlADI also catalyzes the deamination of the arginine side chain in the conserved CRGKA cytoplasmic tails of the variant-specific surface proteins (VSPs) of *Giardia* [10]. Such VSPs citrullination is proposed to influence antigenic switching and antibody-mediated cell death. Furthermore, the release of GlADI to the medium [11] confers to the parasite the ability to impair the availability of free L-Arg to be used for the production of nitric oxide (NO) by IECs [12]. Since NO inhibits replication of *Giardia* and other microbes, depletion of L-Arg is a recognized strategy used to evade immune effector mechanisms [12–15].

Among various adaptations *Giardia* uses for coping with the intestinal environment and immune defense, it is valuable in drug design to know how GlADI participates in subverting the intestinal milieu to benefit itself. Regarding this, we previously demonstrated the potential of GlADI as a target for giardiasis treatment by drug repurposing strategies based on cysteine (Cys)-modification mechanisms [16]. It was reported that GlADI is among 16 immunodominant proteins in *Giardia* [17]; however, its role as a virulent factor modulating the immune system into the intestine has not been elucidated enough yet.

In this regard, Banik and colleagues reported that the immunomodulatory effect of recombinant GlADI on human monocyte-derived dendritic cells is attributable to arginine depletion and NH_4^+ formation instead of preventing NO formation [18]. Furthermore, Muñoz-Cruz and colleagues reported that citrulline but not ammonium induced activation of rat mast cells [19]. Additionally, they reported that recombinant GlADI still stimulated mast cells in an arginine-free medium, although to a lower extent than in the presence of arginine, indicating that GlADI itself can stimulate mast cells [19]. This latter underlines the importance for GlADI to maintain its 3D structure in the intestine milieu to reach immune cells and to establish a lasting communication between the parasite and the host.

An essential family of receptors that might be involved in immunomodulation by GlADI is Toll-like receptors (TLRs). TLRs are present in most immune cells involved in responses against *Giardia.* They are known to be modulated by many pathogenic molecules, specific food components, and pharmaceuticals [20–22]. The involvement of TLRs in immune responses against *Giardia* is not well studied. Still, it might be important as it might lead to new therapeutical approaches to modulate immune responses against *Giardia* in susceptible groups such as children.

Here, we studied the capacity of GlADI to induce activation of the nuclear factor κB (NF-κB) and activator protein 1 (AP-1) via TLRs in cell lines that endogenously express all human TLRs. Furthermore, the possible impact on TLR-dependent immunomodulation of rabeprazole as a drug against *Giardia* was studied. Spectroscopic fluorescence studies in denaturing conditions analyzed the importance of GlADI 3D structure. To understand the mechanisms by which GlADI exerts immunomodulation through TLRs, we used AlphaFold to create a predicted model of GlADI. We applied it for in silico docking studies to propose its specific binding sites to TLRs. Finally, the impact of GlADI on the cytokine release from immature, infant-like dendritic cells (DCs) was studied.

2. Results

2.1. GlADI Exerts Immunomodulation by Activating TLRs

In search of the effects exerted by the direct interaction of GlADI with TLRs, we performed assays to measure the production of NF-κB/AP-1 in THP1-MD2-CD14, a monocyte reporter cell line carrying all TLRs coupled to a SEAP reporter gene. Concentrations of GlADI ranging from 0.05–0.5 μg/mL tended to increase activation of TLRs in a concentration-dependent fashion. On the other hand, GlADI concentrations ranging from 0.5-2 μg/mL had a constant and significantly increased activation of TLRs ($p < 0.05$; Figure 1a).

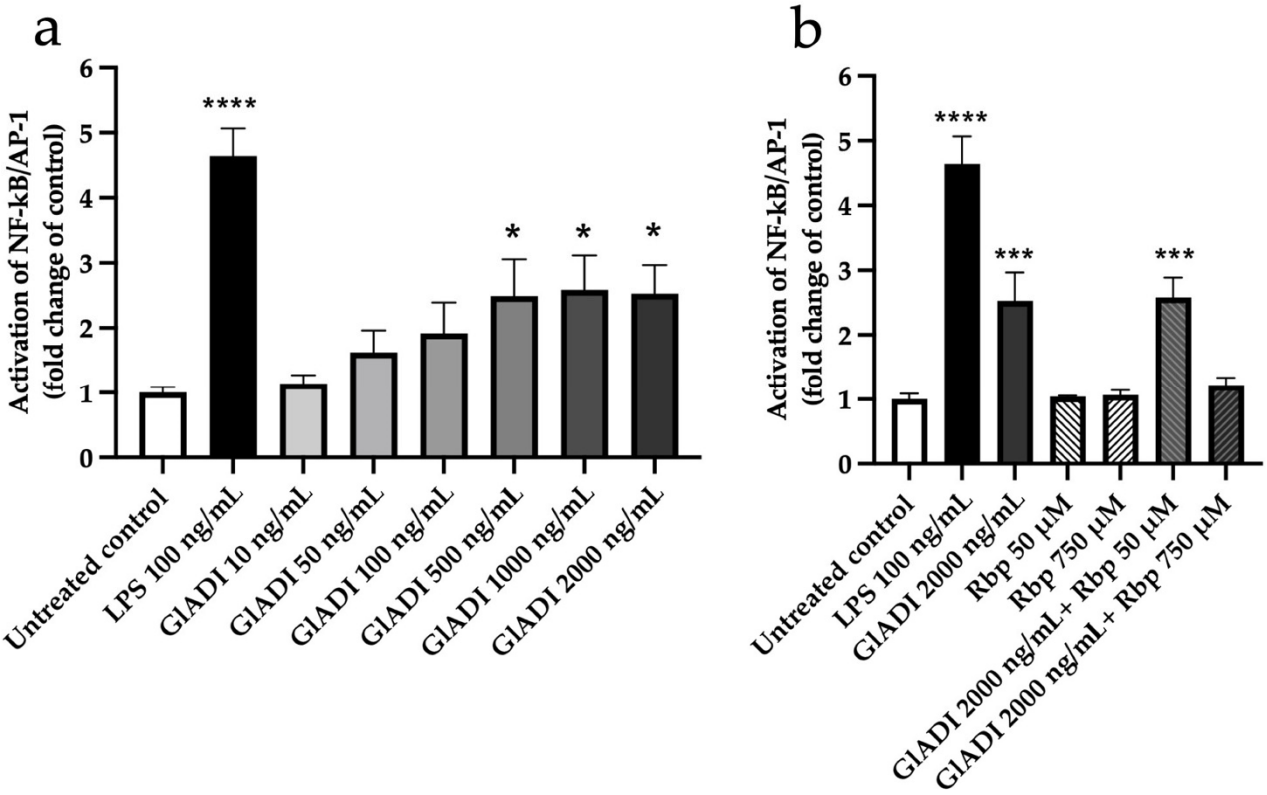

Figure 1. NF-κB/AP-1 activation in THP1-MD2-CD14 reporter cells. (**a**) Cells were stimulated with rising concentrations of GlADI and (**b**) with rabeprazole (Rbp) or the highest concentration of GlADI mixed with Rbp. Activation of NF-κB/AP-1 is presented as the untreated control fold change. Results represent the median with the interquartile range of at least three independent experiments, with three technical replicates. Statistical significance levels compared to the untreated control were determined by the Friedman test (non-parametric statistical test), followed by the Dunn's multiple comparisons test (post hoc test). A p-value < 0.05 was considered as statistically significant (* $p < 0.05$, *** $p < 0.001$, **** $p < 0.0001$).

We assayed two rabeprazole concentrations to study their effects on the process of TLRs activation exerted by GlADI. The addition of 50 μM rabeprazole did not modify the GlADI-induced TLRs activation. In contrast, a concentration of 750 μM inhibited their activation (Figure 1b). Regarding these experiments, it is remarkable that rabeprazole itself does not activate TLRs with the assayed concentrations (Figure 1b). It is remarkable that only the highest concentration of rabeprazole inhibited the TLRs activation by GlADI.

2.2. GlADI Interacts with the Host Immune System through TLR2 and TLR4

To determine which specific TLR was activated in THP1 MD2-CD14 cells, the reporter cell lines expressing either human TLRs two, three, four, five, seven, eight, or nine were used. We found that GlADI activated TLR2 in a dose-dependent manner ranging from

1 μg/mL ($p < 0.001$) to 2 μg/mL ($p < 0.0001$) (Figure 2a). Again, rabeprazole had no effect on this TLR but abolished the activation previously exerted by GlADI (Figure 2b).

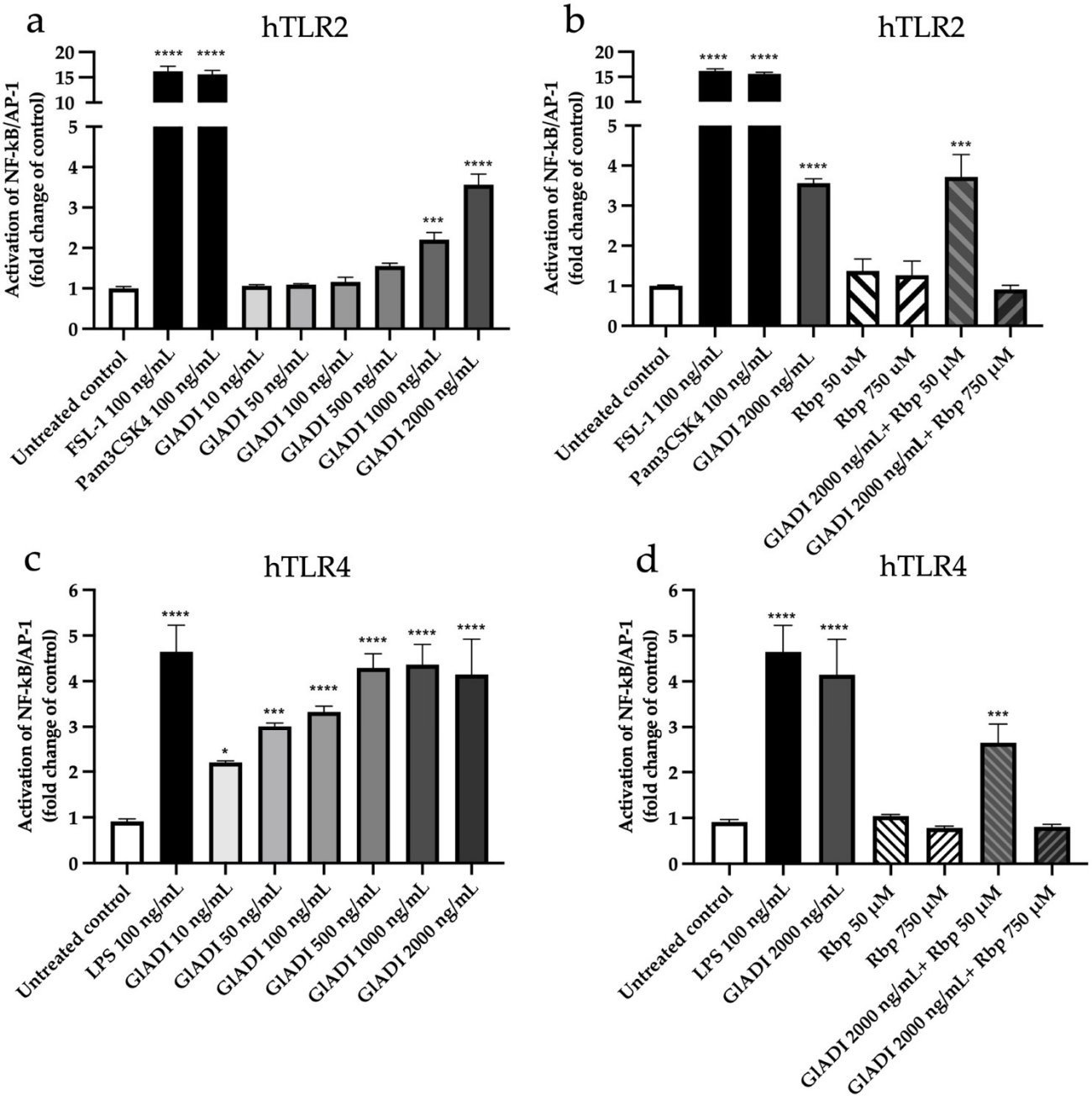

Figure 2. Activation effects of GlADI on HEK-Blue™ reporter cell lines. Each cell line was incubated for 24 h with rising concentrations of GlADI, with rabeprazole (Rbp), or with a mix of GlADI 2000 ng/mL and Rbp. Afterward, NF-κB/AP-1 release was determined. Activation of TLRs is presented as a fold change of the untreated control. NF-κB/AP-1 activation effect of GlADI (**a**,**c**) and the Rbp (**b**,**d**) on human TLR2 (**a**,**b**) and human TLR4 (**c**,**d**), respectively. Appropriate agonists for each TLR served as positive controls. At least five independent assays, each one with three technical replicates. These data were normally distributed. Therefore, the results are represented as the mean ± SD. Statistical significance levels compared to the negative control were determined by one-way ANOVA with Holm-Sidak's multiple comparisons test. A p-value < 0.05 was considered as statistically significant (* $p < 0.05$, *** $p < 0.001$, **** $p < 0.0001$).

GlADI with all assayed concentrations also activated TLR4 in a dose-dependent manner from the lowest ($p < 0.05$) to the highest ($p < 0.0001$) (Figure 2c). Interestingly, the activation of TLR4 was significantly more sensitive to GlADI than that of TLR2 (Figure 2a vs. Figure 2c). Furthermore, rabeprazole at a high concentration abolished the activation of GlADI on TLR4. In contrast, the low concentration did not affect this activation process (Figure 2d). GlADI activated neither TLRs three, five, seven, eight, nor nine at any assayed concentrations (Supplementary Figure S1).

2.3. The Forces Maintaining the 3D Structure of GlADI Could Be a Pivotal Factor in Activating TLRs

The protein thermal shift assay showed that GlADI exhibited a stable melting point (~56 °C) in a wide range of pH (pH 5.0 to 9.5) and under a high ionic strength (Table 1).

Table 1. Thermal shift assays on GlADI varying pH and salinity.

	Melting Temperatures of GlADI (°C)							
[NaCl] mM	**pH 5.0**	**pH 6.0**	**pH 6.5**	**pH 7.0**	**pH 7.5**	**pH 8.0**	**pH 9.0**	**pH 9.5**
0	55.98	59.14	55.88	55.64	60.34	58.96	50.04	56.99
200	49.82	60.94	60.97	63.01	70.56	56.4	59.74	56.24
400	57.04	50.59	47.17	48.12	53.57	52.05	51.93	56.84

To explore whether the tertiary structure of GlADI is involved in the TLRs activation described above, we analyzed the intrinsic fluorescence of this protein by spectroscopic techniques. The quantum yield of GlADI barely varies and is strongly conserved even under extreme denaturing conditions, as can be observed when using increasing concentrations of the chaotropic agent guanidium chloride (GdnHCl) (Figure 3a). The fluorescence emission spectra of GlADI under denaturing conditions showed a maximum of around 340 nm at pH 8.0 (Figure 3a). Such results support that GlADI is highly resistant to denaturing conditions and that the interactions between its constituent amino acids strongly stabilize its 3D structure.

To correlate the above results showing that the low concentration of rabeprazole did not interfere with the TLRs activation by GlADI, whereas high concentrations did interfere, we assayed the influence of different concentrations of rabeprazole combined with increasing concentrations of GndHCl to determine whether rabeprazole can potentiate denaturing of GlADI. The emission spectra showed that rabeprazole concentrations between 50 and 100 μM could not potentiate GndHCl to denature GlADI (Figure 3b,c). On the other hand, higher concentrations of rabeprazole (500 and 750 μM) strongly potentiated denaturing of GlADI with GndHCl (Figure 3d,e). Furthermore, the data from fluorescence spectra demonstrate the ability of rabeprazole itself to denature GlADI at high concentrations even in the absence of GndHCl (Figure 3f).

Since disulfide bonds can stabilize the 3D structure in proteins, we studied the role they could play in the immunomodulation observed for GlADI. Based on the primary structure of GlADI, the DiANNA 1.1 software (Chestnut Hill, MA, USA) [23] predicted the probability of GlADI forming eight intra-disulfide bonds. Experimentally, we determined only three intra- and possibly one inter-disulfide bond on recombinant GlADI [16]. Furthermore, in the AlphaFold-predicted structure of GlADI, we found 6 Cys residues (C216, C223, C469, C576, C283, C365) per subunit, showing distances propitious to establish three disulfide bonds per subunit (Figure 4).

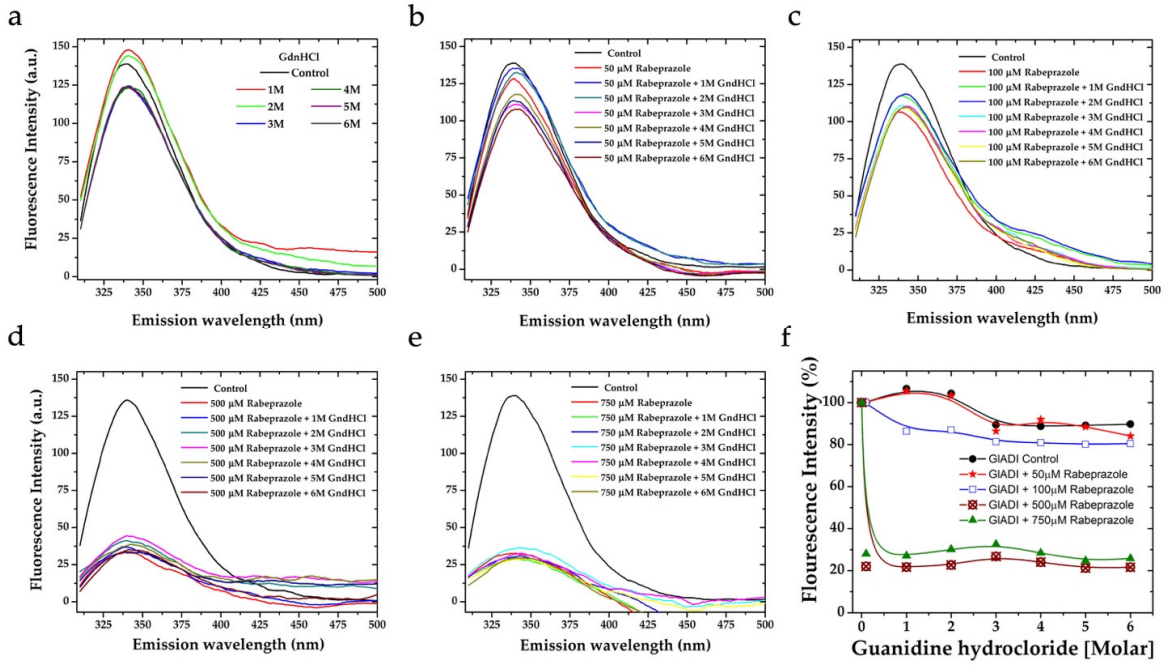

Figure 3. Fluorescence emission spectra of GlADI at rising concentrations of the chaotropic agent guanidine hydrochloride (GdnHCl). The intensity of intrinsic fluorescence of GlADI is almost not decreased by increasing concentrations of GdnHCl tested in a range of denaturing concentrations (**a**), even when rabeprazole 50 µM (**b**) or 100 µM (**c**) are added. The intensity of intrinsic fluorescence of GlADI is strongly decreased when rabeprazole 500 µM (**d**) or 750 µM (**e**) are added. The overall data show the effects of low and high concentrations of rabeprazole on the intrinsic fluorescence of GlADI in the presence or absence of GdnHCl (**f**).

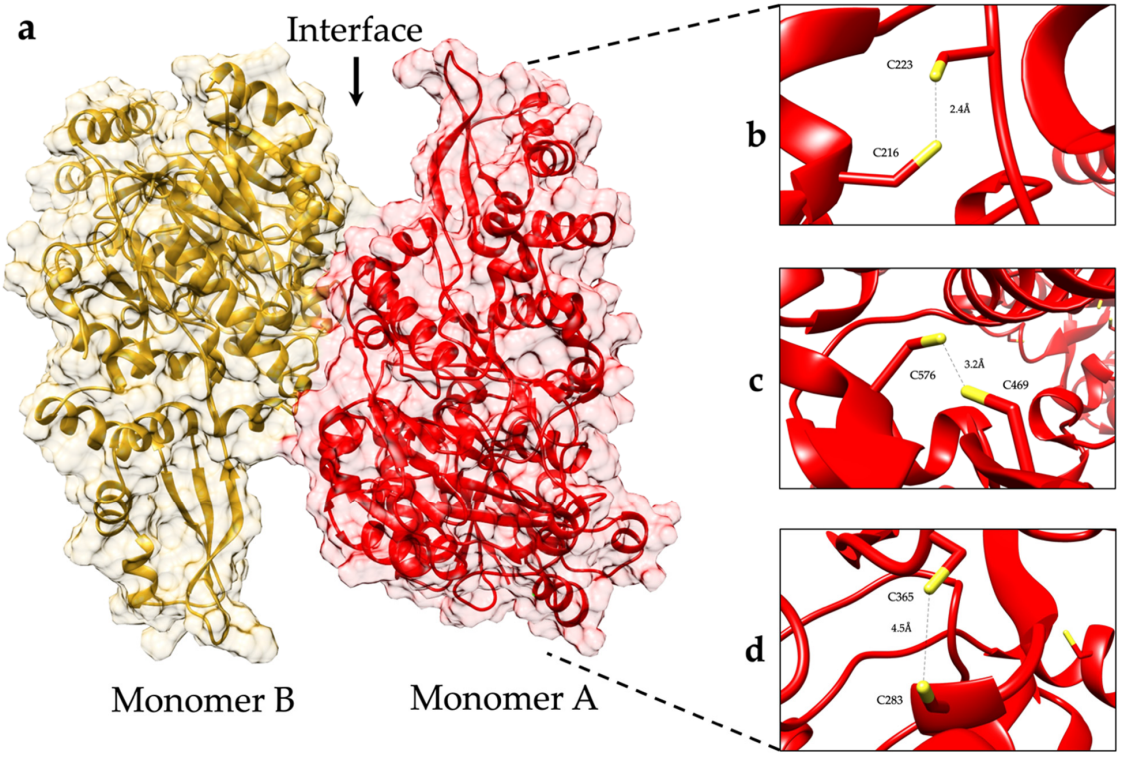

Figure 4. Ribbons and surface representation of the AlphaFold-predicted structure of GlADI. (**a**) The homo dimer with two identical subunits is the described biological active form of GlADI. (**b**–**d**) Based on the distance between their sulfur atoms, three pairs of cysteines might be forming disulfide bonds.

As observed in Figure 3a, the 3D structure of GlADI is hardly denatured; therefore, we analyzed its intrinsic fluorescence in the presence of increasing DTT (Dithiothreitol-reducing agent used to break disulfide bonds). In the presence of DTT, the forces that maintain the 3D structure of GlADI (it is, disulfide bonds) were broken, and, finally, the protein was denatured with the addition of 6 M GndHCl (Figure 5a). Furthermore, lower concentrations of GndHCl combined with DTT were able to promote the denaturation of GlADI.

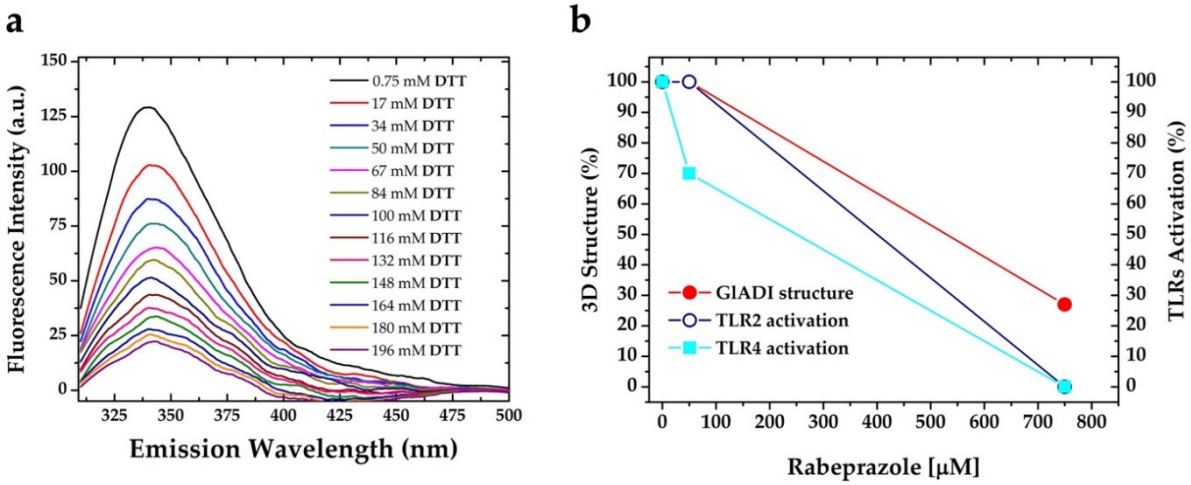

Figure 5. Relationship between 3D structure of GlADI and activation of TLRs. Fluorescence emission spectra of GlADI added with 6 M GndHCl dropped off by increasing concentrations of DTT (disulfide disrupting agent) as a reflection of its denaturing (**a**). The 3D structure stability of GlADI correlates with low concentrations of rabeprazole and activation of TLRs. In contrast, a lack of 3D structure stability correlates with a lack of TLRs activation and high concentrations of rabeprazole (**b**).

Altogether, our results show the reinforcement of GlADI 3D structure by intra-disulfide bonds. Moreover, on this stable structure, GlADI can activate TLRs. Along with this, both low and high concentrations of rabeprazole can inhibit the enzyme activity of GlADI. Still, only the high ones can break disulfide bonds and impair its 3D structure, with the concomitant inability to activate TLRs. Figure 5b interprets and summarizes the data from the effects of rabeprazole concentrations, protein 3D structure, and TLRs activation.

2.4. Predicted Interactions between the AlphaFold-Predicted Structure of GlADI and TLR2-TLR1

To propose an explanation of the molecular mechanisms that drive the activation effects exerted by GlADI on TLRs, protein–protein docking analyses were performed with the HDOCK server [24]. To that end, the AlphaFold-predicted structure of GlADI and the experimentally determined crystallographic coordinates of human TLR2-TLR1 heterodimer and TLR4-MD-2 heterotetramer (PDB codes: 2Z7X and 3FXI, respectively) were used.

Molecular docking analysis of TLR2-TLR1 with the dimer of the AlphaFold-predicted structure of GlADI located it in different sites of these receptors. The best-ranked pose of GlADI with human heterodimer TLR2-TLR1 (Figure 6a) had a docking score of −219.48 kcal/mol. The binding affinity (ΔG) prediction of the protein–protein complex was −11.8 kcal $mol^{-1,}$ while the dissociation constant (K_D) predicted was 2.3×10^{-9} M at 25 °C. According to this approach, monomer A of GlADI established an interface of interaction with the central and C-term ectodomains of human TLR2 (Figure 6a); of which, an area of 557 $Å^2$ comprising six amino acid residues of the monomer A of GlADI interacts with an area of 469 $Å^2$ containing 11 amino acid residues of TLR2. Such interactions include one salt bridge, three hydrogen bonds, and 73 non-bonded contacts (Figure 6b). Furthermore, monomer A of GlADI established interaction with TLR1, of which an area of 73 $Å^2$ at the region of Arg 153 interacts with an area of 68 $Å^2$ comprising three amino acid residues of TLR1. Such interaction formed through 8 non-bonded con-

tacts (Figure 6c) includes important TLR1 residues (V311, F312, and G313), previously reported as part of the ligand binding site [25].

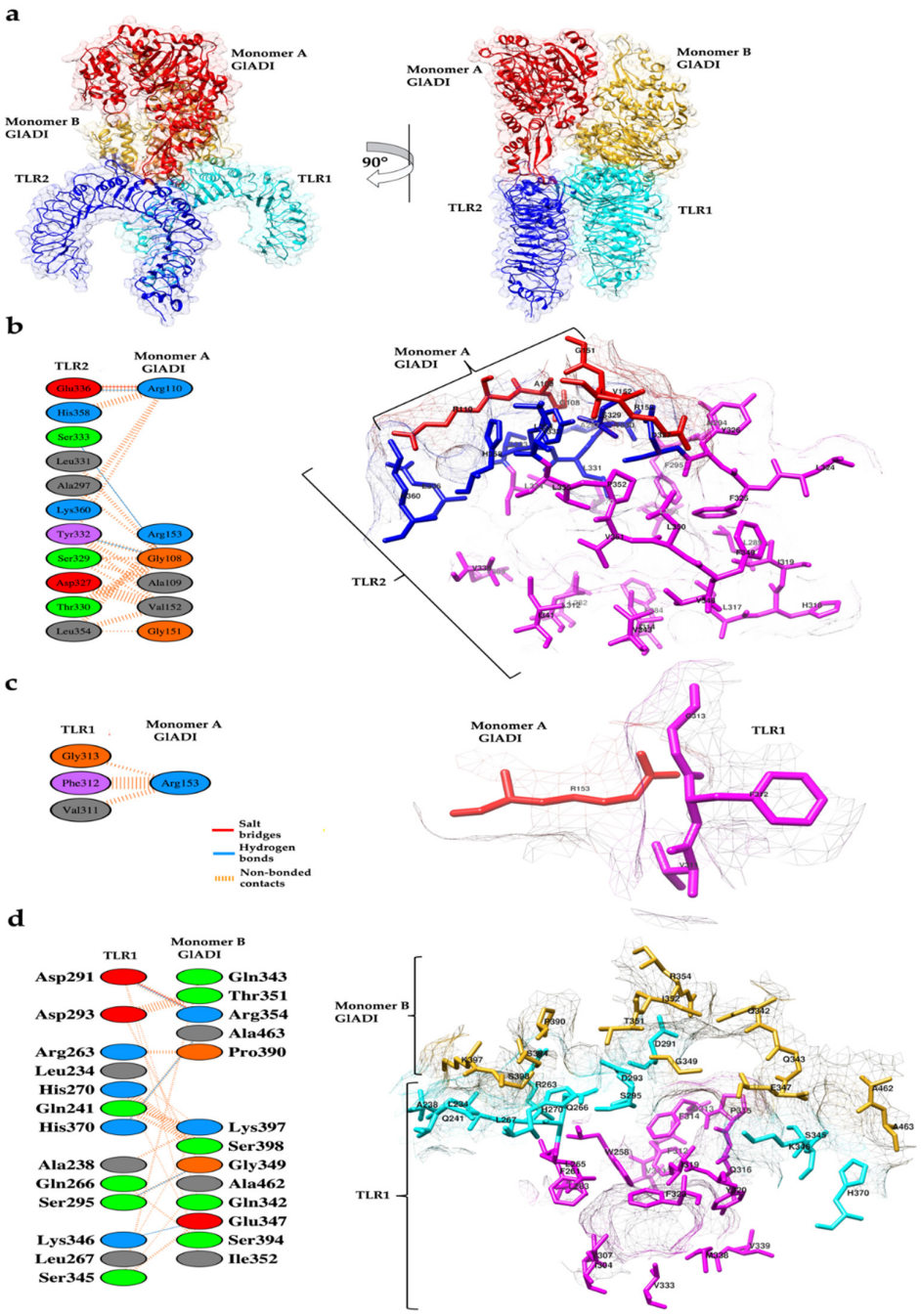

Figure 6. Predicted interactions between AlphaFold-predicted structure of GlADI and human TLR2-TLR1 heterodimer. (**a**) Two views of the predicted protein–protein interactions of GlADI with the ectodomains of human TLR2-TLR1. (**b**) Amino acid residues interacting between GlADI monomer A (red-colored, right side) and TLR2 (blue-colored, right side). (**c**) Amino acid residues interacting between GlADI monomer A (red-colored, right side) and TLR1 (magenta-colored, right side). (**d**) Amino acid residues interacting between GlADI monomer B (gold-colored, right side) and TLR1 (cyan-colored, right side). Amino acid residues magenta-colored (right side) are part of the ligand binding site of the TLR2-TLR1 heterodimer. Interacting amino acid residues are shown (left side). Structures displayed with UCSF Chimera. Docking was performed with HDOCK. Interactions analyses were made with PDBSum.

An area of 673 Å^2 of the monomer B of GlADI comprising 13 amino acid residues interacts with an area of 698 Å^2 of TLR1, containing 13 amino acid residues. These interactions include one salt bridge, four hydrogen bonds, and 77 non-bonded contacts (Figure 6d). Interestingly, these interactions (Figure 6d, cyan-colored residues) are surrounded by the ligand binding pocket (Figure 6d, magenta-colored residues).

We analyzed the interacting interfaces between TLR2 and the AlphaFold-predicted GlADI structure, identifying amino acids involved in protein–protein interactions, which are in the region involved in the TLR2 activation process. The GlADI-predicted structure was found to interact with TLR2 mainly through amino acid residues next to the ligand binding site and amino acid residues important for dimerization (Figure 6b, magenta-colored residues). Remarkably, monomer A of GlADI established hydrogen bonds with Y332, S333, and E336 of TLR2 (Figure 6b, blue-colored residues), which are embedded in the ligand binding region where important residues such as L334, V338, I341, and V343 (Figure 6b, magenta-colored residues), are located. These residues were previously reported to interact with acylated lipopeptides [25].

2.5. Predicted Interactions between the AlphaFold-Predicted Structure of GlADI and TLR4-MD-2

The heterodimer of TLR4 and myeloid differentiation factor 2 (MD-2) recognizes Gram-negative bacteria's lipopolysaccharide (LPS). Since HEK-Blue-TLR4-MD2-CD14 cells express the TLR4-MD-2 heterodimer, we performed the molecular docking analysis on human TLR4-MD-2 tetramer with the dimer of GlADI (Figure 7). GlADI established five regions of interaction with the TLR4-MD2 tetramer (Figures 7 and 8). The best pose of this interaction had a docking score of −261.63 kcal/mol. The binding affinity (ΔG) prediction of the protein–protein complex was −14.6 kcal/mol$^{-1,}$ while the dissociation constant (K_D) predicted was 1.8 × 10^{-11} M at 25 °C.

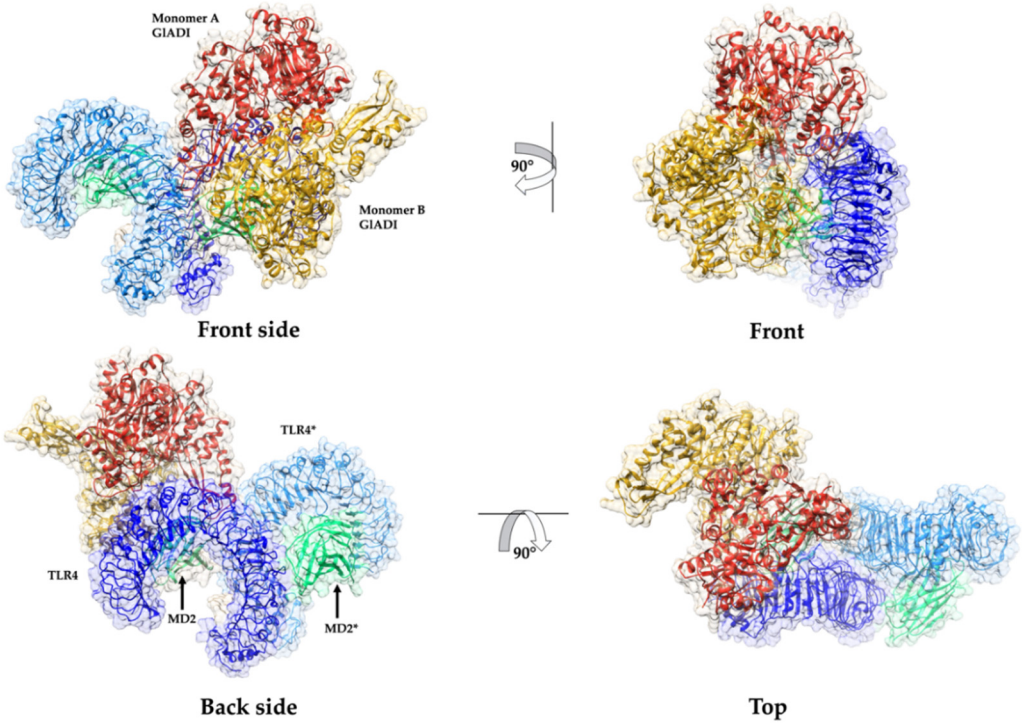

Figure 7. Predicted interactions between AlphaFold-predicted structure of GlADI and the ectodomain of human TLR4 in complex with MD-2. Ribbons combined with surface representation show four different views of the docking prediction between GlADI and TLR4-MD2 tetramer. Structures displayed with UCSF Chimera.

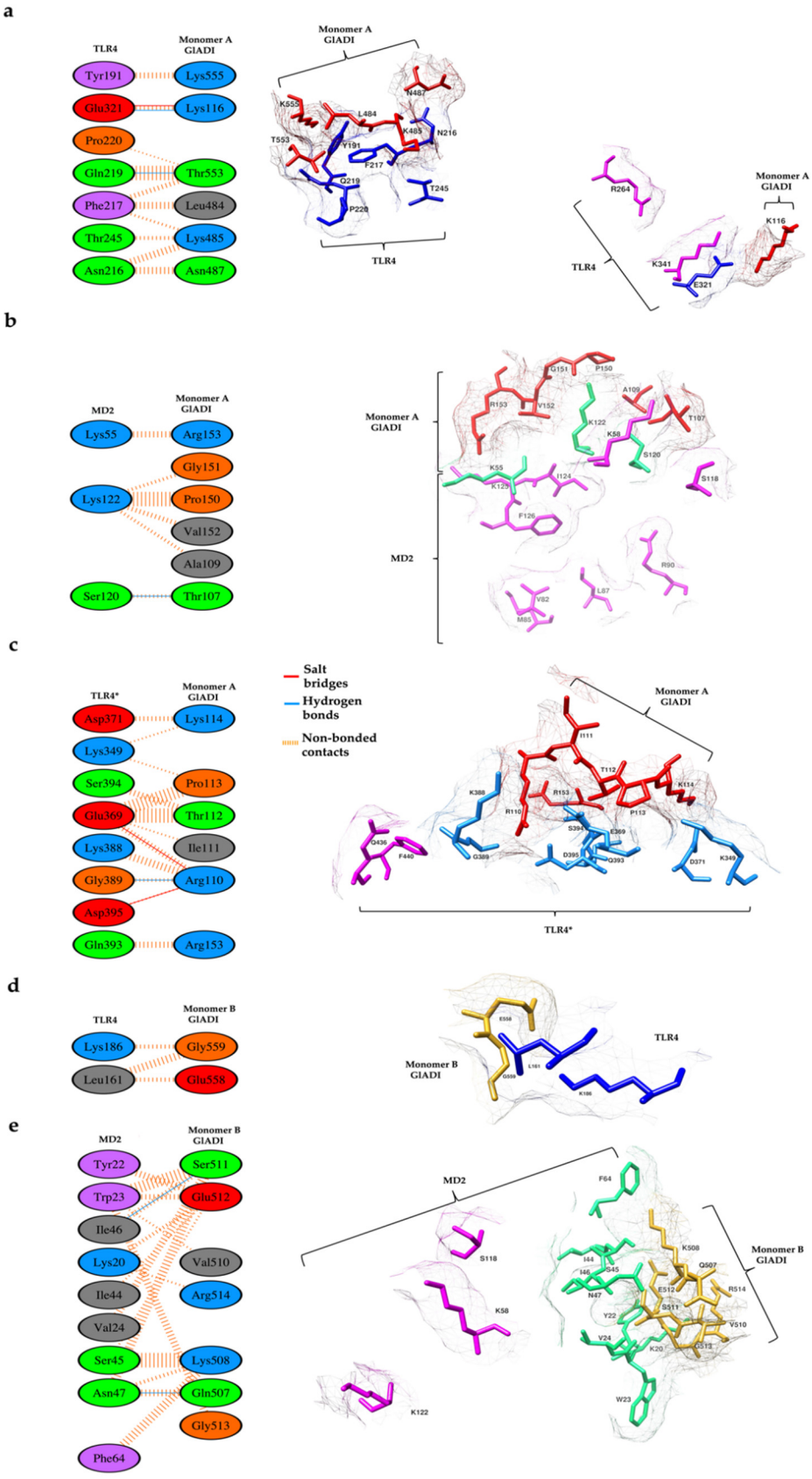

Figure 8. Amino acid residues proposed to interact between AlphaFold-predicted structure of GlADI and the ectodomain of human TLR4 dimer in complex with MD-2. (**a**) Protein–protein interaction

of monomer A of GlADI (red-colored, right side) with TLR4 (blue-colored, right side) and the interactions between their amino acid residues (left side). (**b**) The amino acid residues of monomer A of GlADI (red-colored, right side) interact with MD2 (green-colored, right side). (**c**) The amino acid residues of monomer A of GlADI (red-colored, right side) interact with TLR4*(cyan-colored, right side). (**d**) The amino acid residues of monomer B of GlADI (gold-colored, right side) interact with TLR4 (blue-colored, right side). (**e**) The amino acid residues of monomer B of GlADI (gold-colored, right side) interact with MD2 (green-colored, right side). Amino acid residues magenta-colored (right side) are part of the ligand binding site of the TLR4-MD2 tetramer. Interacting amino acid residues are shown (left side). Structures displayed with UCSF Chimera. Docking was performed with HDOCK. Interactions analyses made with PDBSum.

An area of 476 $Å^2$ comprising six amino acid residues of the monomer A of GlADI interacts with an area of 454 $Å^2$ containing seven amino acid residues of TLR4. This interaction region includes two hydrogen bonds, one salt bridge, and 49 non-bonded contacts (Figure 8a). Moreover, monomer A of GlADI established interaction with MD2. Six amino acid residues of GlADI monomer A, which comprised an area of 256 $Å^2$, interact with three amino acid residues of MD2, which comprised an area of 289 $Å^2$. These interactions include one hydrogen bond and 23 non-bonded contacts (Figure 8b). This interface consists of an important interaction with the K122 residue of MD2, which is part of the ligand binding region. This monomer of GlADI also established interaction with TLR4* by an area of 423 $Å^2$ comprising six amino acid residues of the monomer A of GlADI, interacting with an area of 401 $Å^2$, containing eight amino acid residues of TLR4* (Figure 8c). The K388 residue of TLR4* is involved in these interactions and is recognized as part of the ligand binding region.

The monomer B of GlADI established interaction with two residues of TLR4 through 2 amino acid residues, contributing to areas of 95 and 96 $Å^2$, respectively. This interaction includes four non-bonded contacts (Figure 8d). Furthermore, monomer B of GlADI interacts with MD2 through an area of 357 $Å^2$ comprising seven amino acid residues of the monomer B of GlADI interacting with an area of 324 $Å^2$ containing nine amino acid residues of MD2. This interaction region includes two hydrogen bonds and 56 non-bonded contacts (Figure 8e).

2.6. GlADI Induces Cytokine Production of DCs

We investigated whether GlADI can influence cytokine production of DCs from umbilical cord blood. We found that GlADI had no significant effect on the production neither of Macrophage Inflammatory Protein 1A (MIP-1A), Interleukin 1 receptor antagonist (IL-1RA), or Interleukin 6 (IL-6) (Figure 9a–c). On the other hand, GlADI caused a significant decrease on the production of chemokine ligand of monocyte chemoattractant protein-1 (MCP-1)/CC (CCL2) ($p < 0.0001$) (Figure 9d) and IL-10 ($p < 0.05$) (Figure 9e), whereas it caused a significant increase in IL-1β ($p < 0.0001$) (Figure 9f) and Tumor Necrosis Factor (TNFα) ($p < 0.05$) (Figure 9g).

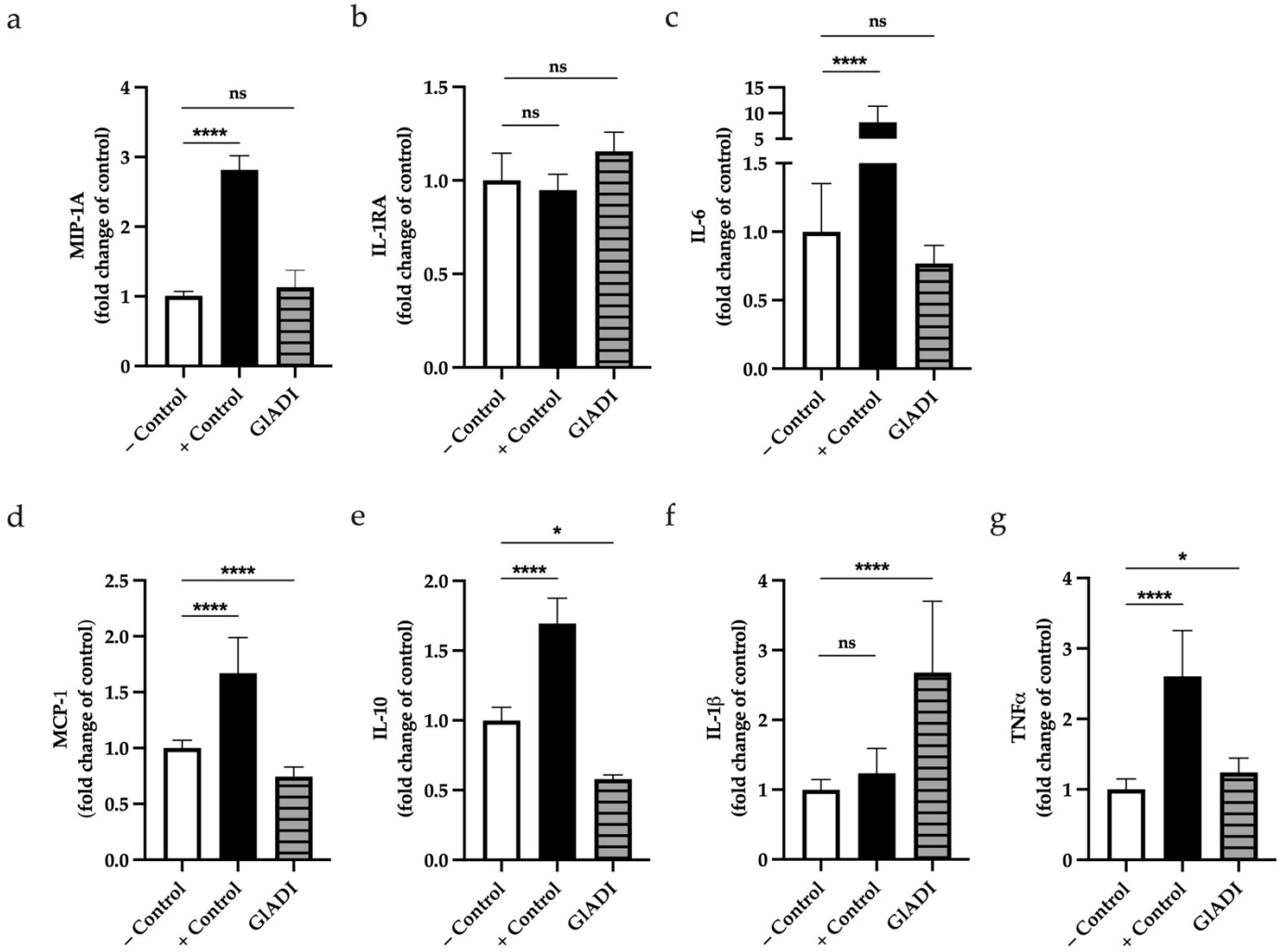

Figure 9. Cytokine production by DCs pre-treated with GlADI 500 ng/mL. GlADI had no effect on the production of (**a**) MIP-1A), (**b**) IL-1RA, and (**c**) (IL-6), whereas it caused a significant decrease in the production of (**d**) MCP-1 and (**e**) IL-10. Significant increases in the production of (**f**) IL-1β and (**g**) TNFα are shown. Results are shown as fold change of the untreated control. Positive and negative control experiments are shown as − Control and + Control, respectively. A p-value < 0.05 was statistically significant (* $p < 0.05$, **** $p < 0.0001$, ns = no significant).

3. Discussion

In the present study, we demonstrate, until the best of our knowledge for the first time, the direct effect of GlADI on human TLR signaling and report the prediction of its 3D structure based on the AlphaFold artificial intelligence program, as well as the probable mode of interaction of GlADI with human TLRs two and four by molecular docking. Moreover, we show that this immunomodulatory capacity is GlADI 3D structure dependent. We also show that GlADI can influence human infant-like DCs responses.

Inflammation through TLRs signaling is a protective response of the host to accelerate the healing process against infectious agents. Th1-type cytokines tend to produce the pro-inflammatory responses responsible for killing parasites, whereas Th2 is associated with anti-inflammatory responses. The Th1-biased inflammatory consequences that TLRs exert can also induce fatal pathological outcomes such as septic shock. Additionally, a pathogen modulated TLR signaling can induce a Th2 response, which promotes the progression of the disease. Thus, pro- and anti-inflammatory immune responses must be effectively balanced to restore the homeostasis of the host during and after a pathogenic infection [26].

Various studies on macromolecules show that different TLRs and their downstream pathways can be activated or inhibited in a structure-dependent way [21,27–30]. The effects of GlADI on TLRs stimulation observed herein are likely to be regulated by factors such as its 3D structure rather than the presence of its metabolic products (citrulline and NH_4^+) or depletion of arginine (its substrate). Our findings do not discard the previously described role of the reaction products of GlADI in the immunomodulatory process [18] but contribute to a better understanding of the variety of mechanisms used by *Giardia* to interact with the human immune system.

Also, as suggested by others [11,18,19], we reinforced that GlADI is a remarkable virulence and pathogenicity factor of *G. lamblia*. Previous studies have found that GlADI can induce immune responses. Muñoz et al. demonstrated the direct role of GlADI in causing the activation of mast cells [19]. However, the authors did not study further implications that structural factors of GlADI could be playing on the observed phenomenon.

We show that GlADI stimulates the membrane-bounded TLRs two and four. Moreover, our results show that rabeprazole not only inhibits GlADI enzyme activity, as previously reported [16] but also interferes with its immunomodulatory effects on TLRs, likely by breaking GlADI disulfide bonds and inducing its denaturation. The enzyme activity of GlADI is susceptible to rabeprazole since C424 is part of the catalytic triad. Because of this, concentrations of rabeprazole as low as 50 μM can completely inhibit the enzyme [16], whereas high concentrations of rabeprazole start affecting the rest of the cysteine residues and even break disulfide bridges.

VSPs and other Cys-rich proteins found in *G. lamblia* are exposed to the milieu. They are thought to protect the parasite under the digestive conditions of the upper small intestine [31]. Cysteines are widely distributed in the proteome of *Giardia* [32], and they potentially can bond their sulfur atoms to form the so-called disulfide bonds. These covalent linkages are formed from nonadjacent Cys residues and stabilize the protein 3D structure. In several microorganisms, protein stability often relies on the formation of disulfide bonds to tackle extra cytoplasmic environments [33,34]. Although GlADI is not classified as a Cys-rich protein, its 16 Cys residues per subunit and its ability to be found extracellularly allowed us to assume that it can possess a strong stabilized 3D structure. Our findings of GlADI intrinsic fluorescence under denaturing and reducing conditions support the hypothesis that the disulfide bridges are reinforcing its 3D structure, which could allow it to resist adverse conditions such as those found in the intestinal milieu.

To gain insight into how the 3D structure of GlADI influences the TLR's immunomodulatory effect observed, we performed molecular docking studies to identify the sites of interaction of GlADI with TLRs. To that end, GlADI crystallographic structure was needed; however, since it is still unknown, we constructed it by using the neural network AlphaFold, which is the first computational approach capable of predicting protein structures to near experimental accuracy in most cases [35]. For TLR2-TLR1, we show that the AlphaFold-predicted GlADI homodimer structure docked over a previously described region important for ligand binding and dimerization. This prediction suggests that GlADI possibly establishes contacts with TLR1 amino acid residues such as V311, F312, and G313, which participate in the binding of ligands to induce immune activation and cytokine release [25]. Such interactions have an important role in the interaction of TLR1 with agonistic ligands such as the di and tri-acylated synthetic lipopeptides Pam_2CSK_4, Pam_3CSK_4, and macrophage-activating lipopeptide-2 (MALP-2) and FSL-1 [25,36]. This finding is in line with others since various proteins have been described as newly discovered TLR2 ligands [37]. Altogether these findings allow us to hypothesize that GlADI might be activating the TLR2-TLR1 heterodimer through mechanisms not defined yet, which could be different from those reported for bacterial lipopeptides. Therefore, further studies are needed to understand the mechanisms underlying the stimulation of TLR2 by GlADI.

Molecular docking supports the possibility of establishing interactions of both TLR4 and MD2 with GlADI through amino acid residues previously described as part of the ligand binding region. This could explain the capacity of GlADI to activate TLR4 more

sensitively than that of TLR2. TLR4 is a membrane-bound innate immune receptor protein of 96 kDa that acts as an innate immune sensor against a broad group of invading pathogens, from viruses to multicellular parasites [26,38–40]. GlADI is not the first protein from *G. lamblia* with TLR4 activation capacity; others, such as VSPs, have been found to stimulate host innate immune responses in a TLR4-dependent manner [31]. Moreover, TLR4 can bind other ligands in addition to LPS, such as various small molecules and endogenous or exogenous proteins [26,39,41–51], as demonstrated for other diseases such as lymphatic filariasis [40]. Since our in silico proposal predicts protein–protein interactions, it is important to note that molecular docking studies of TLR4 with other proteins, such as the native spike protein of SARS-CoV-2 virus (PDB ID: 6VYB), demonstrated significant binding to TLR4 [52]. Without leaving aside the current lack of experimental evidence about the accuracy of AlphaFold-predicted structures applied in docking predictions, it is interesting to compare the results obtained by using an experimentally resolved 3D structure (as in the case of SARS-CoV-2 spike glycoprotein) and those obtained by us with the AlphaFold-predicted GlADI structure. Compared with those studies, we propose that GlADI might interact with amino acid residues from the leucine-rich repeats (LRR) 3–5 of TLR4, while spike protein is predicted to interact with LRRs 9–13. Furthermore, while spike protein does not interact with residues involved in the canonical activation pathway of TLR4, our results suggest a probability of GlADI doing it (i.e., K388). Additionally, GlADI could interact with K122 from MD2, which is part of the ligand binding region.

DCs are key players in the intestine immunity present under the epithelial lining of the gastrointestinal tract. They can sample the luminal content by protruding their dendrites into the lumen to distinguish harmful from harmless antigens [53–55]. DCs are important initiators of mucosal immune responses both in adults and children. However, the clinical impact of giardiasis seems to be stronger in the first five years of life [56]. Thus we used DCs from umbilical cord blood since they are the most infant-like DCs than other DC models.

Here, the incubation of human infant-like DCs in the presence of GlADI provoked an enhanced release of the pro-inflammatory cytokines TNFα and IL-1β but decreased the release of MCP-1. This would be explained by the activation of the inflammatory response mediated by NF-κB signaling, which is essential for host defense against pathogens or their virulence factors such as GlADI. Accordingly, with our results, studies on rat mast cells showed enhanced release of TNFα after treatment with GlADI [19]. Moreover, a rodent model of infection with *Giardia* showed increased levels of TNFα in plasma [57]. Another study in mice proposed a protective role of this pro-inflammatory cytokine in giardiasis since animals devoid of TNFα showed that peak *Giardia* load levels were around 10-fold higher compared with control mice [58]. However, in the same study, transepithelial resistance was reduced to the same extent despite a much lighter parasite burden in TNFα-responsive mice. Certainly, TNF-α has a very important role in the early control of giardiasis, as previously demonstrated in *Giardia* infection using mouse models [58]. On the other hand, the atrophy of intestinal villi and dysfunction of the gut epithelial barrier detected in biopsy specimens from chronically infected patients with giardiasis can also be observed when healthy intestinal biopsy specimens are treated with TNFα [59,60]. Hence, the affectation on epithelial integrity during giardiasis might be due to parasite factors such as GlADI and host-defense factors such as TNFα.

We found that the release of the anti-inflammatory cytokine IL-10 was decreased in those DCs incubated in the presence of GlADI. This is in accordance with a previous report where the IL-10 production was found impaired in LPS-activated human monocyte-derived DCs (moDCs), which were exposed to GlADI [18]. Another study reported that children with symptomatic giardiasis had increased mucosal levels of pro-inflammatory cytokines, including TNFα. Such pro-inflammatory cytokines decreased after antigiardial treatment with the concomitant resolution of symptoms and an increase in IL-10 levels [61].

Regarding IL-1β, we found that GlADI increased the release of this pro-inflammatory cytokine by DCs. This increase in IL-1β has been suggested to be important for the

development and maturation of IL-17A-producing cells [62], which in turn may be essential for the rapid clearance of *Giardia* by humans [63].

Ligand binding to TLRs is the first event in a signaling process that allows defenses to be put in place for clearance of the infection and long-term protection via the molecular memory of the adaptive immunity. Considering the state of the art in cytokines release via TLRs stimulation, our results reinforce the proposal that GlADI could be an important factor in giardiasis that impairs the secretion of anti-inflammatory cytokines while enhancing the pro-inflammatory ones. The strengthened 3D structure of GlADI could help the parasite to long-term modulate the host immune response even after the loss of its enzyme activity. Even though AlphaFold is currently the most robust tool for predicting the 3D structure of proteins, it has not replaced the use of experimentally resolved 3D structures for molecular docking. However, it is important to note that it represents a good strategy to accelerate the design of new ways to treat diseases. Further studies are guaranteed to clarify how GlADI could participate in balancing the pathogenic versus host-protective factors during giardiasis.

4. Materials and Methods

4.1. Recombinant GlADI Expression and Endotoxin Removal

The expression and purification of GlADI were performed as previously described [16]. Once recombinant GlADI was purified, endotoxin levels were determined with the commercial Pierce™ LAL Chromogenic Endotoxin Quantitation Kit (Thermo Fisher, Waltham, MA, USA) according to the manufacturer's instructions. Since endotoxin concentration was above 1 EU/mL, it was removed from pure GlADI fraction by membrane affinity using syringe filters (Acrodisc™ Units with Mustang™ E Membrane, PALL, Port Washington, NY, USA). The endotoxin levels were 1.5 EU/mL before removal and 0.02 EU/mL after this process. As previously reported, these latter endotoxin concentrations do not influence the studied cells [64,65]. Nonetheless, to exclude any influence from endotoxin remnants, we added recombinant GlADI to the cells in the presence of 100 µg/mL of the endotoxin-blocker polymyxin B (Invivogen, Toulouse, France).

4.2. Reporter Cell Lines

THP1-XBlue™-MD2-CD14 human monocytes were used as reporter cell-line. This cell line endogenously expresses all human TLRs and has been genetically modified with the SEAP inducible reporter gene under the control of NF-κB and AP-1 promoters. It also has an extra insert for the expression of MD2 and CD14 accessory proteins, enhancing TLR signaling [30,66]. Human embryonic kidney cells (HEK-Blue™) expressing either human TLRs 2, 3, 4, 5, 7, 8, or 9 were used. Furthermore, this cell line has a SEAP reporter gene system. It is important to note that the HEK-Blue™ TLR2 cell line also expresses the TLRs 1 and 6. TLR2 forms active heterodimers with TLR1 and TLR6 [66]. All these cell lines were acquired from Invivogen (Invivogen, Toulouse, France). THP1-XBlue™-MD2-CD14 and HEK-Blue™ cell lines were cultured in RPMI-1640 medium with 2 mM glutamine and DMEM medium (Lonza, Basel, Switzerland), respectively. RPMI-1640 contained normocin 100 µg/mL (Invivogen, Toulouse, France) and DMEM medium penicillin/streptomycin 50 U/mL and 50 µg/mL. (Gibco, Leicestershire, UK). Both media were supplemented with 10% heat-inactivated fetal bovine serum (Sigma, St. Louis, MO, USA), sodium bicarbonate 1.5 g/L (Sigma, St. Louis, MO, USA), and sodium pyruvate 1 mM (Biowest, Nuaillé, France). Selection antibiotics (Invivogen, Toulouse, France) were the same as those previously reported [21]. Cell lines were passaged twice weekly and worked at 80% confluency, according to the manufacturer's instructions.

4.3. GlADI-TLRs Interaction Assays

In order to test TLRs activation, THP1-XBlue™-MD2-CD14 and HEK-Blue cell lines were incubated for 24 h at 37 °C and 5% CO_2, in 96-well plates, at cell densities previously reported [21] in the presence or absence of 10, 50, 100, 500 1000 and 2000 ng/mL of freshly

purified GlADI with 100 μg/mL of polymyxin B (InvivoGen, Toulouse, France). In order to challenge rabeprazole with the highest dose of GlADI to evaluate how efficiently this drug inhibited the capacity of GlADI to activate TLRs, the highest GlADI working concentration was added alone or in combination with 50 or 750 μM of rabeprazole (Sigma, St. Louis, MO, USA). Culture medium and agonists for each TLR reported [21] were included as positive and negative controls, respectively. Afterward, TLR activation was determined by quantitation of SEAP production. To this end, 20 μL of supernatant were incubated with Quantiblue™ reagent (Invivogen, Toulouse, France) for 1 h at 37 °C. Change in absorbance was measured at 655 nm in a Bio-Rad Benchmark Plus microplate spectrophotometer reader (Bio-Rad Laboratories B.V, Veenendaal, The Netherlands). Data were normalized relative to the negative control, which was set to 1.

HEK TLR2 cell lines express TLR2, TLR1, and TLR6 since signaling of TLR2 activation is dependent on TLR2/TLR6 and TLR1/TLR2 interaction. Activation and dimerization of TLR2/1 and TLR2/6 were confirmed by stimulation with the specific agonists Pam3CysSerLys4 (Pam3CSK4) and lipopeptide (FSL-1), respectively.

4.4. Dendritic Cells Culturing and Stimulation with GlADI

In order to investigate whether GlADI can influence cytokine production of DCs, human dendritic cells (DCs) were generated from CD34+ progenitor cells harvested from umbilical cord blood (MatTek Corporation, Ashland, MA, USA). DCs were defrosted and incubated with a maintenance medium containing cytokines (DC-MM, MatTek Corporation, Ashland, MA, USA) according to the manufacturer's instructions, for 24 h at 37 °C, in 96-well plates at a density of 70×10^4 cells/well to allow them to attach to the well bottom. After 24 h of incubation, DCs were incubated for 48 h at 37 °C and 5% CO_2 in a culture medium containing 500 ng/mL of freshly produced GlADI. In another set of experiments, to challenge DCs with the minimal dose of GlADI that activated TLRs, DCs were incubated with 500 ng/mL of GlADI in combination with 50 μM of Rabeprazole. For all cases, cell supernatants were collected and stored at −80 °C for their subsequent use. Six independent assays were performed. DCs treated with 10 ng/mL of lipopolysaccharide (LPS) from *E. coli* K12 (Invivogen, Toulouse, France) served as positive controls, and cells incubated only with a culture medium were used as negative controls.

4.5. Quantitation of Dendritic Cells Cytokines Production

In order to measure the levels of cytokines TNFα IL-10, IL-6, IL-1β, MCP-1/CCL2, and MIP-1α/CCL3, a magnetic Luminex ® Assay (R&D systems, Biotechne, Minneapolis, MN, USA) was used according to manufacturer's instructions. Briefly, serial dilutions of each cytokine standard were prepared. A mixture of magnetic microbeads with immobilized antibodies was added to a 96-well plate, followed by the addition of undiluted DC supernatants or standards. The plate was incubated overnight at 4 °C in constant shaking. After three washing steps, detection antibodies were added, and the plate was incubated for 30 min at room temperature under continuous shaking. After three more washing steps, the plate was incubated with streptavidin-PE for 30 min in constant shaking. Finally, after washing, magnetic microbeads were resuspended in 100 μL/well of wash buffer, followed by the plate analysis using a Luminex 200 system (Biotechne, Abingdon, UK). Cytokine data were analyzed with xPONENT 4.2 software (Luminex Corporation, 's-Hertogenbosch, The Netherlands).

4.6. Protein Thermal Shift Assay

The thermal shift assay was performed using a Protein Thermal Shift™ Dye Kit (×1000; Thermo Fisher Scientific; Waltham, MA, USA). Each reacted sample (60 μL) was mixed with SYPRO Orange dye (×2) (60 μL), and 20 μL was dispensed into a tube. Using the StepOnePlus real-time PCR system (Applied Biosystems, Carlsbad, CA, USA), the sample was thermally denatured by increasing the temperature from 25 °C to 99 °C at a rate of 0.16 °C/min; the fluorescence intensity was measured. Data were analyzed

using Protein Thermal Shift Software v1.0 (Applied Biosystems; Foster City, CA, USA) to determine the Tm value. The Tm value was used based on the Boltzmann fitting of the fluorescence/temperature raw data (TmB value).

In the thermal shift assay, when a fluorescent dye is added to a protein and heated, the dye binds to exposed hydrophobic sites, which causes it to fluoresce, and the change in fluorescence intensity can be measured to analyze the structural changes in the protein.

4.7. Fluorescence Emission Spectra

The intrinsic fluorescence is used to follow the exposure to solvent of aromatic amino acid residues that occurs during the protein unfolding, which is accompanied by a decrease in quantum yield and a redshift of the maximal emission wavelength. Fluorescence experiments were performed using a Perkin–Elmer LS55 spectrofluorometer (Perkin-Elmer, Waltham, MA, USA) at 25 °C and a protein concentration of 65 µg/mL. The intrinsic fluorescence of the enzymes was determined at an excitation wavelength of 295 nm, and the emission spectra were recorded from 310 to 500 nm, with an integration time of 1s, using excitation and emission slits of 3.5 nm each. Each spectrum was the average of three scans with two experimental repetitions. The spectra of blanks were subtracted from those containing protein.

4.8. Prediction of the Three-Dimensional (3D) Structure of GlADI

Since the experimentally determined 3D structure of GlADI is still unavailable, we used its primary sequence (UniProt code Q27657) to predict the 3D atomic coordinates of folded protein structure. AlphaFold Monomer v2.0 pipeline [35] was used in the Colab server (https://colab.research.google.com/github/sokrypton/ColabFold/blob/main/AlphaFold2.ipynb (accessed on 2 July 2022)). The predicted protein structure started from their sequence, using a slightly simplified version of AlphaFold v2.0 without selecting a specific existing structural template. Notably, the obtained protein structure of the monomer includes the C-terminal end, which is absent in any other homology models previously described [16,67,68]. This latter is relevant since GlADI is the enzyme of its type that shows the most extended C-terminal domain described until today [68]. The dimer was constructed with PyMOL [69] using crystallographic symmetry based on the atomic coordinates of arginine deiminase from *Pseudomonas auruginosa* (PDB code: 2A9G).

4.9. Prediction of the Probably Binding Mode of GlADI to TLRs by Using the AlphaFold-Predicted Structure and Molecular Docking

Before docking analyses, YASARA Energy Minimization Server [70] was used to attain a minimum energy arrangement of the AlphaFold-predicted 3D structure of GlADI. The HDOCK server for integrated protein–protein docking [24] was used to carry out molecular docking between the dimer of the AlphaFold-predicted structure of GlADI and TLR2-TLR1 (PDB code: 2Z7X) or TLR4-MD2 (PDB code: 3FXI) dimers. In our analyses, we established GlADI as the ligand molecule while TLR2-TLR1 or TLR4-MD2 dimers were established as receptor molecules. Results of HDOCK simulations were confirmed by submitting HDOCK-generated protein–protein complexes to PRODIGY [71].

4.10. Statistical Analyses

Data were analyzed with GraphPad Prism™ software (version 8.2.1 for Windows™, San Diego, CA, USA). The normal distribution of data was assessed with the Shapiro–Wilk test. Normally distributed data were analyzed with one-way ANOVA followed by Dunnett's multiple comparisons adjustment. Non-parametric distributed data were analyzed with the Mann–Whitney U test or Friedman test, followed by Dunn's multiple comparisons adjustment test. Results are expressed as mean ± SD or the median and interquartile range (IQR) for data with parametric and non-parametric distribution, respectively. A p-value < 0.05 was statistically significant (* $p < 0.05$, ** $p < 0.01$, *** $p < 0.001$, **** $p < 0.0001$).

Supplementary Materials: The supporting information can be downloaded at: https://www.mdpi.com/article/10.3390/ijms231911552/s1.

Author Contributions: Conceptualization, G.L.-V., C.F.-L.; Supervision, G.L.-V.; Methodology, G.L.-V.; Investigation, C.F.-L., I.d.l.M.-d.l.M., I.G.-T., S.E.-F., L.A.F.-L.; Formal analysis, P.G.-C.; Funding acquisition, G.L.-V., P.G.-C.; Writing original draft, C.F.-L., G.L.-V.; Writing-review and editing, G.L.-V., P.d.V. All authors have read and agreed to the published version of the manuscript.

Funding: This research was partly funded by Programa de Recursos Fiscales para Investigación from Instituto Nacional de Pediatría, grant number 2019/062.

Data Availability Statement: Data are contained within the article.

Acknowledgments: C.F.-L. was financially supported by Abel Tasman Talent Program Sandwich Ph.D. from the University of Groningen—University Medical Center Groningen, UG/UMCG in collaboration with Universidad Nacional Autónoma de México, UNAM, and CONACyT (#260625).

Conflicts of Interest: The authors declare no conflict of interest.

References

1. Dizdar, V.; Gilja, O.H.; Hausken, T. Increased visceral sensitivity in *Giardia*-induced postinfectious irritable bowel syndrome and functional dyspepsia. Effect of the 5HT3-antagonist ondansetron. *Neurogastroenterol. Motil.* **2007**, *19*, 977–982. [CrossRef] [PubMed]
2. Kamda, J.D.; Singer, S.M. Phosphoinositide 3-kinase-dependent inhibition of dendritic cell interleukin-12 production by *Giardia lamblia*. *Infect. Immun.* **2009**, *77*, 685–693. [CrossRef] [PubMed]
3. Buret, A.G.; Cacciò, S.M.; Favennec, L.; Svärd, S. Update on Giardia: Highlights from the seventh International *Giardia* and Cryptosporidium Conference. *Parasite* **2020**, *27*, 49. [CrossRef]
4. Singer, S.M.; Fink, M.Y.; Angelova, V.V. Recent insights into innate and adaptive immune responses to *Giardia*. *Adv. Parasitol.* **2019**, *106*, 171–208. [PubMed]
5. Balmer, E.A.; Faso, C. The Road Less Traveled? Unconventional Protein Secretion at Parasite-Host Interfaces. *Front. Cell Dev. Biol.* **2021**, *9*, 662711. [CrossRef] [PubMed]
6. Rabouille, C.; Malhotra, V.; Nickel, W. Diversity in unconventional protein secretion. *J. Cell Sci.* **2012**, *125*, 5251–5255. [CrossRef] [PubMed]
7. Schofield, P.; Costello, M.; Edwards, M.; O'sullivan, W. The arginine dihydrolase pathway is present in *Giardia intestinalis*. *Int. J. Parasitol.* **1990**, *20*, 697–699. [CrossRef]
8. Schofield, P.J.; Edwards, M.R.; Matthews, J.; Wilson, J.R. The pathway of arginine catabolism in *Giardia intestinalis*. *Mol. Biochem. Parasitol.* **1992**, *51*, 29–36. [CrossRef]
9. Eckmann, L.; Laurent, F.; Langford, T.D.; Hetsko, M.L.; Smith, J.R.; Kagnoff, M.F.; Gillin, F.D. Nitric oxide production by human intestinal epithelial cells and competition for arginine as potential determinants of host defense against the lumen-dwelling pathogen *Giardia lamblia*. *J. Immunol.* **2000**, *164*, 1478–1487. [CrossRef]
10. Touz, M.C.; Rópolo, A.S.; Rivero, M.R.; Vranych, C.V.; Conrad, J.T.; Svard, S.G.; Nash, T.E. Arginine deiminase has multiple regulatory roles in the biology of *Giardia lamblia*. *J. Cell Sci.* **2008**, *121*, 2930–2938. [CrossRef]
11. Ringqvist, E.; Palm, J.E.; Skarin, H.; Hehl, A.B.; Weiland, M.; Davids, B.J.; Reiner, D.S.; Griffiths, W.J.; Eckmann, L.; Gillin, F.D.; et al. Release of metabolic enzymes by *Giardia* in response to interaction with intestinal epithelial cells. *Mol. Biochem. Parasitol.* **2008**, *159*, 85–91. [CrossRef] [PubMed]
12. Rópolo, A.S.; Touz, M.C. A lesson in survival, by *Giardia lamblia*. *ScientificWorldJournal* **2010**, *10*, 2019–2031. [CrossRef] [PubMed]
13. Stadelmann, B.; Merino, M.C.; Persson, L.; Svärd, S.G. Arginine consumption by the intestinal parasite *Giardia intestinalis* reduces proliferation of intestinal epithelial cells. *PLoS ONE* **2012**, *7*, e45325. [CrossRef]
14. Bronte, V.; Zanovello, P. Regulation of immune responses by L-arginine metabolism. *Nat. Rev. Immunol.* **2005**, *5*, 641–654. [CrossRef]
15. Das, P.; Lahiri, A.; Lahiri, A.; Chakravortty, D. Modulation of the arginase pathway in the context of microbial pathogenesis: A metabolic enzyme moonlighting as an immune modulator. *PLoS Pathog.* **2010**, *6*, e1000899. [CrossRef] [PubMed]
16. Fernández-Lainez, C.; de la Mora-de la Mora, I.; García-Torres, I.; Enríquez-Flores, S.; Flores-López, L.A.; Gutiérrez-Castrellón, P.; Yépez-Mulia, L.; Matadamas-Martínez, F.; de Vos, P.; López-Velázquez, G. Multilevel Approach for the Treatment of Giardiasis by Targeting Arginine Deiminase. *Int. J. Mol. Sci.* **2021**, *22*, 9491. [CrossRef]
17. Palm, J.E.; Weiland, M.E.; Griffiths, W.J.; Ljungström, I.; Svärd, S.G. Identification of immunoreactive proteins during acute human giardiasis. *J. Infect. Dis.* **2003**, *187*, 1849–1859. [CrossRef]
18. Banik, S.; Renner Viveros, P.; Seeber, F.; Klotz, C.; Ignatius, R.; Aebischer, T. *Giardia duodenalis* arginine deiminase modulates the phenotype and cytokine secretion of human dendritic cells by depletion of arginine and formation of ammonia. *Infect. Immun.* **2013**, *81*, 2309–2317. [CrossRef]

19. Muñoz-Cruz, S.; Gomez-García, A.; Matadamas-Martínez, F.; Alvarado-Torres, J.A.; Meza-Cervantez, P.; Arriaga-Pizano, L.; Yépez-Mulia, L. *Giardia lamblia*: Identification of molecules that contribute to direct mast cell activation. *Parasitol. Res.* **2018**, *117*, 2555–2567. [CrossRef]
20. Bryant, C.E.; Gay, N.J.; Heymans, S.; Sacre, S.; Schaefer, L.; Midwood, K.S. Advances in Toll-like receptor biology: Modes of activation by diverse stimuli. *Crit. Rev. Biochem. Mol. Biol.* **2015**, *50*, 359–379. [CrossRef]
21. Fernández-Lainez, C.; Akkerman, R.; Oerlemans, M.; Logtenberg, M.; Schols, H.; Silva-Lagos, L.; López-Velázquez, G.; de Vos, P. β (2→6)-Type fructans attenuate proinflammatory responses in a structure dependent fashion via Toll-like receptors. *Carbohydr. Polym.* **2022**, *277*, 118893. [CrossRef] [PubMed]
22. Zhang, Y.; Liang, X.; Bao, X.; Xiao, W.; Chen, G. Toll-like receptor 4 (TLR4) inhibitors: Current research and prospective. *Eur. J. Med. Chem.* **2022**, *235*, 114291. [CrossRef] [PubMed]
23. Ferrè, F.; Clote, P. DiANNA: A web server for disulfide connectivity prediction. *Nucleic Acids Res.* **2005**, *33* (Suppl. S2), W230–W232. [CrossRef]
24. Yan, Y.; Tao, H.; He, J.; Huang, S.Y. The HDOCK server for integrated protein-protein docking. *Nat. Protoc.* **2020**, *15*, 1829–1852. [CrossRef] [PubMed]
25. Jin, M.S.; Kim, S.E.; Heo, J.Y.; Lee, M.E.; Kim, H.M.; Paik, S.G.; Lee, H.; Lee, J.O. Crystal structure of the TLR1-TLR2 heterodimer induced by binding of a tri-acylated lipopeptide. *Cell* **2007**, *130*, 1071–1082. [CrossRef] [PubMed]
26. Mukherjee, S.; Karmakar, S.; Babu, S.P. TLR2 and TLR4 mediated host immune responses in major infectious diseases: A review. *Braz. J. Infect. Dis.* **2016**, *20*, 193–204. [CrossRef]
27. Kucera, K.; Koblansky, A.A.; Saunders, L.P.; Frederick, K.B.; De La Cruz, E.M.; Ghosh, S.; Modis, Y. Structure-based analysis of Toxoplasma gondii profilin: A parasite-specific motif is required for recognition by Toll-like receptor 11. *J. Mol. Biol.* **2010**, *403*, 616–629. [CrossRef]
28. Rana, A.; Akhter, Y. A multi-subunit based, thermodynamically stable model vaccine using combined immunoinformatics and protein structure based approach. *Immunobiology* **2016**, *221*, 544–557. [CrossRef]
29. Safavi, A.; Kefayat, A.; Mahdevar, E.; Abiri, A.; Ghahremani, F. Exploring the out of sight antigens of SARS-CoV-2 to design a candidate multi-epitope vaccine by utilizing immunoinformatics approaches. *Vaccine* **2020**, *38*, 7612–7628. [CrossRef]
30. Cheng, L.; Kiewiet, M.B.; Groeneveld, A.; Nauta, A.; de Vos, P. Human milk oligosaccharides and its acid hydrolysate LNT2 show immunomodulatory effects via TLRs in a dose and structure-dependent way. *J. Funct. Foods* **2019**, *59*, 174–184. [CrossRef]
31. Serradell, M.C.; Rupil, L.L.; Martino, R.A.; Prucca, C.G.; Carranza, P.G.; Saura, A.; Fernández, E.A.; Gargantini, P.R.; Tenaglia, A.H.; Petiti, J.P.; et al. Efficient oral vaccination by bioengineering virus-like particles with protozoan surface proteins. *Nat. Commun.* **2019**, *10*, 361. [CrossRef]
32. Emery-Corbin, S.J.; Grüttner, J.; Svärd, S. Transcriptomic and proteomic analyses of *Giardia intestinalis*: Intestinal epithelial cell interactions. *Adv. Parasitol.* **2020**, *107*, 139–171. [PubMed]
33. Heras, B.; Kurz, M.; Shouldice, S.R.; Martin, J.L. The name's bond.....disulfide bond. *Curr. Opin. Struct. Biol.* **2007**, *17*, 691–698. [CrossRef] [PubMed]
34. Goemans, C.; Denoncin, K.; Collet, J.F. Folding mechanisms of periplasmic proteins. *Biochim. Biophys. Acta* **2014**, *1843*, 1517–1528. [CrossRef] [PubMed]
35. Jumper, J.; Evans, R.; Pritzel, A.; Green, T.; Figurnov, M.; Ronneberger, O.; Tunyasuvunakool, K.; Bates, R.; Žídek, A.; Potapenko, A.; et al. Highly accurate protein structure prediction with AlphaFold. *Nature* **2021**, *596*, 583–589. [CrossRef] [PubMed]
36. Buwitt-Beckmann, U.; Heine, H.; Wiesmüller, K.H.; Jung, G.; Brock, R.; Akira, S.; Ulmer, A.J. TLR1- and TLR6-independent recognition of bacterial lipopeptides. *J. Biol. Chem.* **2006**, *281*, 9049–9057. [CrossRef]
37. Van Bergenhenegouwen, J.; Plantinga, T.S.; Joosten, L.A.; Netea, M.G.; Folkerts, G.; Kraneveld, A.D.; Garssen, J.; Vos, A.P. TLR2 & Co: A critical analysis of the complex interactions between TLR2 and coreceptors. *J. Leukoc. Biol* **2013**, *94*, 885–902.
38. Mukherjee, S.; Karnam, A.; Das, M.; Babu, S.P.S.; Bayry, J. Wuchereria bancrofti filaria activates human dendritic cells and polarizes T helper 1 and regulatory T cells via toll-like receptor 4. *Commun. Biol.* **2019**, *2*, 169. [CrossRef]
39. Mukherjee, S.; Mukherjee, S.; Bhattacharya, S.; Sinha Babu, S.P. Surface proteins of Setaria cervi induce inflammation in macrophage through Toll-like receptor 4 (TLR4)-mediated signalling pathway. *Parasite Immunol.* **2017**, *39*, e12389. [CrossRef]
40. Mukherjee, S.; Mukherjee, S.; Maiti, T.K.; Bhattacharya, S.; Sinha Babu, S.P. A Novel Ligand of Toll-like Receptor 4 From the Sheath of Wuchereria bancrofti Microfilaria Induces Proinflammatory Response in Macrophages. *J. Infect. Dis.* **2017**, *215*, 954–965. [CrossRef]
41. Bryant, C.E.; Spring, D.R.; Gangloff, M.; Gay, N.J. The molecular basis of the host response to lipopolysaccharide. *Nat. Rev. Microbiol.* **2010**, *8*, 8–14. [CrossRef] [PubMed]
42. Bulut, Y.; Faure, E.; Thomas, L.; Karahashi, H.; Michelsen, K.S.; Equils, O.; Morrison, S.G.; Morrison, R.P.; Arditi, M. Chlamydial heat shock protein 60 activates macrophages and endothelial cells through Toll-like receptor 4 and MD2 in a MyD88-dependent pathway. *J. Immunol.* **2002**, *168*, 1435–1440. [CrossRef] [PubMed]
43. Tang, Y.; Zhou, Y.; Fan, S.; Wen, Q. The Multiple Roles and Therapeutic Potential of HSP60 in Cancer. *Biochem. Pharmacol.* **2022**, *201*, 115096. [CrossRef]
44. Asea, A.; Rehli, M.; Kabingu, E.; Boch, J.A.; Baré, O.; Auron, P.E.; Stevenson, M.A.; Calderwood, S.K. Novel signal transduction pathway utilized by extracellular HSP70: Role of toll-like receptor (TLR) 2 and TLR4. *J. Biol. Chem.* **2002**, *277*, 15028–15034. [CrossRef]

45. Lee, J.H.; Jeon, J.; Bai, F.; Jin, S.; Wu, W.; Ha, U.H. The Pseudomonas aeruginosa HSP70-like protein DnaK induces IL-1β expression via TLR4-dependent activation of the NF-κB and JNK signaling pathways. *Comp. Immunol. Microbiol. Infect. Dis.* **2019**, *67*, 101373. [CrossRef] [PubMed]
46. Smiley, S.T.; King, J.A.; Hancock, W.W. Fibrinogen stimulates macrophage chemokine secretion through toll-like receptor 4. *J. Immunol.* **2001**, *167*, 2887–2894. [CrossRef]
47. Guillot, L.; Balloy, V.; McCormack, F.X.; Golenbock, D.T.; Chignard, M.; Si-Tahar, M. Cutting edge: The immunostimulatory activity of the lung surfactant protein-A involves Toll-like receptor 4. *J. Immunol.* **2002**, *168*, 5989–5992. [CrossRef]
48. Okamura, Y.; Watari, M.; Jerud, E.S.; Young, D.W.; Ishizaka, S.T.; Rose, J.; Chow, J.C.; Strauss, J.F., 3rd. The extra domain A of fibronectin activates Toll-like receptor 4. *J. Biol. Chem.* **2001**, *276*, 10229–10233. [CrossRef]
49. Vabulas, R.M.; Braedel, S.; Hilf, N.; Singh-Jasuja, H.; Herter, S.; Ahmad-Nejad, P.; Kirschning, C.J.; Da Costa, C.; Rammensee, H.G.; Wagner, H.; et al. The endoplasmic reticulum-resident heat shock protein Gp96 activates dendritic cells via the Toll-like receptor 2/4 pathway. *J. Biol. Chem.* **2002**, *277*, 20847–208453. [CrossRef]
50. Park, J.S.; Svetkauskaite, D.; He, Q.; Kim, J.Y.; Strassheim, D.; Ishizaka, A.; Abraham, E. Involvement of toll-like receptors 2 and 4 in cellular activation by high mobility group box 1 protein. *J. Biol. Chem.* **2004**, *279*, 7370–7377. [CrossRef]
51. Zhao, Y.; Kuang, M.; Li, J.; Zhu, L.; Jia, Z.; Guo, X.; Hu, Y.; Kong, J.; Yin, H.; Wang, X.; et al. SARS-CoV-2 spike protein interacts with and activates TLR41. *Cell Res.* **2021**, *31*, 818–820. [CrossRef]
52. Choudhury, A.; Mukherjee, S. In silico studies on the comparative characterization of the interactions of SARS-CoV-2 spike glycoprotein with ACE-2 receptor homologs and human TLRs. *J. Med. Virol.* **2020**, *92*, 2105–2113. [CrossRef]
53. Stagg, A.J. Intestinal Dendritic Cells in Health and Gut Inflammation. *Front. Immunol.* **2018**, *9*, 2883. [CrossRef]
54. Tezuka, H.; Ohteki, T. Regulation of IgA Production by Intestinal Dendritic Cells and Related Cells. *Front. Immunol.* **2019**, *10*, 1891. [CrossRef]
55. Mowat, A.M. Anatomical basis of tolerance and immunity to intestinal antigens. *Nat. Rev. Immunol.* **2003**, *3*, 331–341. [CrossRef]
56. Kotloff, K.L.; Nataro, J.P.; Blackwelder, W.C.; Nasrin, D.; Farag, T.H.; Panchalingam, S.; Wu, Y.; Sow, S.O.; Sur, D.; Breiman, R.F.; et al. Burden and aetiology of diarrhoeal disease in infants and young children in developing countries (the Global Enteric Multicenter Study, GEMS): A prospective, case-control study. *Lancet* **2013**, *382*, 209–222. [CrossRef]
57. Abo-Zaid, M.A.; Hamdi, A.A. Evaluation of immune response and haematological parameters in infected male albino rats by giardiasis. *Parasite Immunol.* **2022**, *44*, e12908. [CrossRef]
58. Zhou, P.; Li, E.; Shea-Donohue, T.; Singer, S.M. Tumour necrosis factor alpha contributes to protection against *Giardia lamblia* infection in mice. *Parasite Immunol.* **2007**, *29*, 367–374. [CrossRef]
59. Troeger, H.; Epple, H.J.; Schneider, T.; Wahnschaffe, U.; Ullrich, R.; Burchard, G.D.; Jelinek, T.; Zeitz, M.; Fromm, M.; Schulzke, J.D. Effect of chronic *Giardia lamblia* infection on epithelial transport and barrier function in human duodenum. *Gut* **2007**, *56*, 328–335. [CrossRef]
60. Schmitz, H.; Fromm, M.; Bentzel, C.J.; Scholz, P.; Detjen, K.; Mankertz, J.; Bode, H.; Epple, H.J.; Riecken, E.O.; Schulzke, J.D. Tumor necrosis factor-alpha (TNFalpha) regulates the epithelial barrier in the human intestinal cell line HT-29/B6. *J. Cell Sci.* **1999**, *112*, 137–146. [CrossRef]
61. Maciorkowska, E.; Kaczmarski, M.; Kemona, A. The role of cytokines in giardiasis in children. *Med. Wieku Rozw.* **2005**, *9*, 665–673.
62. Annunziato, F.; Romagnani, C.; Romagnani, S. The 3 major types of innate and adaptive cell-mediated effector immunity. *J. Allergy Clin. Immunol.* **2015**, *135*, 626–635. [CrossRef] [PubMed]
63. Saghaug, C.S.; Sørnes, S.; Peirasmaki, D.; Svärd, S.; Langeland, N.; Hanevik, K. Human memory CD4+ T cell immune responses against *Giardia lamblia*. *Clin. Vaccine Immunol.* **2016**, *23*, 11–18. [CrossRef]
64. Lépine, A.; de Vos, P. Synbiotic Effects of the Dietary Fiber Long-Chain Inulin and Probiotic *Lactobacillus acidophilus* W37 Can be Caused by Direct, Synergistic Stimulation of Immune Toll-Like Receptors and Dendritic Cells. *Mol. Nutr. Food Res.* **2018**, *62*, 1800251. [CrossRef]
65. Vogt, L.; Ramasamy, U.; Meyer, D.; Pullens, G.; Venema, K.; Faas, M.M.; Schols, H.A.; de Vos, P. Immune modulation by different types of β2→ 1-fructans is toll-like receptor dependent. *PLoS ONE* **2013**, *8*, e68367. [CrossRef]
66. Sahasrabudhe, N.M.; Beukema, M.; Tian, L.; Troost, B.; Scholte, J.; Bruininx, E.; Bruggeman, G.; van den Berg, M.; Scheurink, A.; Schols, H.A. Dietary fiber pectin directly blocks toll-like receptor 2–1 and prevents doxorubicin-induced ileitis. *Front. Immunol.* **2018**, *9*, 383. [CrossRef]
67. Li, Z.; Kulakova, L.; Li, L.; Galkin, A.; Zhao, Z.; Nash, T.E.; Mariano, P.S.; Herzberg, O.; Dunaway-Mariano, D. Mechanisms of catalysis and inhibition operative in the arginine deiminase from the human pathogen *Giardia lamblia*. *Bioorganic Chem.* **2009**, *37*, 149–161. [CrossRef]
68. Trejo-Soto, P.J.; Aguayo-Ortiz, R.; Yépez-Mulia, L.; Hernández-Campos, A.; Medina-Franco, J.L.; Castillo, R. Insights into the structure and inhibition of *Giardia intestinalis* arginine deiminase: Homology modeling, docking, and molecular dynamics studies. *J. Biomol. Struct. Dyn.* **2016**, *34*, 732–748. [CrossRef]
69. Schrödinger, L.; DeLano, W. PyMOL. In *The PyMOL Molecular Graphics System*; Version 1.2r3pre; Schrödinger, LLC: New York, NY, USA, 2010.

70. Krieger, E.; Joo, K.; Lee, J.; Lee, J.; Raman, S.; Thompson, J.; Tyka, M.; Baker, D.; Karplus, K. Improving physical realism, stereochemistry, and side-chain accuracy in homology modeling: Four approaches that performed well in CASP8. *Proteins* **2009**, *77*, 114–122. [CrossRef]
71. Xue, L.C.; Rodrigues, J.P.; Kastritis, P.L.; Bonvin, A.M.; Vangone, A. PRODIGY: A web server for predicting the binding affinity of protein–protein complexes. *Bioinformatics* **2016**, *32*, 3676–3678. [CrossRef]

CAPÍTULO 8

Discusión General y Conclusiones

El intestino es un complejo ecosistema, el cual juega un papel crucial en la salud humana. Los componentes que coexisten en este sistema están altamente concentrados en el epitelio intestinal. Ellos establecen una comunicación continua en el mismo sitio en donde se asimilan los nutrientes y donde ocurre la modulación del sistema inmune (Martín, Miquel, Ulmer, Langella, & Bermudez-Humaran, 2014). Los factores que regulan el ambiente intestinal tienen implicaciones locales y sistémicas, las cuales dependen de los alimentos que consumimos y continúan junto con los microorganismos que acompañan dichos alimentos. Es por ello que una dieta occidentalizada, rica en grasas y carbohidratos de alto índice glicémico, junto con un consumo insuficiente de fibras dietéticas (FDs), causan un incremento en la incidencia global de enfermedades no transmisibles (Patry & Nagler, 2021).

Por el contrario, un alto consumo de FDs ayuda al envejecimiento sano y disminuye el riesgo de desarrollar enfermedades crónicas (Dreher, 2018). El tracto gastrointestinal (GI) y el sistema inmune intestinal son piezas esenciales en este círculo virtuoso, destacándolos como blancos para contrarrestar varias enfermedades. Sin embargo, los mecanismos que subyacen dichos efectos benéficos de las FDs no han sido descubiertos por completo. El papel de la ingestión de fibra en la salud depende fuertemente del tipo de fibra. Los fructanos son un grupo importante de FDs que poseen benéficos directos a la salud. Los fructanos son carbohidratos a base de fructosa cuya longitud de cadena o grado de polimerización (GP)son variables (Roberfroid, 2005). Aquellos extraídos de plantas son carbohidratos no estructurales y solubles en agua que sirven como reservorios de energía (Van den Ende, 2013).

El tipo de FD consumida varía marcadamente por región geográfica (Stephen et al., 2017). En Europa, los fructanos extraídos de la planta de la achicoria (*Cichorium intybus*) son los más utilizados en suplementos alimenticios como fuente de FD (Fan, Cao, & Zhang, 2016). Mientras que en regiones como Latinoamérica, las plantas de la familia del agave (*Agave tequilana*, *A. americana*, *A. angustifolia*, etc.), las cuales son endémicas de la región, representan una fuente rica en fructanos. Debido a que estos fructanos también podrían ser utilizados como FDs para la suplementación de los alimentos (López & Urías-Silvas, 2007; López-Velázquez et al., 2015), comprender los mecanismos que subyacen los efectos de los fructanos, podría ayudar al desarrollo de estrategias nutricionales. Dichas estrategias podrían ser dirigidas a poblaciones vulnerables que habitan las regiones donde el agave es endémico y mas allá.

El consumo de los fructanos influencia benéficamente el desarrollo inmune y la función de la barrera intestinal (Vogt et al., 2015). Más aún, sus beneficios dependen del tipo de fructano y de su GP. Estos oligosacáridos pasan por el estómago sin mayor hidrólisis debido a que resisten las enzimas humanas digestivas. Posteriormente, alcanzan el colon, donde la microbiota intestinal los utiliza para generar productos metabólicos, tales como los ácidos grasos de cadena corta (SCFAs, por sus siglas en inglés) (Lambertz, Weiskirchen, Landert, & Weiskirchen, 2017). La achicoria y el agave son dos plantas estudiadas principalmente por sus fructanos y su influencia en la salud (**Capítulo 1**). La evidencia científica más extensa acerca del papel de los fructanos en la salud es atribuible a sus propiedades prebióticas (Vandeputte et al., 2017). Por ejemplo, el impacto de los fructanos incorporados a la fórmula infantil y su efecto en los perfiles de la microbiota intestinal a es vasto campo de estudio (Closa-Monasterolo et al., 2013; Costalos, Kapiki, Apostolou, & Papathoma, 2008; Kapiki et al., 2007; Knol et al., 2005; López-Velázquez et al., 2013; López-Velázquez et al., 2015; Wernimont, Northington, Kullen, Yao, & Bettler, 2015). Evidencia creciente indica que las enfermedades intestinales, la obesidad e incluso el cáncer podrían ser tratados con fructanos de la achicoria o del agave (Espinosa-Andrews, Urias-Silvas, & Morales-Hernández, 2021; Quiñones-Muñoz, Villanueva-Rodríguez, & Torruco-Uco, 2022; Wan et al., 2020), como se muestra en el **Capítulo 1**. Aunque también cruciales en la salud, los efectos directos de los fructanos, especialmente los del agave, en las células inmunes y su potencial de proteger la barrera intestinal no han sido estudiados tan extensivamente.

En esta tesis nos propusimos comprender cómo y en qué medida los fructanos del agave pueden modular y proteger contra enfermedades, así como apoyar a la salud. Para determinar los efectos directos inmunomoduladores de los fructanos del agave, los estudiamos y comparamos con los efectos de los fructanos de la achicoria para evaluar el impacto de estos dos fructanos estructuralmente diferentes (lineales vs ramificados) en la señalización de los receptores tipo Toll (TLRs). Mediante técnicas de docking molecular, estudiamos el modo de interacción de estos fructanos con los TLRs y propusimos una explicación mecanística de los resultados experimentales. También, se utilizaron inhibidores de las vías MyD88 y TRIF para determinar la vía por la cual estos fructanos ejercen sus efectos en la activación de NF- κB/AP-1. Además, pudimos identificar diferencias atribuibles al GP al probar diferentes longitudes de cadena de estos dos tipos de fructanos. Dichas características de los fructanos nos permitieron revelar el impacto que tiene la estructura en: a) la producción de citocinas por las células dendríticas (DCs) expuestas a estos fructanos, b) su efecto protector en in modelo *in vitro* de epitelio intestinal dañado, c) sus efectos en la expresión del mRNA de las uniones estrechas en células Caco-2 bajo condiciones fisiológicas e inflamatorias, y d) su influencia en la expresión de genes relacionados a la mucosa y al estrés del retículo endoplásmico (RE) en cálulas intestinales caliciformes (goblets, por su terminología en inglés (GCs)).

Yendo más allá de los efectos de los fructanos e inspirados en sus efectos en los TLRs, en la segunda parte de esta tesis tomamos provecho de nuestra experiencia previa para estudiar al parásito *Giardia lamblia* y sus proteínas como otros factores que participan en la modulación del ambiente intestinal. *G. lamblia* es un modelo celular para estudiar diferentes manera en las que tratar las parasitosis intestinales y para comprender la compleja comunicación hospedero-parásito via factores de virulencia y TLRs. Este microorganismo causa la enfermedad diarréica llamada giardiasis, la cual afecta principalmente a niños, adultos mayores y sujetos inmunocomprometidos (Ankarklev, Jerlström-Hultqvist, Ringqvist, Troell, & Svärd, 2010). La giardiasis puede causar diferentes grados de severidad, variando de una diarrea autolimitante, al desarrollo de enfermedad intestinal crónica inflamatoria (Troeger et al., 2007). Sin embargo, la existencia de diferentes grados de severidad en la giardiasis aún no ha sido completamente elucidada. Ésta podría resultar de la inmunomodulación provocada por la interacción hospedero-parásito.

Varias proteínas de Giardia han sido propuestas como factores utilizados por el parásito para evadir al sistema inmune (Prucca & Lujan, 2009; Rópolo, Feliziani, & Touz, 2019). Entre varias proteínas multifuncionales en G. lamblia, la arginina deiminasa (GlAD) es de especial interés por ser considerada una enzima que juega múltiples papeles regulatorios durante el ciclo de vida de este parásito (Touz et al., 2008). Uno de los más importantes papeles de GlADI es facilitar la comunicación entre el parásito y el hospedero. Debido a que los TLRs son de los componentes humanos que median dicha comunicación molecular con los parásitos, también nos propusimos estudiar cómo GlADI interactúa con los TLRs para comprender mejor las propiedades inmunomoduladoras de esta proteína cuando es liberada al lumen intestinal.

Estudiamos las interacciones potenciales de los TLRs con la enzima GlADI y las respuestas de DCs semejantes a las de infantes después de ser expuestas a esta enzima. Se realizaron estudios espectroscópicos para establecer la influencia de la estructura 3D en en proceso de activación de los TLRs. Además, probamos a GlADI como un blanco contra la giardiasis mediante socking molecular y ensayos de inhibición enzimática con fármacos modificadores de cisteínas para proponer un nuevo método de tratamiento para la giardiasis. Esos ensayos fueron realizados con la proteína recombinante GlADI, así como la enzyma aislada de lisados de trofozoitos de *G. lamblia*. Finalmente, también investigamos cómo dichos fármacos impactan la capacidad de enquistamiento de *G. lamblia*.

La estructura molecular de las fibras dietéticas dirige en gran parte sus capacidades inmunomoduladoras y de protección de la barrera intestinal cuando pasan a través del sistema gastrointestinal.

Los fructanos junto con los galactooligosacáridos (GOS), los oligosacáridos de le lecha humana (hMOs, por sus siglas en inglés), los almidones y las pectinas son carbohidratos no digeribles (NDCs, por sus siglas en inglés). Estos NDCs han sido ampliamente estudiados, demostrando la relación cercana que existe entre su estructura y sus funciones cuando pasan a través del tracto gastrointestinal (Beukema, Akkerman, et al., 2021; Beukema, Jermendi, et al., 2021; Cheng, Akkerman, Kong, Walvoort, & de Vos, 2020; Cheng et al., 2021; Figueroa-Lozano et al., 2020; Fransen et al., 2017; Kong, de Jong, de Haan, Kok, & de Vos, 2022; Kong et al., 2019; Lépine et al., 2019; Logtenberg et al., 2021; Prado et al., 2020; Vogt et al., 2014). De estos NDCs, los fructanos de la raíz de la achicoria han sido ampliamente estudiados. En cuanto a su estructura química, los fructanos de la achicoriason llamados fructanos de tipo inulina (ITFs) debido a su composición de unidades de fructosa unidas mediante enlaces glicosídicos $\beta(2\rightarrow1)$-D-fructosil-fructosa. Esto les confiere una estructura lineal.

Algunos de ellos pueden contener un residuo terminal unido mediante un enlace α-(1→2)-D-glucopiranosil (Vogt et al., 2013). Los fructanos del agave pertenecen a los fructanos de tipo graminano (GTFs, por sus siglas en inglés) debido a que son una mezcla de enlaces glicosídicos $\beta(2\rightarrow1)$ y $\beta(2\rightarrow6)$ (Lopez, Mancilla-Margalli, & Mendoza-Diaz, 2003). Esto les da la estructura ramificada más compleja que se ha descrito hasta la fecha (Pérez-López & Simpson, 2020).

La capacidad de activación o inhibición de los TLRs ha sido estudiada para algunos hMOs, pectinas e ITFs (Cheng, Kiewiet, Groeneveld, Nauta, & de Vos, 2019; Sahasrabudhe et al., 2018; Vogt et al., 2014; Vogt et al., 2013). En el capítulo 3 estudiamos la capacidad inmunomoduladora de los GTFs y la comparamos con la de los ITFs. Independientemente del GP, encontramos que solo los GTfs inhiben fuertemente la activación de los TLRs 2 y 4. Este efecto inhibidor ha sido observado previamente en el TLR2 por las pectinas (Sahasrabudhe et al., 2018). Estos hallazgos revelan las actividades inmunomoduladoras diferenciales que poseen los NDCs, las cuales están íntimamente relacionadas a su estructura química. La fuerte capacidad inhibitoria de los GTFs podría tener apkicaciones prometedoras principalmente en desórdenes inflamatorios intestinales, o en el campo de los trasplantes como adyuvantes para la reducción de la respuesta inflamatoria contra cápsulas inmunoaislantes para el trasplante celular, justo como fue propuesto para las pectinas (Hu et al., 2021). Estas aplicaciones, entre otras, representan un campo de investigación promisorio y aportan más evidencia acerca del efecto benéfico que estas FDs tienen en la salud humana.

El uso de estudios de docking molecular para proponer potenciales explicaciones mecanísticas acerca de los fenómenos biológicos observados (revelando las interacciones moleculares de las fibras dietéticas u otras moléculas con los TLRs)

El modo de interacción a nivel molecular de los fructanos de la achicoria y del agave nunca se había estudiado antes. Los GTFs poseen un fuerte efecto inhibidor de la activación inducida de los TLRs 2 y 4 como se demostró en el **Capítulo 3**. Basados en estudios de docking molecular, propusimos una explicación mecanística para este fenómeno biológico observado. Dicho efecto inhibitorio de la activación de TLR2 y TLR4 podría ser debido a la competencia de los GTFs con el sitio de unión al agonista natural de dichos TLRs. Estos hallazgos han allanado el camino para el diseño experimental de futuros estudios in vitro o in vivo para la demostración de nuestras predicciones realizadas mediante docking. Se podría utilizar mutagénesis sitio dirigida para confirmar experimentalmente el papel de las interacciones predichas entre los GTFs y los TLRs. Nuestra estrategia de docking también sirvió para proponer una explicación mecanística acerca del fuerte efecto inhibidor del del TLR2 ejercido por las pectinas (Jermendi et al., 2022). Considerados en conjunto, estos hallazgos dan lugar al uso del docking

molecular para la predicción de la interacción de los NDCs con componentes del sistema inmune. Esto podría ser una poderosa herramienta para proponer nuevas aplicaciones de los NDCs dirigidos a desórdenes inflamatorios específicos.

Inspirados en cómo los fructanos de la achicoria y del agave interactúan con los TLRs, en el **Capítulo 7** describimos la interacción de la enzima de *G. lamblia* arginina deiminasa (GlADI) con los TLRs. Más aún, los estudios espectroscópicos mostraron que la capacidad inmunomoduladora de GlADI es dependiente de su estructura 3D. También, eoncontramos que la estructura 3D de GlADI está reforzada por enlaces disulfuro. Además de la interacción encontrada de GlADI con residuos clave de los TLRs 2 y 4, el perfil de citocinas que encontramos después de la interacción de GlADI con las células dendríticas, nos permitió demostrar la capacidad inmunomoduladora de GlADI via los TLRs. Nuestros resultados podrían tener implicaciones más allá del nivel molecular, podrían estar contribuyendo a explicar parcialmente la existencia de la pléyade de cuadros clínicos que se observan en sujetos con giardiasis (Troeger et al., 2007). Más aún, en el caso de *G. lamblia*, muchas de sus proteínas son exportadas al medio intestinal mediante una secreción no convencional, y GlADI forma parte de estas proteínas (Balmer & Faso, 2021). Una vez que GlADI es secretada, se piensa que compite por las pozas de arginina como estrategia para impedir la síntesis de óxido nítrico del hospedero (Touz et al., 2008). Todo esto da origen a más preguntas acerca de la influencia de esta proteína en otros componentes del sistema inmune o de las células epiteliales intestinales. Estos hallazgos contribuyen al mejor entendimiento de los mecanismos que *G. lamblia* utiliza para evadir al sistema inmune y garantizar su supervivencia en el intestino humano.

Estudios de docking como base del diseño experimental de investigación en fármacos de reposicionamiento

Debido a la existencia de cepas de *G. lamblia* que son resistentes a los fármacos de primera línea para tratar la giardiasis (Leitsch, 2015), aún es necesaria la investigación dirigida hacia la búsqueda de tratamientos alternativos. El reposicionamiento de fármacos es una estrategia bien conocida que ahorra tiempo y recursos económicos en la búsqueda de nuevos fármacos efectivos (Farha & Brown, 2019). Consiste en la búsqueda de nuevas aplicaciones a los fármacos previamente aprobados para su uso en humanos (Pushpakom et al., 2019). En el **Capítulo 2**, fuimos más allá de la caracterización de GlADI como un potencial blanco de fármacos para combatir la giardiasis. Tomamos nuestra previa experiencia en el diseño racional de fármacos como modelo (Enríquez-Flores et al., 2011; García-Torres et al., 2016; Hernández-Alcántara et al., 2013; López-Velázquez et al., 2019; Reyes-Vivas et al., 2014). El diseño racional de fármacos consiste en la búsqueda de ciertas moléculas a partir de la predicción in silico de su acción potencial en determinado blanco, por ejemplo, en la inhibición de la actividad enzimática. Usualmente el diseño de fármacos termina en el ensayo de la molécula en estudios clínicos, hasta su liberación final en el mercado farmacéutico (Gupta et al., 2021). Siguiendo los pasos del diseño racional de fármacos, comenzamos con la realización de estudios de docking molecular para predecir la potencial interacción de los fármacos omeprazol, rabeprazol, sulbutiamina y aurotiomalato con GlADI. Encontramos que GlADI puede ser un buen blanco para la propuesta de antigiardiásicos alternativos, debido a que todos estos fármacos establecieron interacción con diferentes residuos de cisteína de la proteína. Esto nos dio argumentos científicos para proceder con los estudios experimentales *in vitro*, donde encontramos que la proteína recombinante es inactivada en una manera dosis dependiente por todos estos fármacos. Posteriormente, demostramos *in vivo* que sólo el omeprazol y el rabeprazol inactivaron a la enzima junto con la disminución de la sobrevida del parásito. Nuestro grupo de investigación previamente había descrito a la enzima de *Giardia* triosafosfato isomerasa como otro blanco del omeprazol, rabeprazol y otros derivados (García-Torres et al., 2016; Reyes-Vivas et al., 2014). Todos estos hallazgos en conjunto, soportan futuros estudios clínicos para el reposicionamiento de estas moléculas, que actúan como inhibidores de la bomba estomacal de protones, como antigiardiásicos alternativos.

El docking molecular también podría dar una explicación para la posible modulación de los fructanos a la barrera epitelial intestinal

En el **Capítulo 4** demostramos el efecto protector de los fructanos en la barrera epitelial intestinal. Este efecto fue observado en cultivos de células epiteliales intestinales (IECs, por sus siglas en inglés), las cuales fueron expuestas a moléculas que dañan la barrera intestinal. Basados en reportes previos (Demel, Dorrepaal, Ebskamp, Smeekens, & De Kruijff, 1998; Vereyken, Chupin, Demel, Smeekens, & De Kruijff, 2001; Vereyken, Van Kuik, Evers, Rijken, & de Kruijff, 2003), propusimos como posible explicación de nuestros hallazgos que los fructanos fortalecen la barrera mucosa intestinal mediante el establecimiento de una interacción con las IECs, mientras que, al mismo tiempo, compiten con los sitios de unión de las moléculas disruptoras en la barrera intestinal. Dicha interacción es dependiente de la estructura del fructano aplicado. Entonces, los fructanos lineales podrían tener una mayor área de interacción con la membrana citoplasmática, comparado con los fructanos ramificados, los cuales poseen una estructura más compleja. Como se hizo con los TLRs (**Capítulo 3**), la predicción mediante docking molecular de dichas interacciones de los fructanos con los componentes intestinales, tales como la barrera de mucosa, la membrana citoplasmática, el glicocálix, las proteínas de membrana, y/o las células del tejido linfoide asociado al intestino (GALT, por sus siglas en inglés) tales como las células de Paneth y las células microplegadas (células M), podrían aportar evidencia de otros potenciales sitios intestinales de unión para los fructanos. Más aún, estas predicciones podrían servir para el diseño de experimentos para estudiar dichas interacciones a nivel molecular. No se sabe si estos fructanos pueden ser absorbidos en el intestino por las IECs, lo cual podría ser otra hipótesis a estudiar. Para ir más allá, estudios complementarios en la localización celular de los fructanos mediante, por ejemplo, microscopía, podrían ayudar a confirmar o refutar nuestra hipótesis. Estos planteamientos podrían contribuir a los mecanismos que expliquen los efectos benéficos de estas FDs en la salud humana. Con este conocimiento, el diseño de FDs específicas para ciertos desórdenes inflamatorios podría ser más racional.

Las condiciones inflamatorias fueron inducidas por el uso de moléculas que dañan la integridad del epitelio (Lucioli et al., 2013; Tai et al., 1996). Más aún, incluimos disruptores que actúan mediante diferentes vías de señalización, esto para investigar los posibles mecanismos que subyacen los efectos observados. Encontramos que los efectos protectores observados por los fructanos fueron dependientes de las diferentes vías que llevaron a la disrupción. Para estudiar más a detalle los mecanismos que expliquenn nuestros hallazgos, la realización de estudios funcionales que incluyan moléculas que inhiben dichas vías de señalización (González-Mariscal, Tapia, & Chamorro, 2008), podrían proporcionar más evidencia mecanística.

Para la elucidación de los mecanismos que subyacen los efectos benéficos de los fructanos en la salud intestinal, los estudios de expresión génica necesitan ser complementados con estudios funcionales y/o estudios *in vivo* y viceversa

Para tener un panorama general de los efectos directos de los fructanos de la achicoria y del agave en la salud intestinal, en los **Capítulos 4-6** estudiamos las diferentes células especializadas que constituyen el epitelio intestinal. Entonces, como células tipo enterocito incluímos a las células Caco-2 y T84, como células productoras de mucosa incluimos a la línea celular tipo goblet LS174T, y como representantes de las células inmunes intestinales, incluímos a las células dendríticas. Primeramente, en el **Capítulo 4** mediante estudios funcionales de resistencia transepitelial, demostramos que ambos, los fructanos de la achicoria y los del agave tuvieron efecto protector y antiinflamatorio en la disrupción de la barrera inducida químicamente. Sin embargo, los estudios de expresión génica realizados en los **Capítulos 5 y 6** mostraron que los efectos de protección fueron dependientes del tipo de fructano. Estos hallazgos indican la necesidad de ambos, los estudios funcionales,

así como los estudios de expresión génica para una caracterización integral de los efectos de los fructanos en las IECs. Más aún, futuros estudios in vivo también podrían contribuir a disectar los efectos observados de una manera más extensiva.

El impacto de los fructanos de la achicoria en la comunicación entre las células epiteliales intestinales con aquellas del sistema inmune intestinal, tales como las células dendríticas fue previamente descrito por nuestro grupo de investigación (Bermudez-Brito et al., 2015). Esto no había sido investigado para los fructanos del agave. En el **Capítulo 6** mostramos que las células dendríticas exhibieron respuesta antiinflamatoria cuando fueron expuestos a los fructanos. Más aún, demostramos que dichas respuestas reguladoras de las DCs son más fuertes cuando son expuestas al medio de cultivos que fue previamente utiulizado por las IECs, mismas que a su vez, fueron incubadas en presencia de los fructanos. Estos hallazgos revelan que los fructanos de la achicoria y del agave juegan un papel importante en dicha intercomunicación intestino-sistema inmune. Los componentes celulares y/o metabolitos responsables de estos hallazgos siuen desconocidos. Entonces, los estudios de expresión génica en ambos tipos celulares, las IECs y las dendríticas podría apoyar a la elucidación de los mecanismos que subyacen dicha intercomunicación. La metabolómica podría ser una herramienta promisoria para un estudio más a profundidad en este campo de investigación (Spacova et al., 2020).

Conclusiones y perspectivas futuras

Tomados en conjunto los capítulos de esta tesis contribuyen a un mejor conocimiento de los efectos inmunomoduladores directos de moléculas como los fructanos y las proteínas de parásitos como GlADI, así como los mecanismos compartidos por los cuales interfieren con la inmunidad del hospedero. En el caso de los fructanos, el conocimiento generado aquí podría ser útil para el diseño de alimentos funcionales enriquecidos con fructanos del agave, especialmente en regiones como Latinoamérica donde el agave es endémico.

Como se discutió previamente, las investigaciones conducidas en esta tesis han abierto la breha para varias líneas de investigación a futuro. Los estudios más promisorios son los que permitirán la aplicación de los fructanos del agave como prebióticos . como se demostró para los fructanos de la achicoria (Logtenberg et al., 2020), sería interesante investigar si hay alguna preferencia de la microbiota intestinal por la fermentación de fructanos del agave dependiendo de su GP. Los pasos necesarios para proponer a los fructanos del agave como prebióticos podrían ser dirigidos para determinar si dichos efectos varían con el sexo y/o la edad del hospedero (desde la infancia hasta la adultez). El efecto prebiótico de los fructanos del agave también podría ser estudiado en la prevención y el tratamiento de condiciones como la resistencia a antibióticos, la enfermedad inflamatoria intestinal, la obesidad y el cáncer.

En el caso de GlADI, el conocimiento generado nos permite entender mejor cómo se lleva a cabo la intercomunicación hospedero-parásito. Además podríamos utilizar los fármacos de reposicionamiento estudiados para dañar la estructura 3D de GlADI y de esta manera impedir su interacción con los TLRs. Con esto se podría modular o atenuar la intercomunicación hospedero-parásito para apoyar la expulsión del parásito por el hospedero. El impacto general de las moléculas estudiadas en las IECs y las DCs descrito en esta tesis se muestra en la Figura 1.

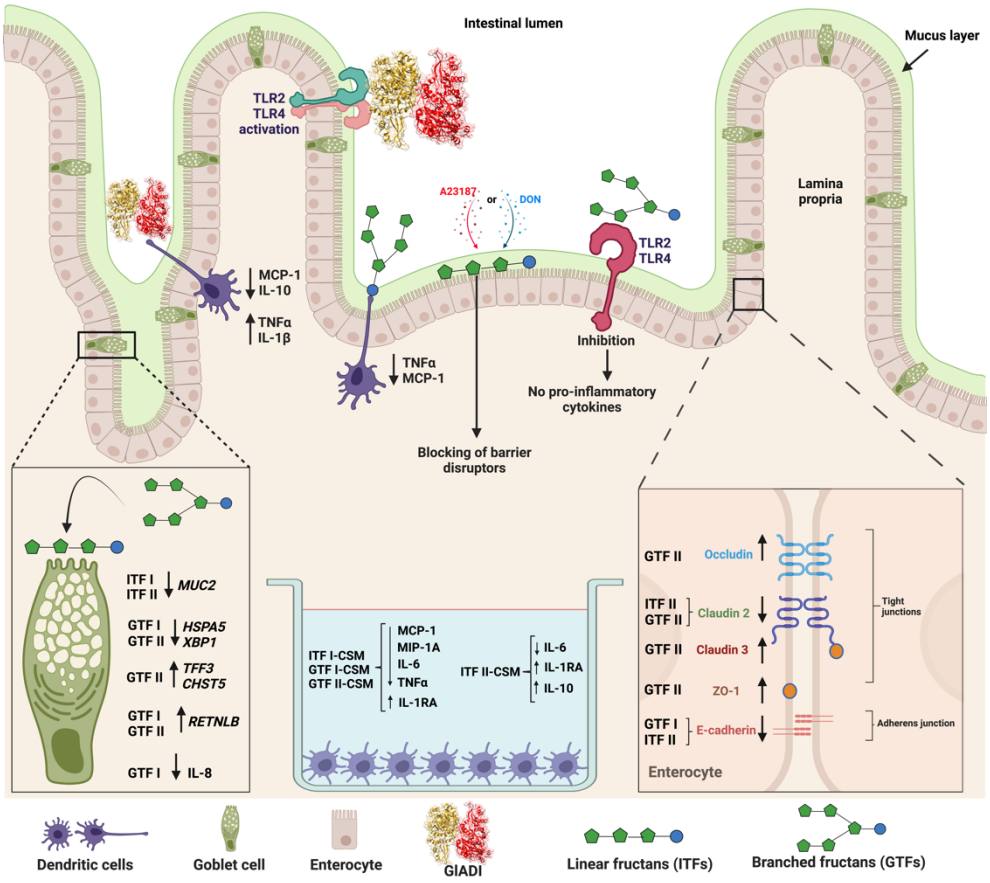

Figure 1. Impacto general de los fructanos de la achicoria y del agave, así como de GIADI en las células epiteliales intestinales. Abreviaturas: A23187, ionóforo de clacio; DON, deoxinivalenol; ITF I, fructano tipo inulina I; ITF II, fructano tipo inulina II; GTF I, fructano tipo graminano I; GTF II, fructano tipo graminano II; MUC2, mucina-2; HSPA5, miembro 5 de las proteínas de choque térmico familia A (Hsp70) (BiP); XBP1, proteína 1 de unión a caja X; TFF3, factor trébol; CHST5, sulfotransferasa 5 de carbohidrato (N-acetilglucosamina-6-O); RETNLB, beta tipo resistina; IL-8, interleucina 8; CSM, medio utilizado por Caco-2; MCP-1, proteína quimioatractora 1; MIP-1A, proteína 1-alfa inflamatoria; IL-6, interleucina 6; TNFα, factor de necrosis tumoral alfa; IL-1RA, proteína antagonista del receptor de interleucina 1; IL-10, interleucina 10; IL-1β, interleucina 1β, GIADI arginina deiminasa de *Giardia*; TLR2, receptor tipo Toll 2; TLR4, receptor tipo Toll 4.

Referencias bibliográficas

Ankarklev, J., Jerlström-Hultqvist, J., Ringqvist, E., Troell, K., & Svärd, S. G. (2010). Behind the smile: cell biology and disease mechanisms of Giardia species. *Nature Reviews Microbiology,* 8(6), 413-422.

Balmer, E. A., & Faso, C. (2021). The Road Less Traveled? Unconventional Protein Secretion at Parasite-Host Interfaces. *Front Cell Dev Biol,* 9, 662711.

Bermudez-Brito, M., Sahasrabudhe, N. M., Rösch, C., Schols, H. A., Faas, M. M., & de Vos, P. (2015). The impact of dietary fibers on dendritic cell responses in vitro is dependent on the differential effects of the fibers on intestinal epithelial cells. *Molecular nutrition & food research,* 59(4), 698-710.

Beukema, M., Akkerman, R., Jermendi, É., Koster, T., Laskewitz, A., Kong, C., . . . de Vos, P. (2021). Pectins that Structurally Differ in the Distribution of Methyl-Esters Attenuate Citrobacter rodentium-Induced Colitis. *Molecular nutrition & food research,* 65(19), 2100346.

Beukema, M., Jermendi, É., Koster, T., Kitaguchi, K., de Haan, B. J., van den Berg, M. A., . . . de Vos, P. (2021). Attenuation of Doxorubicin-Induced Small Intestinal Mucositis by Pectins is Dependent on Pectin's Methyl-Ester Number and Distribution. *Molecular nutrition & food research,* 65(18), 2100222.

Cheng, L., Akkerman, R., Kong, C., Walvoort, M. T., & de Vos, P. (2020). More than sugar in the milk: human milk oligosaccharides as essential bioactive molecules in breast milk and current insight in beneficial effects. *Critical reviews in food science and nutrition*, 1-17.

Cheng, L., Kiewiet, M. B., Groeneveld, A., Nauta, A., & de Vos, P. (2019). Human milk oligosaccharides and its acid hydrolysate LNT2 show immunomodulatory effects via TLRs in a dose and structure-dependent way. *Journal of Functional Foods,* 59, 174-184.

Cheng, L., Kong, C., Wang, W., Groeneveld, A., Nauta, A., Groves, M. R., . . . de Vos, P. (2021). The Human Milk Oligosaccharides 3-FL, LNnT, and LDFT Attenuate TNF-α Induced Inflammation in Fetal Intestinal Epithelial Cells In Vitro Through Shedding or Interacting with TNF Receptor 1. *Molecular nutrition & food research*, e2000425-e2000425.

Closa-Monasterolo, R., Gispert-Llaurado, M., Luque, V., Ferre, N., Rubio-Torrents, C., Zaragoza-Jordana, M., & Escribano, J. (2013). Safety and efficacy of inulin and oligofructose supplementation in infant formula: results from a randomized clinical trial. *Clinical Nutrition,* 32(6), 918-927.

Costalos, C., Kapiki, A., Apostolou, M., & Papathoma, E. (2008). The effect of a prebiotic supplemented formula on growth and stool microbiology of term infants. *Early human development,* 84(1), 45-49.

Demel, R., Dorrepaal, E., Ebskamp, M., Smeekens, J., & De Kruijff, B. (1998). Fructans interact strongly with model membranes. *Biochimica et Biophysica Acta (BBA)-Biomembranes,* 1375(1-2), 36-42.

Dreher, M. L. (2018). Whole fruits and fruit fiber emerging health effects. *Nutrients,* 10(12), 1833.

Enríquez-Flores, S., Rodríguez-Romero, A., Hernández-Alcántara, G., Oria-Hernández, J., Gutiérrez-Castrellón, P., Pérez-Hernández, G., . . . Mendez, S. T. (2011). Determining the molecular mechanism of inactivation by chemical modification of triosephosphate isomerase from the human parasite Giardia lamblia: a study for antiparasitic drug design. *Proteins: Structure, Function, and Bioinformatics,* 79(9), 2711-2724.

Espinosa-Andrews, H., Urias-Silvas, J. E., & Morales-Hernández, N. (2021). The role of agave fructans in health and food applications: A review. *Trends in Food Science & Technology,* 114, 585-598.

Fan, C., Cao, J., & Zhang, F. (2016). The prebiotic inulin as a functional food-a review. *Eur. Rev. Med. Pharmacol. Sci,* 20(15), 3262-3265.

Farha, M. A., & Brown, E. D. (2019). Drug repurposing for antimicrobial discovery. *Nature microbiology,* 4(4), 565-577.

Figueroa-Lozano, S., Valk-Weeber, R. L., Akkerman, R., Abdulahad, W., Van Leeuwen, S. S., Dijkhuizen, L., & De Vos, P. (2020). Inhibitory effects of dietary n-glycans from bovine lactoferrin on toll-like receptor 8; comparing efficacy with chloroquine. *Frontiers in immunology,* 11, 790.

Fransen, F., Sahasrabudhe, N. M., Elderman, M., Bosveld, M., El Aidy, S., Hugenholtz, F., . . . van der Gaast-de Jongh, C. (2017). β2→ 1-fructans modulate the immune system in vivo in a microbiota-dependent and-independent fashion. *Frontiers in immunology,* 8, 154.

García-Torres, I., Marcial-Quino, J., Gómez-Manzo, S., Vanoye-Carlo, A., Navarrete-Vázquez, G., Colín-Lozano, B., . . . Enríquez-Flores, S. (2016). Proton pump inhibitors drastically modify triosephosphate isomerase from Giardia lamblia at functional and structural levels, providing molecular leads in the design of new antigiardiasic drugs. *Biochimica et Biophysica Acta (BBA)-General Subjects,* 1860(1), 97-107.

González-Mariscal, L., Tapia, R., & Chamorro, D. (2008). Crosstalk of tight junction components with signaling pathways. *Biochimica et Biophysica Acta (BBA)-Biomembranes,* 1778(3), 729-756.

Gupta, R., Srivastava, D., Sahu, M., Tiwari, S., Ambasta, R. K., & Kumar, P. (2021). Artificial intelligence to deep learning: machine intelligence approach for drug discovery. *Molecular Diversity,* 25(3), 1315-1360.

Hernández-Alcántara, G., Torres-Larios, A., Enríquez-Flores, S., García-Torres, I., Castillo-Villanueva, A., Méndez, S. T., . . . López-Velázquez, G. (2013). Structural and functional perturbation of Giardia lamblia triosephosphate isomerase by modification of a non-catalytic, non-conserved region. *PloS one,* 8(7), e69031.

Hu, S., Kuwabara, R., Chica, C. E. N., Smink, A. M., Koster, T., Medina, J. D., . . . García, A. J. (2021). Toll-like receptor 2-modulating pectin-polymers in alginate-based microcapsules attenuate immune responses and support islet-xenograft survival. *Biomaterials,* 266, 120460.

Jermendi, É., Fernández-Lainez, C., Beukema, M., López-Velázquez, G., van den Berg, M. A., de Vos, P., & Schols, H. A. (2022). TLR 2/1 interaction of pectin depends on its chemical structure and conformation. *Carbohydrate polymers*, 120444.

Kapiki, A., Costalos, C., Oikonomidou, C., Triantafyllidou, A., Loukatou, E., & Pertrohilou, V. (2007). The effect of a fructo-oligosaccharide supplemented formula on gut flora of preterm infants. *Early human development,* 83(5), 335-339.

Knol, J., Scholtens, P., Kafka, C., Steenbakkers, J., Gro, S., Helm, K., . . . Wells, J. (2005). Colon microflora in infants fed formula with galacto-and fructo-oligosaccharides: more like breast-fed infants. *Journal of pediatric gastroenterology and nutrition,* 40(1), 36-42.

Kong, C., de Jong, A., de Haan, B. J., Kok, J., & de Vos, P. (2022). Human milk oligosaccharides and non-digestible carbohydrates reduce pathogen adhesion to intestinal epithelial cells by decoy effects or by attenuating bacterial virulence. *Food Research International,* 151, 110867.

Kong, C., Elderman, M., Cheng, L., de Haan, B. J., Nauta, A., & de Vos, P. (2019). Modulation of intestinal epithelial glycocalyx development by human milk oligosaccharides and non-digestible carbohydrates. *Molecular nutrition & food research,* 63(17), 1900303.

Lambertz, J., Weiskirchen, S., Landert, S., & Weiskirchen, R. (2017). Fructose: a dietary sugar in crosstalk with microbiota contributing to the development and progression of non-alcoholic liver disease. *Frontiers in immunology,* 8, 1159.

Leitsch, D. (2015). Drug resistance in the microaerophilic parasite Giardia lamblia. *Current tropical medicine reports,* 2(3), 128-135.

Lépine, A. F., Konstanti, P., Borewicz, K., Resink, J.-W., de Wit, N. J., de Vos, P., . . . Mes, J. J. (2019). Combined dietary supplementation of long chain inulin and Lactobacillus acidophilus W37 supports oral vaccination efficacy against Salmonella typhimurium in piglets. *Scientific reports,* 9(1), 1-13.

Logtenberg, M. J., Akkerman, R., An, R., Hermes, G. D., de Haan, B. J., Faas, M. M., . . . de Vos, P. (2020). Fermentation of Chicory Fructo-Oligosaccharides and Native Inulin by Infant Fecal Microbiota Attenuates Pro-Inflammatory Responses in Immature Dendritic Cells in an Infant-Age-Dependent and Fructan-Specific Way. *Molecular nutrition & food research,* 64(13), 13.

Logtenberg, M. J., Akkerman, R., Hobe, R., Donners, K. M., Van Leeuwen, S. S., Hermes, G. D., . . . Zoetendal, E. G. (2021). Structure-Specific Fermentation of Galacto-Oligosaccharides, Isomalto-Oligosaccharides and Isomalto/Malto-Polysaccharides by Infant Fecal Microbiota and Impact on Dendritic Cell Cytokine Responses. *Molecular nutrition & food research*, 2001077.

Lopez, M. G., Mancilla-Margalli, N. A., & Mendoza-Diaz, G. (2003). Molecular structures of fructans from Agave tequilana Weber var. azul. *Journal of Agricultural and Food Chemistry,* 51(27), 7835-7840.

López, M. G., & Urías-Silvas, J. E. (2007). Agave fructans as prebiotics. *Recent Advances in Fructooligosaccharides Research,* 37, 1-14.

López-Velázquez, G., Díaz-García, L., Anzo, A., Parra-Ortiz, M., Llamosas-Gallardo, B., Ortiz-Hernández, A. A., . . . Gutiérrez-Castrellón, P. (2013). Safety of a dual potential prebiotic system from Mexican agave" Metlin® and Metlos®", incorporated to an infant formula for term newborn babies: A randomized controlled trial. *Rev. Investig. Clin,* 65, 483-490.

López-Velázquez, G., Fernández-Lainez, C., de la Mora-de, J. I., de la Portilla, D. C., Reynoso-Robles, R., González-Maciel, A., . . . Olivos-García, A. (2019). On the molecular and cellular effects of omeprazole to further support its effectiveness as an antigiardial drug. *Scientific reports,* 9(1), 1-14.

López-Velázquez, G., Parra-Ortiz, M., Mora, I. D. I. M.-D. I., García-Torres, I., Enríquez-Flores, S., Alcántara-Ortigoza, M. A., . . . Cruz-Rubio, J. M. (2015). Effects of fructans from Mexican agave in newborns fed with infant formula: a randomized controlled trial. *Nutrients,* 7(11), 8939-8951.

Lucioli, J., Pinton, P., Callu, P., Laffitte, J., Grosjean, F., Kolf-Clauw, M., . . . Bracarense, A. P. F. (2013). The food contaminant deoxynivalenol activates the mitogen activated protein kinases in the intestine: interest of ex vivo models as an alternative to in vivo experiments. *Toxicon,* 66, 31-36.

Martín, R., Miquel, S., Ulmer, J., Langella, P., & Bermudez-Humaran, L. (2014). Gut ecosystem: how microbes help us. *Beneficial Microbes,* 5(3), 219-233.

Patry, R. T., & Nagler, C. R. (2021). Fiber-poor Western diets fuel inflammation. *Nature Immunology*, 1-3.

Pérez-López, A. V., & Simpson, J. (2020). The Sweet Taste of Adapting to the Desert: Fructan Metabolism in Agave Species. *Frontiers in Plant Science,* 11, 324.

Prado, S. B., Beukema, M., Jermendi, E., Schols, H. A., de Vos, P., & Fabi, J. P. (2020). Pectin interaction with immune receptors is modulated by ripening process in papayas. *Scientific reports,* 10(1), 1-11.

Prucca, C. G., & Lujan, H. D. (2009). Antigenic variation in Giardia lamblia. *Cellular microbiology,* 11(12), 1706-1715.

Pushpakom, S., Iorio, F., Eyers, P. A., Escott, K. J., Hopper, S., Wells, A., . . . McNamee, C. (2019). Drug repurposing: progress, challenges and recommendations. *Nature reviews Drug discovery,* 18(1), 41-58.

Quiñones-Muñoz, T. A., Villanueva-Rodríguez, S. J., & Torruco-Uco, J. G. (2022). Nutraceutical Properties of Medicago sativa L., Agave spp., Zea mays L. and Avena sativa L.: A Review of Metabolites and Mechanisms. *Metabolites,* 12(9), 806.

Reyes-Vivas, H., Castillo-Villanueva, A., Yépez-Mulia, L., Hernández-Alcántara, G., Figueroa-Salazar, R., García-Torres, I., . . . Marcial-Quino, J. (2014). Giardial triosephosphate isomerase as possible target of the cytotoxic effect of omeprazole in Giardia lamblia. *Antimicrobial agents and chemotherapy,* 58(12), 7072-7082.

Roberfroid, M. B. (2005). Introducing inulin-type fructans. *British Journal of Nutrition,* 93(S1), S13-S25.

Rópolo, A. S., Feliziani, C., & Touz, M. C. (2019). Unusual proteins in Giardia duodenalis and their role in survival. *Advances in Parasitology,* 106, 1-50.

Sahasrabudhe, N. M., Beukema, M., Tian, L., Troost, B., Scholte, J., Bruininx, E., . . . Schols, H. A. (2018). Dietary fiber pectin directly blocks Toll-like receptor 2–1 and prevents doxorubicin-induced ileitis. *Frontiers in immunology,* 9, 383.

Spacova, I., Dodiya, H. B., Happel, A.-U., Strain, C., Vandenheuvel, D., Wang, X., & Reid, G. (2020). Future of probiotics and prebiotics and the implications for early career researchers. *Frontiers in microbiology,* 11.

Stephen, A. M., Champ, M. M.-J., Cloran, S. J., Fleith, M., Van Lieshout, L., Mejborn, H., & Burley, V. J. (2017). Dietary fibre in Europe: current state of knowledge on definitions, sources, recommendations, intakes and relationships to health. *Nutrition research reviews,* 30(2), 149-190.

Tai, Y. H., Flick, J., Levine, S. A., Madara, J. L., Sharp, G. W., & Donowitz, M. (1996). Regulation of tight junction resistance in T84 monolayers by elevation in intracellular Ca2+: a protein kinase C effect. *J Membr Biol,* 149(1), 71-79.

Touz, M. C., Rópolo, A. S., Rivero, M. R., Vranych, C. V., Conrad, J. T., Svard, S. G., & Nash, T. E. (2008). Arginine deiminase has multiple regulatory roles in the biology of Giardia lamblia. *Journal of cell science,* 121(17), 2930-2938.

Troeger, H., Epple, H.-J., Schneider, T., Wahnschaffe, U., Ullrich, R., Burchard, G.-D., . . . Schulzke, J.-D. (2007). Effect of chronic Giardia lamblia infection on epithelial transport and barrier function in human duodenum. *Gut,* 56(3), 328-335.

Van den Ende, W. (2013). Multifunctional fructans and raffinose family oligosaccharides. *Frontiers in Plant Science,* 4, 247.

Vandeputte, D., Kathagen, G., D'hoe, K., Vieira-Silva, S., Valles-Colomer, M., Sabino, J., . . . Darzi, Y. (2017). Quantitative microbiome profiling links gut community variation to microbial load. *Nature,* 551(7681), 507-511.

Vereyken, I. J., Chupin, V., Demel, R. A., Smeekens, S. C., & De Kruijff, B. (2001). Fructans insert between the headgroups of phospholipids. *Biochimica et Biophysica Acta (BBA)-Biomembranes,* 1510(1-2), 307-320.

Vereyken, I. J., Van Kuik, J. A., Evers, T. H., Rijken, P. J., & de Kruijff, B. (2003). Structural requirements of the fructan-lipid interaction. *Biophysical Journal,* 84(5), 3147-3154.

Vogt, L., Meyer, D., Pullens, G., Faas, M., Smelt, M., Venema, K., . . . De Vos, P. (2015). Immunological properties of inulin-type fructans. *Critical reviews in food science and nutrition,* 55(3), 414-436.

Vogt, L., Meyer, D., Pullens, G., Faas, M. M., Venema, K., Ramasamy, U., . . . de Vos, P. (2014). Toll-Like Receptor 2 Activation by b2→ 1-Fructans Protects Barrier Function of T84 Human Intestinal Epithelial Cells in a Chain Length–Dependent Manner. *The Journal of nutrition,* 144, 1002-1008.

Vogt, L., Ramasamy, U., Meyer, D., Pullens, G., Venema, K., Faas, M. M., . . . de Vos, P. (2013). Immune modulation by different types of β2→ 1-fructans is toll-like receptor dependent. *PloS one,* 8(7), e68367.

Wan, X., Guo, H., Liang, Y., Zhou, C., Liu, Z., Li, K., . . . Wang, L. (2020). The physiological functions and pharmaceutical applications of inulin: A review. *Carbohydrate polymers,* 246, 116589.

Wernimont, S., Northington, R., Kullen, M. J., Yao, M., & Bettler, J. (2015). Effect of an α-lactalbumin-enriched infant formula supplemented with oligofructose on fecal microbiota, stool characteristics, and hydration status: a randomized, double-blind, controlled trial. *Clinical pediatrics,* 54(4), 359-370.